The role of ubiquitin, heat shock proteins, and inducible proteasome subunits in major histocompatibility class I antigen presentation

Dissertation

zur Erlangung des akademischen Grades eines
Doktors der Naturwissenschaften (Dr. rer. nat.)
des Fachbereiches für Biologie
an der Universität Konstanz

vorgelegt von

Michael Basler

Tag der mündlichen Prüfung: 18.02.2005
1. Referent: Prof. Dr. M. Scheffner
2. Referent: Prof. Dr. M. Groettrup

Abbreviations

20S	20S proteasome
2D	two-dimensional gel electrophoresis
A	alanine
aa	amino acid
AAA-ATPases	ATPases associated with a variety of cellular activities
Ag	antigen
Ala	alanine
AMC	7-amino-4-methylcoumarin
APC	antigen presenting cell
Arm	armstrong
Asp	asparagine
ATP	adenosine triphosphate
β2m	beta 2-microglobuline
βNA	beta-naphthylamide
BAG	Bcl-2-associated athanogene
BFA	brefeldin A
BH	bleomycin hydrolase
Bz	benzoyl
CD	clusters of differentiation
cDNA	complementary DNA
CDR	complementarity-determining regions
CHIP	carboxyl terminus of Hsc70-interacting protein
CMV	cytomegalovirus
ConA	concanavalin A
cTEC	cortical epithelial cells
CTL	cytotoxic T lymphocytes
Cys	cysteine
D	aspartic acid
d	day
DC	dendritic cell
dd	deionized distilled
DMSO	dimethylsulfoxide
DNA	deoxyribonucleic acid
Doc	docile
DRiP	defective ribosomal product
DTT	1,4-Dithreothiol
E:T	effector to target
E1	ubiquitin activating enzyme
E2	ubiquitin-carrier enzyme
E3	ubiquitin-ligase
EDTA	ethylenediaminetetraacetic acid
eGFP	enhanced GFP
Em	emission
ER	endoplasmic reticulum
ERAP	ER-associated aminopeptidases
F	phenylalanine
FACS	fluorescence activated cell sorting
FCS	fetal calf serum
Fig.	figure

FITC	fluorescin-isothiocyanat
Fl	fluorescence
FPLC	fast performance liquid chromatography
FSC	forward scatter
G	glycin
GA	geldanamycin
GFP	green fluorescent protein
Glu	glutamic acid
Gly	glycine
GP	glycoprotein
GPC	glycoprotein precursor
h	hour
HA	hemagglutinin
HA	herbimycin A
HAT	hypoxanthine aminopterin thymidine
HCMV	human cytomegalovirus
HEV	high endothelial venules
HIV	human immunodeficiency virus
Hop	Hsp-organizing protein
HPLC	high performance liquid chromatography
HPLC-ESI-MS	HPLC electron spray ionisation mass spectrometry
HRP	horse radish peroxidase
Hsc	heat shock cognate
Hsp	heat shock protein
Hyb	hybridoma
i.p.	intra-peritoneal
i.v.	intra-venous
ICS	intracellular cytokine staining
IEF	isoelectric focusing
IFN	interferon
Ig	immunoglobulin
IL	interleukine
IMDM	iscove’s modified dulbecco’s medium
K	lysine
kb	kilo base
kDa	kilo dalton
kV	kilo volt
L	large
LAP	leucine aminopeptidase
LB	Luria-Bertani
LCMV	lymphocytic choriomeningitis virus
Leu	leucine
LMP	low molecular weight protein
LPS	lipopolysaccharide
m.o.i.	multiplicity of infection
mA	milli ampere
mAb	monoclonal antibody
MCMV	mouse cytomegalovirus
MDa	mega dalton
MECL	multicatalytic endopeptidase complex subunit
MEF	mouse embryonic fibroblasts

Met	methionine
MHC	major histocompatibility
min	minute
mM	milli molar
mRNA	messenger RNA
MS	mass spectrometry
mTEC	medullary thymic epithelial cells
NEPHGE	non-equilibrium pH gradient gel electrophoresis
NK	natural killer cells
nm	nanometer
NP	nucleoprotein
ova	ovalbumin
P1	position 1
PA	proteasome activator
PAGE	polyacrylamide gel electrophoresis
PBS	phosphate-buffer saline
PCR	polymerase chain reaction
PE	phycoerythrin
pep	peptide
pfu	plaque forming unit
pGP-C	pre-glycoprotein C
PGPH	peptidyl-glutamyl-peptide hydrolysing
PI	proteasome inhibitor
PSA	puromycin-sensitive aminopeptidase
R	arginine
rad	radiation absorbed dose
REG	regulator
RNA	ribonucleic acid
Rpn	regulatory particle non-ATPase
Rpt	regulatory particle triple-A protein
RT-PCR	reverse transcriptase-PCR
rVV	recombinant vaccinia virus
rVVG2	vaccinia virus expressing the LCMV-WE glycoprotein
S	short
SD	standard deviation
SDS	sodium dodecyl sulphate
siRNA	RNA interference
SP	signal peptide
SPP	signal peptide peptidase
SR-A	scavenger receptor class-A
SSC	sideward scatter
STAT	signaling transduction transcription factor
SV40	simian virus 40
T	threonine
$t_{1/2}$	half-life
TAP	transporter associated with antigen processing
TCA	trichloroacetic acid
TCR	T cell receptor
tet	tetracycline
T_H	T helper cells
Thr	threonine

TM	transmembrane region.
TNF	tumor necrosis factor
TOP	thimet oligopeptidase
TPPII	tripeptidyl aminopeptidase II
TRiC	TCP1-ring complex
tTA	transactivator
Ub	ubiquitin
v/v	volume per volume
Vh	volt hours
VV	vaccinia virus
w/v	weight per volume
WE	LCMV-WE strain
µM	micro molar

Zusammenfassung

Mit Hilfe von Peptiden, die auf MHC-Klasse-I Molekülen präsentiert werden, können zytotoxische T-Lymphocyten mit ihrem T-Zellrezeptor Zellen erkennen, die von Pathogenen infiziert oder zu einer Tumorzelle entartet sind. Das Proteasom, eine abundante Protease eukaryontischer Zellen, spielt dabei eine zentrale Rolle. Das Ziel dieser Doktorarbeit war die Analyse verschiedener Parameter des MHC-Klasse-I Weges, wobei die Rolle der drei induzierbaren, proteolytisch aktiven Untereinheiten LMP2, LMP7 und MECL-1 im Mittelpunkt stand. Als Werkzeug, um dies zu untersuchen, wurde das gut charakterisierte Lymphozytäre Choriomeningits Virus (LCMV) verwendet.

In der Vergangenheit wurden widersprüchliche Resultate erhalten, ob Ubiquitin für die Präsentation von MHC-I-Liganden benötigt wird. Um Klarheit zu schaffen, wurde in dieser Arbeit Ubiquitin und dominant negative Formen von Ubiquitin in einem Tetrazyklin-induzierbaren System exprimiert. Nach der Induktion von Ubiquitin oder mutiertem Ubiquitin wurden keine Veränderungen in der Ubiquitylierung und in der MHC-I Oberflächenexpression festgestellt.

Um die Rolle von Hsp90 in der Antigenprozessierung zu analysieren, wurden Zellen mit Geldanamycin, einem Inhibitor für Hsp90, behandelt. Diese zeigten eine dosisabhängige Reduktion in der Präsentation des LCMV-spezifischen Epitopes NP118-126. Andere LCMV-spezifische Peptide waren dagegen nicht betroffen. Verschiedene Experimente zur Spezifizierung der Rolle von Hsp90 in der Prozessierung von NP118-126 schlugen fehl. Es scheint, dass der Effekt von Geldanamycin auf NP118-126 Zell- und Virus-spezifisch ist. Die Untersuchung des Einflusses von Geldanamycin auf die Präsentation von Epitopen, die am N- oder C-terminalen Ende eines stabilen Proteins exprimiert wurden, zeigte, dass Epitope unabhängig von ihrer Position verschlechtert präsentiert werden.

Im Hauptteil dieser Doktorarbeit wurde die Funktion der drei induzierbaren Proteasomuntereinheiten LMP2, LMP7 und MECL-1 in der Antigenprozessierung LCMV-spezifischer Epitope untersucht. Dabei wurde gezeigt, dass Interferon-γ-behandelte Zellen das LCMV-spezifische Epitop GP33-41 verbessert und das aus dem gleichen Glykoprotein stammende subdominante Epitop GP276-286 verschlechtert präsentieren. *In vitro* wie auch *in vivo* Experimente enthüllten, dass die proteasomale Prozessierung von GP276-286 besser durch das konstitutive Proteasom als durch das Immunoproteasom vollzogen werden kann. Zahlreiche Veröffentlichungen zur Unteruchung der Subdominanz von GP276-286 blieben ohne schlüssige Resultate. Die zuvor erwähnte Zerstörung von GP276-286 durch Immunoproteasome könnte der Grund dafür sein.

Der Einfluss von MECL-1 in der Antigenprozessierung wurde mit Hilfe von MECL-1 defizienten Mäusen analysiert. Die Infektion dieser Mäuse mit LCMV zeigte eine reduzierte CTL-Antwort gegen zwei verschiedene Epitope, NP205-212 und GP276-286. Die verschlechterte CTL-Antwort gegen GP276-286 in MECL-$1^{-/-}$ Mäusen konnte nicht mit einem Präsentationsdefekt in diesen Mäusen erklärt werden. CD8-positive Zellen in MECL-1-defizienten Milzen waren im Vergleich zu Wildtyp Mäusen um 20% reduziert. CTLs von MECL-1-defizienten Mäusen, welche das variabe Segment $V_{\beta}10$ in ihrem T Zellrezeptor tragen, proliferierten nicht nach einer LCMV-Infektion. Dieser Befund sowie die Tatache, dass MECL-1 in Zellen, welche die negative Selektion im Thymus vermitteln, konstitutiv exprimiert ist, deuten auf ein verändertes T-Zellrepertoire in MECL-1 defizienten Mäusen hin. Somit konnte gezeigt werden, dass MECL-1 eine wichige Komponente des MHC-I Antigenprozessierungsweg ist.

Ein weiterer Faktor, der die Immundominanz einzelner Epitope bestimmt, ist die Kinetik der viralen Proteinexpression. Es wurde gezeigt, dass eine geringe LCMV-Dosis zu einer Dominanz von NP-spezifischen CTLs führt, wohingegen GP-spezifische CTLs nach einer hohen Virus-Dosis dominieren.

Die Relevanz von Immunoproteasomen wurde mit Hilfe von Cytomegaloviren (MCMV und HCMV), welche in ihrem Genom zahlreiche Proteine kodieren, die dem Virus helfen, dem Immunsystem zu enkommen, untermauert. Es konnte *in vitro* gezeigt werden, dass der Einbau von Immunoproteasomuntereinheiten in MCMV- und HCMV-infizierten Fibroblasten stark vermindert ist. Eine Deletion im Gen M27 von MCMV, welches einen Inhibitor für STAT2 kodiert und somit den IFN-γ Rezeptor Signalweg hemmt, hatte zur Folge, dass die Transkription und Proteinexpression der induzierbaren Proteasomeuntereinheiten wieder normal funktionierten.

Das ungewöhnlich lange Signalpeptid des LCMV-Glykoproteins (GP) wurde in transfizierten und LCMV-infizierten Zellen untersucht. Dabei wurde gefunden, dass das Signalpeptid von GP langlebig ist und in Viruspartikeln akkumuliert. Diese Besonderheiten weisen darauf hin, dass das Signalpeptid nicht nur den Glykoproteinvorläufer in die Membran des Endoplasmatischen Retikulums führt, sondern auch eine zusätzliche bis jetzt unbekannte Funktion im Lebenszyklus des LCMV hat.

Preface and summary

The class I pathway allows the immunosurveillance of proteins, which are synthesized within virtually all types of cells. Proteasomes are highly abundant in eukaryotic cells and play a major role in antigen processing. The aim of this study was to analyse different parameters in the MHC-I antigen processing pathway, focused on the role of the three proteasome inducible immune subunits LMP2, LMP7, and MECL-1. As a tool to address the topics of these thesis the well-characterised lymphocytic choriomeningitis virus model was chosen.

A general introduction to the topics addressed in the chapters (2-9) was described in chapter 1, focused on proteasomal degradation.

Chapter 2 addressed the role of ubiquitylation in antigen processing. Ubiquitin and dominant negative mutant forms of ubiquitin were expressed in a tetracycline inducible manner to investigate whether ubiquitin is required for the presentation of ligands for MHC-I. No change in total ubiquitylation and MHC-I surface expression was observed after induction of ubiquitin or its mutant forms.

In chapter 3 the role of Hsp90 in the processing of LCMV derived epitopes was investigated. Treatment of LCMV infected cells with geldanamycin, an inhibitor of Hsp90, led to a dose dependent reduction in presentation of the LCMV-derived epitope NP118, but other LCMV-derived epitopes were not affected. Different experiments to assign the role of Hsp90 in processing of NP118 failed. The dependency of NP118 on Hsp90 seems to be cell and virus specific. Analysis whether an epitope is differently affected by geldanamycin when expressed at the N-terminus compared to the C-terminus within a stable protein, revealed that both are reduced independently of their site of expression.

The main part of these thesis, Chapter 4 and 5, described the role of LMP2, LMP7 and MECL-1 in the processing of LCMV-derived epitopes. Chapter 4 analysed the proteasomal processing of GP276-286, a subdominant epitope in LCMV-WE infected C57BL/6 mice. The treatment of cells with IFN-γ enhanced the presentation of GP33–41, whereas presentation of the GP276–286 epitope from the same glycoprotein was markedly reduced. Different read-out systems proved that GP276-286 is made more efficiently by constitutive proteasomes compared to immunoproteasomes.

In chapter 5 the contribution of MECL-1 in antigen processing was analysed with the help of MECL-1 gene targeted mice. Infection of these mice with LCMV-WE markedly reduced the intensity of the CTL response to two different epitopes, NP205-212 and GP276-286. The reduced CTL response to GP276-286 in MECL-1$^{-/-}$ mice could not be assigned to a defect in presentation of this epitope. Staining of CD8 in splenocytes showed that MECL-1 deficient

mice have a 20% reduction of CD8 positive cells compared to wildtype mice. MECL-1$^{-/-}$-derived CTLs using the V$_ß$10 variable segment for their T cell receptors, the preferred V$_ß$-chain of GP276-specific CTLs, didn't proliferate after LCMV infection. Therefore and as MECL-1 is constitutively expressed in cells responsible for negative selection in the thymus one can assume that MECL-1 gene targeted mice have an altered CTL-repertoire. Taken together, it is demonstrated that MECL-1 is an important component in the MHC-I antigen processing pathway.

Another factor that determines immunodominance is the kinetic of viral protein expression (chapter 6). It was reported that a small load of LCMV led to immunodominance of NP-CTL, whereas a large viral load resulted in dominance of GP-CTL.

Chapter 7 described that the incorporation of immunoproteasome subunits was prevented in MCMV infected, as well as HCMV-infected, fibroblasts *in vitro*. Quantitative assessment of LMP2, MECL-1, and LMP7 transcripts revealed that the inhibition of immunoproteasome formation occurred at a pretranscriptional level. Remarkably, a targeted deletion of the MCMV gene *M27*, encoding an inhibitor of STAT2 that disrupts IFN-γ receptor signaling, largely restored transcription and protein expression of immunoproteasome subunits in infected cells.

In chapter 8 we have investigated the cleavage and fate of the unusually long LCMV-glycoprotein (GP) signal peptide (SP) in transfected and LCMV-infected cells. Thereby we found that the cleaved signal peptide is rather long-lived and accumulates in virus particles. These unusual features of the cleaved SP suggest that it not only targets the nascent glycoprotein precursor (pGP-C) to the endoplasmic reticulum membrane but also has additional so far unknown functions in lymphocytic choriomeningitis virus life cycle.

Finally, the results from chapter 2 to 8 are discussed in chapter 9. To obtain a more profound overview of the results from chapter 2 to 8, I recommend reading the discussions at the end of each chapter. The reference list in chapter 10 is linked to chapter 1 to 9.

Michael Basler
November 2004

Chapter 1

Introduction

1. Overview of the antiviral immune response

Vertebrates posses complex immunological defence systems, which protect them from invading pathogens. At the beginning of an infection unspecific defence mechanism (called innate or unspecific immunity) like anatomical (skin, mucous membranes) or physiological (temperature, pH) barrier, complement system, natural killer cells (NK), and phagocytes play an important role to suppress the infection till the adaptive (acquired) immune system can control the infection. In contrast to the adaptive immunity, the innate immunity has no memory.

The adaptive immune response can be classified into the humoral and cell-mediated responses. The humoral response is mediated by B cells, which recognize the three dimensional structure of viral antigens. In contrast, T cells, which are the executors of the cellular immune response, recognize antigens in the form of small peptides presented on major histocompatibility (MHC) molecules by their T cell receptor (Zinkernagel and Doherty, 1974) (Townsend et al., 1985).

The effector cells of the cellular immunity against viruses are T helper (T_H) and cytotoxic T lymphocytes (CTL) (Swain, 1983). CTLs carry the CD8 coreceptor and recognize through their T cell receptor endogenous viral peptides presented on MHC-I of virus infected cells. An infected cell can be killed by CTLs due to perforin release (Kägi et al., 1994). T helper cells expressing the CD4 coreceptor are MHC-II restricted and their function is to induce and modulate the immune response by cytokines (Swain, 1983).

2. T lymphocytes

T lymphocyte precursors develop in the bone marrow from stem cells and migrate to the thymus for maturation. In the thymus, the T cell receptor is generated due to gene recombination and positive as well as negative selection occurs.

The T cell receptor is a heterodimer consisting of α and β or γ and δ polypeptide chains, which are connected via disulfide bonds (Garcia et al., 1996). The extracellular part of α and β consists of a variable and constant immunoglobulin like domain (Yanagi et al., 1984). The highest variability is constrained to the complementarity-determining regions 1-3 (CDR1-3) of the variable domain. The diversity of T cell receptors results from genomic rearrangement of V, D, and J gene segments for the β chain and of V and J segments for the α chain.

Additional deletion and addition of nucleotides between different gene segments increase the diversity of T cell receptors (Davis and Bjorkman, 1988). Different coreceptors like CD4, CD8, and CD3 are essential for MHC recognition and signal transduction.
In a first step, rearranged T cell receptors are examined to recognize the individuals MHC molecules (positive selection) (Bevan and Fink, 1978; Fowlkes and Schweighoffer, 1995; Zinkernagel et al., 1978). Thereafter, auto reactive T cells, which bind a MHC-self antigen – complex with too high affinity are eliminated (negative selection) (Hengartner et al., 1988). Functional T cells leave the thymus to enter the blood as so called naïve T cells and build the T cell repertoire.
T cells circulating in the blood reach secondary lymphatic organs (homing) via high endothelial venules (HEV). This process is directed by chemokines. Naïve T cells circulate through secondary lymphatic organs till they encounter their corresponding antigen presented on MHC of professional antigen presenting cells in T cell zones, triggering clonal expansion of the activated T cell. Activated CTLs leave secondary lymphatic organs and screen our body for infected cells presenting foreign antigen on MHC-I (Campbell et al., 1998) (Sallusto et al., 1999) (Forster et al., 1999).

3. The 26S proteasome

The 26S proteasome (2000kDa) is the main protease in the cytoplasm and the nucleus and is responsible for the degradation of the bulk (80-90%) of cellular proteins (Rock et al., 1994). It is implicated in the degradation of abnormal and damaged proteins, or regulating proteins like cell-cycle regulators, oncogenes, or transcription factors. Recent studies have shown that not only cytosolic and nuclear proteins are proteasome substrates: integral membrane and even ER-luminal proteins have been identified to be degraded by proteasomes, the latter being accessible only after re-export to the cytosol (Lord et al., 2000; Romisch, 1999; Tiwari and Weissman, 2001). The 26S complex, which degrades ubiquitylated proteins, is composed of two distinct complexes: A 20S (700kDa) proteolytic cylinder flanked by two distinct 19S regulatory caps (Fig. 1).

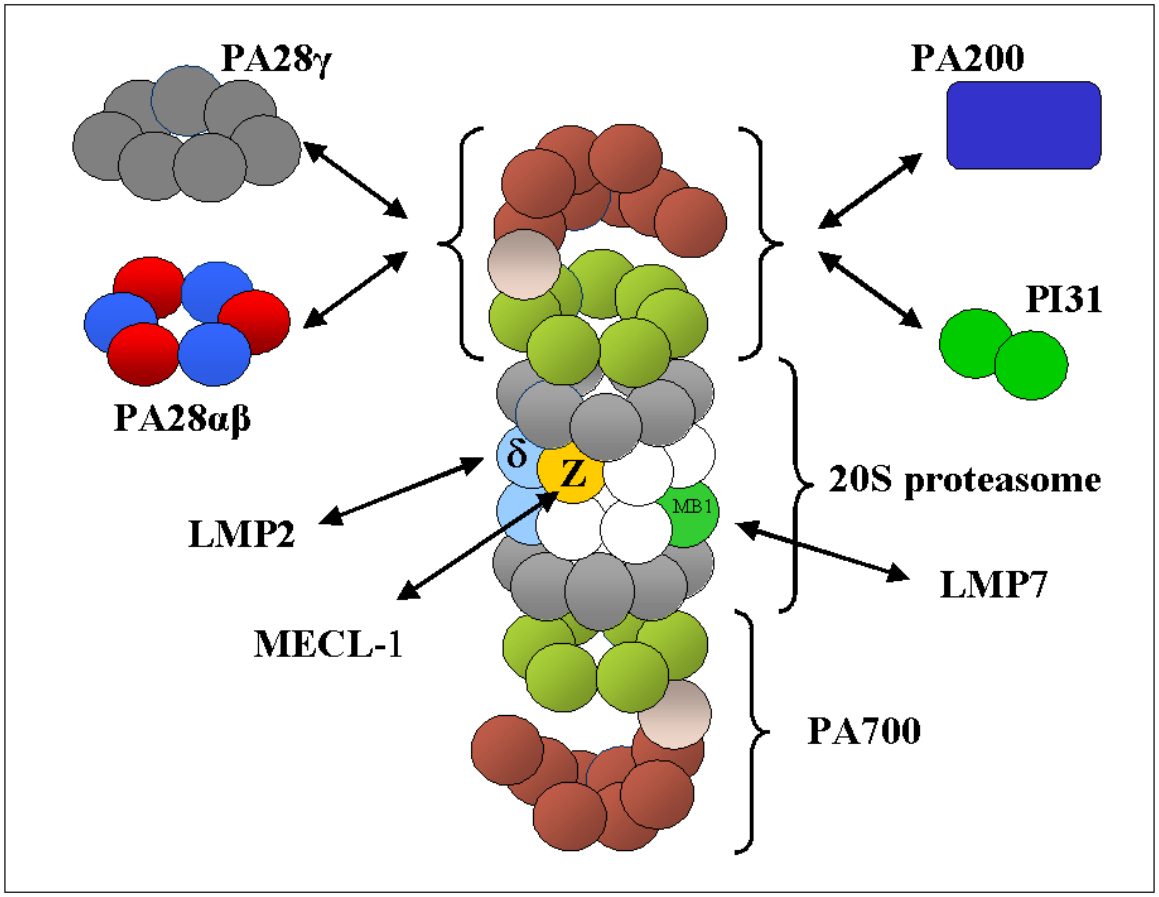

Figure 1: Scheme of the 20S proteasome and its regulators. The α-rings of the 20S proteasome are highlighted in grey and the β-rings in white. The regulators (PA28αβ, PA28γ, PI31, and PA200) are discussed in section 4.4.2 and the interferon-γ inducible subunits (LMP2, LMP7, MECL-1) in 4.4.1

3.1 20S proteasome

The proteolytic core complex of the proteasome system is the 20S proteasome, which is constructed like a cylinder of four stacked rings. The outer two rings consist of seven different α-type subunits that bind to regulatory complexes of the 20S core particle, whereas the two inner rings are made up of seven different subunits of the β-type (α_7-β_7-β_7-α_7). Together, the four rings enclose three inner compartments, two antechambers and one central proteolytic chamber formed by the β-type subunits. Three of the β-subunits designated β_1 (δ), β_2 (Z, MC14), and β_5 (X, MB1) bear the active centers of the 20S proteasome. They (β_1, β_2, and β_5) all posses a N-terminal threonine (Thr-1) responsible for the nucleophilic attack of the carbonyl carbon of a peptide bond. The catalytic activities of the 20S proteasome have been characterized with the help of fluorogenic peptide substrates and inhibitors and were classified as chymotrypsin-like (cleavage C-terminal of hydrophobic aa), trypsin-like (cleavage C-terminal of basic aa), and caspase-like (also known as peptidyl-glutamyl-peptide

hydrolysing (PGPH); cleavage C-terminal of acidic aa). Proteasome assembly is a slow process that involves detectable intermediate complexes with half-lives of several hours (Nandi et al., 1997). These ‘preproteasome‘ intermediates contain one complete α-ring, an incomplete and variable complement of unprocessed β-subunits, and an assembly chaperone, ‘proteassemblin‘. Completion of assembly involves completion of the β-ring, juxtaposition of two preproteasomes at the β-ring interface, autolysis of β-subunit N-terminal propeptides, and degradation of proteassemblin (Nandi et al., 1997) (Schmidtke et al., 1997) (Griffin et al., 2000).

3.2 PA700

The 20S proteasome must be viewed as a proteolytic core complex that needs to associate with regulatory complexes that control the cleavage activity of the proteasome and the access of substrates to the lumen of the 20S proteasome. The PA700 complex (or 19S regulator) which seems to function as the “mouth” for the 20S‘s digestive machinery consists of 17 different subunits, and is thought to be required for the binding and unfolding of ubiquitylated proteins (Braun et al., 1999). The 19S particle can be further subdivided into two assemblages: the “base” and the “lid” (Glickman et al., 1998). The base, which generates a direct contact with the α ring of the 20S complex, is made up of six AAA-ATPases (ATPases associated with a variety of cellular activities; family of chaperone-like ATPases) (Rpt1-6) together with three non–ATPase subunits (S1/Rpn2, S2/Rpn1, S5a/Rpn10). The lid complex forms the distal mass of the 19S regulatory complex and is made of multiple non-ATPase subunits (Rpn) (Glickman et al., 1998; Glickman et al., 1999; Voges et al., 1999).

One important function of PA700 is to recognize ubiquitylated proteins and other potential substrates of the proteasome. Two ubiquitin-binding subunits of PA700 have been identified, referred to as Rpn10 (S5a in mammalian) and Rpt5 (S6’) (Deveraux et al., 1994; Lam et al., 2002). A second function of the 19S regulator is to open a gate in the α ring that will allow entry of the substrate into the proteolytic chamber. Both the channel opening function and the unfolding of the substrate require metabolic energy, which is probably provided by ATP and the six base ATPase subunits (Kohler et al., 2001b) (Kohler et al., 2001a).

4. Antigen processing for MHC-I

4.1 A short overview

The generation of peptide-MHC-class-I complexes results from a multi-step process (Fig. 2). Endogenous viral or bacterial proteins of infected cells as well as cellular proteins are degraded to small peptides of 8 to 10 amino acids (aa), which are presented on MHC-I to T cells. This process is referred to antigen processing and antigen presentation (York et al., 1999) (Rock and Goldberg, 1999).

Proteins (short lived, long lived, misfolded) are degraded by the ubiquitin-proteasome system. Thereby the proteasome releases peptides that range in size from 2-25 amino acids (Kisselev et al., 1998) (Toes et al., 2001). Peptides can be further trimmed or destroyed by cytosolic proteases like leucine aminopeptidase (LAP) (Beninga et al., 1998), bleomycin hydrolase (BH) (Stoltze et al., 2000), puromycin-sensitive aminopeptidase (PSA) (Stoltze et al., 2000), thimet oligopeptidase (TOP) (Saric et al., 2001; York et al., 2003), and tripeptidyl aminopeptidase II (TPPII) (Geier et al., 1999) (Seifert et al., 2003) (Reits et al., 2004). Cytosolic peptides designated for MHC-I presentation are then transported into the lumen of the endoplasmic reticulum (ER) via the transporter associated with antigen processing (TAP), an ER-resident heterodimeric peptide transporter. TAP binds cytosolic peptides and hydrolyses one ATP molecule to open its pore for peptide trans-location and one ATP molecule to complete the cycle, expelling the peptide into the ER lumen in the process (Neefjes et al., 1993; van Endert et al., 2002). TAP is one subunit of the approximately 1MDa MHC-class-I-loading complex, that increases the efficiency of peptide loading by clustering the relevant molecules (including tapasin, calreticulin, the thiol oxidoreductase Erp57, TAP, and MHC-class-I-beta 2 microglobulin dimer) that are involved in MHC-class-I loading in a single location (Dick et al., 2002; Garbi et al., 2000; Ortmann et al., 1997). In the ER, further N-terminal trimming of peptides can occur by the ER- associated aminopeptidases ERAP1 (York et al., 2002) (Saric et al., 2002) or ERAP2 (not yet shown) (Tanioka et al., 2003). Once the class I molecule binds an appropriate peptide, it is released from the MHC-I-loading complex and rapidly transported via golgi to the cell surface, where they present the loaded peptide to cytotoxic T cells (Fig. 2).

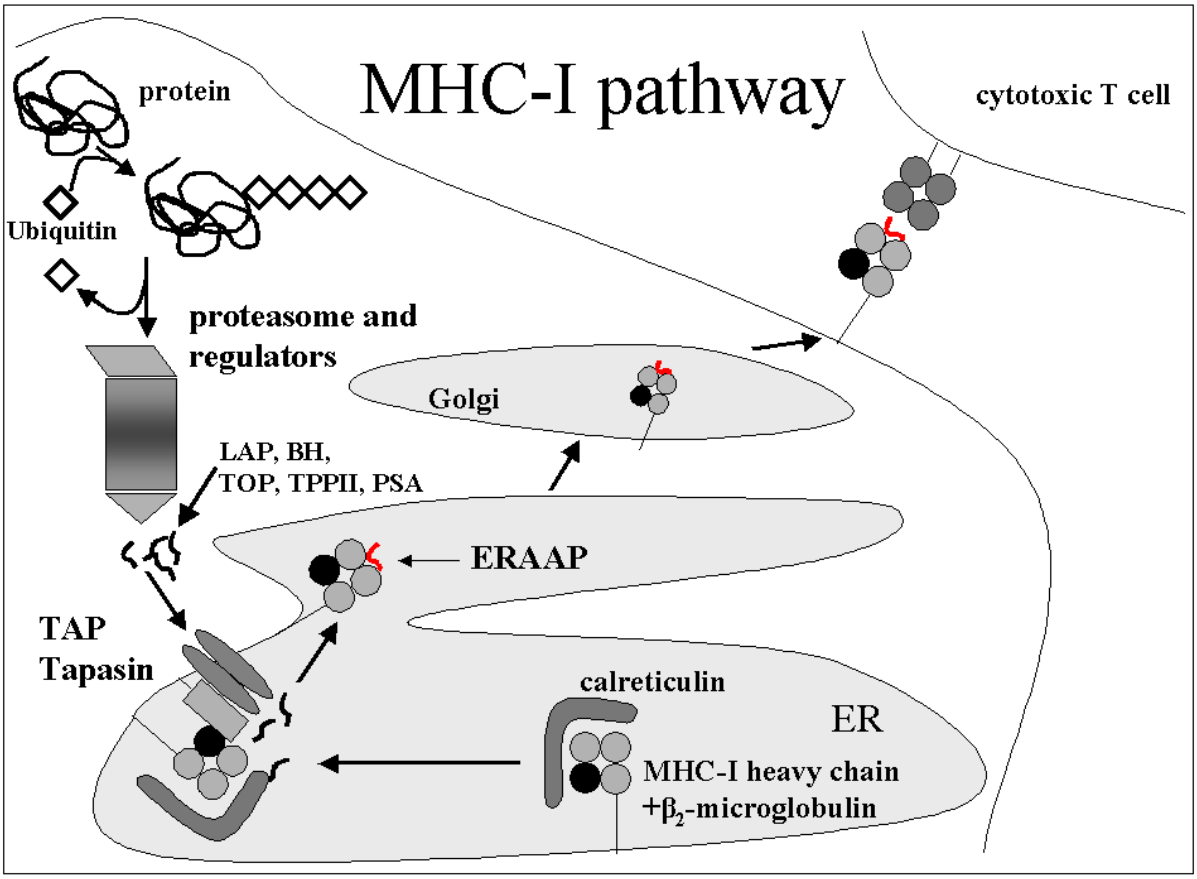

Figure 2: Model of the major histocompatibility complex class I pathway (MHC-I). For explanations see text.

4.2 The source of antigenic peptides

Class-I-presented peptides can originate from virtually any cellular protein, including viral and bacterial proteins (Hunt et al., 1992). Recent evidence suggests that a large portion of ligands for MHC-I may derive from newly synthesized proteins (Khan et al., 2001a; Princiotta et al., 2003; Reits et al., 2000; Schubert et al., 2000). It was proposed, that these MHC-I peptides originate from mistakes in the translation process, like mis-incorporation of amino acids (aa), premature termination, deletion of residues, unsuccessful folding, failure to associate with proper partners, etc.. The products of all these errors can be grouped together as a source of antigenic peptides, generally termed DRiP's (defective ribosomal products) (Yewdell et al., 1996). Studies of TAP with green fluorescent protein (GFP) showed that its lateral mobility in the ER membrane is inversely proportional to the amount of transportable peptides. Inhibition of protein synthesis decreased the mobility of TAP drastically (Reits et al., 2000). This finding indicates that newly synthesized proteins constitute most of the TAP-transported peptides. The efficiency of peptide generation for MHC-I can be estimated to be

in the order of 1 per several 1000 proteins degraded (Princiotta et al., 2003). 20% to 50% of all peptides presented on MHC-I derive from DRiP's (Princiotta et al., 2003). There is increasing evidence that peptides derived from ´noncoding´ regions of mRNA 5´ or 3´ of the open reading frame, and from alternate reading frames can serve as a source of antigenic peptides (Hahn et al., 1991; Schwab et al., 2003; Shastri and Gonzalez, 1993). But this might be rather an exception to the rule. Recently, Vigneron et al. reported that CD8 T lymphocytes were found to recognize a nonameric peptide on melanoma cells that comprises two noncontiguous segments of melanocytic glycoprotein $gp100^{PMEL17}$. The production of this peptide involves the excision of four amino acids and splicing of the fragments; both steps executed by the proteasome. These results indicate, that antigenic peptides can emerge even from two noncontiguous peptides (Vigneron et al., 2004).

4.3 Ubiquitin and its role in antigen processing

Ubiquitin is a small protein (76 amino acids) whose structure is highly conserved through evolution and is abundant in the cytoplasm and nucleus of all eukaryotic cells (Finley and Chau, 1991; Schlesinger et al., 1975). There are only three differences in the sequence of ubiquitin from yeast compared to human. This strong sequence conservation suggests that the vast majority of amino acids that make up ubiquitin are essential, as apparently any mutation that has occurred over evolutionary history has been removed by natural selection. Ubiquitin is encoded by a family of genes whose translation products are fusion proteins. The ubiquitin genes typically exist in two states: 1. The ubiquitin gene can be fused to a ribosomal protein gene giving rise to a translation product that is a ubiquitin-ribosomal fusion protein (Finley et al., 1989); 2. Ubiquitin genes can exist as a linear repeat, meaning the translation product is comprised of a linear chain of ubiquitin-molecules fused together (a polyubiquitin molecule) (Ozkaynak et al., 1984). After the fusion proteins are synthesized, another protein called ubiquitin-C-terminal-hydrolase cleaves the fusion proteins at the C-terminal end of ubiquitin. This either liberates an individual ubiquitin and ribosomal protein or liberates a set of ubiquitin monomers from the polyubiquitin (Pickart and Rose, 1985).

Ubiquitin fulfils essential functions (like the progression of cell cycle, the induction of the inflammatory response, substrate degradation, regulation of DNA repair, etc.) in eukaryotes through its covalent conjugation to other intracellular proteins. Conjugation of ubiquitin to its substrates is achieved by the sequential action of three different enzymes (Fig. 3). Free ubiquitin is activated in an ATP-dependent manner by the activity of an ubiquitin-activating

enzyme (E1), which hydrolyses ATP and forms a complex with ubiquitin via a thioester bond. Subsequently, ubiquitin is transferred to one of many distinct ubiquitin-conjugating enzymes (E2s). In some reactions, E2s can directly ubiquitylate substrates, whereas others require the help of ubiquitin ligases (E3s). Each ubiquitin molecule is conjugated via an isopeptide bond between the C-terminus of ubiquitin (G76) and the epsilon amino group of a lysine side chain to the substrate or to other previously bound ubiquitin moieties (via the K48) to form a long chain (Fig. 3). Multiubiquitylation serves mainly to label substrates for degradation (at least four ubiquitin moieties), whereas monoubiquitylation regulates several processes, such as endocytosis, DNA repair and transcriptional regulation (Hershko and Ciechanover, 1998) (Hershko et al., 2000) (Weissman, 2001) .

At present, it is unclear to what extent ubiquitylation is required to generate MHC-I-presented peptides from different proteins. It is clear that ubiquitylation is not required for the generation of all substrates. When cells were injected with ovalbumin (ova) in which all potential sites for ubiquitylation have been blocked, presentation of an ova-derived peptide still occurred (Michalek et al., 1996). Contradictory results have been obtained with a cell line containing a temperature sensitive E1. At the nonpermissive temperature some antigens were presented normally (Cox et al., 1995) but others displayed an impaired presentation (Michalek et al., 1993). To study the role of ubiquitin in antigen presentation this approach is not really suitable because these E1 cells have remaining E1-activity at nonpermissive temperature and antigen presentation may change under heat shock condition. Given that ubiquitylation plays an important role in overall protein degradation, it seems likely that it has a major role in generating many MHC-I ligands, but conclusive data are still lacking.

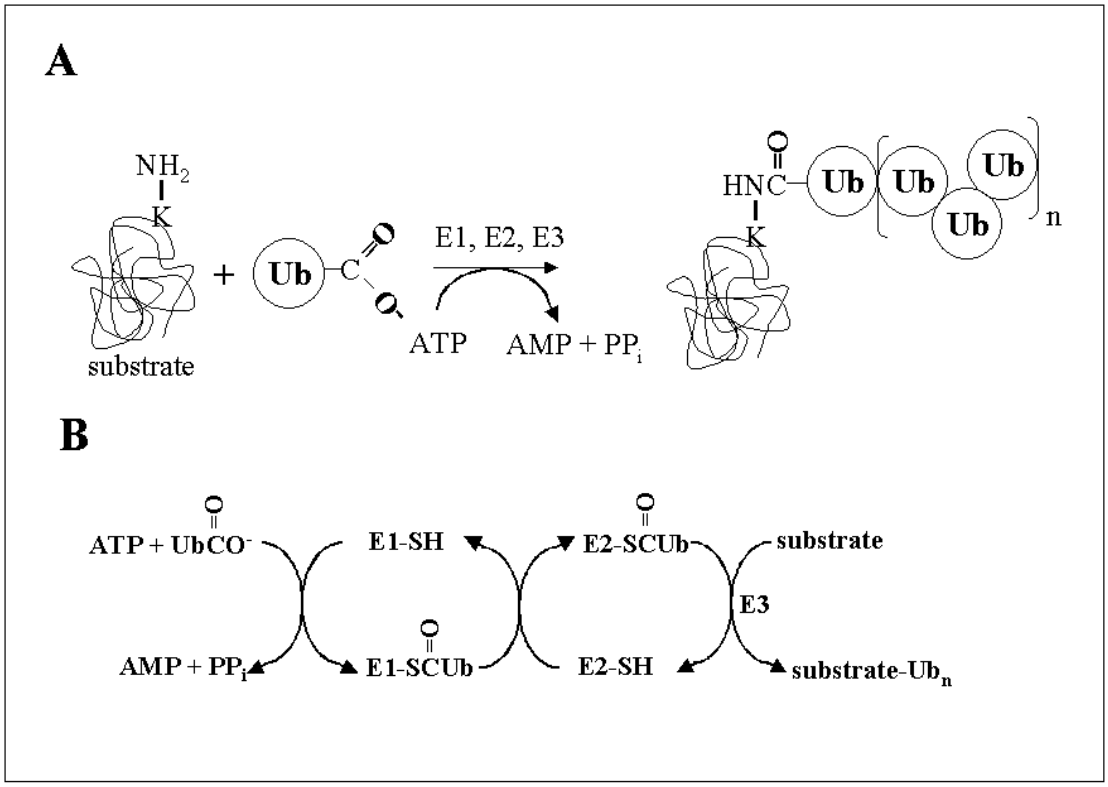

Figure 3: Enzymatic reaction of the ubiquitin system. (**A**) Overview of signalling by ubiquitin. ub: ubiquitin (with carboxyl group G76). As indicated by brackets, the number of ubiquitins may vary. (**B**) Enzymatic pathway of ubiquitin conjugation.

4.4 The proteasome as a source of MHC class I ligands

The proteasome plays a critical role in the generation of the majority of MHC class I-presented peptides. Analysis with proteasome inhibitors showed a reduction of MHC-I surface expression and a blocking of peptide-presentation derived from many proteins (Gallimore et al., 1998c; Harding et al., 1995; Rock et al., 1994; Schwarz et al., 2000a). Proteasome inhibited cells showed normal presentation of antigenic peptides expressed as minigenes in this cells, which shows, that blocking antigen presentation with proteasome inhibitors is due to a loss of peptide generation by proteasomes rather than to a disruption of other required steps (affected by the inhibitors) in the pathway (Rock et al., 1994).

Furthermore, it has been demonstrated that purified proteasomes can generate antigenic peptides or their precursor, which are trimmed by other proteases, from protein or oligopeptide substrates (Eggers et al., 1995) (Niedermann et al., 1995; Schwarz et al., 2000c). Estimates are that approximately 60% of proteasome-generated fragments are too small, 15%

are of the appropriate size and 20% are too large for direct presentation by MHC-I (Cascio et al., 2001). This implies that most of the longer peptides need to be further trimmed before properly fitting MHC-I molecules.

4.4.1 The interferon-γ inducible proteasome subunits LMP2, LMP7, and MECL-1

Some elements of the vertebrate proteasomal system are upregulated by interferon-γ, an immunomodulatory cytokine secreted by T_H, CTLs and NK cells. Upon stimulation of cells with IFN-γ, the constitutive proteolytically active β-subunits designated β_1 (δ), β_2 (MC14, Z), and β_5 (MB1) are replaced by inducible subunits named β_{1i} (LMP2), β_{2i} (MECL-1), and β_{5i} (LMP7) during the *de novo* assembly of 20S proteasomes. Proteasomes containing the IFN-γ inducible–subunits are commonly referred to as 'immunoproteasomes'. In contrast to mecl-1, the lmp2 and lmp7 genes are located in the mammalian MHC locus. In some tissues, (like spleen, thymus, lungs) considerable amounts of immunoproteasomes are constitutively expressed (Barton et al., 2002) (Stohwasser et al., 1997). Differences in organ specific proteasome composition were proposed to be linked to CD8+ T cell-mediated autoimmunity (Kuckelkorn et al., 2002). The substitution of active site subunits changes the proteolytic specificity of the proteasome (Driscoll et al., 1993; Eleuteri et al., 1997) and leads to marked changes in the distribution of fragments that are produced from polypeptides (Boes et al., 1994; Groettrup et al., 1995). Based on comparison of *in vitro* digests of enolase from constitutive and immunoproteasomes by mass spectrometry (MS), algorithms were developed to predict cleavage patterns. This analysis showed that even aa, which are four aa apart from the cleavage site, can influence whether proteasomes exert cleavage. The average length of fragments produced by either set of proteasome was the same. Immunoproteasomes have a much stronger preference for Leu at P1 (first aa N-terminal of the cleavage site), as well as other hydrophobic aa in this position. In contrast, the acidic aa Asp (D) and Glu (E) were clearly disfavoured by immunoproteasomes (Toes et al., 2001). Incorporation of the three subunits occurs interdependently, so that under physiological conditions formation of homogeneous immunoproteasomes or constitutive proteasomes is favoured (Griffin et al., 1998; Groettrup et al., 1997). The β_5-subunits (LMP7, X) are relatively late incorporated into proteasomes and absent from most preproteasomes. Interestingly, immunoproteasome assembly proceeds in a different order from constitutive proteasome assembly with LMP2 being an early component of pre-immunoproteasomes, whereas its homologue, Delta, is a late

component of constitutive preproteasomes (Nandi et al., 1997). LMP2 is required for efficient MECL-1 incorporation and LMP7 is incorporated preferentially over X into proteasomes containing LMP2 and MECL-1, which is dependent on differences between LMP7 and X propeptides (De et al., 2003; Griffin et al., 1998; Groettrup et al., 1997). Immunoproteasomes from mice deficient in LMP7 showed a reduced incorporation of LMP2 and MECL-1 and an accumulation of their precursors (De et al., 2003). Additionally, De et al. published that incorporation of MECL-1 into proteasomes is dependent on LMP2 and to a lesser extent on LMP7. In contrast, LMP2 and LMP7 are integrated independently of MECL-1 into proteasomes. Contradictory results were obtained in mouse fibroblasts overexpressing LMP2 and LMP7, which displayed a poor incorporation of LMP2 into proteasomes. After supertransfecting these cells, which expressed nearly no endogenous MECL-1, with MECL-1, delta was fully replaced by LMP2 (Groettrup et al., 1997).

The majority of class-I-restricted epitopes known to date can be presented by cells carrying standard proteasomes. In the past years, several antigenic peptides including tumor epitopes, were found to be processed differentially by the two proteasome types (Schwarz et al., 2000c) (Sijts et al., 2000b) (Morel et al., 2000).

Why does an organism take on such a tremendous effort to replace all the constitutive proteasomes by immunoproteasomes when only a minor part of CTL epitopes is affected? Different concepts have been proposed: (a) The LMP subunits may have a docking function to physically link proteasomes to TAP. Electron microscopic studies have shown that a small proportion of proteasomes is associated with the ER, and subcellular fractionation studies have demonstrated an enrichment of the LMPs in the microsomal fraction (Palmer et al., 1996; Rivett et al., 1992; Yang et al., 1992). However, proteasomes containing a LMP2-green fluorescent protein fusion appeared to be more or less evenly distributed throughout the cytoplasm and nucleus even after treatment of the cells with IFN-γ. (Reits et al., 1997) (b) The ‘optimal loading‘ argument is implying that the subunit exchanges produce a better-suited set of peptides for loading and stabilizing MHC-I molecules. (c) Another concept is that of ‘optimal diversity‘, which suggests, that a broader set of peptides is produced. It was reported that during an ongoing infection constitutive proteasomes were completely replaced by immunoproteasomes in infected organs at the peak of the CTL response (Khan et al., 2001b) (Barton et al., 2002). To present the most diverse set of peptide an exchange of constitutive to immunoproteasome of more than 50% would not make sense. Another argument against the ‘diversity‘ concept is that dendritic cells, the main inducer of a CTL response, express after maturation mostly immunoproteasomes (Macagno et al., 1999). The authors of Khan et al.

came up with another concept. (d) They postulated that the almost complete replacement of constitutive proteasomes by immunoproteasomes serves to generate different T cell epitopes in inflamed as opposed to uninflamed tissues. This change in epitope production may contribute to avoid autoimmune assaults if different peptide epitopes are processed from endogenous housekeeping genes in uninflamed sites as opposed to sites of viral infection (Khan et al., 2001b).

4.4.1.1 LMP2

GFP fusion studies with LMP2, which replaces delta, showed that LMP2 is evenly distributed throughout the cytoplasm and nucleus (Reits et al., 1997). Overexpression of LMP2 reduces the caspase-like activity of the proteasome and enhances C-terminal cleavage of hydrophobic aa (leads to better suited MHC-I ligands), while proteasomes from spleen cells of LMP2 deficient mice displayed an enhancement in caspase-like activity compared to wildtype mice. LMP2 gene targeted mice displayed no change in MHC class I ligand expression, but the numbers of $CD8^+$ were reduced in blood, spleen and thymus. Some epitopes are affected by LMP2, but the bulk of MHC class I ligands can still be generated in cell lines or mice which are deficient in LMP2 (Arnold et al., 1992; Momburg et al., 1992; Van Kaer et al., 1994). Recently Chen et al. reported that in $LMP2^{-/-}$ mice the CTL response to influenza virus follows a different hierarchy than in wild-type mice, which was due both to differences in the CTL precursor frequency as well as to changes in epitope presentation (Chen et al., 2001).

4.4.1.2 LMP7

The exchange of LMP7 for MB1 is poorly understood and inconclusive results (regarding cleavage preference) were obtained using fluorogenic peptides (Gaczynska et al., 1994; Stohwasser et al., 1996) (Groettrup et al., 1995). LMP7-deficient mice display reduced MHC class I surface expression (Fehling et al., 1994). A mutated form of LMP7 (T1A) revealed that for the production of certain epitopes only the correct structure of LMP7 is required but not its catalytical activity (Gileadi et al., 1999; Sijts et al., 2000a). Like for LMP2, only a minor part of the bulk of MHC-I ligands is affected by LMP7 (Arnold et al., 1992; Momburg et al., 1992).

4.4.1.3 MECL-1

The MECL-1 subunit is unlike LMP2 and LMP7 not encoded in the MHC locus. The discovery of this third subunit exchange (MECL-1 for MC14) lagged behind five years and the *in vivo* function of this subunit is poorly characterized (Groettrup et al., 1996a; Hisamatsu et al., 1996; Nandi et al., 1996). Overexpression of a mutant MECL-1 (T1A) led to a complete loss in trypsin-like activity (Salzmann et al., 1999).

4.4.2 Regulators of the proteasome and their implication in antigen processing

4.4.2.1 PA28 or 11S REG

PA28 (200kDa) also referred as 11S REG forms a hexa- or heptameric ring-shaped complex of 28kDa subunits. Similar to PA700, the 11S regulator binds to one or both α–rings of the 20S proteasome. The 19S regulatory complex and 11S regulatory complex can simultaneously bind the proteasome to build the so-called hybrid proteasomes (Hendil et al., 1998) (Cascio et al., 2002). The PA28 family consists of three members: α, β, and γ. Unlike PA700, the PA28 proteins do not enable proteasomes to digest full-length proteins or ubiquitylated substrates *in vitro* (Ma et al., 1992).

4.4.2.1.1 PA28αβ

Degradation of small peptides (but not denatured or ubiquitylated proteins) by the 20S proteasome is greatly stimulated by PA28αβ (Song et al., 1996) (Kuehn and Dahlmann, 1996). PA28αβ predominantly forms hetero-oligomers (Ahn et al., 1996; Song et al., 1996), which have been found mostly in the cytoplasm (Wojcik et al., 1998). X-ray crystallography studies displayed that the 11 S REG is a barrel traversed by a central channel. This structural analysis did not reveal the mechanism by which PA28 activates the 20S proteasome, but conformational changes in proteasomal α- and β-type subunits have been implicated (Knowlton et al., 1997). The N-terminal sequences in α subunits completely seal off the antechambers of the 20S proteasome. Therefore it seems likely, that PA28αβ cause a conformation change in proteasome α-subunits, such that substrate access to the chambers of the 20S proteasome is relieved. It has also been proposed that PA28 binding may facilitate the egress of peptide products by forming a continuous channel leading from the upper surface of PA28 to the interior of the proteasome. Studies with small fluorogenic peptides have revealed,

that the 11S REG stimulates the chymotrypsin-like and PGPH activity of the 20S proteasome to a greater extent than the trypsin-like activity (Dubiel et al., 1992) (Ustrell et al., 1995). In the absence of 11S REG, the 20S proteasome cleaves its substrate only at one site. In contrast, different groups have shown that binding of the 11 S REG to the 20S proteasome promotes the excision of dual-cleavage peptides (Groettrup et al., 1995) (Dick et al., 1996) (Niedermann et al., 1997). Whitby et al. solved the X-ray structure of *S. cerevisiae* 20S proteasome bound to PA26 (the 11S regulator of *Trypanosoma brucei*) and proposed another model of how PA28αβ may operate. PA26 induced a conformational change in the α-subunits, which opened a gate in the α-rings, but no changes in the β-subunits were observed (Whitby et al., 2000). It has been reported that 75% of peptide products of 20S and 26S proteasome are too short to serve as ligands for MHC-I molecules (Kisselev et al., 1999). Therefore, by opening the α-ring, PA28αβ may affect antigen processing by permitting the exit of larger peptide products better suited for MHC-I ligands.

PA28αβ only occurs in vertebrates and is upregulated by interferon-γ (IFN-γ) (Honore et al., 1993) (Jiang and Monaco, 1997). Although the α- and β-subunits are not encoded in the MHC locus (McCusker et al., 1999), their relatively high expression in cells and organs of the immune system suggests a role in antigen processing (Knowlton et al., 1997; Ma et al., 1993). One of the first direct hints for a role in antigen processing was the observation that PA28α overexpression in fibroblasts led to an increased presentation of two CTL epitopes (Groettrup et al., 1996b). Further insights into the role of PA28αβ in the immune system were expected from knockout mice. But contradictory results were obtained with PA28β (Preckel et al., 1999) and PA28αβ (Murata et al., 2001) deficient mice. Disruption of the PA28β-gene, which led to a complete absence also of the PA28α protein, caused a severe immunological phenotype. Processing of several endogenous (HY male antigen) and exogenous (OVA-derived SIINFEKL, influenza virus derived NP366-374) epitopes as well as primary *in vivo* CTL responses against MCMV and LCMV were drastically impaired. Two-dimensional gels of proteasome from these mice revealed, that compared to wildtyp mice, the immunoproteasome subunits LMP2, LMP7 and MECL-1 are not incorporated (Preckel et al., 1999). Completely different results were obtained from PA28αβ double gene disrupted mice. Immunoproteasome assembly in these mice was not impaired and no difference in presentation of OVA-derived SIINFEKL and influenza virus derived NP366-374 was observed compared to wildtype mice. These mice responded normal to influenza A virus infection, but the TRP2 derived epitope$_{181\text{-}188}$ presentation was impaired in these mice (Murata et al., 2001). Taken together, it appears that PA28αβ leads to an enhanced presentation of

some epitopes, but others are not affected (Groettrup et al., 1996b; Murata et al., 2001; Schwarz et al., 2000b; Schwarz et al., 2000c).

4.4.2.1.2 PA28γ

PA28γ (also called Ki, or REGγ) was discovered as a major autoantigen in patients suffering from lupus erythematosus (Nikaido et al., 1990). REGγ forms homo heptamers, which activate the 20S proteasome and is mainly found in the nucleus. In contrast to PA28αβ, REGγ is barely induced by interferon-γ (Jiang and Monaco, 1997). PA28γ enhanced trypsin-like activity of the proteasome, but only a weak enhancement of the caspase-like and chymotrypsin-like activity was observed (Li et al., 2001) (Realini et al., 1997).
PA28γ deficient mice have only a minor phenotype. They display a reduction in body size coupled with defects in mitotic progression of cultured embryonic fibroblasts (MEF) (Murata et al., 1999). Recently, PA28γ gene targeted mice have been thoroughly analysed in respect to immune defects (Barton et al., 2004). These mice showed normal surface MHC-I expression, but had a slightly reduced number of $CD8^+$ T cells. The proportions of $CD8^+$ T cells responding to a panel of influenza virus epitopes after influenza infection as well as to a SV40 T Ag epitope (expressed by a recombinant vaccinia virus) were normal. The only immunological defect was a slightly impaired clearance of the intracellular fungal pathogen *Histoplasma capsulatum*. Taken together, PA28γ has, if at all, only a minor effect on MHC-I antigen presentation.

4.4.2.2 PA200

PA200 is a 200 kDa nuclear protein that activates the proteasome. It promotes the proteasomal hydrolysis of peptides, but not proteins. Following gamma-irradiation of HeLa cells the uniform nuclear distribution of PA200 changes to a strikingly punctuate pattern, a behaviour characteristic of many DNA repair proteins. These findings implicate PA200 in DNA repair, possibly by recruiting proteasomes to double strand breaks (Ustrell et al., 2002). Homologs of PA200 are present in organism without an adaptive immune system (worms, plants and yeast), which indicates that PA200 has no role in antigen presentation.

4.4.2.3 PI31

PI31 (Proteasome Inhibitor) is a 31kDa protein that inhibits the hydrolysis of small synthetic substrates and large unfolded proteins by the 20S proteasome (McCutchen-Maloney et al., 2000). PI31 localizes at the nuclear envelop/endoplasmic reticulum membrane (Zaiss et al., 2002). Immunosubunits do not influence the affinity of PI31 to the 20S proteasome. Kinetic analysis showed that PA28 compete with PI31 for proteasome binding and this competition is due to distinct affinities of the two molecules for the 20S proteasome, strongly biased towards PI31. PI31 may function by hindering substrate access to the 20S catalytic channel (Zaiss et al., 1999).

Zaiss et al. reported that in cells overexpressing PI31 immunoproteasome subunit precursors were accumulating, which resulted in an impaired immunoproteasome formation. The failure of immunoproteasomes to mature properly implicated a diminished processing of an immunoproteasome-dependent CTL epitope ($E1B_{912-200}$). In parallel to impaired immunoproteasome formation, IFN-γ treated cells (overexpressing PI31) exhibit a severely reduced MHC-I surface expression, which suggests that generation of a large number of CTL epitopes is inhibited in PI31-transfected cells. They proposed that PI31 may serve to control immunoproteasome formation and may thereby maintain an intracellular balance between constitutive-and immunoproteasomes (Zaiss et al., 2002).

4.5 Hsp90 and its role in antigen processing

The control and maintenance of the three-dimensional structure of proteins is a prerequisite for cell survival, and involves a cooperation of molecular chaperones and energy-dependent proteases. Molecular chaperones recognize hydrophobic regions exposed on unfolded proteins and stabilize nonnative conformations. As a consequence, formation of insoluble protein aggregates in the highly crowded cellular environment is prevented and folding to the native state promoted. Different chaperones follow distinct strategies to achieve the general goal of preventing protein misfolding and aggregation and they often cooperate (McClellan and Frydman, 2001; Wickner et al., 1999).

The Hsp90 chaperone family is evolutionary highly conserved and includes the Hsp90 (90kDa heat shock protein) of the eukaryotic cytosol (termed: Hsp90α and β in humans; Hsp86 and Hsp84 in mice; Hsc82 and Hsc84 in yeast) and Grp94/gp96 of the eukaryotic ER. Other family members are the Hsp75/TRAP1 in the mitochondrial matrix and the HtpG in the bacterial cytosol (Argon and Simen, 1999; Felts et al., 2000). The homodimer Hsp90 is one of

the most abundant proteins in eukaryotic cells, comprising 1-2% of total cellular proteins even in nonstress conditions and can be induced through heat shock and cell stress (Nemoto et al., 1995) (Young et al., 2001). Functional Hsp90 is ATP dependent and can be inhibited by the ansamycin drugs geldanamycin (GA) or herbimycin A (HA) occupying the ATP-binding pocket (Whitesell et al., 1994).

Hsp90 functions as a protein-folding machinery collaborating with other chaperone molecules, such as Hsp70 and Hsp40, and cochaperones p23 and Hop (Buchner, 1999) and is essential for maintenance of functional integrity of various fragile proteins, such as steroid hormone receptors and many protein kinases (Picard et al., 1990; Stepanova et al., 1996; Xu and Lindquist, 1993). BAG-1 as well as CHIP, an ubiquitin ligase, have been proposed to act as a link between molecular chaperones and the ubiquitin/proteasome pathway (Connell et al., 2001) (Meacham et al., 2001) (Luders et al., 2000). Association with CHIP seems to convert the Hsc/Hsp70 chaperone into a substrate recognition factor of a functional ubiquitin ligase complex, whereas BAG-1 supports binding of the ligase complex to the proteasome and triggers the release of ubiquitylated substrates from Hsc/Hsp70 for their transfer to the proteasome (Cyr et al., 2002; Hohfeld et al., 2001).

Hsp90 directly associates with the 20S proteasome and thus appears to be closely linked to protein degradation in the cell (Tsubuki et al., 1993; Wagner and Margolis, 1995). In addition, it has been reported that Hsp90 links misfolded proteins to the ubiquitylation pathway for selective elimination (Connell et al., 2001) and that Hsp90 binds to tumor-associated MHC-I ligands or their precursors (Ishii et al., 1999). Complexes of peptides with Hsp90 can be taken up by macrophages and dendritic cells through the CD91 receptor or scavenger receptor class-A (SR-A) and these peptides are re-presented on MHC-I (Binder et al., 2000) (Basu et al., 2001) (Berwin et al., 2003). A more direct link to MHC-I antigen presentation was provided by Yamano et al. who showed that geldanamycin, an inhibitor of Hsp90, suppressed antigen presentation of an ova-derived epitope in LPS blasts derived from PA28αβ-deficient mice, but not in wildtype cells. This indicates that Hsp90 can compensate for the loss of PA28 and is essential in a PA28-independent pathway (Yamano et al., 2002).

5. Immunodominance

CTL responses are usually directed against a few dominant epitopes and some minor epitopes. The phenomenon that a CTL response is dominated by a few epitopes is termed

immunodominance. Factors that contribute to immunodominance have been extensively described (Chen et al., 2000; Deng et al., 1997; Yewdell and Bennink, 1999) (Probst et al., 2002). Knowledge of these factors is important for the design of vaccines that elicit optimal $CD8^+$ T cell responses.

In order to be immunogenic, a peptide has to be generated by a professional antigen presenting cell (APC) from a polypeptide and delivered to the MHC-I molecule to which it has to bind with sufficient affinity. This complex has to trigger the activation and proliferation of a T_{CD8+} with a complimentary T cell receptor. Many obstacles have to be cleared to achieve a strong CTL response:

(a) The proteasome has to make the perfect C-terminal cut of a T cell epitope (Craiu et al., 1997) (Mo et al., 1999) (Serwold and Shastri, 1999). (b) Cytosolic or ER-associated proteases have to trim peptide precursors to correct size (Mo et al., 1999; Serwold et al., 2002) (Saric et al., 2002). (c) Cytosolic as well as ER-associated proteases can destroy peptides or their precursors (Reits et al., 2003). (d) Peptides have to bind to the transporter associated with antigen processing (TAP) as well as to a given MHC class I molecule with respect to their length and the availability of anchor residues (Rammensee et al., 1999). (e) A sufficient number of peptide-MHC-I complexes has to be produced (Kageyama et al., 1995). (f) An adequate avidity of the T cell receptor for the class I/peptide complex is pivotal (Lanzavecchia et al., 1999) (g) The precursor frequency of T cells with a particular specificity (T cell repertoire) will determine whether a given epitope achieves immunodominance over competing epitopes (Chen et al., 2000; Slifka et al., 2003). (f) Specific viral proteins can suppress efficient presentation of viral proteins (Basta and Bennink, 2003; Khan et al., 2004). (g) Kinetic of viral protein expression can shape immunodominance (Probst et al., 2003).

6. Lymphocytic choriomeningitis virus

The prototypic arenavirus lymphocytic choriomeningitis virus (LCMV) is a prominent model to study immunological mechanism. Using the LCMV model important concepts of immunology and viral pathogenesis have been developed. The natural host of the noncytopathic virus is the mouse. LCMV is an enveloped bisegmented negative-strand RNA virus. Virions of LCMV are composed of a nucleocapsid, which is surrounded by a lipid envelope containing the envelope glycoprotein GP. After interaction of LCMV with its

receptor alpha-dystroglycan (Cao et al., 1998) and internalisation of the virions within vesicles, LCMV GP mediates fusion of the viral and cellular membranes, resulting in delivery of the nucleocapsids into the cytoplasm. The two genome segments L (large) and S (short) have approximate sizes of 7.2 and 3.4kb, respectively (Meyer et al., 2002; Salvato and Shimomaye, 1989). Each segment directs the synthesis of two gene products, encoded in ambisense orientation. The S segment encodes the virus nucleoprotein (NP; 63kDa) and the glycoprotein (GP) precursor (GPC; 75kDa) (Riviere et al., 1985). Posttranslational processing of GPC produces GP-1 (40-46kDa) and GP-2 (35kDa) (Buchmeier and Oldstone, 1979), which is mediated by the cellular subtilase SKI-1/S1P in a late-Golgi or post-Golgi compartment (Beyer et al., 2003). The LCMV N-terminal signal peptide (SP) of GPC is unusual large (58aa) (Froeschke et al., 2003). The L RNA segment codes for the virus RNA-dependent RNA polymerase (L; 200kDa) and a small 11kDa RING finger protein (Z), whose role in the virus life cycle is poorly understood (Salvato and Shimomaye, 1989).

Infection of C57BL/6 (H-2^b) mice with LCMV induces a strong and protective CTL response. In C57BL/6 mice, this response is strongly dominated by CTLs specific for the GP-derived GP33-41D^b, GP34-41K^b, and the NP-derived NP396-404D^b and the subdominant epitopes GP276-286/D^b, GP92-101/D^b, GP118-125/K^b and NP205-212/K^b (van der Most et al., 1996) (Gallimore et al., 1998a) (van der Most et al., 2003). The response in BALB/c (H-2^d) mice is dominated by a single epitope, the NP118-126/L^d, but also GP283-292/K^d specific CTLs are detectable (van der Most et al., 1996) (Fig. 4). After infection with LCMV-WE, LCMV-Docile, or LCMV-Arm Clone13 the CTL response in C57BL/6 mice is dominated by GP33-specific CTLs, whereas infection of mice with the slower replicating strain LCMV-Armstrong results in NP396 dominance (Gallimore et al., 1998a; Probst et al., 2003; Zajac et al., 1998). NP118 is the first CTL epitope known to emerge exclusively from the DRiP pathway (Khan et al., 2001a).

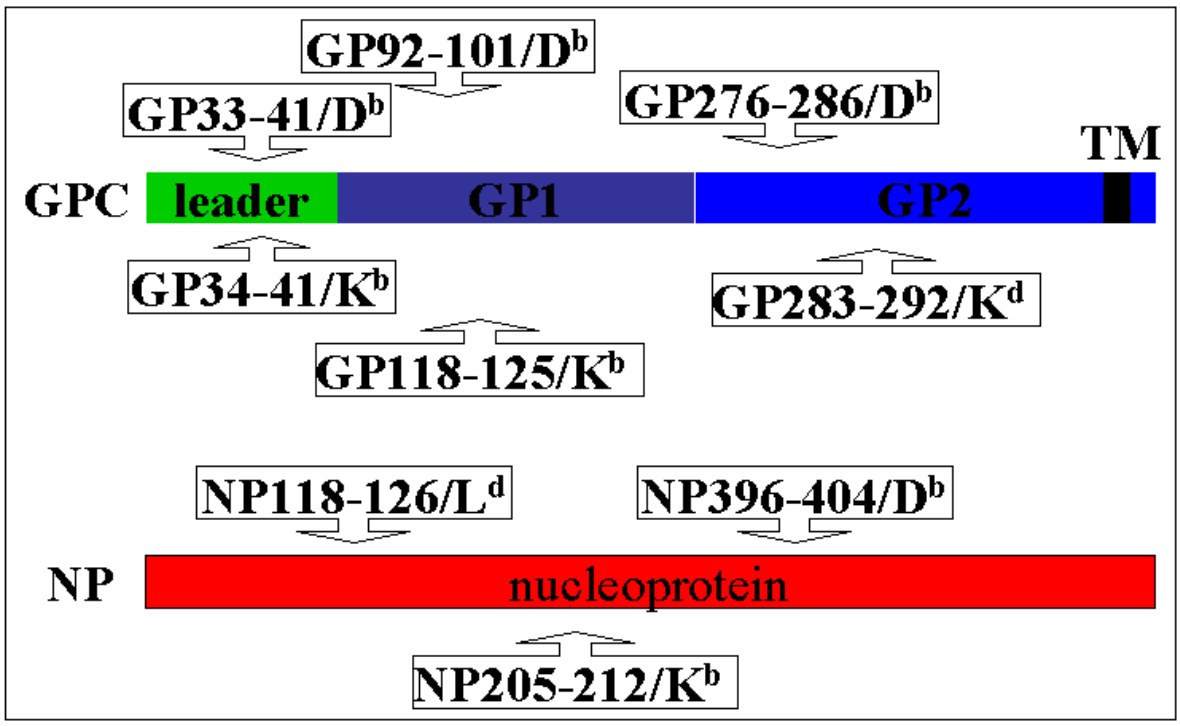

Figure 4: Scheme of antigenic epitopes of lymphocytic choriomeningitis virus (LCMV). TM: transmembrane region.

Infection with low doses of LCMV-WE (200pfu i.v.) leads to a peak in virus titer on day four after infection. Shortly after infection the cytokines IFN-α/β and IFN-γ are induced impairing viral replication. This cytokines activate NK cells, which are not able to control the virus infection (Bukowski et al., 1983; Welsh and Kiessling, 1980). The LCMV-specific CTL response peaks at day 7-9 post infection and eliminates the virus (Moskophidis et al., 1993; Zinkernagel et al., 1986). Experiments with CD4-deficient or CD4-depleted mice showed that the LCMV specific CTL response in the acute phase is independent of T help (Leist et al., 1987; Rahemtulla et al., 1991). But for a long-term elimination of the virus neutralising antibodies are essential to control virus replication (Ciurea et al., 2000; Planz et al., 1997).

The reason why CTLs are emerging in great numbers to only one or a few epitopes while CTLs to other potential epitopes are virtually not detectable has been profoundly investigated in the LCMV system but the phenomenon remains poorly understood (Gallimore et al., 1998b) (van der Most et al., 1996) (van der Most et al., 1998) (Gallimore et al., 1998a). GP33, GP276, and NP396 epitopes were eluted from H-2D^b proteins of LCMV infected MC57 fibroblast cells and the approximate number of epitopes per cell was determined. The calculated numbers were 1080 for GP33, 92 for GP276, and 162 for NP396 which implies that the copies of GP276 and NP396 epitopes generated in MC57 cells and presented on the cell surface are in a range, where recognition by CTLs could become limiting (Gallimore et

al., 1998a) (Christinck et al., 1991). However, it must be pointed out that MC57 cells infected with LCMV *in vitro* may not be representative for the physiological situation because infected cells *in vivo* are confronted with IFN-γ produced by NK cells and T_{h1} cells which has dramatic effects on the class I processing and presentation pathway. Recently, it has been shown that the immunodominance of the LCMV specific CTL response can be shaped by the kinetics of viral protein expression (Probst et al., 2003). But it is still not clear why GP276 is a subdominant epitope in C57BL/6 mice after infection with LCMV. The affinity of GP276 for the peptide binding groove of H-2D^b seems superior to that of GP33 since an about 10 fold lower concentration of GP276 was required to achieve optimal lysis (Gallimore et al., 1998a) (van der Most et al., 1998). Also the recognition and elimination of LCMV infected target cells by GP276 specific CTLs seems to be more efficacious compared to GP33 specific CTLs as evidenced by adoptive transfer experiments thus indicating that the binding of the GP276 specific T cell receptors to H-2D^b/GP276 complexes on the surface of LCMV infected cells is not a limitation (Gallimore et al., 1998a). It has been proposed that the GP276-286-specific T cell repertoire might be a limiting factor because T cell lines specific for GP276 were strongly biased for the usage of $V_\alpha 4$ and $V_\beta 10$ variable segments for their T cell receptors, but it has not been investigated whether this bias imposes a limit on the availability of GP276 specific T cells in the repertoire (Aebischer et al., 1990; Gallimore et al., 1998a). Butz and Bevan showed that LCMV-infected fibroblasts are more efficient in restimulating GP276-286 specific CTLs than the LCMV-infected dendritic cell line jawsII (Butz and Bevan, 1998). In contrast to fibroblasts, dendritic cells constitutively express high levels of immunoproteasome subunits (Macagno et al., 1999). Hence, the observed reduced capacity of jawsII to restimulate GP276-286 specific CTLs might be due to a destruction of the epitope GP276-286 by immunoproteasomes. This idea is supported by the fact that in persistently infected mice GP276-286 becomes immunodominant and GP276-286 specific CTLs are attracted to non-lymphoid tissues where low levels of immunoproteasomes are expressed. It hence appears that the intracellular processing of GP276 is less efficient than the processing of the GP33 epitope derived from the same glycoprotein. It has been reported that the proteasome is involved in the processing of both GP33 and GP276 (Schwarz et al., 2000a).

Chapter 2

Generation of a cell line expressing wildtype ubiquitin and ubiquitin mutant forms in an inducible manner

Michael Basler & Marcus Groettrup

1. Abstract

The proteasome plays a critical role in the generation of the majority of MHC class I-presented peptides. Ubiquitin is required for the degradation of most cellular proteins, but to date it is unclear whether ubiquitin is also required for antigen processing for MHC-I. To address this topic ubiquitin and dominant negative mutant forms of ubiquitin were expressed in a tetracycline inducible manner. Induction of ubiquitin or its mutant forms did neither change total ubiquitylation nor MHC-I surface expression.

2. Introduction

At present, it is unclear to what extent ubiquitylation is required to generate MHC-I-presented peptides from different proteins (see chapter 1; 4.3). Contradictory results have been obtained with a cell line containing a temperature sensitive E1. At the nonpermissive temperature some antigens were presented normally (Cox et al., 1995) but others displayed an impaired presentation (Michalek et al., 1993). To study the role of ubiqutin in antigen presentation this approach is not really suitable because these E1 cells have remaining E1-activity at nonpermissive temperature and antigen presentation may change under heat shock condition. To establish a more appropriate system to study the role of ubiquitylation in antigen processing an inducible dominant negative ubiquitin construct was created. To target a protein for degradation at least four ubiquitin moieties connected via K48 have to be attached to a lysine of a target protein. A lysine 48 to an arginine mutation (K48R) disturbs the formation of ubiquitin chains und therefore degradation of a target protein. UbiquitinK48R (UbK48R) is fully competent as a conjugative donor but when added to a target protein or an ubiquitin UbK48R fails to regenerate a free K48 for chain elongation, and thus can act as a terminator of chain growth. This mechanism suggests that UbK48R should be a dominant negative inhibitor of chain formation and degradation. A problem arising with the K48R mutation is that the chain stopping UbK48R can be removed by a deubiquitin enzyme and be replaced by wildtype ubiquitin. Finley et al. showed that overexpression of the double mutant UbK48R,G76A led to a bias toward short chain lengths (Finley et al., 1994). Although UbK48R,G76A is a poor substrate for the ubiquitin-activating enzyme this construct was more effective in stabilizing a short lived protein than the single K48R mutation. It has been shown that the Gly to Ala mutation at position 76, which forms the C-terminus of ubiquitin, inhibits deubiquitylation, and therefore degradation (Hodgins et al., 1992).

3. Results

To study the role of ubiquitylation in antigen processing it was decided to overexpress the following three different proteins in an inducible manner (Fig. 1):

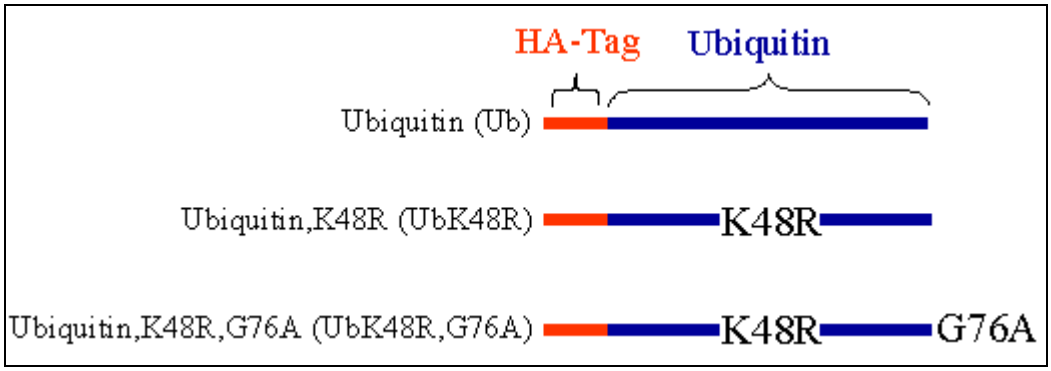

Figure 1: Scheme of wildtype ubiquitin and ubiquitin mutants. HA-Tag is shown in red; Ubiquitin in blue.

A N-terminal hemagglutinin (HA) epitope tag, which is well-characterized and highly immunoreactive, was placed at the N-terminus of ubiquitin or its mutants to discriminate them from endogenous wildtype ubiquitin.

Generation of ubiquitin, ubiquitinK48R, and ubiquitinK48R,G76A constructs by PCR

With the help of ubiquitin specific primers containing a KpnI or an EcoRI restriction site, mouse cDNA was used as a template to amplify mouse ubiquitin by PCR. The amplified fragment (wildtype ubiquitin) was purified and used as template for the K48R and K48R,G76A mutants. The K48R and K48R,G76A mutants were generated as displayed in figure 2.

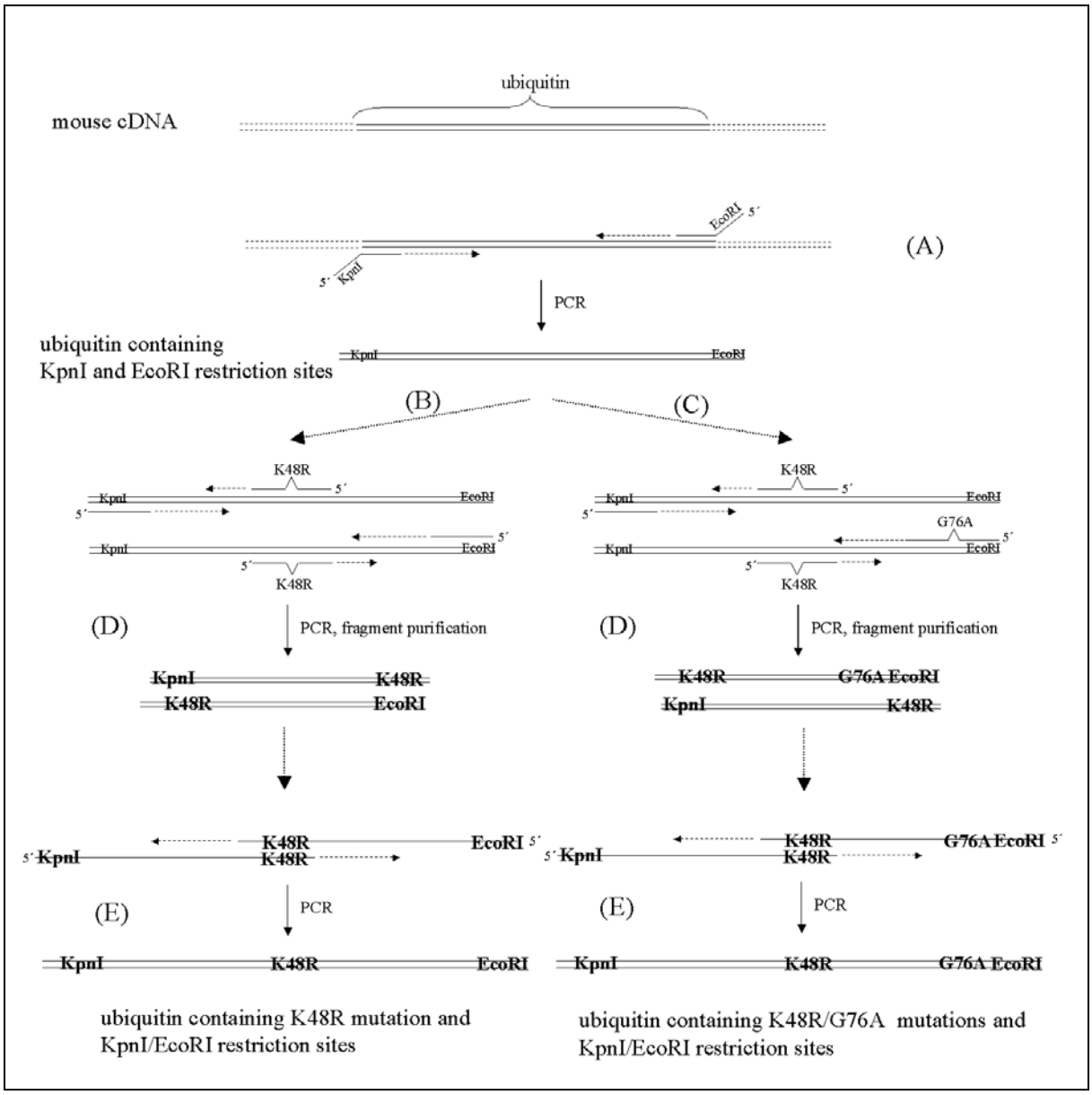

Figure 2: Scheme of PCR strategies. (**A**) Mouse cDNA was amplified with primers containing EcoRI and KpnI restriction sites. The resulting fragment was used to create two fragments containing the K48R mutation (**D**). Pathway (**B**) generates the UbK48R fragment, pathway (**C**) the fragment UbK48R,G76A. The two fragments created in (**D**) were annealed and completed by PCR (**E**). Dotted arrows indicate that strands are completed by PCR. Short lines (———) characterize primers and mutations are designated with ^.

Insertion of constructs in pTet-splice

The three generated fragments were cleaved with KpnI and EcoRI, purified and inserted into the multiple cloning site of pcDNA3.1 (containing HA-Tag); C-terminal of the HA-Tag. The vector was amplified in E.Coli XL-1 blue, isolated, purified, and cleaved with the restriction enzymes HindIII and XbaI. pTet-splice was opened with the help of the restriction enzymes HindIII and SpeI. Due to compatible overhanging ends of XbaI and SpeI restriction sites the

HindIII and XbaI cleaved fragments were cloned into the multiple cloning site of pTet-splice (Fig. 3). All sequences were verified via dedesoxy sequencing (Microsynth, Balgach Switzerland).

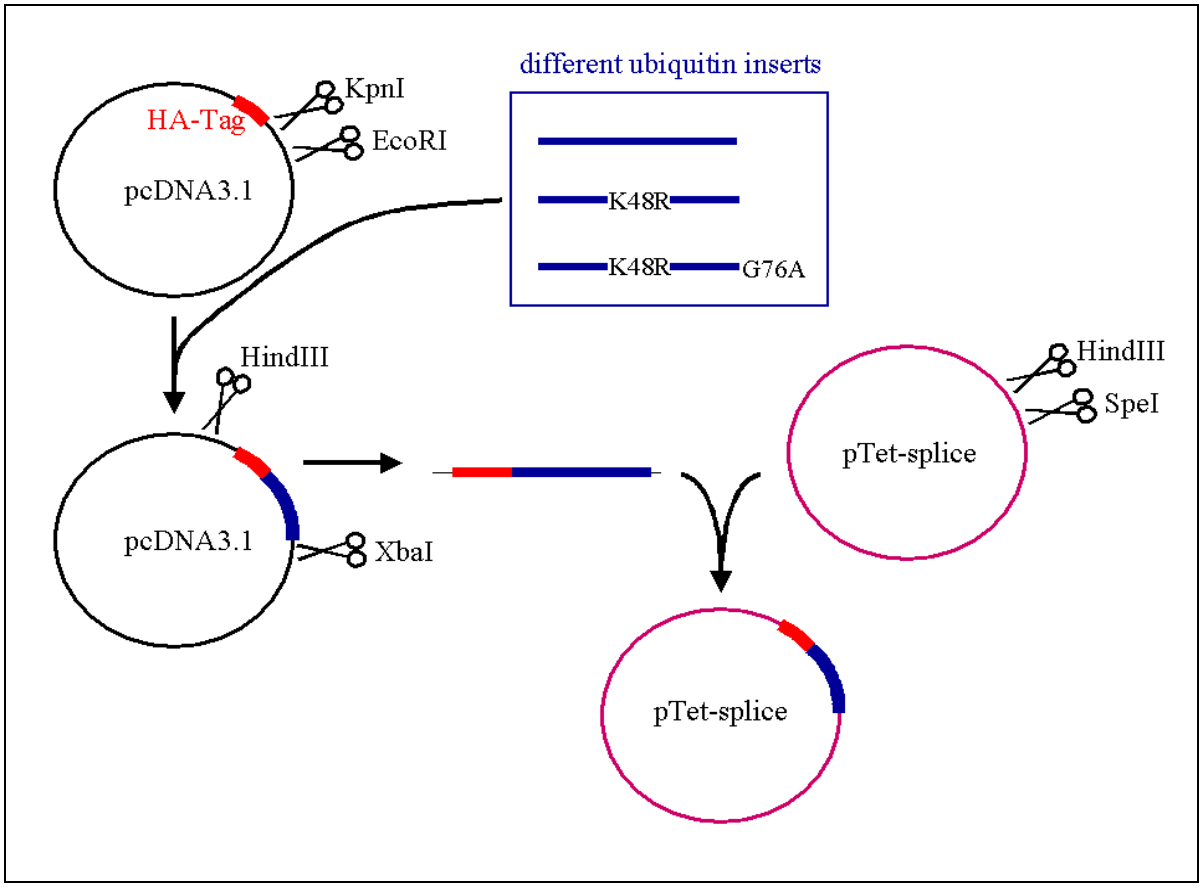

Figure 3: Scheme of cloning strategy. Different ubiquitin constructs were inserted in KpnI and EcoRI cleaved pcDNA3.1 C-terminal of an HA-Tag. The ubiquitin fragment containing an HA-Tag was excised via HindIII and XbaI and inserted into pTet-splice (opened with HindIII and SpeI).

Generation of Ub, UbK48R, and UbK48R,G76A inducible cell lines

To express the different ubiquitins in an inducible manner, the well-characterized tet-off system was chosen (Gossen and Bujard, 1992; Khan et al., 2001; Raasi et al., 2001; Shockett et al., 1995). Autoregulatory expression of tetracycline-controlled transactivator (tTA) is accomplished in a vector called pTet-tTAk by placing the tTAk gene (Fig. 4; green) under the control of tetP (tet promoter; Fig. 4; red) upstream of the minimal hcmv promoter region (Fig. 4; blue) containing a TATA box and transcription start site. The gene of interest is controlled by tetP as well. The tTA protein is consisting of two domains, one for DNA binding and one for transactivation. In the presence of tetracycline (Fig.4; A), the basal activity of the minimal hCMV promoter results in expression of very low levels of the tTA

protein, and any tTA protein is blocked from binding to the tet repressor binding site. Both tTAk and gene of interest are therefore maintained at low levels. When tetracycline is removed (Fig. 4; B), the small amounts of tTA present bind to the tet repressor binding site and thus stimulate expression of the tTAk gene. Higher levels of the tTA protein now stimulate higher levels of tTA protein and, thus, gene of interest expression.

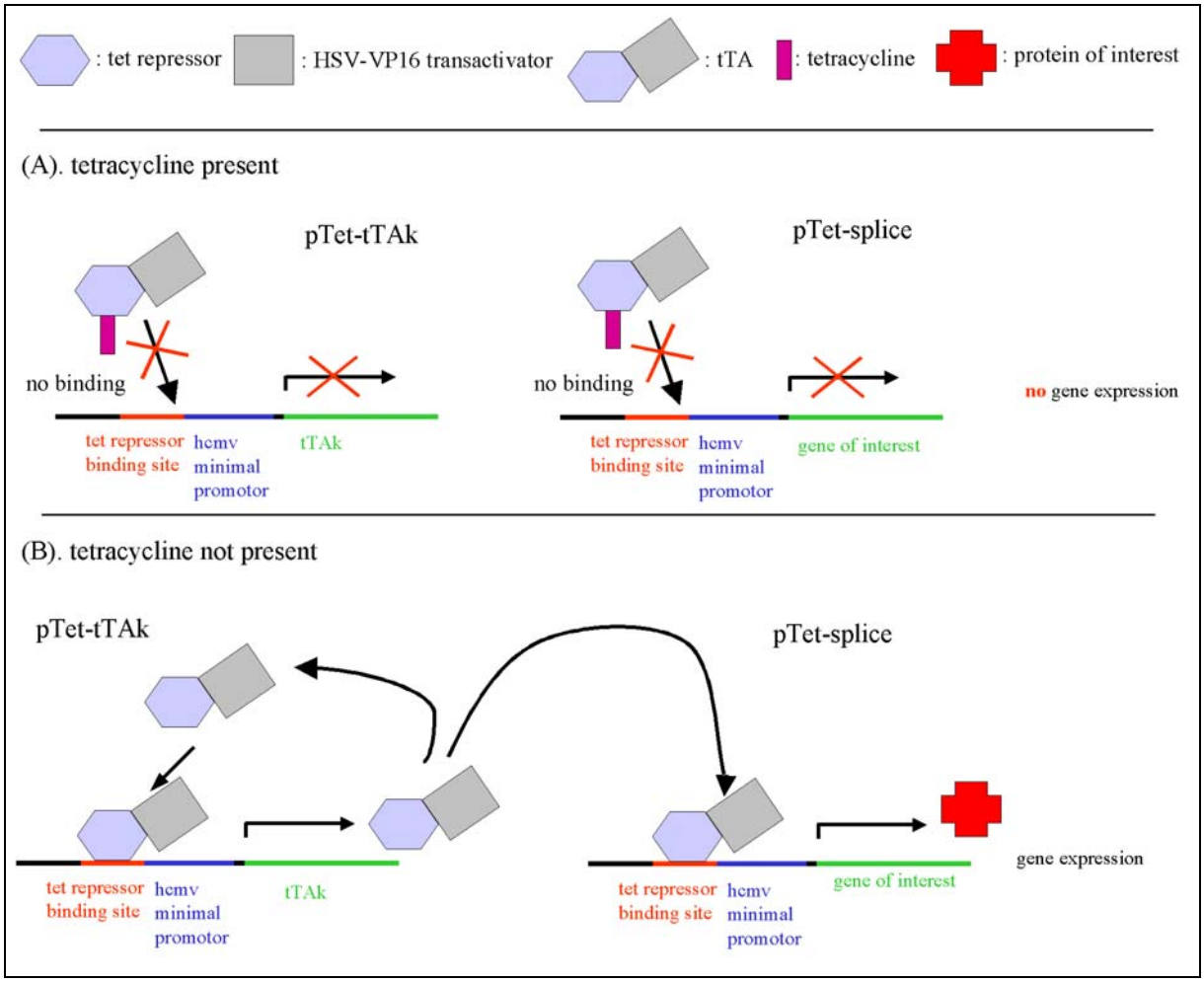

Figure 4: Scheme of a tetracycline regulated gene expression system. For explanations see text.

Initially, B8 cells were stably transfected with the expression construct pTet-tTAk, which encodes a tet-responsive transcriptional inducer (Shockett et al., 1995). The transfectants were tested by transient transfection of tet-regulated β-galactosidase or luciferase reporter constructs, and a clone designated B8tTA.F4 was selected that showed a strong expression of β-galactosidase and luciferase in the absence of tetracycline but very little expression of β-galactosidase and luciferase in the presence of tetracycline (Raasi et al., 2001).

Ptet-splice vector containing the gene of interest (Ub; UbK48R; UbK48R,G76A) and pLXSP puromycin resistance plasmid were stably transfected into B8tTA.F4. Clonal and selection drug-resistant cells were extensively washed to remove tetracycline and protein expression was analysed by western blot using an HA-Tag specific monoclonal antibody. Four positive clones termed W14 (wildtype ubiquitin), K6 (ubiquitin containing K48R mutation), K8 (ubiquitin containing K48R mutation), and G4 (ubiquitin containing K48R and G76A mutation) could be detected (Fig. 5).

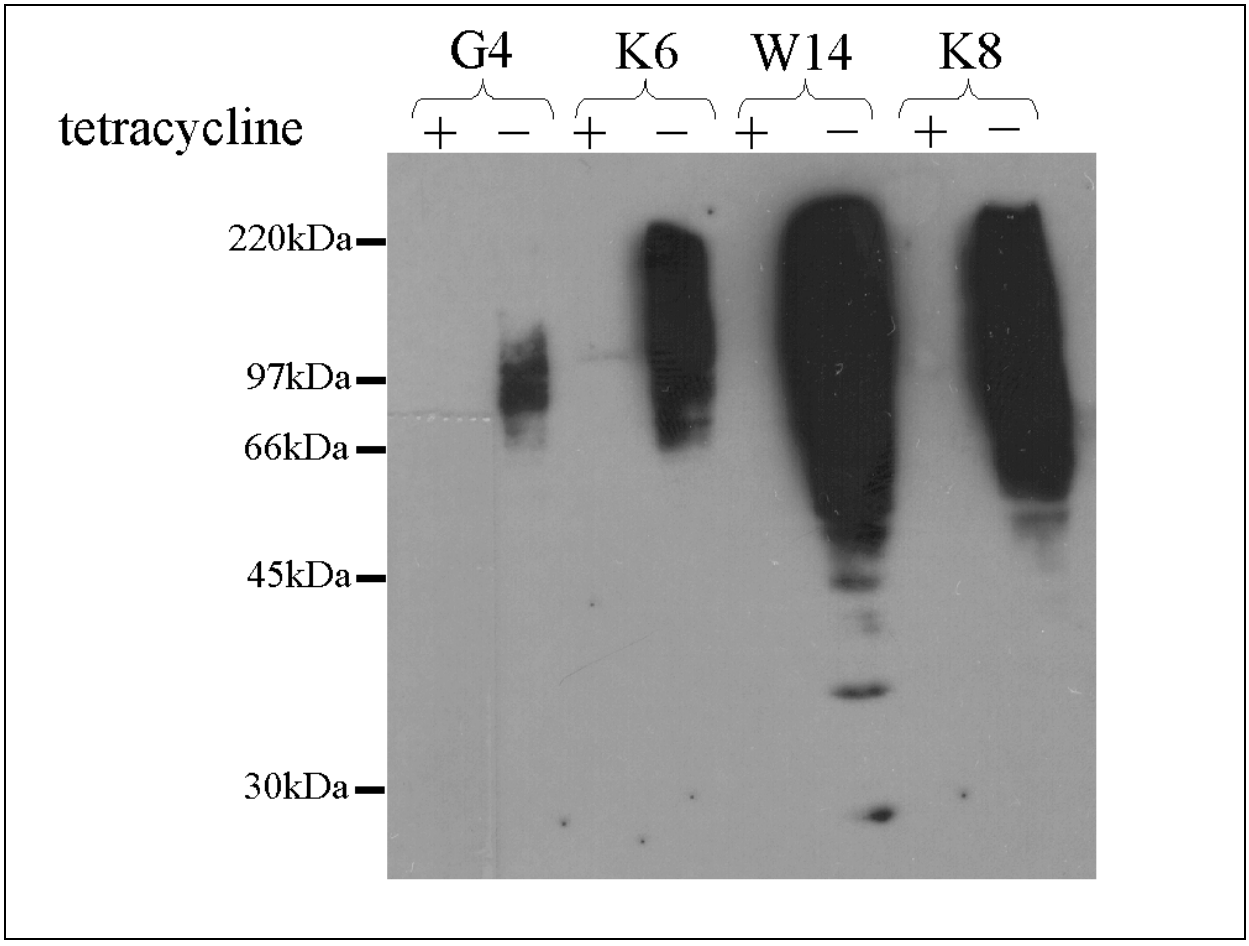

Figure 5: Western blot analysis of HA-ubiquitin and its mutants. G4, K6, W14, and K8 were induced by extensive washing and grown in the presence (+; not induced) or absence (-; induced) of tetracycline. Two days post induction, total lysates were analysed by western blot with a monoclonal HA-specific antibody. The molecular masses are indicated on the left.

HA-ubiquitin expression was completely absent in non-induced cells. W14 showed a stronger induction of HA-ubiquitin than G4, K6, and K8. Ubiquitylation with UbK48R,G76A led to a clear shift of ubiquitin conjugates to lower molecular masses, compared to Wt14, K6, and K8.

Is total ubiquitin changed after induction?

To test whether total ubiquitin (endogenous plus induced ubiquitin) is changed after induction of mutated ubiquitins the different cell lines were induced by extensive washing and analysed by western blot with an ubiquitin specific antibody (Fig. 6). Induction of mutated ubiquitin was confirmed by HA western blot.

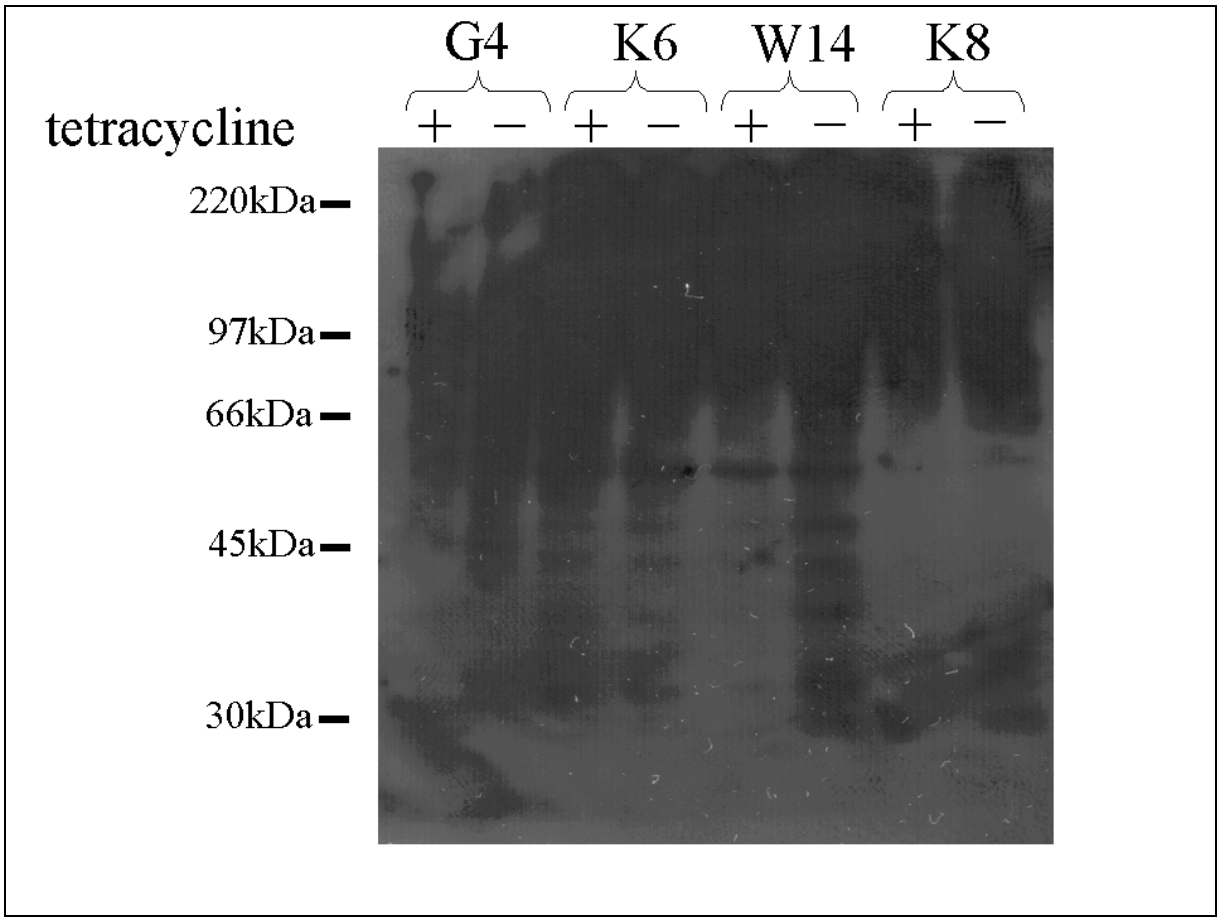

Figure 6: Western blot analysis of ubiquitin expression. G4, K6, W14, and K8 were induced by extensive washing and grown in the presence (+; not induced) or absence (-; induced) of tetracycline. Two days post induction, total lysates were analysed by western blot with an ubiquitin specific polyclonal antibody. The molecular masses are indicated on the left.

No change in total ubiquitylation was observed between induced and non-induced cells. G4 + and - showed a reduced ubiquitylation, especially of higher molecular weight proteins, probably due to loading less protein.

Does induction of mutant ubiquitin forms change MHC-I expression on the cell surface?

If ubiquitin is important for MHC-I antigen presentation, the ubiquitin mutants should affect total MHC-I surface expression. W14, K8, and G4 were induced by extensive washing and two days later the cells were analysed by flow cytometrie with the help of D^d, K^d and L^d-specific antibodies (Fig. 7). B8 cells were used as a negative control.

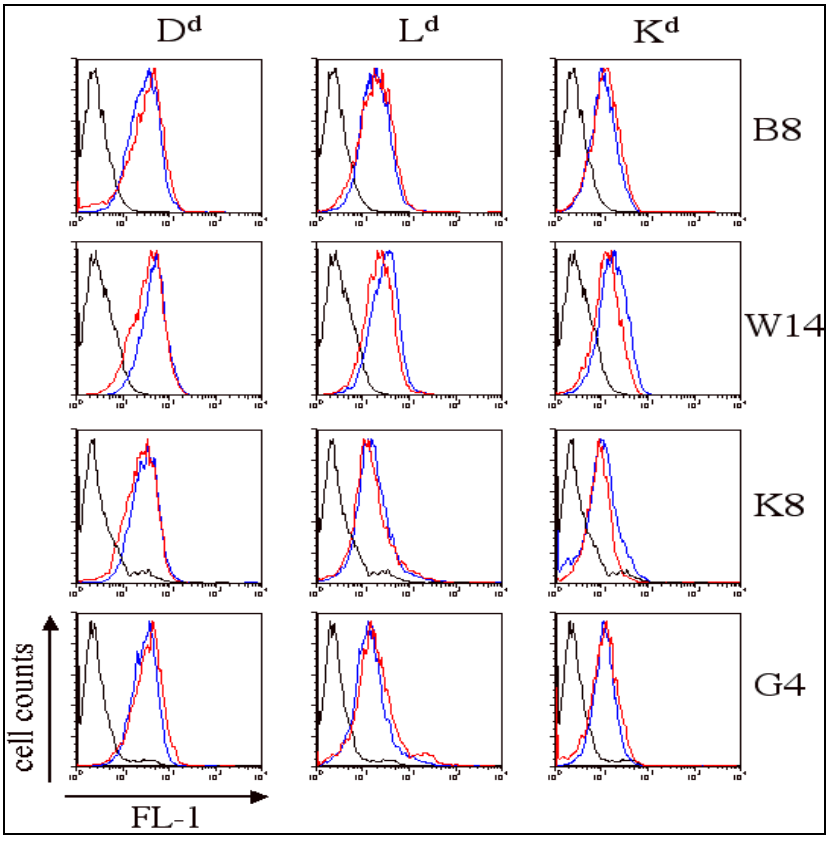

Figure 7: Flow-cytometric analysis of MHC class I surface expression of B8, W14, K8, and G4. Cells were induced by extensive washing and grown in the presence (blue) or absence (red) of tetracycline. Two days post induction, cells were stained with an H-2D^d, H-2L^d, or H-2K^d class I molecules specific antibody (indicated on top) followed by FITC-conjugated (FL-1) sheep anti-mouse Ig secondary antibody. The black curves are stainings with the secondary Ab alone.

Inducing the cell lines did not lead to a change in D^d, L^d, and K^d MHC-I surface expression of B8, W14, K8 or G4 cells compared to non-induced cells.

4. Discussion

At present, the necessity of ubiquitin for antigen presentation is not clear. Analysis with a temperature sensitive E1 enzyme led to contradictory results (Cox et al., 1995; Michalek et al., 1993). To shed light into the dark a more convenient new system was created. Wildtype ubiquitin and the mutant ubiquitin forms UbK48R and UbK48R,G76A were overexpressed in fibroblasts in a tetracycline inducible manner. Ubiquitin containing a K48R mutation leads to a stop in ubiquitin branch formation. At least four ubiquitin moieties are required to target proteins for degradation. Hence, cells overexpressing ubiquitin containing a K48R mutation should have an impaired degradation of proteins, which should lead to cell death after prolonged induction. UbK48R blocking branch growth can be removed by deubiquitylating enzymes and be replaced by wildtype ubiquitin. It has been shown that the Gly to Ala mutation at position 76, which forms the C-terminus of ubiquitin, inhibits deubiquitylation (Hodgins et al., 1992). Finley et al. showed that overexpression of the double mutant UbK48R,G76A stabilized a short lived protein more effectively than the single K48R mutation, although UbK48R,G76A is a poor substrate for the ubiquitin-activating enzyme (Finley et al., 1994). This inspired us to overexpress UbK48R as well as the double mutant UbK48R,G76A in a tetracycline inducible manner.

Western blot analysis of induced cells showed that the proteins UbWt, UbK48R, UbK48R,G76A (clones were termed W14, K6, K8, and G4) can be induced and conjugated to target proteins (Fig. 5). UbK48R,G76A overexpression led to ubiquitin conjugation shifted to lower molecular masses, like it was reported in Finley et al. (Finley et al., 1994). Induction of mutant ubiquitin did not cause cell death after prolonged induction. Probably, these transfectants do not overexpress mutated ubiquitin to an extent were they can disturb the cells ubiquitylation process. It is important to notice, that ubiquitin is highly abundant in the cytosol and nucleus of all eucaryotic cells. Hence, it is not surprising, that endogenous wildtype ubiquitin is competing successfully with its mutated form. To disturb the cells ubiquitylation system the mutated ubiquitin should reach an expression level at which endogenous ubiquitin is negligible. G4, K6, and K8 do not fulfil this. To find clones able to compete with endogenous ubiquitin further screening for new clones is needed, in case endogenous ubiquitin can ever be outcompeted. Cell lysates derived from induced W14, K6, K8, and G4 did not display an altered ubiquitylation pattern compared to non-induced cells (Fig. 6). Again, this indicates, that neither the induced W14 can increase total ubiquitylation nor do the overexpressed mutants reduce total ubiquitylation or shift ubiquitin conjugates to lower molecular weights.

The bulk of MHC-I ligands are dependent on proteasomal degradation. Treatment of cells with inhibitors for proteasome leads to a reduction in MHC-I on the cell surface (Harding et al., 1995; Rock et al., 1994). Therefore, it seems reasonable that MHC-I surface expression is dependent on ubiquitylation. W14, K6, K8, and G4 did not display an altered MHC-I surface expression after induction, neither for H-2D^d, H-2L^d, nor H-2K^d class I molecules (Fig. 7). Induction of wildtype ubiquitin did not increase MHC-I suggesting that the cells ubiquitin content is not limiting for presentation of MHC-I surface expression or that ubiquitylation is not needed at all. In case MHC-I antigen processing is ubiquitin dependent, the mutated forms of ubiquitin should decrease MHC-I surface levels. But neither K48R nor K48R,G76A mutations displayed reduced MHC-I expressions (Fig. 7). This might indicate, that ubiquitin is not essential for MHC-I antigen processing or that, more likely, the induced mutated ubiquitin cannot outcompete endogenous ubiquitin (discussed above).

It has been reported (Tsirigotis et al., 2001) that cells overexpressing UbK48R are highly sensitive to canavanine (an amino acid analog that substitutes for arginine during translation) or the heavy metal cadmium. Both substances induce protein misfolding; cadmium via a poorly defined mechanism. High molecular weight proteins were accumulating during canavanine and cadmium treatment leading to increased cell death (Tsirigotis et al., 2001). Treatment of W14, K6, K8, and G4 with canavanine and cadmium might be an alternative to explore the role of ubiquitin in antigen presentation. Ubiquitin might become limiting under these conditions. But inducing protein misfolding can affect a lot of proteins required for MHC-I antigen presentation, like it is the case with the temperature sensitive E1.

To obtain more conclusive data further investigations and screening for better clones are required.

5. Material and methods

Primers and DNA constructs

For amplifying ubiquitin mouse cDNA (a kind gift of R. de Giuli) the following primer set was used: 5′-TACGGGGTACCAATGCAGATCTTCGTGAAGACCC-3′; 5′-TCTGCAGAA TTCTCAGCCACCTCTCAGGCGAAGGAC-3′. To create the UbK48R mutant two primer sets were used: 1. 5′-TACGGGGTACCAATGCAGATCTTCGTGAAGACCC-3′; 5′GCCA TCTTCCAGCTGCCTGCCGGCAAAGATCAG-3′ and 2. 5′-TCTGCAGAATTCTCAGCC ACCTCTCAGGCGAAGGAC-3′; 5′-CTGATCTTTGCCGGCAGGCAGCTGGAAGATG

GC -3′. For the generation of the UbK48R mutant two the following primer sets were used: 1. 5′-TACGGGGTACCAATGCAGATCTTCGTGAAGACCC-3′; 5′GCCATCTTCCA GCTGCCTGCCGGCAAAGATCAG-3′ and 2. 5′-TCTGCAGAATTCTCAGGCACCTCTC AGGCGAAGGACCAG-3′; 5′-CTGATCTTTGCCGGCAGGCAGCTGGAAGATGGC-3′. All primers were purchased from Mycrosynth (Balgach, Switzerland). pcDNA3.1 (invitrogen) containing HA-Tag was a kind gift of G. Schmidtke. pTet-splice was purchased from invitrogen.

Restriction digests

Restriction digests with a single restriction enzyme were performed in a volume of 10µl containing 1µl restriction enzyme, 1µl 10x restriction enzyme buffer, and variable volumes of DNA. The difference to 10µl was equalled with ddH_2O. Digests were incubated for 1h at 37°C and analysed by agarose gel electrophoresis. Restriction digests with two restriction enzymes were performed similarly in a volume of 20µl. All restriction enzymes (KpnI, EcoRI, XbaI, and SpeI) and buffers were purchased from Promega (Germany). All fragments were analysed by agarose gel electrophoresis and purified with the NucleoSpin® extract kit (Machinery Nagel, Germany).

Polymerase chain reaction (PCR)

All PCRs were performed in a volume of 30µl containing 3µl 10x PCR buffer, 3µl dNTPs (2mM), 0.5µl sense primer (50µM), 0.5µl antisense primer (50µM), 0.5-2µl template and 0.2µl PFU polymerase (Promega, Germany). The difference to 30µl was equalled with ddH_2O. The following PCR program was used: 1. step: 5min 95°C, 2. step: 1min 95°C, 3. step 0.5min 60°C 4. step: 1min 72°C 5. step: 5min 72°C. Step 2 to 4 were repeated 30 times. To combine the two K48R fragments a PCR without primers was performed (assembly PCR; the fragments anneal and complete). Step 2 to 4 were repeated 7 times. To amplify the generated fragment a PCR with the outer primers was performed.

All PCR products were analysed by agarose gel electrophoresis and purified with the QIAquick gel extraction kit.

Transformation and vector amplification

Electrocompetent E. Coli XL-1 blue (Stratagene, US) were thawed on ice and transferred to an ice cold electrocuvette (2mm; Eurogentec, Belgium). 1µl of DNA (1ng to 1pg) was added and incubated for 1min on ice. Electrotransformation was performed using the following setup: 25µF, 1.8kV and 200ohm. After pulsing 500µl SOC (2% bacto-tryptone (w/v), 0.5% bacto-yeast extract (w/v), 0.05%NaC (w/v), 2.5mM KCl, 10mM $MgCl_2$, 20mM glucose) was added, bacteria were shaked for 1h at 37°C and plated on LB agar plates (LB-medium plus 1.5% bacto-agar) containing 50µg/ml ampicilin. Bacteria were grown over night at 37°C and single colonies were transferred to 5ml LB-medium containing 50µg/ml ampicilin. For the production of small amounts of DNA the culture was shaked over night at 37°C and the DNA was isolated using the NucleoSpin® plasmid kit (Machinery Nagel, Germany). To produce large amounts of DNA 2ml of the 5ml bacteria culture were transferred after 8h to 500ml LB-medium containing 50µg/ml ampicilin. The DNA was isolated using the Gen Elute™ HP Plasmid Maxiprep kit (Sigma, Germany).

Cell lines and transfection

B8tTA.F4 (Raasi et al., 2001) are B8 (Groettrup et al., 1995) cells stably transfected with the plasmid pTet-tTAk and hygromycin resistant plasmid pLXSH. They are cultured in IMDM10%+100 units/ml penicillin/streptomycin + 400 µg/ml hygromycin (Calbiochem) + 400ng/ml tetracycline (Sigma).

B8tTA.F4 cells were stably transfected with pTet-splice containing the gene for Ub, UbK48R, or UbK48R,G76A and puromycin resistance plasmid (pLXSP) according to the manufactures protocol (FuGENE 6, Roche) in 6-well plate. The cells were termed Ub, UbK48R, or UbK48R,G76A according to the transfected plasmid. Two days later cells were transferred to 96-well round bottom plates and selected with puromycin (0.25µg/ml). Cells were plated at different densities reaching from 1 to 10000 cells per plate. After 3 weeks clonal and selection drug resistant cells were transferred to 24-well plates and propagated. Cells were washed four times with PBS (to induce ubiquitin) in a 6-well plate and analysed two days later for protein expression by western blot.

Western blotting

Ub, UbK48R, or UbK48R,G76A cells (confluent 6-well) were lysed in 100µl lysis buffer (20mM Tris pH7.8, 50mM NaCl, 0.1% SDS) on ice for 15 minutes and sonificated. After centrifugation, 10µl aliquots of the crude lysates were boiled for 5min at 95 °C in 10 µl 2x reducing Laemmli sample buffer and separated by SDS-PAGE (10% gel). Proteins were blotted onto nitrocellulose (0.45µm, 12Vh, 200mA) (Schleicher & Schuell BioSciences, Dassel, Germany). Membranes were blocked (PBS containing 0.4% Tween (v/v) and 5% dry milk (w/v)) for 1h at room temperatures and incubated over night at 4 °C with a monoclonal antibody recognizing HA (1:10000 in PBS containing 0.4% Tween (v/v) and 5% dry milk (w/v) (Sigma). After 3 washes with PBS containing 0.4% Tween (v/v) the membrane was incubated with the HRP-conjugated goat anti-mouse antibody (DakoCytomation, Glostrup, Denmark, diluted 1:1000 in containing 0.4% Tween (v/v) and 5% dry milk (w/v)). Membranes were washed 3 times and proteins were visualized on x-ray films by enhanced chemiluminescence.

Flow cytometry

A number of $5x10^5$ induced or non-induced cells in 100 µl of PBS + 2% FCS were incubated in a round-bottom 96-well plate on ice for 20 min with 1 µg of mAb specific for H-$2L^d$, H-$2K^d$, or H-$2D^d$ molecules (28-14-81, 15-5-5S, or 19/191), washed twice, and subsequently stained by a FITC-conjugated sheep anti-mouse Ig (Silenus, Victoria, Australia) for another 20 min on ice. Samples were washed twice, acquired with the use of FACScan flow cytometer (BD Biosciences), and analyzed by the FlowJo software (Tree Star).

6. References

Cox, J.H., Galardy, P., Bennink, J.R. and Yewdell, J.W. (1995) Presentation of endogenous and exogenous antigens is not affected by inactivation of E1 ubiquitin-activating enzyme in temperature-sensitive cell lines. *J. Immunol.*, **154**, 511-519.

Finley, D., Sadis, S., Monia, B.P., Boucher, P., Ecker, D.J., Crooke, S.T. and Chau, V. (1994) Inhibition of proteolysis and cell cycle progression in a multiubiquitination-deficient yeast mutant. *Mol. Cell. Biol.*, **14**, 5501-5509.

Gossen, M. and Bujard, H. (1992) Tight control of gene expression in mammalian cells by tetracyclin-response promotors. *Proc. Natl. Acad. Sci. USA*, **89**, 5547-5551.

Groettrup, M., Ruppert, T., Kuehn, L., Seeger, M., Standera, S., Koszinowski, U. and Kloetzel, P.M. (1995) The interferon-γ-inducible 11S regulator (PA28) and the LMP2/LMP7 subunits govern the peptide production by the 20S proteasome in vitro. *J. Biol. Chem.*, **270**, 23808-23815.

Harding, C.V., France, J., Song, R., Farah, J.M., Chatterjee, S., Iqbal, M. and Siman, R. (1995) Novel Dipeptide aldehydes are proteasome inhibitors and block the MHC-I antigen-processing pathway. *J. Immunol.*, **155**, 1767-1775.

Hodgins, R.R.W., Ellison, K.S. and Ellison, M.J. (1992) Expression of a ubiquitin derivate that conjugates to protein irreversible produces phenotypes consistent with a ubiquitin deficiency. *J. Biol. Chem.*, **267**, 8807-8812.

Khan, S., de Giuli, R., Schmidtke, G., Bruns, M., Buchmeier, M., van den Broek, M. and Groettrup, M. (2001) Cutting Edge: Neosynthesis is required for the presentation of a T cell epitope from a long lived viral protein. *J. Immunol.*, **167**, 4801-4804.

Michalek, M.T., Grant, E.P., Gramm, C., Goldberg, A.L. and Rock, K.L. (1993) A role for the ubiquitin-dependent proteolytic pathway in MHC class I-restricted antigen presentation. *Nature*, **363**, 552-554.

Raasi, S., Schmidtke, G. and Groettrup, M. (2001) The ubiquitin-like protein FAT10 forms covalent conjugates and induces apoptosis. *J. Biol. Chem.*, **276**, 35334-35343.

Rock, K.L., Gramm, C., Rothstein, L., Clark, K., Stein, R., Dick, L., Hwang, D. and Goldberg, A.L. (1994) Inhibitors of the proteasome block the degradation of most cell proteins and the generation of peptides presented on MHC class I molecules. *Cell*, **78**, 761-771.

Shockett, P., Difilippantonio, M., Hellman, N. and Schatz, D.G. (1995) A modified tetracycline-regulated system provides autoregulatory, inducible gene expression in cultured cells and transgenic mice. *Proc. Natl. Acad. Sci. USA*, **92**, 6522-6526.

Tsirigotis, M., Zhang, M., Chiu, R.K., Wouters, B.G. and Gray, D.A. (2001) Sensitivity of mammalian cells expressing mutant ubiquitin to protein- damaging agents. *J Biol Chem*, **276**, 46073-46078.

Chapter 3

The role of Hsp90 in processing of LCMV-WE derived epitopes

Michael Basler, Jacqueline Möbius, & Marcus Groettrup

1. Abstract

The control and maintenance of the three-dimensional structure of proteins is pivotal for cell survival. Molecular chaperones recognize hydrophobic regions exposed on unfolded proteins and stabilize nonnative conformations. The Hsp90 chaperone family is evolutionarily conserved and highly abundant in cells. In this chapter the role of Hsp90 in antigen processing of LCMV-derived epitopes is investigated. Treatment of the macrophage cell line J774 with an Hsp90 specific inhibitor (geldanamycin) led to a dose-dependent reduction in the presentation of the LCMV-derived epitope NP118. Other LCMV-derived epitopes were not affected. Analysis whether an epitope is differently affected by geldanamycin when expressed at the N-terminus compared to the C-terminus within a stable protein revealed that both are reduced independently of their site of expression.

2. Introduction

Different aspects of the role of Hsp90 in antigen processing have been addressed (see chapter 1; 4.5). It has been reported that Hsp90 links misfolded proteins to the ubiquitylation pathway for selective elimination (Connell et al., 2001) and that Hsp90 binds to tumor-associated MHC-I ligands or their precursor (Ishii et al., 1999). The experiments of Yamano et al. (Yamano et al., 2002), which showed that geldanamycin, an inhibitor of Hsp90, suppressed antigen presentation of an ovalbumin (ova) derived epitope in LPS blasts derived from PA28αβ-deficient mice, but not in wildtype cells, inspired us to investigate the role of Hsp90 in processing of LCMV-WE derived epitopes.

3. Results

NP118-presentation is affected by Hsp90

Due to the fact that the LCMV-WE specific CTL response in BALB/c mice is mostly directed to the NP118 CTL epitope (van der Most et al., 1996), CTLs from these mice can be used to exclusively detect the NP118 epitope. After a short *in vitro* restimulation with cells presenting the corresponding peptide, CTLs start to produce IFN-γ. The activation of these CTLs can be detected by double staining for CD8 and intracellular IFN-γ (intracellular cytokine staining for IFN-γ (ICS)). The portion of activated CTLs corresponds with the amount of antigen

presented, making it an appropriate system to detect antigen presented on MHC-I. The macrophage cell line J774 (H-2^d) was infected with LCMV-WE (moi of 0.5) and treated with different concentrations of geldanamycin (GA), ranging from 0.1 to 10µM. Geldanamycin is a well-characterized specific inhibitor for Hsp90, binding into the ATP binding site of Hsp90 (Stebbins et al., 1997). Primary splenocytes from LCMV-WE infected BALB/c mice (d8 post infection) were used to compare the amount of MHC-I-NP118 complexes on the cell surface of GA and untreated LCMV infected cells using ICS (Fig. 1).

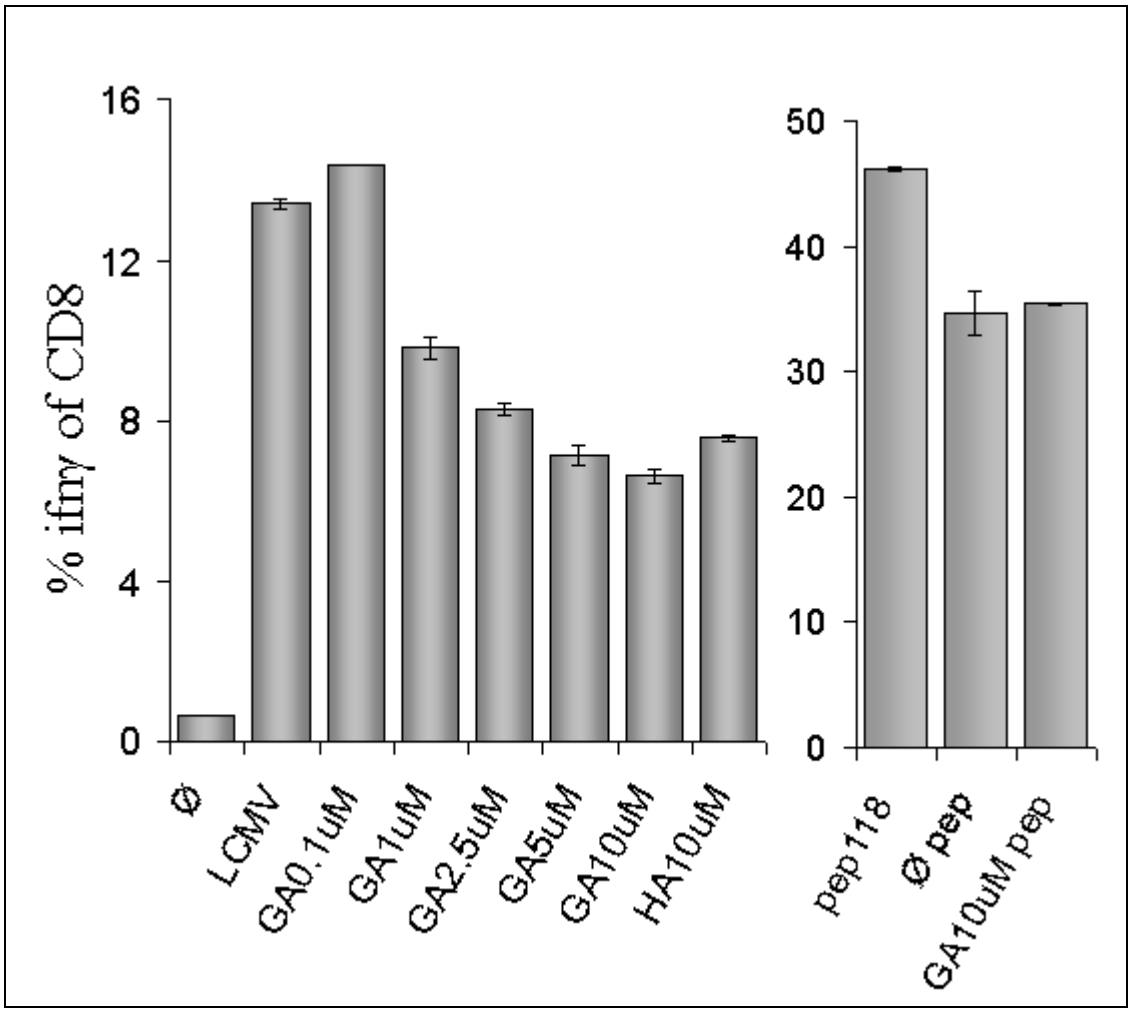

Figure 1: Comparison of the presentation of the LCMV epitope NP118 in GA treated and LCMV-infected J774 cells. J774 cells were infected with LCMV-WE (moi of 0.5, o/n) and treated with different concentrations of GA (0.1µM, 1µM, 2.5µM, 5µM, 10µM) or HA (10µM). The y-axis shows intracellular IFN-γ produced by CD8-positive splenocytes (derived from LCMV-WE infected (200pfu i.v.) BALB/c mice (8d post infection)). LCMV infected but untreated J774 are marked with 'LCMV'. As a negative control uninfected cells (Ø) and peptide loaded cells (pep118) were used. To exclude possible inhibition effects of GA on splenocytes, LCMV-infected untreated J774 (Ø pep) and LCMV-infected 10µM GA treated J774 (GA10µM pep) were pulsed with peptide.

The activation status of splenocytes decreased from 13% (untreated cells) with increasing concentrations of GA to 7%. Treatment (10µM) of LCMV-infected cells with another Hsp90-specific inhibitor, designated herbimycin A (HA), led to a reduction comparable to treatment with 5µM GA. Schnaider et al. reported that GA blocks CD28-mediated activation of human T lymphocytes (Schnaider et al., 1998). To exclude that GA from GA-treated cells inhibits CTLs (used to detect amount of antigen presented), and thus falsifying activation status of CTLs, GA-treated cells were extensively washed and part of the cells were pulsed with peptide NP118. LCMV-infected untreated (pulsed with peptide) and GA treated cells (pulsed with peptide) activated CTLs to the same extend, thus excluding an inhibition effect of GA on CTLs in this assay.

Effect of geldanamycin shortly after LCMV infection

In order to examine the effect of GA on presentation of NP118 shortly after infection, the amount of NP118 presented on LCMV-infected ±GA treated J774 cells was analysed at 2h, 4h and 5h post infection. As a read-out to detect antigen, ICS with splenocytes from LCMV-WE infected BALB/c mice (200pfu; d8) was used (Fig. 2).

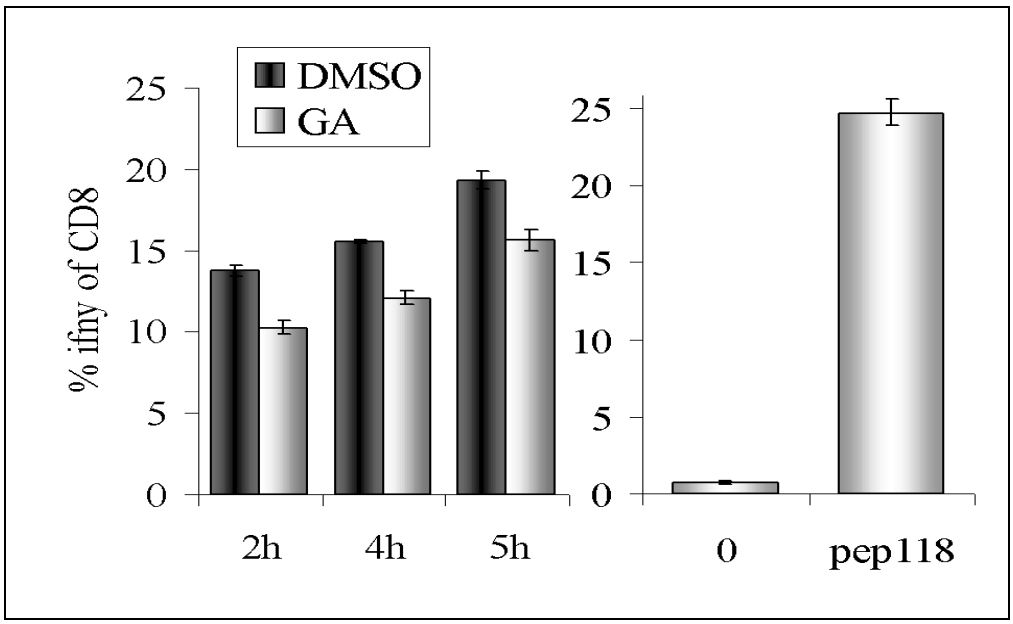

Figure 2: Comparison of the presentation of the LCMV epitope NP118 in GA treated and LCMV-infected J774 cells shortly after infection. J774 cells were pretreated for 1h with 10µM GA. Then cells were infected with LCMV-WE (moi of 10) for 2h, 4h, 5h and treated ± 10µM GA. Antigen was detected by ICS with splenocytes from LCMV-WE infected BALB/c mice (8d post infection; 200pfu). The y-axis shows intracellular IFN-γ produced by CD8-positive splenocytes. As a negative control uninfected cells (Ø) and peptide-loaded cells (pep118) were used.

LCMV infection could be detected already 2h post infection. GA treated cells showed a slight but consistent reduction in NP118 presentation 2h, 4h, and 5h post infection. Hence, the effect of Hsp90 on the presentation of NP118 is exerted shortly after translating the protein.

Generation of cell lines expressing LCMVNP or ubiquitin-LCMVNP

Khan et al. demonstrated that the NP118 epitope exclusively derives from DRiPs (Khan et al., 1994). This might indicate that Hsp90 exerts its effect on NP118 presentation in the DRiP pathway. Hsp90, probably binding to newly synthesized proteins, could function as linkage between defective ribosomal products and the proteasome. To proof this hypothesis, B8 cells were transfected with either LCMV-derived nucleoprotein (NP) or a nucleoprotein containing an N-terminal ubiquitin moiety (UbNP). The N-terminal ubiquitin moiety leads to a rapid degradation of the nucleoprotein in UbNP transfected cells (Rodriguez et al., 1997). Proteasome inhibitors led to an accumulation of the full nucleoprotein, thus, the full protein is correctly made, but immediately degraded after synthesis. Therefore, in contrast to NP transfected cells, GA should not have an effect on the presentation of NP118 in UbNP transfected cells, if the above mentioned hypothesis (concerning Hsp90 participating in the DRiP pathway) is true (Fig. 3).

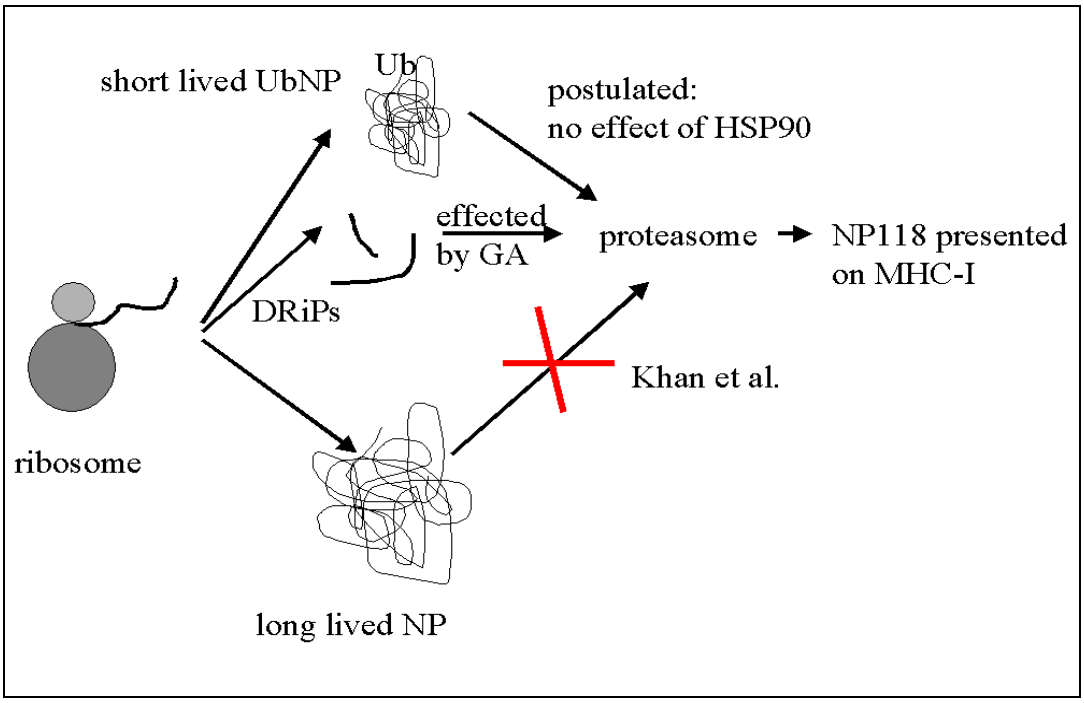

Figure 3: *Postulated model of Hsp90 effecting processing of NP118. For explanations see text.*

B8 cells were stably transfected with NP or UbNP and screened for NP118 presentation by ICS with splenocytes derived from LCMV-WE infected BALB/c mice (d8 post infection). Several positive NP and UbNP clones displayed in Fig. 4 were obtained.

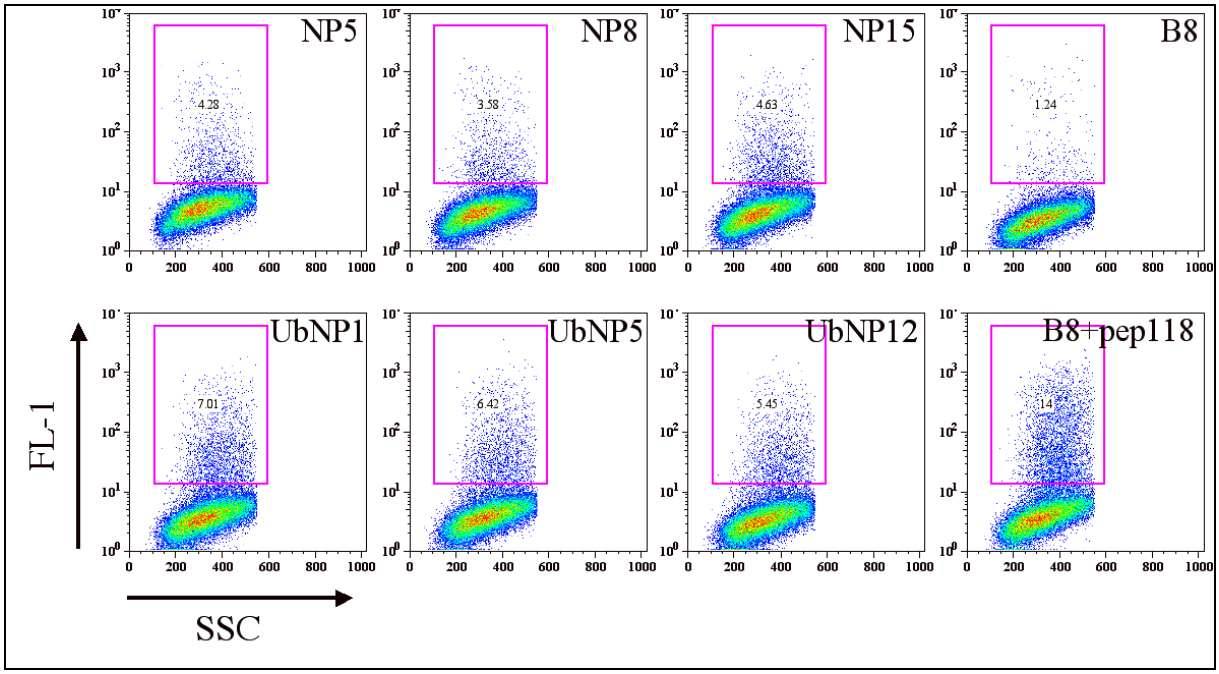

Figure 4: FACS dot blots of NP or UbNP transfected cells. B8 cells were transfected with plasmids containing NP or UbNP and NP118 presentation was analysed by ICS with splenocytes from LCMV-WE infected BALB/c mice (8d post infection; 200pfu). Three different stably transfected clones are shown for NP and UbNP. The y-axis shows intracellular IFN-γ (FL-1) produced by CD8-positive splenocytes (lymphocytes were gated on CD8). As a negative control untransfected cells (B8) and peptide-loaded cells (B8+pep118) were used.

Nucleoprotein containing a N-terminal ubiquitin (UbNP) transfected B8 cells displayed a general higher activation of CTLs resulting from an enhanced NP118 presentation as it was reported by Rodriguez et al. (Rodriguez et al., 1997).

Effect of geldanamycin on NP and UbNP cells

To proof the afore mentioned theory, UbNP1, UbNP12, NP5, and NP15 were treated over night with GA or as a negative control with DMSO and NP118 presentation was analysed by ICS with splenocytes derived from LCMV-WE infected BALB/c mice (Fig. 5).

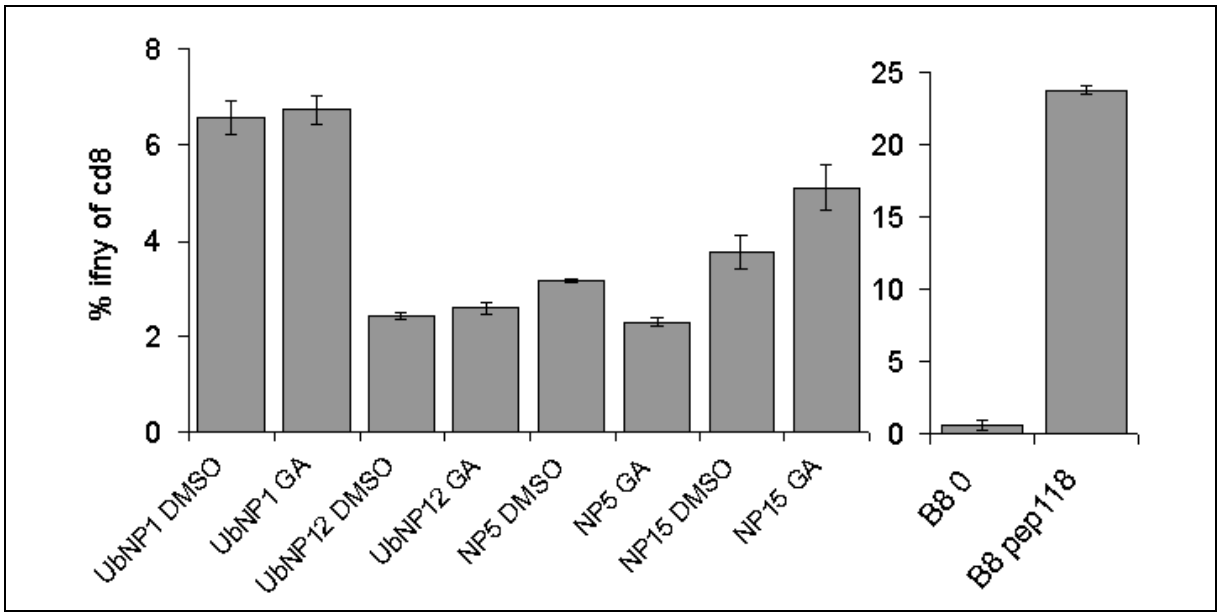

Figure 5: Comparison of the presentation of the LCMV epitope NP118 in GA or DMSO treated UbNP1, UbNP12, NP5, and NP15 cells. UbNP1, UbNP12, NP5, and NP15 cells were treated over night with either 10µM GA or DMSO. NP118 presentation was analysed by ICS. The y-axis shows intracellular IFN-γ produced by CD8-positive splenocytes (derived from LCMV-WE infected (200pfu i.v.) BALB/c mice (8d post infection)). As a negative control uninfected cells (B8 0) and peptide-loaded cells (B8 pep118) were used.

No significant reduction of NP118 presentation was observed in neither NP nor UbNP transfected cells. UbNP1, UbNP12, NP5, and NP15 cells are stably transfected cells, thus continuously producing NP. Probably, the overnight treatment with GA is not sufficient to reduce the existing NP118 (is already at the surface before GA treatment). To circumvent this problem cells were incubated for 10h with brefeldin A, a drug inhibiting transport from the ER to the cell surface (Fujiwara et al., 1988), to reduce MHC-I expression and thus NP118 presentation (Fig. 6A). BFA pre-incubated cells were treated over night with GA or as a negative control with DMSO and NP118 presentation was analysed by ICS with splenocytes derived from LCMV-WE infected BALB/c mice (Fig. 6B).

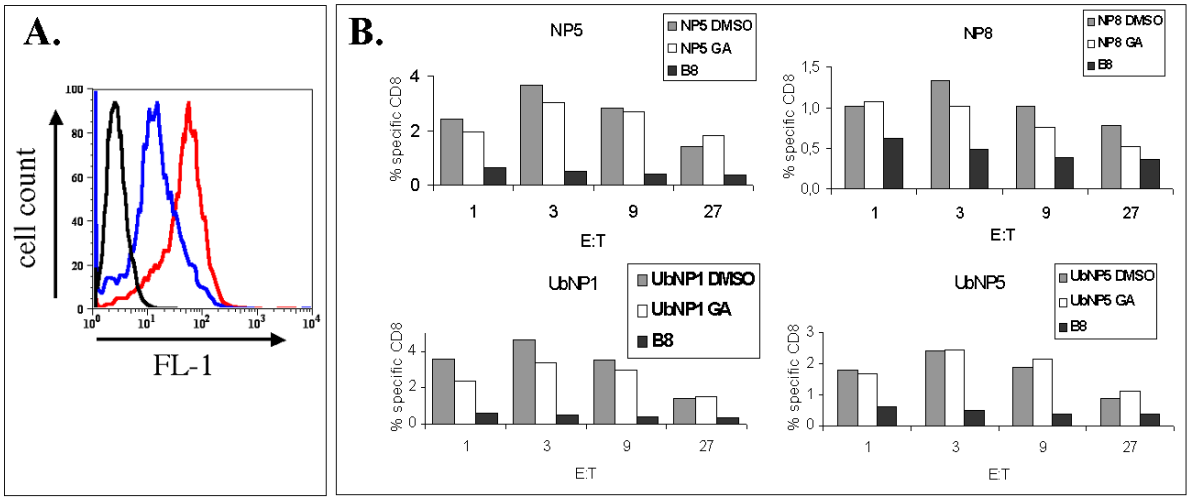

Figure 6: Comparison of the presentation of the LCMV-derived epitope NP118 in GA or DMSO treated BFA preincubated UbNP1, UbNP5, NP5, and NP8 cells. **A.** B8 cells were incubated for 10h with 10µg/ml BFA (blue curve) or left untreated (red curve). Cells were stained with an antibody specific for L^d and analysed by FACS followed by FITC-conjugated (FL-1) sheep anti-mouse Ig secondary antibody. The black curve is a staining with the secondary antibody alone. **B.** BFA pre-treated or untreated UbNP1, UbNP5, NP5, and NP8 cells were incubated o/n with 10µM GA or DMSO. NP118 presentation was analysed by ICS. The x-axis displays different (1;3;9;27) effector (splenocytes) to target (UbNP1, UbNP5, NP5, or NP8) ratios. The y-axis shows intracellular IFN-γ produced by CD8-positive splenocytes (derived from LCMV-WE infected (200pfu i.v.) BALB/c mice (8d post infection)). As a negative control untreated B8 cells (B8) were used.

No significant and consistent difference was observed for GA treated NP and UbNP cells compared to untreated cells. It seems that for unknown reasons GA had no effect on these cells in contrast to LCMV infected J774 cells (Fig. 1), indicating that the effect seen in Fig. 1 is cell type and virus specific.

Effect of geldanamycin on minimal NP118 epitope

To test whether the impact of Hsp90 on NP118 presentation (Fig. 1) is a processing phenomenon J774 cells were treated ±GA and infected with either a vaccinia virus expressing the full length nucleoprotein (VVYN4) or the minimal NP118 epitope (VV118). The infected cells were analysed (5h post infection) by ICS with splenocytes derived from LCMV-WE infected BALB/c mice (Fig. 7).

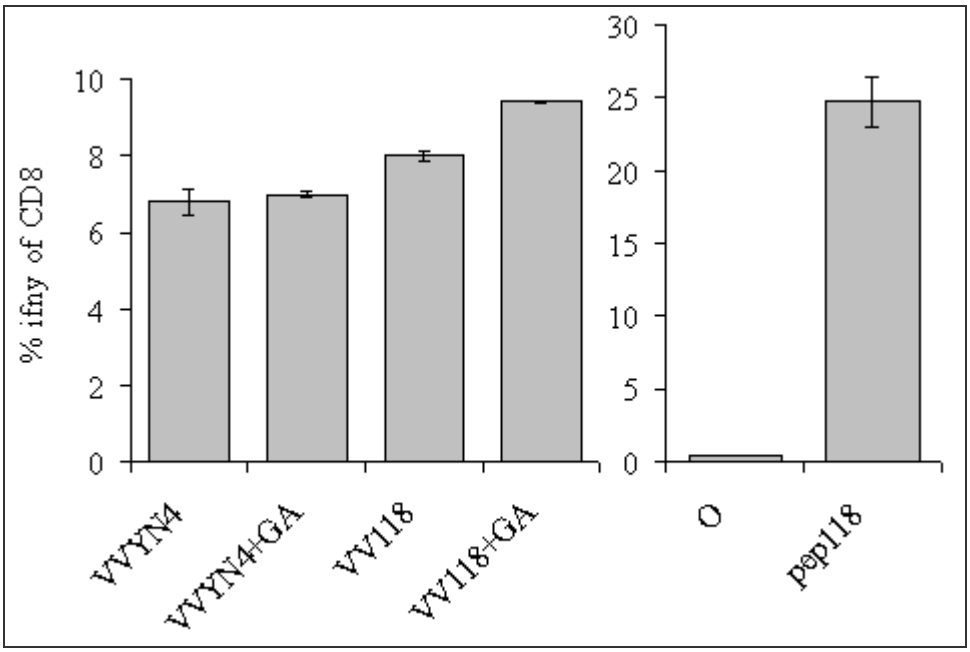

Figure 7: Comparison of the presentation of the LCMV epitope NP118 in ±GA treated VVYN4 or VV118 infected J774 cells. J774 cells were pretreated with GA (10μM) for 2h followed by infection with either VVYN4 or VV118 for 5h. NP118 presentation was analysed by ICS with splenocytes derived from LCMV-WE infected (200pfu i.v.) BALB/c mice (8d post infection). The y-axis shows intracellular IFN-γ produced by CD8-positive splenocytes. As a negative control uninfected cells (0) and peptide loaded cells (pep118) were used.

Neither VVYN4 nor VV118 infected J774 cells displayed a significant change in NP118 presentation after GA treatment, compared to uninfected cells. Therefore, no conclusion can be drawn whether Hsp90 plays a role in the presentation of the minimal epitope. For unknown reasons, GA treatment had no effect on the presentation of NP118 when the full length LCMV-derived nucleoprotein was expressed by a vaccinia virus, indicating, that the phenomena discovered in Fig. 1 seems to be virus specific.

Effect of Hsp90 on other LCMV-derived epitopes

To examine whether other LCMV-derived epitopes are affected by Hsp90, C57BL/6 (H-2^b) derived thioglycollate-elicited peritoneal macrophages were treated ±GA and infected with LCMV. The infected cells were analysed (15h post infection) by ICS with *in vitro* restimulated splenocytes (CTL lines specific for GP33, GP276, and NP396) derived from LCMV-WE infected BALB/c mice (Fig. 7).

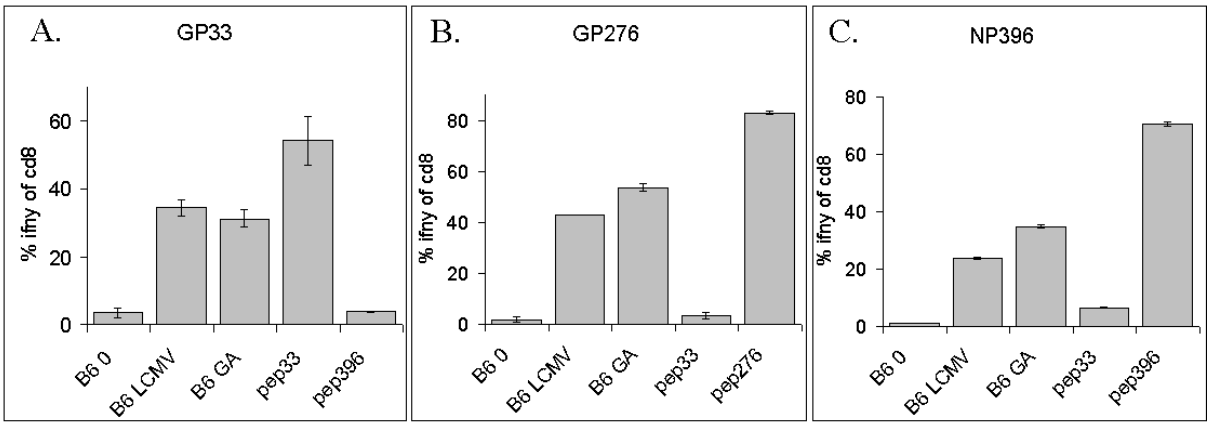

Figure 7: Comparison of the presentation of the LCMV-derived epitopes GP33, GP276, and NP396 in ±GA treated C57BL/6 derived macrophages. Thioglycollate-elicited peritoneal macrophages were infected over night with LCMV-WE (moi of 0.5) and treated with 10µM GA (B6 GA) or DMSO (B6 LCMV). GP33 (**A.**), GP276 (**B.**), and NP396 (**C.**) presentation was analysed by ICS with CTL-lines specific for GP33, GP276 or NP396. The y-axis shows intracellular IFN-γ produced by CD8-positive CTL-lines specific for GP33 (**A.**), GP276 (**B.**), and NP396 (**C.**). As a negative control uninfected macrophages (B6 0) were used. To point out the specificity of the different CTL-lines macrophages were pulsed with peptide (pep33, pep276, and pep396).

No reduction in CTL activation after GA treatment can be observed for the H-2D^b derived epitopes GP33, GP276, and NP396. On the contrary GP276 and NP396 presentation were even slightly increased.

Generation of cell lines expressing NP118 N- or C-terminal of GFP

The fact that two epitopes derived from the same nucleoprotein (NP118 and NP396) behave differently in respect to Hsp90 led to speculations that Hsp90 could affect epitopes expressed at the N-terminus differently than epitopes derived from the C-terminus. It has been shown that the NP118 epitope exclusively derives from DRiP's (Khan et al., 2001). Therefore an epitope derived from the N-terminus should be a better 'DRiP' than an epitope derived from the C-terminus due to premature chain termination derived from translational errors. To test this hypothesis the NP118 epitope was expressed at the N- (termed NGFP) or C- (termed GFPC) terminus of the very stable green fluorescent protein (GFP) (Fig. 8) in a tetracycline inducible manner (see chapter 2).

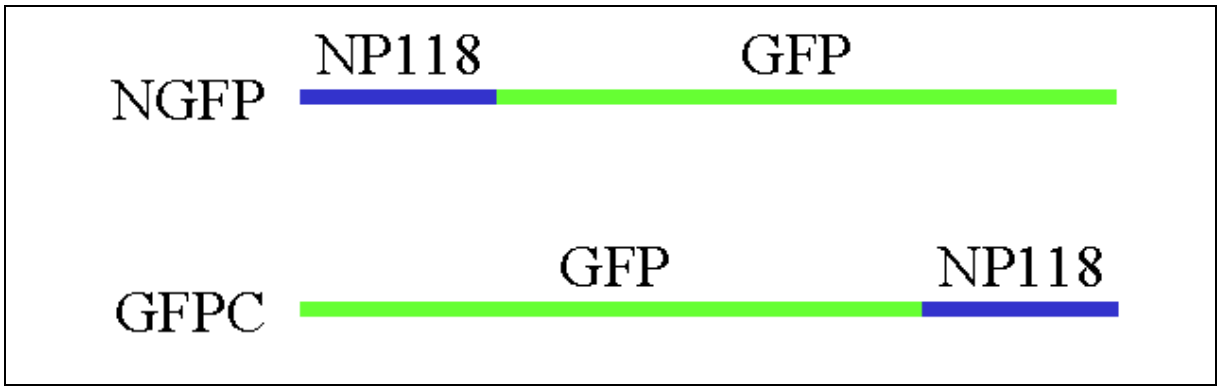

Figure 8: Scheme of two different GFP constructs. GFP expressing a N-terminal NP118-126 epitope was termed NGFP; C-terminal NP118-126 expressing GFP was named GFPC.

Ptet-splice vector containing the gene of interest (NGFP or GFPC) and pLXSP puromycin resistance plasmid were stably transfected into B8tTA.F4. Clonal and selection drug-resistant cells were extensively washed to remove tetracycline and protein expression was analysed due to excitation of eGFP (enhanced GFP) at 488nm and excision at 507nm by flow cytometry measured in FL-1 (Fig. 9).

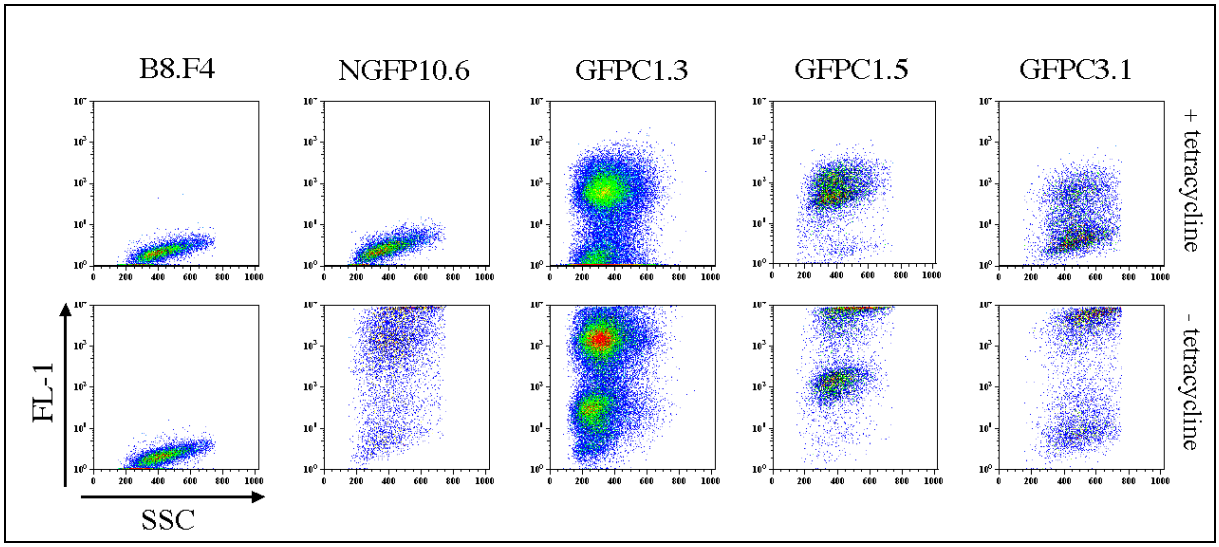

Figure 9: FACS blots of NGFP or GFPC transfected B8tTA.F4 cells. B8tTA.F4 cells were transfected with plasmids containing NGFP or GFPC and eGFP expression (FL-1) was determined 2d after intensive washing (to remove tetracycline) by flow cytometrie. One clone expressing NGFP (NGFP10.6) and three clones for GFPC (GFPC1.3, GFPC1.5, and GFPC3.1) were obtained. Live cells are displayed as a FL-1 (y-axis) vs. ssc (x-axis) plot. Cells containing tetracycline are marked with '+tetracycline' (not induced), transfectants without tetracycline are labelled with '-tetracycline' (induced).

One clone expressing the NP118-126 N-terminal of GFP fluoresced in induced state but was completely silent in the presence of tetracycline. In contrast, all three GFPC expressing clones

displayed a background expression, even in the presence of tetracycline (not induced). Whether this background expression is a systematic error arising with GFPC transfected cells has to be determined with screening for more GFPC clones.

Do NGFP and GFPC present NP118?

In order to test whether the stably transfected NGFP or GFPC cells present the NP118 epitope, these cells were induced by extensive washing and NP118 presentation was analysed by ICS with splenocytes derived from LCMV-WE infected (200pfu i.v.) BALB/c mice (8d post infection) (Fig. 10).

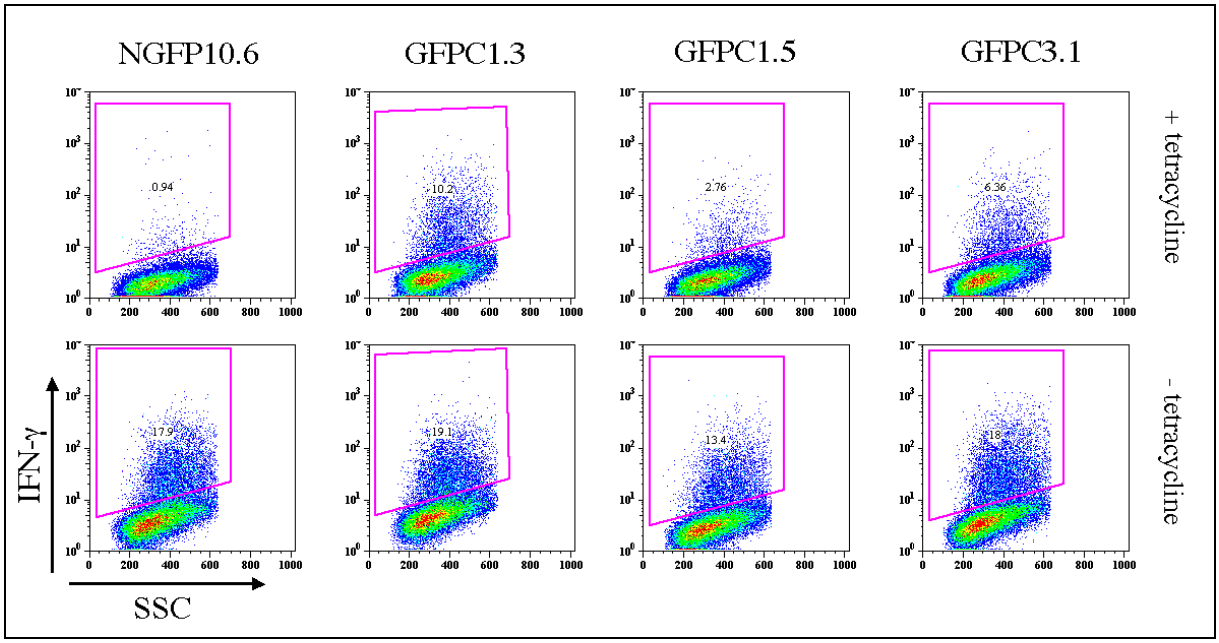

Figure 10: Comparison of the presentation of the LCMV-derived epitopes NP118 of stably transfected NGFP or GFPC cells by ICS. Cells were extensively washed and NP118 presentation was analysed 2d later by ICS using splenocytes derived from LCMV-WE infected (200pfu i.v.) BALB/c mice (8d post infection). The y-axis shows intracellular IFN-γ produced by CD8-positive splenocytes. Cells containing tetracycline are marked with '+tetracycline' (not induced), transfectants without tetracycline are labelled with '-tetracycline' (induced).

All four clones were able to present the NP118 epitope, but no difference in activating CTLs could be observed between N-terminal and C-terminal expression of NP118. GFPC cells stimulated CTLs even when not induced, confirming results obtained in Fig. 9, where GFP was partially expressed in the presence of tetracycline.

Stability of NGFP and GFPC

To investigate the stability of the two constructs NGFP and GFPC, NGFP10.6 and GFPC1.5 cells were extensively washed, metabolically labelled and pulsed for 0h, 2h, 6h, 24h, 36h, 48h, and 96h. GFP was precipitated with anti-GFP mAb and analysed by SDS-PAGE (Fig. 11).

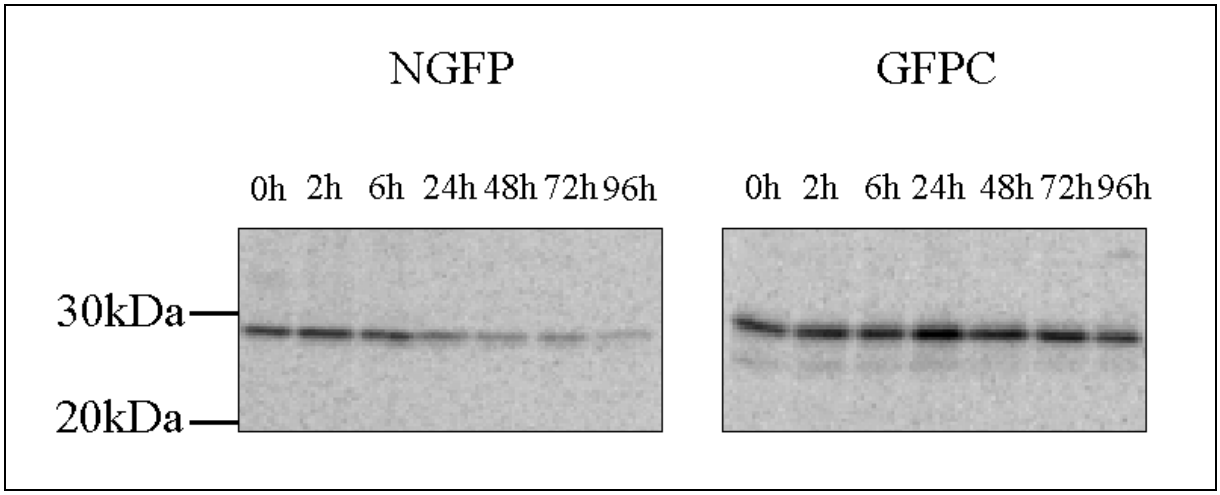

Figure 11: Stability of NGFP and GFPC. NGFP10.6 and GFPC1.5 cells were labeled for 2h with [^{35}S]Cys/Met and chased for the indicated times prior to GFP-specific immunoprecipitation, SDS-PAGE, and autoradiography. Molecular mass markers are indicated to the left in kDa, and immunoprecipitated proteins are indicated on top.

GFPC proofed to be a very stable protein barely degraded over the time course of 4d ($t_{1/2}$>4d). In contrast, NGFP was degraded with increased rate compared to GFPC but can still be considered as a quite stable protein with a half-life of approximately 40h.

Neosynthesis is required to present NGFP and GFPC

Khan et al. showed that two days after terminating nucleoprotein synthesis the presentation of the LCMV-nucleoprotein-derived epitope NP118 was not detectable anymore, although the full nucleoprotein was still present. To investigate the role of protein neosynthesis for the presentation of the nucleoprotein epitope NP118 in stably transfected NGFP and GFPC cells, these cells were grown in the absence of tetracycline and were subsequently cultivated for 0, 1, 2, and 3 days in the presence of tetracycline. NP118 presentation on NGFP and GFPC cells was monitored by ICS using splenocytes derived from LCMV infected BALB/c mice (Fig. 12).

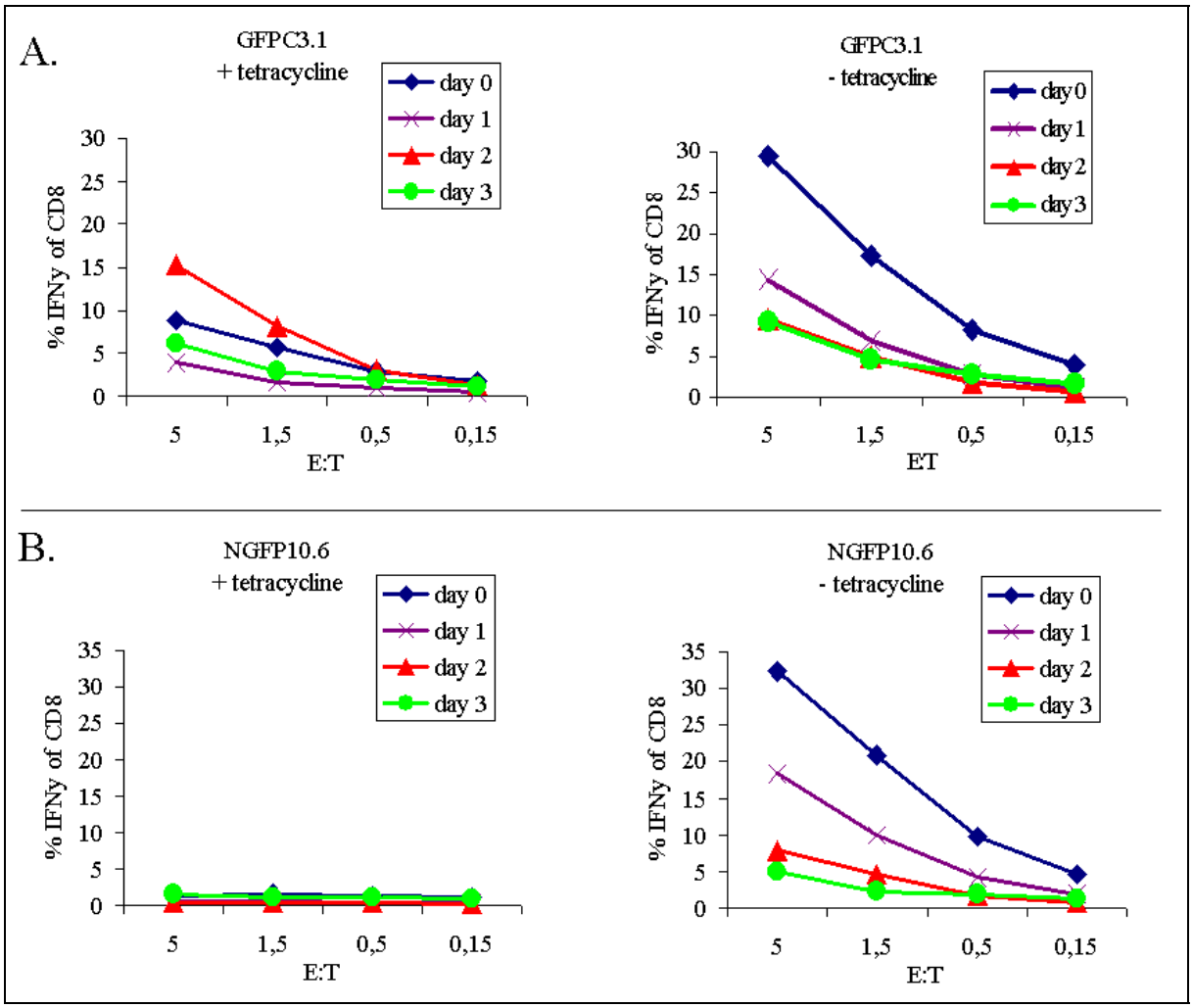

Figure 12: Analysis of NP118 presentation by NGFP and GFPC cells by ICS. NP118 presentation was determined on NGFP10.6 (**A.**) and GFPC3.1 (**B.**) cells, which had been cultured in the absence of tetracycline and were then grown in the presence of tetracycline for the indicated number of days (d1-3) (right panel of **A.** and **B.**). The x-axis displays different effector (splenocytes) to target (NGFP10.6 and GFPC3.1) ratios. The y-axis shows intracellular IFN-γ produced by CD8-positive splenocytes (derived from LCMV-WE infected (200pfu i.v.) BALB/c mice (8d post infection)). As a negative control cells were grown continuously in the presence of tetracycline (left panel of **A.** and **B.**).

Only 1 day after cultivation of NGFP10.6 and GFPC3.1 with tetracycline NP118 presentation was reduced by 50%. On the second and third day of tetracycline treatment of NGFP10.6 the NP118 presentation stagnated slightly over background levels (compare not induced NGFP10.6), presumably due to diminutive degradation of the full-length stable nucleoprotein (seen in Fig. 11). GFPC3.1 displayed on the second day of tetracycline treatment a reduction of the NP118 presentation to almost background levels obtained with noninduced GFPC3.1. It is therefore evident that nucleoprotein neosynthesis is required to maintain full NP118 presentation. In GFPC3.1 cells presentation of this epitope cannot be fuelled from the long-lived nucleoprotein molecules, which remained at the same level in GFPC3.1 cells over 4 days (Fig. 11). A sharp drop in NP118 presentation was detected 1 day after the termination of

nucleoprotein synthesis in NGFP10.6 cells but a small residual NP118 presentation remained on the second and third day of cultivation in the presence of tetracycline. Taken together, this data demonstrate a requirement for nucleoprotein neosynthesis for the full presentation of the immunodominant epitope NP118.

Effect of geldanamycin on NGFP and GFPC

In order to determine the effect of Hsp90 on NGFP or GFPC these cells were induced by extensive washing and incubated over night with 10µM GA. NP118 presentation was analysed by ICS using splenocytes derived from LCMV infected BALB/c mice (Fig. 13).

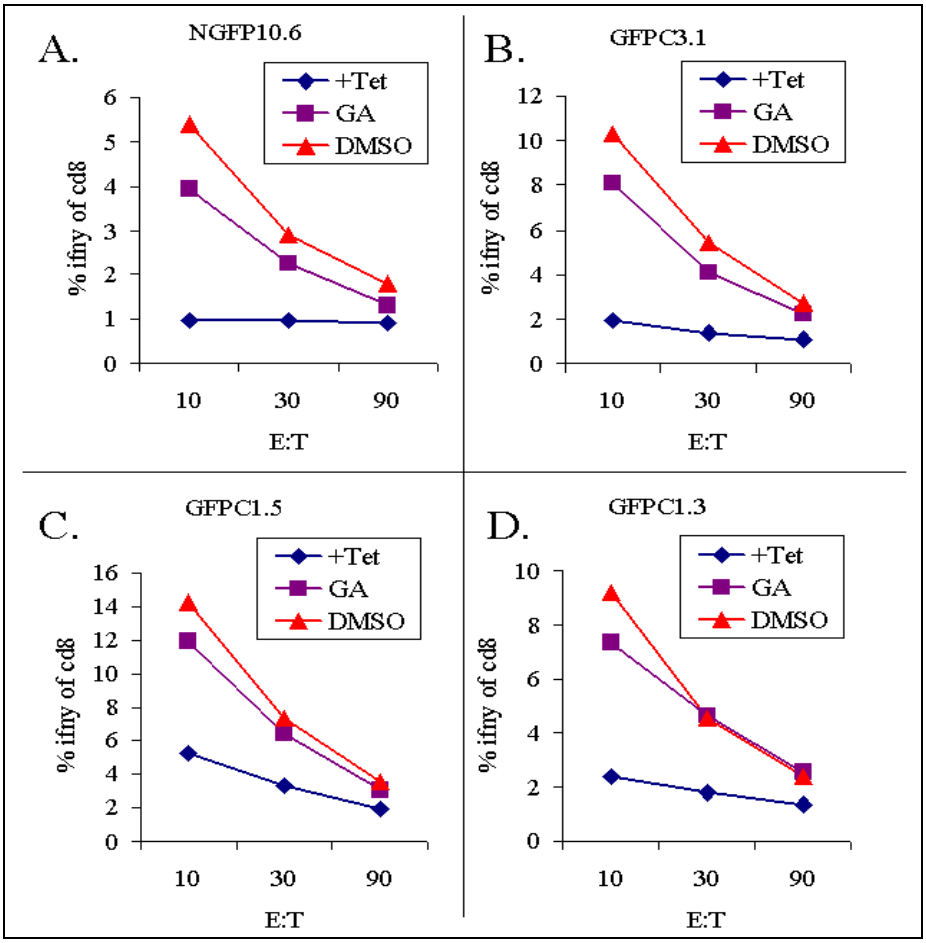

Figure 13: Comparison of the presentation of the LCMV epitope NP118 in GA treated NGFP10.6, GFPC3.1, GFPC1.5, and GFPC1.3 cells. NGFP10.6 (**A.**), GFPC3.1 (**B.**), GFPC1.5 (**C.**), and GFPC1.3 (**D.**) cells were induced by extensive washing and treated over night with either 10µM GA or DMSO. NP118 presentation was analysed by ICS. The y-axis shows intracellular IFN-γ produced by CD8-positive splenocytes (derived from LCMV-WE infected (200pfu i.v.) BALB/c mice (8d post infection)). As a negative control cells grown in the presence of tetracycline (+Tet) are shown (not induced cells).

Presentation of NP118 on MHC-I on the cell surface in geldanamycin treated NGFP and GFPC cells was impeded compared to untreated cells (GFPC1.3 to a lesser extent) (Fig. 13). No difference could be observed between N- and C-terminal NP118-GFP-fusion, suggesting that Hsp90 is not discriminating between N- and C-terminal epitopes.

4. Discussion

A role of heat shock proteins in antigen presentation, probably by protecting peptide intermediates from degradation, has been suggested several years ago (Srivastava and Das, 1984; Tamura et al., 1997; Udono and Srivastava, 1993). Heat shock proteins play an important role in eliciting innate and adaptive immunity by chaperoning peptides for antigen presentation and providing endogenous danger signalling (Chen et al., 1999; Millar et al., 2003). Recently, Kunisawa et al. showed by tracking proteolytic intermediates in living cells, that some of these peptides were bound to the group II chaperonin TRiC and were protected from degradation. Destabilization of TRiC by RNA interference inhibited the expression of peptide-loaded MHC-I molecules on the cell surface. Thus, the TRiC chaperonin serves a function in protecting proteolytic intermediates in the MHC-I antigen processing pathway (Kunisawa and Shastri, 2003). Yamano et al. showed that geldanamycin, an inhibitor of Hsp90, suppressed antigen presentation of an ova derived epitope in LPS blasts derived from PA28αβ-deficient mice, but not in wildtype cells. This indicates that Hsp90 can compensate for the loss of PA28 and is essential in a PA28-independent pathway (Yamano et al., 2002).
The results of Yamano et al. inspired us to investigate role of Hsp90 in the presentation of LCMV-derived epitopes. It has been shown, that geldanamycin (GA), an inhibitor for Hsp90, reduces NP118 presentation in a dose-dependent manner (Fig. 1). Experiments to confirm these data with RNA interference (siRNA) failed, probably due to stability and high abundance of Hsp90 (data not shown). Even two hours LCMV infection reduced the NP118-presentation about 30% in geldanamycin treated cells, compared to untreated cells (Fig. 2). Khan et al. proofed that the NP118 epitope is exclusively emerging from ‘DRiP’s’ (Khan et al., 2001). This finding suggests that Hsp90 might be involved in transporting DRiP’s to the proteasome (Fig. 3). To confirm this hypothesis two cell lines either expressing the full-length nucleoprotein or an ubiquitin-nucleoprotein fusion protein were generated (Fig. 4). In contrast to the very long-lived nucleoprotein, Rodriguez et al. showed that the N-terminal ubiquitin fusion leads to a rapid degradation of the nucleoprotein (Rodriguez et al., 1997). Assuming that most of the generated NP118 peptides derive from the short lived but full length

ubiquitin-nucleoprotein fusion protein, and not from DRiP's, cells expressing UbNP should be less affected by geldanamycin than cells expressing the stable wildtype nucleoprotein (Fig. 3). This theory was not supported by data obtained in Fig. 5,6. Hsp90 inhibition did even not disturb NP118 presentation in B8 cells transfected with wildtype nucleoprotein, suggesting that the effect of Hsp90 displayed in Fig. 1 is a cell- or viral-specific phenomenon. The results of Yamano et al. indicate that the Hsp90-dependent processing pathway is common, but the contribution of Hsp90 in antigen processing seems to depend on the cell type (Yamano et al., 2002). Infection of the geldanamycin treated macrophage cell line J774 with a vaccinia virus expressing the LCMV nucleoprotein (VVYN4) did not affect NP118 presentation (Fig. 7), suggesting the effect of Hsp90 to be a LCMV specific phenomena.

Yamano et al. reported that Hsp90 acts in an epitope-specific manner (Yamano et al., 2002). None of the H-2D^b-restricted LCMV-derived epitopes GP33, GP276, and NP396 were negatively affected by geldanamycin (Fig. 8). In contrast Hsp90 inhibition led even to a slightly increased GP276 and NP396 presentation. The result that GA affected the presentation of the two epitopes NP118 and NP396, derived from the same nucleoprotein, differently, led to speculations that epitopes expressed at different positions within a certain protein are differently dependent on Hsp90. To proof this theory the NP118 epitope was expressed at the N- or C-terminus of green fluorescent protein (GFP) in a tetracycline inducible manner (Fig. 9,10). GA treatment reduced the amount of NP118 presented on MHC-I for both NGFP and GFPC, but no altered presentation was observed when the epitope was expressed at the N- or C-terminus of GFP.

The existence of DRiPs is certain, as biological processes cannot occur with 100% fidelity. There are translational errors that result in amino acid substitutions and truncations. Further errors occur post-translationally, including improper interaction with molecular chaperones (therefore incorrect folding), mistargeting to organelles, failure to associate with proper partners to create multisubunit structures and improper post-translational covalent modifications. The above-mentioned system, with the NP118 epitope fused N- or C-terminal to GFP, is an excellent approach to investigate whether DRiPs derive predominantly from translational errors or from post-translational events. If DRiPs originate mainly from translational errors, resulting in premature translation termination, than an epitope near the N-terminus should be produced in larger quantities than an epitope expressed at the C-terminus, because there is an increased probability that the translation process is terminated before the C-terminal epitope is made. To address this question the presentation of the NP118 epitope in NGFP and GFPC cells should derive exclusively from DRiPs. To fulfil this, these proteins

have to be long lived so that the pool of fully matured proteins (of NGFP or GFPC) does not contribute significantly to MHC-I presentation. Both proteins were quite stable, but NGFP was degraded more efficient than GFPC (Fig. 11). No significant difference was observed between NGFP and GFPC in activating splenocytes in ICS (Fig. 10), but no conclusion can be drawn, because all GFPC clones were slightly presenting NP118 in noninduced conditions, making it difficult to compare NGFP to GFPC. Screening for tight GFPC clones, expressing comparable amounts of eGFP to NGFP, should clarify whether the epitope position within a certain protein is important for efficient antigen presentation.

5. Materials and methods

Primers and DNA constructs

To generate NGFP the NP118 epitope (plus four additional N- and C-terminal aa: NP114-122; plus a N-terminal kosak sequence (GCCACC)) was amplified from pTet-SpliceLCMV-NP (Khan et al., 2001) using following primers containing the EcoRI and SalI restriction site: 5`-CCGGAATTCGCCACCATGAGAACTGAGAGGCCTC-3`; 3`-ATGTACCCTTTAAACTGTCGTCAGCTGGCGT-5`. The amplified NP118 epitope was cloned into the tetracycline (tet)-regulated expression construct pTet-Splice (Shockett et al., 1995) via EcoRI and SalI sites, thus yielding the plasmid pTet-SpliceNNP118. EGFP was amplified from pEGFP-C1 (Clontech) using primers containing a stop codon (TAA) and SalI and SpeI restriction site (5`-ACGCGTCGACATGGTGAGCAAGGGCGAG-3`; 3`-GTACCTGCTCGACATGTTCATTTGATCACC -5`) and cloned into pTet-SpliceNNP118 C-terminal of the NP118 epitope via SalI and SpeI restriction sites. The resulting construct was named pTet-SpliceNGFP.

To generate GFPC, EGFP was amplified from pEGFP-C1 (Clontech) using primers (5`-CCGGAATTCGCCACCATGGTGAGCAA-3`; 3`-GTACCTGCTCGACATGTTCCAGCTGGCT-5`) containing a start codon (ATG), the EcoRI and SalI restriction sites plus a N-terminal kosak sequence and cloned into pTet-Splice via EcoRI and SalI sites, thus yielding the plasmid pTet-SpliceGFP. The NP118 epitope (plus four additional N- and C-terminal aa: NP114-122) was amplified from pTet-SpliceLCMV-NP (Khan et al., 2001) using following primers containing the SalI and SpeI restriction sites and the C-terminal stop codon (TAA): 5`-ACGCGTCGACATGAGAACTGAGAGGCCTC-3`; 3`-ATGTACCCTTTAAACTGTCGTATTTGATCACC-5`. The amplified NP118 epitope was cloned into pTet-SpliceGFP via SalI and SpeI restriction sites, thus yielding the plasmid pTet-SpliceGFPC. All primers were

purchased from Mycrosynth (Balgach, Switzerland). pTet-splice was purchased from invitrogen.

Restriction digests

Restriction digests with a single restriction enzyme were performed in a volume of 10µl containing 1µl restriction enzyme, 1µl 10x restrction enzyme buffer, and variable volumes of DNA. The difference to 10µl was equalled with ddH_2O. Digests were incubated for 1h at 37°C and analysed by agaraose gel electrophoresis. Restriction digests with two restriction enzymes were performed similarly in a volume of 20µl. All restriction enzymes (SpeI, EcoRI, SalI) and buffers were purchased from Promega (Germany). Fragments were purified with the NucleoSpin® extract kit or the NucleoTrap® kit (Machinery Nagel, Germany).

Polymerase chain reaction (PCR)

All PCRs were performed in a volume of 30µl containing 3µl 10x PCR buffer, 3µl dNTPs (2mM), 0.5µl sense primer (50µM), 0.5µl antisense primer (50µM), 0.5-2µl template and 0.2µl PFU polymerase (Promega, Germany). The difference to 30µl was equalled with ddH_2O. The following PCR program was used: 1. step: 5min 95°C, 2. step: 1min 95°C, 3. step 0.5min 60°C 4. step: 1min 72°C 5. step: 5min 72°C. Step 2 to 4 were repeated 30 times. All PCR products were analysed by agarose gel electrophoresis and purified with NucleoSpin® extract kit or the NucleoTrap® kit (Machinery Nagel, Germany).

Transformation and vector amplification

Electrocompetent E. Coli XL-1 blue (Stratagene, US) were thawed on ice and transferred to an ice cold electrocuvette (2mm; Eurogentec, Belgium). 1µl of DNA (1ng to 1pg) was added and incubated for 1min on ice. Electrotransformation was performed using the following setup: 25µF, 1.8kV and 200ohm. After pulsing 500µl SOC (2% bacto-tryptone (w/v), 0.5% bacto-yeast extract (w/v), 0.05%NaC (w/v), 2.5mM KCl, 10mM $MgCl_2$, 20mM glucose) was added. Bacteria were shaked for 1h at 37°C and plated on LB agar plates (LB-medium plus 1.5% bacto-agar) containing 50µg/ml ampicilin. Bacteria were grown over night at 37°C and single colonies were transferred to 5ml LB-medium containing 50µg/ml ampicilin. For the production of small amounts of DNA the culture was shaken over night at 37°C and the DNA was isolated using the NucleoSpin® plasmid kit (Machinery Nagel, Germany). To produce

large amounts of DNA 2ml of the 5ml bacteria culture were transferred after 8h to 500ml LB-medium containing 50µg/ml ampicilin. The DNA was isolated using the Gen Elute^{TM} HP Plasmid Maxiprep kit (Sigma, Germany).

Cell lines and transfection

IMDM and RPMI media were purchased from Invitrogen-Life Technologies (Karlsruhe, Germany) and contained GlutaMAX, 10% FCS, and 100U/ml penicillin/streptomycin.

J774 (cultured in RPMI10%) is a mouse macrophage cell line (kind gift of S. Basta) and B8 (cultured in IMDM10%) is a BALB/c-derived fibroblast line (H-2^{d}) obtained by SV40 infection *in vitro* (Groettrup et al., 1995). B8tTA.F4 (Raasi et al., 2001) are B8 cells stably transfected with the plasmid pTet-tTAk and hygromycin resistant plasmid pLXSH. They are cultured in IMDM10%+100 units/ml penicillin/streptomycin + 400 µg/ml hygromycin (Calbiochem), + 400ng/ml tetracycline (Sigma).

B8tTA.F4 cells were stably transfected with the plasmids pTet-SpliceGFPC or pTet-SpliceNGFP and puromycin resistance plasmid (pLXSP) according to the manufactures protocol (FuGENE 6, Roche) in 6-well plates. The cells were termed NGFP or GFPC according to the transfected plasmid. Two days later cells were transferred to 96-well round bottom plates and selected with puromycin (0.25µg/ml). Cells were plated at different densities reaching from 1 to 10000 cells per plate. After 3 weeks clonal and selection drug resistant cells were transferred to 24-well plates and propagated. Cells were washed four times with PBS (to induce NGFP or GFPC) in a 6-well plate and protein expression was analysed two days later due to excitation of eGFP (enhanced GFP) at 488nm and emission at 507nm by flow cytometry measured in FL-1. NGFP and GFPC are cultured in IMDM10% + 400 µg/ml hygromycin (Calbiochem), + 2.5µg/ml puromycin (Sigma) + 400ng/ml tetracycline (Sigma).

To generate NP and UbNP cells, B8 cells were transfected similarly to NGFP and GFPC with the plasmids pCMV-NP (NP) and pCMV-U-NP (UbNP) (Rodriguez et al., 1997) (kind gift of L. Whitton). Clonal and selection drug resistant cells were analysed for NP118 presentation by ICS. NP and UbNP are cultured in IMDM10% + 2.5µg/ml puromycin (Sigma).

Synthetic peptides, mice and viruses

The synthetic peptides GP33-41/D^b (KAVYNFATC), GP276-286/D^b (SGVENPGGYCL), NP396-404/D^b (FQPQNGQFI), and NP118-126/L^d (RPQASGVYM) were obtained from Echaz Microcollections (Tubingen, Germany).

BALB/c (H-2^d) and C57BL/6 (H-2^b) mice were originally obtained from Charles River, Germany. The animals were kept at the University of Constance in a pathogen-free facility and used at 6-10 weeks of age.

LCMV-WE was originally obtained from F. Lehmann-Grube (Hamburg, Germany) and propagated on the fibroblast line L929. Recombinant vaccinia virus encoding the LCMV nucleoprotein (VVYN4) (was originally obtained from Dr. D. Bishop, Institute of Virology, Oxford, U.K.) or the NP118 minigene (VV118) (Schwarz et al., 2000) was propagated on BSC40 cells.

Intracellular cytokine staining for interferon-γ (ICS)

$2x10^6$ splenocytes or $2x10^5$ restimulated cells and $2\text{-}4x10^5$ stimulator cells were incubated in round-bottom 96-well plates with 10^{-7}M of the specific peptide in 100µl IMDM10% + brefeldin A (10µg/ml) for 5h at 37°C. Cells were incubated for 20min at 4°C with Cy5-conjugated mouse anti-CD8 (clone 53-6.7, BD PharMingen) and washed twice with PBS. Following fixation with 4% paraformaldehyde at 4°C for 5min and two washes with PBS, the cells were incubated overnight with fluorescein-conjugated mouse anti-IFN-γ (clone XMG1.2, BD PharMingen) in PBS containing 2% FCS and 0.1% (w/v) saponin (Sigma). Samples were washed twice and acquired with the use of FACScan™ flow cytometer (Becton Dickinson, Mountain View, CA) and analysed by the FlowJo software (Tree Star, San Carlos, CA).

CTL lines

For generating NP396-404, GP33-41, and GP276-286 specific CTL-lines, memory C57BL/6 mice (at least four weeks post infection with 200pfu LCMV-WE i.v.) were sacrificed and splenocytes were plated at a density of $4x10^6$ in 24-well plates. Splenocytes were restimulated with $2x10^5$ peritoneal-elicited macrophages pulsed with peptide (10^{-7}M). 8d later restimulated cells of one well were transferred to a 6-well plate and restimulated with $6x10^5$ thioglycolate-

elicited peritoneal macrophages pulsed with peptide (10^{-7}M). CTL lines were used in ICS at a E:T ratio of 1:1.

Flow cytometry

A number of approximately $5x10^5$ BFA treated (10µg/ml) or untreated B8 cells in 100µl of PBS + 2% FCS were incubated in a round-bottom 96-well plate on ice for 20 min with 1µg of L^d-specific mAb 28-14-81, washed twice, and subsequently stained by a FITC-conjugated sheep anti-mouse Ig (Silenus, Victoria, Australia) for another 20 min on ice. Samples were washed twice, acquired with the use of FACScan flow cytometer (BD Biosciences), and analyzed by the FlowJo software (Tree Star).

NGFP and GFPC cells were washed four times with PBS and eGFP expression was analysed two days later by flow cytometry in FL-1.

Metabolic labeling, immunoprecipitation, and gel electrophoresis

A total of approximately 10^7 NGFP or GFPC cells were starved in cysteine/methionine-free RPMI 1640, 10% dialyzed FCS for 1 h at 37°C and labeled with 0.2 mCi/ml Met-[^{35}S]-label (Hartmann Analytic, Braunschweig, Germany) for 2h. Cells were washed with PBS and chased for 0h, 2h, 6h, 24h, 48h, 72h, and 96h in the presence of tetracycline to stop neosynthesis. Cells were harvested, and lysed for 30 min on ice in 20mM Tris/HCl, pH 7.5, 150mM NaCl, 1mM $MgCl_2$, and 2% Triton X-100. The lysates were counted for [^{35}S]methionine/cysteine incorporation, and equal aliquots were used for immunoprecipitation. The lysate was precleared for 1 h with protein G-Sepharose CL-4B (Amersham Biosciences, Uppsala, Sweden), followed by overnight immunoprecipitation with an anti-GFP antibody (clone 7.1 and 13.1) (Roche, Germany) bound to protein G-Sepharose at 4°C. The precipitates were washed five times with ripa-buffer (50mM Tris pH8, 150mM NaCl, 1% NP40, 0.5% deoxycholate, 0.1% SDS), separated by SDS-PAGE (12%), and visualized by autoradiography on a Fuji BAS1500 radioimager.

6. References

Chen, W., Syldath, U., Bellmann, K., Burkart, V. and Kolb, H. (1999) Human 60-kDa heat-shock protein: a danger signal to the innate immune system. *J Immunol*, **162**, 3212-3219.

Connell, P., Ballinger, C.A., Jiang, J., Wu, Y., Thompson, L.J., Hohfeld, J. and Patterson, C. (2001) The co-chaperone CHIP regulates protein triage decisions mediated by heat-shock proteins. *Nat Cell Biol*, **3**, 93-96.

Fujiwara, T., Oda, K., Yokota, S., Takatsuki, A. and Ikehara, Y. (1988) Brefeldin A causes disassembly of the Golgi complex and accumulation of secretory proteins in the endoplasmic reticulum. *J Biol Chem*, **263**, 18545-18552.

Groettrup, M., Ruppert, T., Kuehn, L., Seeger, M., Standera, S., Koszinowski, U. and Kloetzel, P.M. (1995) The interferon-γ-inducible 11S regulator (PA28) and the LMP2/LMP7 subunits govern the peptide production by the 20S proteasome in vitro. *J. Biol. Chem.*, **270**, 23808-23815.

Ishii, T., Udono, H., Yamano, T., Ohta, H., Uenaka, A., Ono, T., Hizuta, A., Tanaka, N., Srivastava, P.K. and Nakayama, E. (1999) Isolation of MHC class I-restricted tumor antigen peptide and its precursors associated with heat shock proteins hsp70, hsp90, and gp96. *J Immunol*, **162**, 1303-1309.

Khan, M.T., Wang, K., Auland, M.E., Kable, E.P.W. and Roufogalis, B.D. (1994) Membrane-bound high molecular mass proteinases from human erythrocytes. *Biochim. Biophys. Acta*, **1209**, 215-221.

Khan, S., de Giuli, R., Schmidtke, G., Bruns, M., Buchmeier, M., van den Broek, M. and Groettrup, M. (2001) Cutting Edge: Neosynthesis is required for the presentation of a T cell epitope from a long lived viral protein. *J. Immunol.*, **167**, 4801-4804.

Kunisawa, J. and Shastri, N. (2003) The group II chaperonin TRiC protects proteolytic intermediates from degradation in the MHC class I antigen processing pathway. *Mol Cell*, **12**, 565-576.

Millar, D.G., Garza, K.M., Odermatt, B., Elford, A.R., Ono, N., Li, Z. and Ohashi, P.S. (2003) Hsp70 promotes antigen-presenting cell function and converts T-cell tolerance to autoimmunity in vivo. *Nat Med*, **9**, 1469-1476.

Raasi, S., Schmidtke, G. and Groettrup, M. (2001) The ubiquitin-like protein FAT10 forms covalent conjugates and induces apoptosis. *J. Biol. Chem.*, **276**, 35334-35343.

Rodriguez, F., Zhang, J. and Whitton, J.L. (1997) DNA immunization: Ubiquitination of a viral protein enhances cytotoxic T-lymphocyte induction and antiviral protection but abrogates antibody induction. *J. Virol.*, **71**, 8497-8503.

Schnaider, T., Somogyi, J., Csermely, P. and Szamel, M. (1998) The Hsp90-specific inhibitor, geldanamycin, blocks CD28-mediated activation of human T lymphocytes. *Life Sci*, **63**, 949-954.

Schwarz, K., van den Broek, M., Kostka, S., Kraft, R., Soza, A., Schmidtke, G., Kloetzel, P.M. and Groettrup, M. (2000) Overexpression of the proteasome subunits LMP2, LMP7, and MECL-1 but not PA28α/β enhances the presentation of an immunodominant lymphocytic choriomeningitis virus T cell epitope. *J. Immunol.*, **165**, 768-778.

Shockett, P., Difilippantonio, M., Hellman, N. and Schatz, D.G. (1995) A modified tetracycline-regulated system provides autoregulatory, inducible gene expression in cultured cells and transgenic mice. *Proc. Natl. Acad. Sci. USA*, **92**, 6522-6526.

Srivastava, P.K. and Das, M.R. (1984) The serologically unique cell surface antigen of Zajdela ascitic hepatoma is also its tumor-associated transplantation antigen. *Int J Cancer*, **33**, 417-422.

Stebbins, C.E., Russo, A.A., Schneider, C., Rosen, N., Hartl, F.U. and Pavletich, N.P. (1997) Crystal structure of an Hsp90-geldanamycin complex: targeting of a protein chaperone by an antitumor agent. *Cell*, **89**, 239-250.

Tamura, Y., Peng, P., Liu, K., Daou, M. and Srivastave, P.K. (1997) Immunotherapy of tumors with autologous tumor-derived heat shock protein preparations. *Science*, **278**, 117-120.

Udono, H. and Srivastava, P.K. (1993) Heat shock protein 70-associated peptides elicit specific cancer immunity. *J. Exp. Med.*, **178**, 1391-1396.

van der Most, R.G., Sette, A., Oseroff, C., Alexander, J., Murali-Krishna, K., Lau, L.L., Southwood, S., Sidney, J., Chestnut, R.W., Matloubian, M. and Ahmed, R. (1996) Analysis of cytotoxic T cell responses to dominant and subdominant epitopes during acute and chronic lymphocytic choriomeningitis virus infection. *J. Immunol.*, **157**, 5543-5554.

Yamano, T., Murata, S., Shimbara, N., Tanaka, N., Chiba, T., Tanaka, K., Yui, K. and Udono, H. (2002) Two distinct pathways mediated by PA28 and hsp90 in major histocompatibility complex class I antigen processing. *J Exp Med*, **196**, 185-196.

Chapter 4

Immunoproteasomes down-regulate presentation of a subdominant T cell epitope from lymphocytic choriomeningitis virus

Michael Basler, Nikolay Youhnovski, Maries van den Broek, Michael Przybylski, & Marcus Groettrup

Published in Journal of Immunology 2004:173(6):3925-34.

The Journal of Immunology

Immunoproteasomes Down-Regulate Presentation of a Subdominant T Cell Epitope from Lymphocytic Choriomeningitis Virus[1]

Michael Basler,* Nikolay Youhnovski,† Maries van den Broek,‡ Michael Przybylski,† and Marcus Groettrup[2]*

The cytotoxic T cell response to pathogens is usually directed against a few immunodominant epitopes, while other potential epitopes are either subdominant or not used at all. In C57BL/6 mice, the acute cytotoxic T cell response against lymphocytic choriomeningitis virus is directed against immunodominant epitopes derived from the glycoprotein (gp33–41) and the nucleoprotein (NP396–404), while the gp276–286 epitope remains subdominant. Despite extensive investigations, the reason for this hierarchy between epitopes is not clear. In this study, we show that the treatment of cells with IFN-γ enhanced the presentation of gp33–41, whereas presentation of the gp276–286 epitope from the same glycoprotein was markedly reduced. Because proteasomes are crucially involved in epitope generation and because IFN-γ treatment in vitro and lymphocytic choriomeningitis virus infection in vivo lead to a gradual replacement of constitutive proteasomes by immunoproteasomes, we investigated the role of proteasome composition on epitope hierarchy. Overexpression of the active site subunits of immunoproteasomes LMP2, LMP7, and MECL-1 as well as overexpression of LMP2 alone suppressed the presentation of the gp276–286 epitope. The ability to generate gp276–286-specific CTLs was enhanced in LMP2- and LMP7-deficient mice, and macrophages from these mice showed an elevated presentation of this epitope. In vitro digests demonstrated that fragmentation by immunoproteasomes, but not constitutive proteasomes led to a preferential destruction of the gp276 epitope. Taken together, we show that LMP2 and LMP7 can at least in part determine subdominance and shape the epitope hierarchy of CTL responses in vivo. ***The Journal of Immunology,*** **2004, 173: 3925–3934.**

Cytotoxic T lymphocytes recognize peptide epitopes presented on MHC class I molecules, which allows CTLs to monitor for cells harboring intracellular pathogens. CTL responses are usually directed against one or a few dominant epitopes and some minor epitopes. Several factors that contribute to this phenomenon of immunodominance have been described (1–4). Viral proteins have to be targeted for degradation at a sufficient frequency (5), and they must be fragmented into peptides that meet the requirements for binding to the TAP as well as to a given MHC class I molecule with respect to their length and the availability of anchor residues (6). CTLs need to be triggered by their nominal epitope in the context of the appropriate class I molecule for an extended period of time, which implies that the affinity of the peptide to the binding groove of class I should be high. In addition, an adequate avidity of the TCR for the class I/peptide complex is pivotal (7). Finally, the precursor frequence of T cells with a particular specificity will determine whether a given epitope achieves immunodominance over competing epitopes (3, 8).

The infection of the mouse with lymphocytic choriomeningitis virus (LCMV)[3] is a frequently used model of viral infection, and also, the phenomenon of immunodominance has been thoroughly investigated (2, 8, 9–12). In C57BL/6 mice, this response is dominated by CTLs specific for the H-2D^b-restricted epitopes gp33–41, nucleoprotein 396–404 (NP396–404), and the subdominant epitope gp276–286. The reasons for gp276 subdominance have been thoroughly investigated in the past (11). One contributing factor to the subdominance of gp276 could be that the amount of gp276 epitopes that was eluted from 10^9 LCMV-infected MC57 fibroblasts (0.16 ng) was about twice as low as that of NP396 (0.3 ng) and 12-fold lower than gp33 (2.0 ng). This amount corresponded to 92 H-2D^b-bound gp276 epitopes per MC57 cell, which is in a range in which it could become limiting for the recognition by gp276-specific CTLs (13, 14). It hence appears that the intracellular processing of gp276 is less efficient than processing of the gp33 epitope derived from the same glycoprotein. Because the proteasome is involved in the processing of both epitopes (15), we decided to further investigate its impact on the establishment of the epitope hierarchy.

The proteasome is the main protease in the cytoplasm and the nucleus that generates the C termini of most peptide ligands of MHC class I molecules (16, 17). The proteolytic core complex of the proteasome system is the 20S proteasome, which is constructed like a cylinder of four stacked rings. The outer two rings consist of seven different α-type subunits that bind to regulatory complexes of the 20S core particle, whereas the two inner rings are made up of seven different subunits of the β-type. Three of the β-subunits,

*Division of Immunology, Department of Biology, and †Laboratory of Analytical Chemistry, Department of Chemistry, University of Constance, Konstanz, Germany; and ‡Institute of Experimental Immunology, Department of Pathology, University Hospital Zürich, Zürich, Switzerland

Received for publication October 30, 2003. Accepted for publication July 2, 2004.

The costs of publication of this article were defrayed in part by the payment of page charges. This article must therefore be hereby marked *advertisement* in accordance with 18 U.S.C. Section 1734 solely to indicate this fact.

[1] This work was supported by grants of the Swiss National Science Foundation (31-52284.97/1) and the University of Constance to M.G., and by a grant from the Cloëtta Foundation, Zürich, to M.v.d.B.

[2] Address correspondence and reprint requests to Dr. Marcus Groettrup, Department of Biology, Division of Immunology, University of Constance, P1101 Universitätsstrasse 10, D-78457 Konstanz, Germany. E-mail address: Marcus.Groettrup@uni-konstanz.de

[3] Abbreviations used in this paper: LCMV, lymphocytic choriomeningitis virus; ESI-MS, electrospray ionization mass spectrometry; NP, nucleoprotein; VV, vaccinia virus.

0022-1767/04/$02.00

designated δ (β1), MB1 (β5), and MC14 (Z, β2), bear the active centers of the 20S proteasome. Upon stimulation of cells with the inflammatory cytokine IFN-γ, these constitutively expressed subunits are replaced by inducible subunits named LMP2 (β1i), LMP7 (β5i), and MECL-1 (β2i) during the de novo assembly of 20S proteasomes. This subunit exchange alters the cleavage pattern of the proteasome (16), which can lead to an enhancement of Ag presentation (18–21). However, for a few epitopes from human tumors, the induction of immunoproteasomes was found to negatively affect their presentation (22). Although gene-targeted mice deficient for LMP2 (23) and LMP7 (24) have been generated almost a decade ago, the impact of these two subunits on the hierarchy of epitopes has been barely investigated, except for a recent study by Chen et al. (25), which shows that in LMP2$^{-/-}$ mice the CTL response to influenza virus follows a different hierarchy than in wild-type mice. This effect was due both to differences in the CTL precursor frequency as well as to changes in epitope presentation.

Another IFN-γ-inducible complex, which affects epitope generation and therefore has the potential to shape epitope hierarchies, is the 11S regulator of the proteasome (26) (also called PA28 (27)). PA28 consists of two different subunits, α and β, which form a heptameric ring that binds to the 20S or 26S proteasomes and affects their peptidolytic properties (28). Overexpression of PA28αβ has been shown to enhance the presentation of a number of epitopes (29–32), and, conversely, PA28 deficiency in PA28β$^{-/-}$ or PA28αβ$^{-/-}$ mice interferes with epitope presentation in several cases (33, 34).

In this study, we investigated whether the composition of proteasome active site subunits and PA28 could be involved in determining immunodominance and subdominance in the LCMV system. The finding that the IFN-γ treatment of MC57 fibroblasts enhanced gp33 presentation, but down-regulated the presentation of gp276 inspired our work. With the help of transfectants and knockout mice, we could indeed show that immunoproteasomes negatively affect gp276 processing and presentation in vitro and the generation of gp276-specific CTLs in vivo. Our data are discussed with respect to so far elusive changes of epitope hierarchy in acute vs persistent LCMV infection and in relation to different Ag presentation by fibroblasts as opposed to dendritic cells.

Materials and Methods

Mice and viruses

C57BL/6 mice (H-2^b) were purchased from the animal facility of University of Constance. LMP2$^{-/-}$ (23) and LMP7$^{-/-}$ (24) gene-targeted mice were provided by J. Monaco (Department of Molecular Genetics, Cincinnati Medical Center, Cincinnati, OH), while PA28αβ mice were kindly contributed by T. Chiba (Department of Molecular Oncology, Tokyo Metropolitan Institute of Medical Science, Tokyo, Japan) (34). All knockout mice were backcrossed onto the C57BL/6 background for at least 10 generations. Mice were kept in a specific pathogen-free facility and used at 6–10 wk of age. LCMV-WE was originally obtained from F. Lehmann-Grube (Heinrich Pette Institut, Universität Hamburg, Hamburg, Germany) and propagated on the fibroblast line L929. Recombinant vaccinia virus (rVV) encoding the LCMV glycoprotein (rVVG2) was obtained from D. Bishop (Institute of Virology, Oxford, U.K.) and was propagated on BSC40 cells. Mice were infected with 200 PFU of LCMV-WE i.v. or with 2×10^6 PFU of VVG2 i.p., and the specific CTL response was analyzed at day 8 or 6 after infection, respectively.

Cell lines

MC57 (H-2^b) is a C57BL/6-derived methylcholanthrene-induced fibrosarcoma cell line (35). MCGP (H-2^b) is a MC57-derived transfectant expressing the LCMV glycoprotein. B8 is a BALB/c-derived fibroblast line (H-2^d) obtained by SV40 infection in vitro (28). B27M6 and B27M2 are triple transfectants of B8 cells expressing murine LMP2, LMP7, and MECL-1; BPαβ13 is a double transfectant of B8 cells expressing murine PA28α and PA28β (19); BC2P6 is a transfectant of B8 cells expressing murine LMP2 (28); B7H6 is a transfectant of B8 cells expressing murine LMP7 (28). Hyb33 and Hyb276 are T cell hybridomas specific for gp33–41/H-2K^b or gp276–286/H-2D^b, respectively (15). All cells were grown in IMDM supplemented with 2 mM glutamine, 10% FCS, and 100 U/ml penicillin/streptomycin. Selection drugs were required for MCGP (0.8 mg/ml G418), B27M6Db (0.5 mg/ml G418, 3 μg/ml puromycin, 0.4 mg/ml hygromycin B, 5 μg/ml blasticidin), BPαβ13Db (0.5 mg/ml G418, 3 μg/ml puromycin, 0.4 mg/ml hygromycin B, 5 μg/ml blasticidin), B8Db (5 μg/ml blasticidin), B7H6Db and BC2P6Db (3 μg/ml puromycin, 0.4 mg/ml hygromycin B), and Hyb33 and Hyb276 (1× hypoxanthine thymidine, 0.5 mg/ml hygromycin B).

Synthetic peptides

The synthetic peptides gp33–41 (KAVYNFATC) and gp276–286 (SGVENPGGYCL) were obtained from Echaz Microcollections (Tubingen, Germany). The 25-mer peptide used for proteasome digestion encompassing LCMV-glycoprotein residues 271–295 (TLSSDSSGVEDPG GYCLTKWMILAAE) was synthesized by solid-phase peptide synthesis on a NovaSyn TGA resin (0.21 mmol/g) by Fmoc/tBu chemistry, using a semiautomated Economy Peptide Synthesizer EPS-221 (Abimed, Germany). The crude peptide was purified by reverse-phase HPLC on a C18 column (GROM-SIL 120 ODS-4 HE, 10 μm, 250 × 20 mm; Grom, Herrenberg-Kayh, Germany) using as mobile phases: eluent A (0.1% trifluoroacetic acid in water) and eluent B (80% AcCN, 0.1% trifluoroacetic acid in water). The following gradient was applied: 0 min, 10% eluent B; 45 min, 90% eluent B.

Antibodies

KL 25 is a mouse mAb reactive with the LCMV glycoprotein (36). The mAb KH95 (BD Pharmingen, San Diego, CA) reacts with the H-2D^b MHC class I molecule.

Flow cytometry

A number of 5×10^5 infected and noninfected B8Db, B27M6Db, B27M2Db, B7H6Db, BC2P6Db, and BPαβ13Db cells in 100 μl of PBS + 2% FCS were incubated in a round-bottom 96-well plate on ice for 20 min with 1 μg of mAb KL25, washed twice, and subsequently stained by a FITC-conjugated sheep anti-mouse Ig (Silenus, Victoria, Australia) for another 20 min on ice. Samples were washed twice and analyzed on a FACScan flow cytometer (BD Biosciences, Mountain View, CA). To check transfected B8Db, B27M6Db, B27M2Db, B7H6Db, BC2P6Db, and BPαβ13Db for H-2D^b expression, the staining was performed, as described above, with the H-2D^b-specific Ab KH95.

For Vβ staining splenocytes from uninfected or LCMV (8 days postinfection with 200 PFU of LCMV-WE i.v.)-infected C57BL/6, LMP2$^{-/-}$, and LMP7$^{-/-}$ mice were treated with 1.66% NH_4Cl (w/v), washed twice, and incubated for 30 min with biotin-conjugated anti-Vβ8.1/8.2, anti-Vβ9, or anti-Vβ10b (BD Pharmingen) Abs on ice. Samples were washed twice and incubated for another 30 min with streptavidin-conjugated FITC and Cy5-conjugated mouse anti-CD8 (BD Pharmingen). After two washes, cells were acquired with the use of FACScan flow cytometer (BD Biosciences, Mountain View, CA) and analyzed with the FlowJo software (Tree Star, San Carlos, CA). Differences between groups were assessed by unpaired *t* test (www.graphpad.com). Values of $p < 0.05$ are considered to be statistically significant.

Transfections

B8, B27M6, and BPαβ13 were transfected with an expression plasmid encoding H-2D^b (a kind gift from F. Momburg, Heidelberg, Germany). Cells were plated to 80% confluence and were transfected by the standard calcium phosphate coprecipitation method with 10 μg of H-2D^b plasmid and 2 μg of blasticidin resistance vector pcDNA6/TR (Invitrogen Life Technologies, Karlsruhe, Germany). Two days after transfection, cells were plated in 96-well plates under cloning conditions and selected with 5 μg/ml blasticidin (Invitrogen Life Technologies). Because of instability of blasticidin, the selection medium was replaced every 4 days. Blasticidin-resistant cells were tested for H-2D^b expression by FACS analysis, and positive cells were subcloned to obtain monoclonal cells.

B27M2, BC2P6, and B7H6 cells were stably transfected with H-2D^b plasmid and either hygromycin or puromycin resistance plasmids, according to the manufacturer's protocol (FuGENE 6; Roche, Basel, Switzerland). Clonal and selection drug-resistant cells were tested for H-2D^b expression by flow cytometry.

LacZ assay

For the lacZ assay, 5×10^4 LCMVgp33–41/H-2K^b- or LCMVgp276–286/H-2D^b-specific T cell hybridomas (15) were cocultured overnight with

2.5×10^4 stimulator cells in 96-well plates. As stimulator cells, MCGP, B8Db, B27M6Db, B27M2Db, BC2P6Db, B7H6Db, and PB$\alpha\beta$13Db, or thioglycolate-elicited peritoneal macrophages from C57BL/6, LMP2$^{-/-}$, or LMP7$^{-/-}$ mice were used. MCGP cells were treated for 3 days with 60 U/ml murine rIFN-γ (Roche) to allow a complete replacement of constitutive proteasomes by immunoproteasomes (19). The lacZ-based color reaction was performed and measured, as detailed elsewhere (15).

Restimulation and cytolytic assay

B6, LMP2$^{-/-}$, and LMP7$^{-/-}$ mice were infected with 2×10^6 VVG2 i.p. Six days later, 4×10^6 splenocytes were cocultured with 2×10^6 peptide-loaded (gp33–41 or gp276–286) irradiated (2000 rad) syngeneic splenocytes in 2 ml of IMDM supplemented with 10% FCS, penicillin/streptomycin, 2-ME, and 10% Con A supernatant (Con A-induced rat spleen culture supernatant) in 24-well plates. After 6 days of culture, a standard ^{51}Cr release assay with peptide (gp33–41 or gp276–286)-loaded (10^{-6} M) or unloaded MC57 cells was performed. In brief, target cells were incubated with $Na_2{}^{51}CrO_4$ ± peptide for 90 min. Three-fold dilutions of the restimulated cultures were tested for cytotoxic activity using 10^4 ^{51}Cr-labeled MC57 as targets in a 5-h chromium release assay. The percentage of specific lysis was calculated as follows: percentage of specific release = (experimental release –spontaneous release) ÷ (maximal release –spontaneous release) × 100%. The spontaneous lysis was below 15%; the lysis of unloaded targets was below 10%.

Intracellular staining for IFN-γ

A total of 2×10^6 splenocytes was incubated in round-bottom 96-well plates with 10^{-7} M of the specific peptide in 100 μl of 10% IMDM for 2 h at 37°C. Then brefeldin A (10 μg/ml) was added, and the incubation was continued for another 4 h. Cells were incubated for 20 min at 4°C with Cy5-conjugated mouse anti-CD8 (clone 53-6.7; BD Pharmingen). Following fixation with 4% paraformaldehyde at 4°C for 5 min, the cells were incubated overnight with fluorescein-conjugated mouse anti-IFN-γ (clone XMG1.2; BD Pharmingen) in PBS containing 2% FCS and 0.1% (w/v) saponin (Sigma-Aldrich, St. Louis, MO). Samples were washed twice, acquired with the use of FACScan flow cytometer (BD Biosciences), and analyzed by the FlowJo software (Tree Star).

Metabolic labeling, immunoprecipitation, and two-dimensional gel electrophoresis

A total of 10^7 thioglycolate-elicited peritoneal macrophages from BALB/c mice was starved in cysteine/methionine-free RPMI 1640, 10% dialyzed FCS for 1 h at 37°C and labeled with 0.2 mCi/ml Met-[^{35}S]-label (Hartmann Analytic, Braunschweig, Germany) for 8 h to allow full maturation of the proteasome. Cells were washed with PBS, harvested, and lysed for 30 min on ice in 20 mM Tris/HCl, pH 7.5, 150 mM NaCl, 1 mM $MgCl_2$, and 2% Triton X-100. The lysate was precleared for 1 h with protein A-Sepharose CL-4B (Amersham Biosciences, Uppsala, Sweden), followed by overnight immunoprecipitation with an antiproteasome serum bound to protein A-Sepharose at 4°C. The precipitates were washed four times with NET-TON (650 mM NaCl, 5 mM EDTA, 50 mM Tris-HCl, 0.5% Triton-X-100, 0.05% NaN_3, 1 mg/ml OVA) and twice with NET-T (150 mM NaCl, 5 mM EDTA, 50 mM Tris-HCl, 0.5% Triton X-100, 0.05% NaN_3), and separated by nonequilibrium pH-gradient gel electrophoresis/SDS-PAGE, as previously described (28), and visualized by autoradiography on a Fuji BAS1500 radioimager.

Purification of 20S proteasome

The lysis of organ tissue, the purificaton of 20S proteasomes from liver, and the quantification of the 20S proteasome from uninfected and LCMV-infected (8 days postinfection with 200 PFU of LCMV-WE i.v.) C57BL/6, LMP2$^{-/-}$, and LMP7$^{-/-}$ mouse livers were performed, as previously described (28).

Proteasomal fragmentation of polypeptide and mass spectrometric analysis of peptide products

Digestions of the 25-mer polypeptide spanning LCMV-WE glycoprotein residues 271–295 with purified 20S proteasomes were performed for indicated time periods exactly as previously described (19). HPLC-electrospray ionization mass spectrometry (ESI-MS) analysis was performed on a Q-Trap mass spectrometer (Applied Biosystems, Concord, Canada) equipped with Turbospray Ion Source (Applied Biosystems) and Agilent (Palo Alto, CA) 1100 HPLC system (Autosampler G1313A, Binary Pump G1312A, on-line vacuum degasser G1322A), ACCURATE flow splitter AC-100-VAR with 0.3 mm I.D. splitter capillary CAL-100-0.3 (LC Packings, Amsterdam, Holland), and control software: Analyst 1.3.2 (Applied Biosystems) under Windows 2000 operating system. HPLC conditions: mobile phase solvent A 0.1% aqueous solution of HCOOH, solvent B 0.1% solution of HCOOH in acetonitrile with following gradient: 0 min, 0% B; 4 min, 0% B; 44 min, 80% B. Binary pump flow 100 μl/min and after splitting (on column) 4–10 μl/min. The HPLC column was PepMap C18, 3 μm, 100 Å, 300 μm I.D. × 5 cm (LC Packings). MS conditions: scan type: enhanced MS; positive mode; mass range 340-1400 amu; declustering potential 30 V; entrance potential 10 V; curtain gas 20 PSI; ion source gas 1: 15 PSI; ion spray voltage 5000 V; source temperature 200°C. Sample injection volume 1 μl.

Results

Effect of IFN-γ on the presentation of gp33–41 and gp276–286

The stimulation of cells with IFN-γ strongly induces many proteins along the MHC class I presentation pathway, thus leading to a marked up-regulation of class I cell surface expression (16). When we infected the C57BL/6-derived mouse fibroblast line MC57 with the LCMV strain WE and treated the cells with or without murine IFN-γ for 3 days, we observed that IFN-γ caused a 2- to 3-fold up-regulation in the presentation of the immunodominant epitope gp33 as determined with a gp33-specific T cell hybridoma in a lacZ-based colorigenic assay (37) (Fig. 1A). Despite a ~10-fold increase of bulk H-2D^b and H-2K^b class I cell surface expression (data not shown), the presentation of the subdominant gp276 epitope was consistently down-regulated by IFN-γ treatment by a factor of ~2 in the same assay. Although we confirmed that the cells were equally infected with LCMV by determining the cell surface expression of the LCMV glycoprotein by flow cytometry (data not shown), we wanted to rule out that the obtained result is linked to IFN-γ-dependent changes in viral replication and Ag production. We hence repeated this experiment with the MCGP line, which is a stable MC57 transfectant expressing the LCMV glycoprotein. Also in this virus-independent model, we observed an IFN-γ-dependent up-regulation of gp33 presentation, whereas presentation of the gp276 epitope was markedly reduced (Fig. 1*B*).

Effect of the immunoproteasome subunits LMP2, LMP7, and MECL-1 as well as PA28$\alpha\beta$ on the presentation of gp276–286

Numerous gene products are induced with IFN-γ, which could account for an enhancement of gp33 presentation, but only few candidates are known that could be responsible for the down-regulation of gp276 presentation. Given that immunoproteasomes have been shown to interfere with the presentation of some tumor epitopes (22), we examined whether the IFN-γ-inducible proteasome subunits LMP2, LMP7, and MECL-1, or the IFN-γ-inducible proteasome activator PA28$\alpha\beta$ could mediate the observed down-regulation of gp276 presentation. Previously, we have generated and carefully characterized stable transfectants of the mouse fibroblast line B8, which coexpress either all three active site subunits of immunoproteasomes (designated B27M6 or B27M2) or the α- and β-subunits of the proteasome regulator PA28$\alpha\beta$ (designated BP$\alpha\beta$13) to the same degree as B8 fibroblasts after 3 days of IFN-γ treatment (19). Because the recipient line B8 is derived from a BALB/c mouse (H-2^d), we supertransfected the recipient line B8 as well as B27M6 and BP$\alpha\beta$13 cells with an expression construct encoding the H-2D^b restriction element. Clones named B8Db, B27M6Db, B27M2Db, and BP$\alpha\beta$13Db, respectively, were selected that, according to flow cytometry, expressed similar levels of H-2D^b class I molecules on the cell surface (Fig. 2*B*). Interestingly, when these clones were infected for 1.5 days with LCMV-WE and examined for gp276 presentation with our gp276/H-2D^b-specific hybridoma, we found that the combined overexpression of LMP2, LMP7, and MECL-1 in B27M6Db and B27M2Db cells reduced gp276 presentation 2- to 3-fold compared

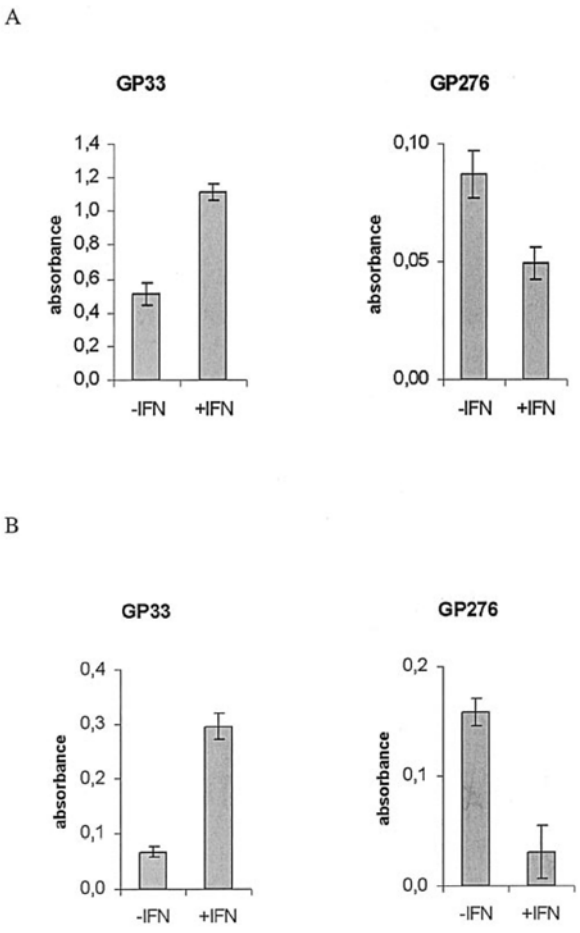

FIGURE 1. Comparison of the presentation of the LCMV epitopes gp33 and gp276 in ±IFN-γ-treated and LCMV-infected MC57 cells (*A*) and the LCMV glycoprotein transfectant MCGP (*B*). Stimulator cells were treated for 3 days with 60 U/ml IFN-γ or left untreated, and LCMV infection was performed in vitro a few hours before initiation of IFN-γ treatment. The stimulation of gp33- and gp276-specific T cell hybridomas was determined in chromogenic lacZ assays. The *y*-axis shows absorbance of enzymatically converted chromogen at 570 nm in lacZ assays. The values are means of three replicate cultures; shown is a representative experiment of three experiments that yielded similar results. Error bars represent SDs.

with B8Db cells, whereas PA28$\alpha\beta$ overexpression had only a minor effect (Fig. 2, *A* and *C*). This result, which was confirmed with independent clones, strongly suggested that the induction of immunoproteasomes is at least in part responsible for the IFN-γ-mediated down-regulation of gp276.

To investigate the effect of LMP2 only and LMP7 only, we stably supertransfected the well-characterized cell lines BC2P6 (B8 cell-overexpressing LMP2) and B7H6 (B8 cell-overexpressing LMP7) (28) with an expression construct encoding the H-2D^b restriction element (Fig. 2, *C* and *D*). These clones were infected with LCMV, and the presentation of gp276 was examined with gp276/H-2D^b-specific hybridomas. Cells overexpressing LMP7 showed no altered presentation of gp276 compared with the parental cells (Fig. 2*C*). In contrast, LMP2 overexpression reduced gp276 presentation ~4-fold, which indicates that the reduced presentation of gp276 in LMP2/LMP7/MECL-1 cells (Fig. 2, *A* and *C*) is mainly due to LMP2.

Comparison of gp33 and gp276 presentation by LCMV-infected macrophages from C57BL/6, LMP2$^{-/-}$, and LMP7$^{-/-}$ mice

To confirm this effect of immunoproteasomes in an independent system and to discriminate whether LMP2 or LMP7 contributes to down-regulation of gp276 presentation, we examined Ag presentation by LCMV-infected thioglycolate-elicited peritoneal macrophages from LMP2$^{-/-}$ and LMP7$^{-/-}$ gene-targeted as well as C57BL/6 control mice. The peritoneal macrophages were infected in vitro for 20 h with LCMV-WE and analyzed for gp33 and gp276 presentation with the respective T cell hybridomas (Fig. 3) using peptide-pulsed MC57 cells as specificity controls (*lanes 1* and *2*) and uninfected peritoneal macrophages from C57BL/6, LMP2$^{-/-}$, and LMP7$^{-/-}$ mice as negative controls (*lanes 3–5*). Although no difference in gp33 presentation was found between C57BL/6 and LMP2$^{-/-}$ macrophages, gp33 presentation was reduced by ~50% in LCMV-WE-infected macrophages from LMP7$^{-/-}$ mice. This result suggests that the induction of LMP7, but not of LMP2, contributes to the IFN-γ-dependent enhancement of gp33 presentation (Fig. 1*A*). The presentation of gp276, in contrast, seems to benefit from the deficiency of LMP7 and to a minor extent from LMP2 as macrophages from the respective knockout mice stimulated gp276-specific hybridomas better than macrophages from the wild-type control. This result is consistent with the aforementioned reduction in gp276 presentation caused by immunoproteasome overexpression (Fig. 2*B*).

To address to which extent LMP2 and LMP7 are expressed in thioglycolate-elicited peritoneal macrophages, these cells were metabolically labeled with [^{35}S]Met/Cys. The proteasomes were immunoprecipitated and the subunit composition was analyzed by nonequilibrium pH-gradient gel electrophoresis/SDS-PAGE. LMP7 (bearing 15 Met/Cys in the primary structure) was prominently expressed in thioglycolate-elicited peritoneal macrophages, as evidenced by the intensity of the LMP7 spots, and the virtually complete replacement of the homologous subunit MB-1 (bearing 9 Met/Cys). LMP2 (bearing 8 Met/Cys), in contrast, was expressed to a lesser extent according to the low spot intensity and the prevalence of its constitutive homologue δ (containing 11 Cys/Met) (Fig. 3*B*). This might explain the only minor effect of LMP2 deficiency on gp276 presentation by peritoneal macrophages.

The generation of gp276-specific CTLs is improved in LMP2$^{-/-}$ and LMP7$^{-/-}$ mice

To investigate how LMP2 and LMP7 would affect the CTL response to gp33, gp276, and NP396 in vivo, we first infected LMP2$^{-/-}$, LMP7$^{-/-}$, and PA28$\alpha\beta^{-/-}$ knockout as well as C57BL/6 control mice with LCMV. However, standard ^{51}Cr release assays performed on day 8 postinfection with peptide-loaded target cells did not detect significant differences between these mice strains irrespective of whether we infected with LCMV-WE or LCMV-Armstrong (data not shown). Moreover, virus titers in the spleen obtained on day 4 postinfection were not different in control and knockout mice (Table I). These results are not unexpected given that LCMV replicates very fast in numerous mouse tissues to high titers and overwhelms the organism with viral Ags. Hence, we turned to infection of these mice with rVVG2. VV replicates much slower in mice, and therefore produces a lower amount of Ag. Splenocytes from rVVG2-infected mice were harvested on day 6 after infection, and the CTLs were restimulated in vitro for another 6 days before they were used as effectors in a chromium release assay. As shown in Fig. 4*A*, the lysis of targets loaded with the gp276 peptide by LMP2$^{-/-}$ and LMP7$^{-/-}$ effectors was much higher (40–75%) as compared with CTLs from C57BL/6 mice (15–25%). This indicates that, in agreement with

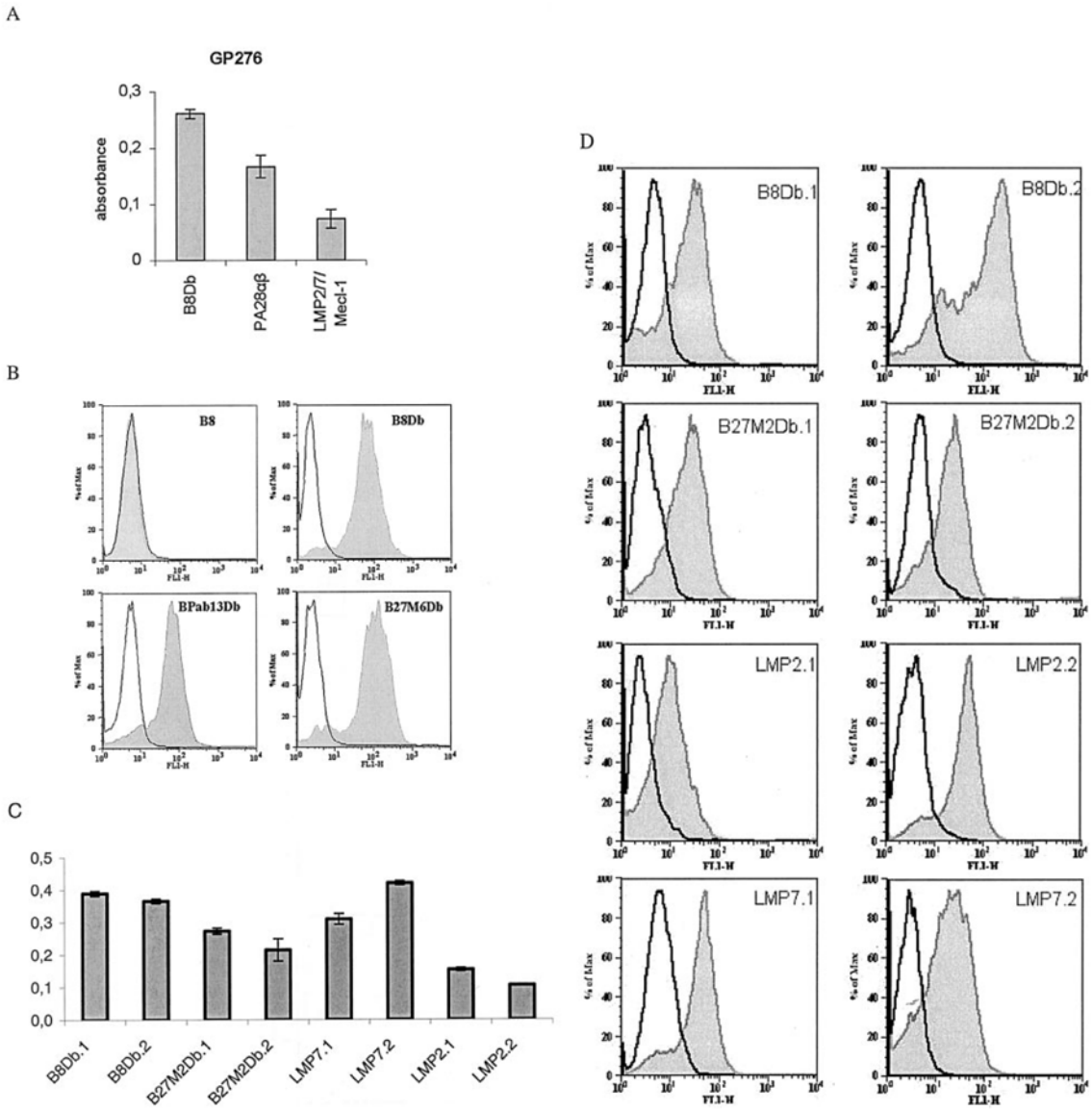

FIGURE 2. *A*, Comparison of the presentation of the LCMV-GP276 epitope by stable cell lines transfected with expression constructs for the restriction element H-2D^b as well as LMP2/LMP7/MECL-1 (B27M6Db) or PA28α and β (BP$\alpha\beta$13Db); B8Db are recipient cells only transfected for H-2D^b. The stimulator cells were infected with LCMV-WE in vitro 24 h before incubation with the gp276-specific hybridoma. The *y*-axis represents absorbance of enzymatically converted chromogen at 570 nm in lacZ assays. The values are the means of three replicate cultures; shown is a representative experiment of three experiments with similar outcome. Error bars represent SDs. *B* and *D*, To verify that H-2D^b cell surface expression was roughly equivalent in the different transfectants, a flow cytometric analysis was performed before every assay. *C*, Comparision of the presentation of gp276 epitope by stable cell lines transfected with H-2D^b (B8Db) as well as LMP2/LMP7/MECL-1 (B27M2Db), LMP7, or LMP2. The stimulator cells were infected with LCMV-WE in vitro 24 h before incubation with the gp276-specific hybridoma. The *y*-axis represents absorbance of enzymatically converted chromogen at 570 nm in lacZ assays. Two independent clones are shown for each transfection construct. The values are the means of three replicate cultures; shown is a representative experiment of three experiments with similar outcome. Error bars represent SDs.

our in vitro data, the gp276 epitope became immunodominant in the absence of either LMP2 or LMP7. The lysis of gp33-loaded targets varied between 20 and 40% for all mice, thus indicating that the replacement of constitutive proteasomes by immunoproteasomes did not significantly affect the generation of gp33-specific CTLs. Even with this more sensitive in vivo system, we failed to detect any differences between PA28$\alpha\beta^{-/-}$ and C57BL/6 wild-type mice with respect to the generation of either gp33- or gp276-specific CTLs (data not shown).

To confirm the observed enhancement in the generation of gp276-specific CTLs in LMP2- and LMP7-deficient mice, we performed double stainings of splenocytes from LMP2$^{-/-}$, LMP7$^{-/-}$, and C57BL/6 control mice for CD8 on the cell surface and for the intracellular content of IFN-γ (intracellular cytokine staining) on day 7 after infection with rVVG2. Also with this ex vivo assay, we observed that the generation of gp276-specific precursors was clearly enhanced in LMP2$^{-/-}$ and LMP7$^{-/-}$ mice (Fig. 4, *B* and *C*). In contrast, there was no difference in the

A

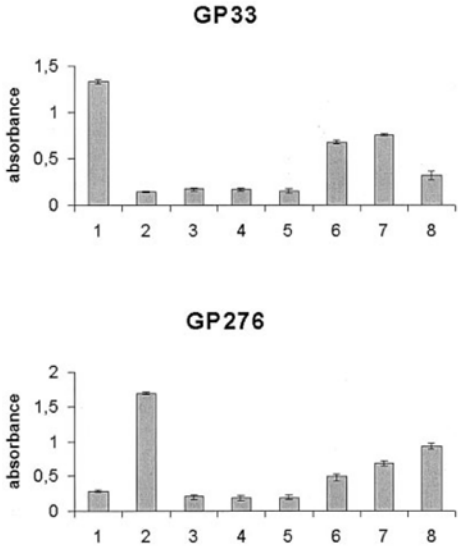

B

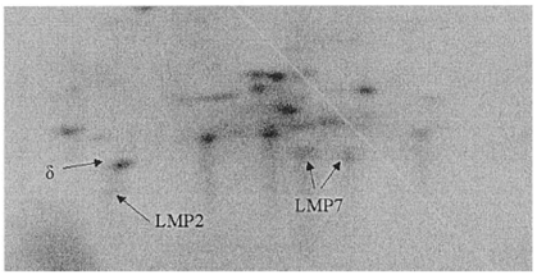

FIGURE 3. *A*, Presentation of gp33–41 and LCMV-gp276–286 epitopes by LCMV-infected macrophages from C57BL/6, LMP2$^{-/-}$, and LMP7$^{-/-}$ mice. Peritoneal macrophages were infected with LCMV-WE in vitro 1 day before addition of T cell hybridomas specific for gp33 (*upper panel*) or gp276 (*lower panel*); peptide-loaded MC57 cells served as specificity controls. The *y*-axis shows absorbance of enzymatically converted chromogen at 570 nm in lacZ assays. The values are the means of three replicate cultures. Error bars represent SDs. *Lane 1*, gp33-pulsed MC57; *lane 2*, gp276-pulsed MC57; *lane 3*, uninfected C57BL/6 macrophages; *lane 4*, uninfected LMP2$^{-/-}$ macrophages; *lane 5*, uninfected LMP7$^{-/-}$ macrophages; *lane 6*, infected C57BL/6 macrophages; *lane 7*, infected LMP2$^{-/-}$ macrophages; *lane 8*, infected LMP7$^{-/-}$ macrophages. The experiment has been repeated twice, giving similar results. *B*, Subunit composition of proteasomes from thioglycolate-elicited peritoneal macrophages. Thioglycolate-elicited peritoneal macrophages were metabolically labeled with [^{35}S]methionine/cysteine. Proteasomes were immunoprecipitated and analyzed for subunit composition on two-dimensional gels by autoradiography. LMP7, LMP2, as well as its constitutive homologue δ are labeled.

generation of gp33-specific CTLs in LMP2- and LMP7-deficient mice, compared with wild-type C57BL/6 mice (Fig. 4*B*). Taken together, it appears that the down-regulation of gp276 epitope presentation through LMP2 and LMP7 in vitro nicely correlates with an enhanced CTL elicitation in the respective gene-targeted mice.

Table I. *LCMV titers in spleen samples from C57BL/6, LMP2$^{-/-}$, and LMP7$^{-/-}$ mice 4 days after infection with 200 PFU of LCMV-WE*[a]

Mouse Strain	LCMV Titer
C57BL/6	$4.0 \pm 0.9 \times 10^5$
LMP2$^{-/-}$	$3.9 \pm 0.9 \times 10^5$
LMP7$^{-/-}$	$7.0 \pm 2.6 \times 10^5$

[a] Titers are given in PFU LCMV-WE per spleen.

The generation of Vβ10b-specific CTLs is impaired in LCMV-infected LMP2- and LMP7-deficient mice

To investigate whether the improved generation of gp276-specific CTLs in LMP2- and LMP7-deficient mice is due to an altered CTL repertoire, splenocytes from naive and LCMV-WE-infected (8 days postinfection with 200 PFU of LCMV-WE) C57BL/6, LMP2$^{-/-}$, and LMP7$^{-/-}$ mice were stained with different TCR-Vβ-specific Abs (Fig. 5). There was a significant difference (2% less) of Vβ8.1/8.2-specific CD8-positive cells in naive LMP2-deficient mice compared with C57BL/6 and LMP7-deficient mice. After LCMV infection, no difference could be detected for Vβ8. Naive LMP7$^{-/-}$ mice showed a slight, but significant difference for Vβ9-specific CTLs, which was abolished after LCMV infection. It has been shown that T cell lines specific for gp276 were using exclusively the Vβ10 variable segment for their TCRs (38). Naive LMP2$^{-/-}$ and LMP7$^{-/-}$ mice showed no difference in Vβ10 usage compared with C57BL/6. In contrast, after LCMV infection, the extent of CTLs using Vβ10 was significantly increased in C57BL/6 mice compared with LMP2- and LMP7-deficient mice.

In vitro fragmentation of the gp271–295 polypeptide by immunoproteasomes and constitutive proteasomes as well as LMP2- and LMP7-deficient proteasomes

Given that the generation of the gp276 epitope is dependent on proteasome activity (19), we hypothesized that gp276 presentation is adversely affected by LMP2 and LMP7 because constitutive proteasomes and immunoproteasomes fragment precursor polypeptides of gp276 in a different way. To test this hypothesis, we investigated how immunoproteasomes and constitutive 20S proteasomes fragment the 25-mer precursor polypeptide covering residues 271–295 of the LCMV-WE glycoprotein (NH_2-TLSDSS GVEDPGGYCLTKWMILAAE-COOH), which contains the underlined 11-meric gp276–286 epitope bearing an aspartate in position 5, which resulted from rapid deamidation of asparagine after systhesis (Fig. 6*A*). We isolated 20S proteasomes from the liver of uninfected mice as a source of constitutive proteasomes. Immunoproteasomes were isolated from the liver of mice on day 8 after LCMV infection. The subunit composition of the two proteasome populations on two-dimensional gels confirmed our previous finding that LCMV infection results in a virtually complete replacement of constitutive proteasomes by immunoproteasomes in vivo (39) (data not shown). The separation of the produced fragments after 8 h of in vitro digest by HPLC shows that constitutive proteasomes and immunoproteasomes fragment the 25-mer polypeptide in a different manner, and these differences in the HPLC profiles were confirmed in several independent experiments (Fig. 6*B*). The fragmentation was not observed in the presence of the proteasome inhibitor lactacystin, suggesting that 20S proteasomes were not contaminated by other proteases (data not shown). The time period of 8 h was chosen because the 25-mer substrate eluting late in the gradient is still by far the predominant peptide and the relative intensities of emerging peaks remained the same over a

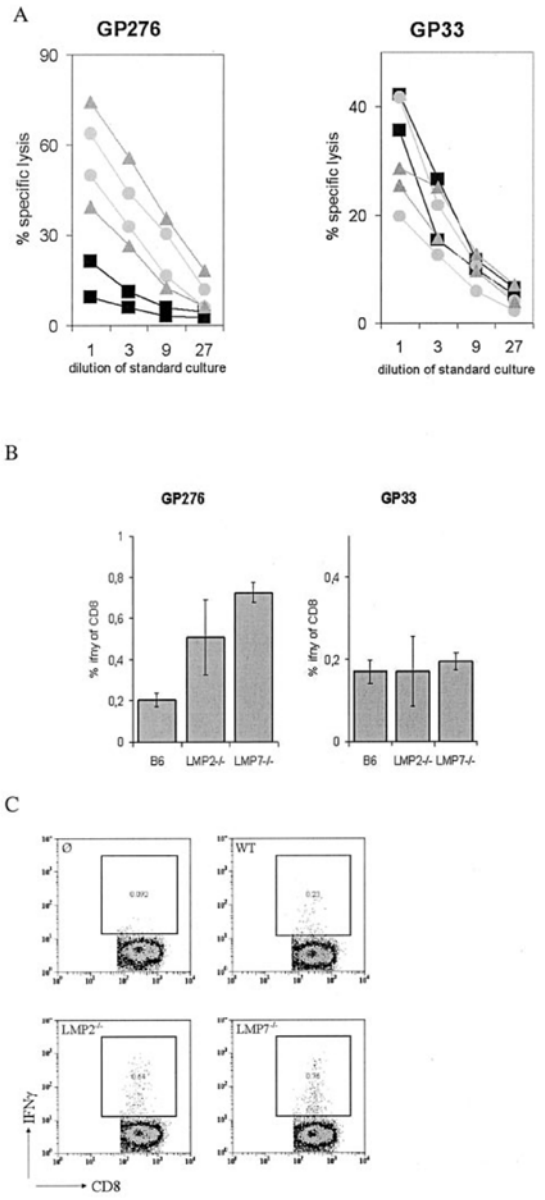

FIGURE 4. Generation of gp33–41- and gp276–286-specific CTLs in LMP2$^{-/-}$, LMP7$^{-/-}$, and C57BL/6 mice. *A*, LMP2$^{-/-}$ mice (circles), LMP7$^{-/-}$ mice (triangles), and C57BL/6 wild-type mice (squares) were infected i.p. with 2×10^6 PFU of rVVG2. Six days after infection, splenocytes were restimulated in vitro with gp33 or gp276 peptide-loaded, irradiated spleen cells. After 6 days, the restimulated spleen cells were used as effectors in a cytolytic assay. As targets, MC57 cells were used after loading with the synthetic epitopes gp276 (*left panel*) and gp33 (*right panel*). The percentage of specific lysis is plotted vs the dilution of restimulation culture. Duplicates were taken for all data points. *B*, B6, LMP2$^{-/-}$, and LMP7$^{-/-}$ mice were infected with 2×10^6 PFU of VVG2 i.p.; 7 days later, the VVG2-induced gp33–41- and gp276–286-specific CTL response was measured in the spleen by staining for CD8 and intracellular IFN-γ. Shown are the percentages of IFN-γ-positive cells of CD8$^+$ cells as determined by flow cytometry. Error bars represent SDs. The experiments have been repeated three times, yielding similar results. *C*, FACS plots of VVG2-infected C57BL/6 (wild type), LMP2$^{-/-}$, and LMP7$^{-/-}$ mice after 5-h in vitro stimulation with gp276. ∅, Represents a VVG2-infected mouse without in vitro peptide stimulation. The *y*-axis shows intracellular IFN-γ produced by CD8-positive (*x*-axis) splenocytes.

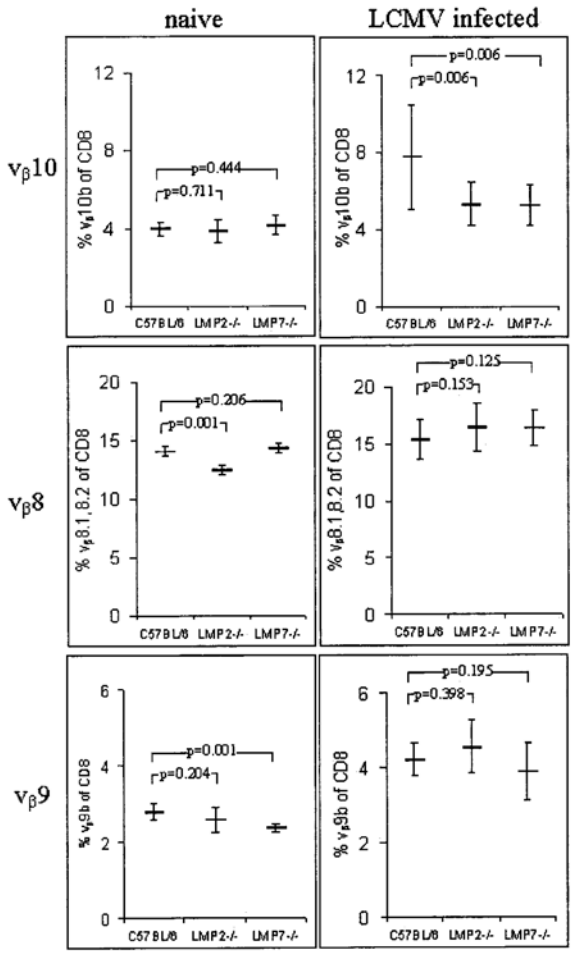

FIGURE 5. Analysis of Vβ variable segments of TCRs from C57BL/6, LMP2$^{-/-}$, and LMP7$^{-/-}$ mice. Splenocytes from naive or LCMV-infected (8 days postinfection with 200 PFU of LCMV-WE i.v.) mice were stained for CD8 and Vβ8.1/8.2, Vβ9, or Vβ10b, and analyzed by flow cytometry. Values are the means of 7 (naive) or 12 (infected) mice from two independent experiments. Values of p were determined by unpaired t test and are considered to be statistically significant when $p < 0.05$.

digestion period of up to 8 h. A further fragmentation of primary fragments was therefore unlikely to occur.

To obtain at least semiquantitative information on how the 25-mer precursor was differentially fragmented by constitutive proteasomes and immunoproteasomes, the fragments of the same digest as shown in Fig. 6*B* were analyzed by ESI-MS. A comparison of the peak intensities of ion currents from selected fragments, which could be unambiguously identified by their mass, revealed that the 11-mer epitope (residues 276–286) as well as a putative 12-mer precursor of the latter (residues 275–286) were made in greater quantity by constitutive proteasomes, whereas fragments that resulted from cleavages within the epitope (residues 280–291 and 281–289) were produced in greater amounts by immunoproteasomes (Fig. 6*C*). These data are in accordance with our Ag presentation assays, as they suggest that immunoproteasomes preferentially destroy the gp276 epitope and their precursors, whereas constitutive proteasomes are able to proteolytically generate these peptides in greater amounts.

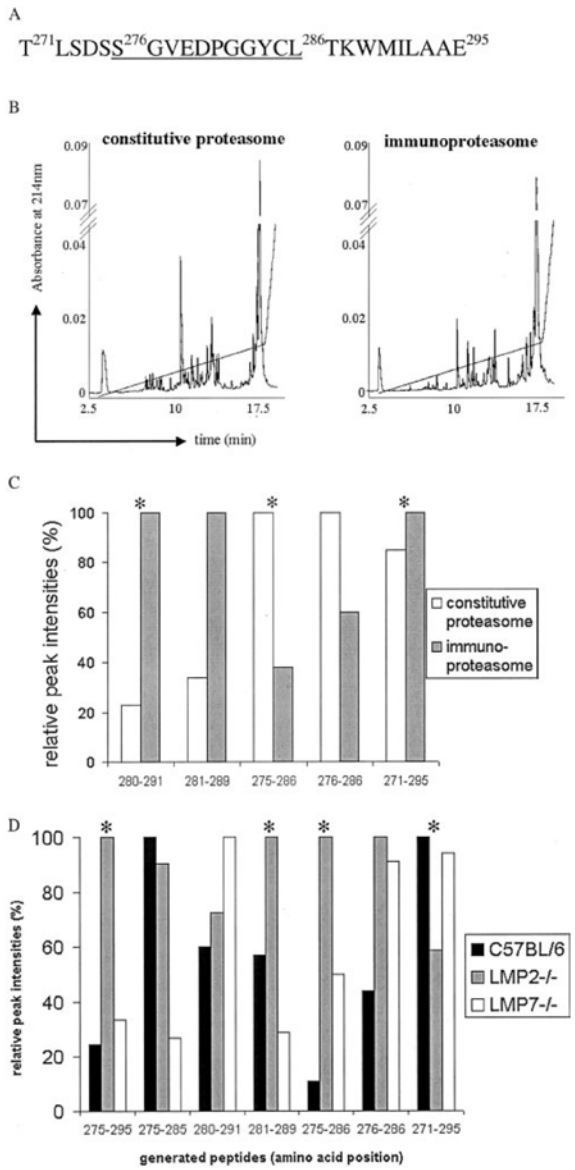

FIGURE 6. Comparison of selected fragments produced from an LCMV-gp 25-mer polypeptide by proteasome in vitro digestions. The 25-mer gp271–296 polypeptide was digested with purified 20S constitutive proteasomes and immunoproteasomes for 8 h and analyzed by HPLC-ESI-MS. *A*, Amino acid sequence of the 25-mer polypeptide containing the CTL epitope gp276–286 (underlined). *B*, Representative HPLC profiles of 25-mer polypeptide in vitro digestions (8 h) by 20S constitutive proteasome or immunoproteasome. Note that the peaks of the educt 25-mer polypeptide are of similar intensity. *C*, Comparison of selected fragments produced in the digests shown in *B*, as analyzed by HPLC-ESI-MS. The integrals of the peaks from the extracted ion chromatograms of the analyzed fragments obtained from digests by constitutive proteasomes and immunoproteasomes were compared and are shown as relative peak intensities. Peptide fragments indicated by stars represent major fragments (*D*). Comparison of selected fragments of a 25-mer (gp271–295) polypeptide in vitro digest, as analyzed by HPLC-ESI-MS with proteasome isolated from livers of LCMV-WE-infected LMP2$^{-/-}$, LMP7$^{-/-}$, and C57BL/6 mice. The integrals of the peaks from the extracted ion chromatograms of the analyzed fragments obtained from digests by proteasome isolated from livers of LCMV-WE-infected LMP2$^{-/-}$, LMP7$^{-/-}$, and C57BL/6 mice were compared and are shown as relative peak intensities. Peptide fragments indicated by stars represent major fragments.

To address the effect of LMP2 only and LMP7 only, 20S proteasome was isolated from liver of LCMV-infected LMP2- and LMP7-deficient mice. Two-dimensional gels confirmed that the two other immunoproteasome subunits were induced (data not shown). Analysis of how the 25 mer was fragmented was obtained exactly as in Fig. 6*C*. The LCMV-derived epitope gp276–286 and its putative precursor gp275–286 were produced in larger amounts by LMP2- and LMP7-deficient immunoproteasome compared with normal immunoproteasome (Fig. 6*D*), which is in accordance with the results obtained in Fig. 4, in which LMP2- and LMP7-deficient mice elicited a stronger CTL response against gp276 than wild-type mice.

Discussion

Immunodominance is an inherent and frequently observed phenomenon associated with T cell responses to viruses and other pathogens. The reason that CTLs are emerging in great numbers to only one or a few epitopes while CTLs to other potential epitopes are virtually not detectable has been profoundly investigated in the LCMV system, but the phenomenon remains poorly understood (2, 8, 9–12). Recently, it has been shown that the immunodominance of an antiviral CTL response can be shaped by the kinetics of viral protein expression (40). Nevertheless, it is still not clear why gp276 is a subdominant epitope in C57BL/6 mice after infection with LCMV. The affinity of gp276 for the peptide-binding groove of H-2D^b seems superior to that of gp33 because a ~10-fold lower concentration of gp276 was required to achieve optimal lysis (10, 11). Also, the recognition and elimination of LCMV-infected target cells by gp276-specific CTLs seem to be more efficacious compared with gp33-specific CTLs, as evidenced by adoptive transfer experiments, thus indicating that the binding of the gp276-specific TCRs to H-2D^b/gp276 complexes on the surface of LCMV-infected cells is not a limitation (11). A factor that was shown to be a determinant of immunodominance at least in influenza infection is the availability of specific CTLs in the repertoire of peripheral T cell specificities (3, 25). T cell lines specific for gp276 were strongly biased for the usage of Vα4 and Vβ10 variable segements for their TCRs (38), but it has not been investigated whether this bias imposes a limit on the availability of gp276-specific T cells in the repertoire.

Finally, gp33, gp276, and NP396 epitopes were eluted from H-2D^b proteins of LCMV-infected MC57 fibroblast cells, and the approximate number of epitopes per cell was determined. The calculated numbers were 1080 for gp33, 92 for gp276, and 162 for NP396, which implies that the copies of gp276 and NP396 epitopes generated in MC57 cells and presented on the cell surface are in a range, in which recognition by CTLs could become limiting (13, 14). However, it must be pointed out that MC57 cells infected with LCMV in vitro may not be representative for the physiological situation because infected cells in vivo are confronted with IFN-γ produced by NK cells and Th1 cells, which has dramatic effects on the class I processing and presentation pathway. In particular, we have shown that the infection of mice with LCMV, with mouse CMV, or with *Listeria monocytogenes* results in an IFN-γ-dependent and almost complete replacement of constitutive proteasomes by immunoproteasomes in the liver as well as other organs on day 7 or 8 after infection (39) (our unpublished data). We found that MC57 fibroblasts, even when they were infected with LCMV in vitro and hence produced type I IFNs, expressed mostly constitutive proteasomes (39). Moreover, not fibroblasts, but dendritic cells are the crucial APCs in the priming phase of the immune response, and these were shown to express high levels of immunoproteasomes (41, 42).

Hence, we set out to investigate immunoproteasomes as determinants of epitope hierarchy in the LCMV system. Our finding that IFN-γ treatment of MC57 cells resulted in enhanced gp33 presentation, whereas gp276 presentation was reduced (Fig. 1), inspired us to perform the experiments described in this work. An in vivo correlate to this finding has recently been reported by Rodriguez et al. (43), who showed that gp276-specific CTLs are much more prominent in IFN-γ-deficient mice, but the gp33-specific CTL response was improved in these mice as well. Another interesting phenomenon was reported by Butz and Bevan (44). They noted that when CTLs from LCMV-infected C57BL/6 mice were weekly restimulated in vitro by LCMV-infected MC57 cells, gp276-specific CTLs outgrew gp33- and NP396-specific cells within 3 wk. However, when the restimulation was performed with the dendritic cell line JawsII, gp276-specific CTLs waned, and gp33- as well as NP396-specific CTLs predominated. Given that IFN-γ stimulation leads to an almost complete replacement of constitutive proteasomes by immunoproteasomes in mouse fibroblasts within 3 days and that dendritic cells constitutively express higher amounts of immunoproteasomes than fibroblasts, we hypothesized that immunoproteasomes may be responsible for both phenomena by down-regulating gp276 peptide presentation. This hypothesis turned out to be correct, as we have shown by two independent approaches. First, we demonstrated that the overexpression of the active site subunits of immunoproteasomes LMP2, LMP7, and MECL-1 in triple transfectants caused a 2- to 4-fold down-regulation of gp276 presentation in T cell hybridoma lacZ assays (Fig. 2, *A* and *C*). Second, we showed that LCMV-infected peritoneal macrophages from LMP7$^{-/-}$ mice and to a minor extent from LMP2$^{-/-}$ were better stimulators of gp276-specific T cell hybridomas than C57BL/6 wild-type macrophages. LMP2- and LMP7-overexpressing cells indicated that mostly LMP2 is responsible for the down-regulation of gp276 in LMP2, LMP7, and MECL-1 triple transfectant (Fig. 2*C*). Comparing the fragmentation of a gp276-containing polypeptide by constitutive proteasomes and immunoproteasomes in vitro suggests that immunoproteasomes produce less gp276 precursors and destroy the gp276 epitope more frequently than constitutive proteasomes through cleavages within the epitope (Fig. 6).

Taken together, it appears that the expression of LMP2 and LMP7 negatively affects the generation of the gp276 epitope. It is, however, not possible to assign this effect to one of the subunits exclusively because their incorporation into the proteasome is to some extent interdependent. We have analyzed the subunit composition of 20S proteasomes purified from livers of LCMV-infected LMP2$^{-/-}$ and LMP7$^{-/-}$ as well as C57BL/6 wild-type mice on Coomassie-stained two-dimensional gels and found that LMP7 incorporation fully occurs in LMP2$^{-/-}$ mice in accordance with previous data (45–47). However, because the incorporation of the subunit MECL-1 barely occurs when LMP2 is missing, the effects observed in LMP2$^{-/-}$ mice could also be caused by a lack of MECL-1. In contrast, we found that the incorporation of LMP2 and MECL-1 in livers of LCMV-infected LMP7$^{-/-}$ mice occurs only to an extent of ~50%, which means that the more prominent enhancement of gp276 presentation in LMP7-deficient macrophages may at least in part be attributed to a reduction in LMP2 and MECL-1 incorporation (data not shown).

One consequence of our finding is that the number of 92 gp276 epitopes that Gallimore et al. (11) calculated to be presented by a single LCMV-infected MC57 cell will probably be much lower in cells containing immunoproteasomes, which almost completely replace constitutive proteasomes during LCMV infection in vivo. It is therefore not unexpected that the further down-regulation of gp276 epitopes by immunoproteasomes reduces gp276 epitope generation to an extent that puts a limit on the generation of gp276-specific CTLs in LCMV-infected mice. Nevertheless, the effect of immunoproteasomes on the generation of gp276-specific CTLs is not as prominent as we expected. It was not observed when LMP2$^{-/-}$ and LMP7$^{-/-}$ mice were infected with either the faster replicating WE strain or the slower replicating Armstrong strain of LCMV. However, when the mice were infected with rVVG2, which produces lower amounts of the LCMV glycoprotein, the impact of immunoproteasomes was nicely detectable (Fig. 4). We cannot rule out, however, that in addition to the effect on gp276 presentation, the greater number of gp276-specific CTLs in LMP2$^{-/-}$ and LMP7$^{-/-}$ knockout mice is due to a difference in the repertoire of peripheral T cells in these mice, as has been demonstrated for the influenza epitope NP366–374 in LMP2$^{-/-}$ mice (25). Differences in Vβ10 usage of LCMV-infected LMP2- and LMP7-deficient mice might indicate that an altered T cell repertoire of gp276-specific T cells exists in these mice (Fig. 5).

Still another interesting phenomenon observed in mice persistently infected with LCMV may be linked to our results. In two different models of chronic LCMV infection, it was recently found that the gp276 epitope that is subdominant in acute infection becomes the immunodominant epitope in chronically infected mice, whereas gp33 and NP396 drop deeply in epitope hierarchy (48, 49). Both research groups report that in chronic infection, the LCMV-specific CTLs stop to produce TNF-α and IFN-γ, which are the cardinal inducers of immunoproteasomes. We propose that this reversion in epitope hierarchy is at least in part due to a drop in the cellular content of immunoproteasomes.

Acknowledgments

We thank Dr. Tomoki Chiba and Dr. John Monaco for the contribution of mice, and Katrin Schwarz for the performance of some initial experiments. Dr. Cornelia Kolb is acknowledged for supplying purified proteasomes, and Dr. Frank Momburg for providing the H-2D^b expression construct. We are grateful to Eugene N. Damoc for help with mass spectroscopy.

References

1. Deng, Y., J. W. Yewdell, L. C. Eisenlohr, and J. R. Bennink. 1997. MHC affinity, peptide liberation, T cell repertoire, and immunodominance all contribute to the paucity of MHC class I-restricted peptides recognized by antiviral CTL. *J. Immunol. 158:1507*.
2. Gallimore, A., J. Hombach, T. Dumrese, H. G. Rammensee, R. M. Zinkernagel, and H. Hengartner. 1998. A protective cytotoxic T cell response to a subdominant epitope is influenced by the stability of the MHC class I/peptide complex and the overall spectrum of viral peptides generated within infected cells. *Eur. J. Immunol. 28:3301*.
3. Chen, W., L. C. Anton, J. R. Bennink, and J. W. Yewdell. 2000. Dissecting the multifactorial causes of immunodominance in class I-restricted T cell responses to viruses. *Immunity 12:83*.
4. Yewdell, J. T., and J. R. Bennink. 1999. Immunodominance in major histocompatibility complex class I-restricted T lymphocyte responses. *Annu. Rev. Immunol. 17:51*.
5. Townsend, A., J. Bastin, K. Gould, G. Brownlee, M. Andrew, B. Coupar, D. Boyle, S. Chan, and G. Smith. 1988. Defective presentation to class I-restricted cytotoxic T lymphocytes in vaccinia-infected cells is overcome by enhanced degradation of antigen. *J. Exp. Med. 168:1211*.
6. Rammensee, H. G., J. Bachmann, N. P. N. Emmerich, O. A. Bachor, and S. Stevanovic. 1999. SYFPEITHI: database for MHC ligands and peptide motifs. *Immunogenetics 50:213*.
7. Lanzavecchia, A., G. Iezzi, and A. Viola. 1999. From TCR engagement to T cell activation: a kinetic view of T cell behavior. *Cell 96:1*.
8. Slifka, M. K., J. N. Blattman, D. J. Sourdive, F. Liu, D. L. Huffman, T. Wolfe, A. Hughes, M. B. Oldstone, R. Ahmed, and M. G. Von Herrath. 2003. Preferential escape of subdominant CD8$^+$ T cells during negative selection results in an altered antiviral T cell hierarchy. *J. Immunol. 170:1231*.
9. Van der Most, R. G., A. Sette, C. Oseroff, J. Alexander, K. Murali-Krishna, L. L. Lau, S. Southwood, J. Sidney, R. W. Chestnut, M. Matloubian, and R. Ahmed. 1996. Analysis of cytotoxic T cell responses to dominant and subdominant epitopes during acute and chronic lymphocytic choriomeningitis virus infection. *J. Immunol. 157:5543*.
10. Van der Most, R. G., K. MuraliKrishna, J. L. Whitton, C. Oseroff, J. Alexander, S. Southwood, J. Sidney, R. W. Chesnut, A. Sette, and R. Ahmed. 1998. Identification of D-b- and K-b-restricted subdominant cytotoxic T- cell responses in lymphocytic choriomeningitis virus-infected mice. *Virology 240:158*.

11. Gallimore, A., T. Dumrese, H. Hengartner, R. M. Zinkernagel, and H.-G. Rammensee. 1998. Protective immunity does not correlate with the hierarchy of virus-specific cytotoxic T cell responses to naturally processed peptides. *J. Exp. Med. 187:1647*.
12. Weidt, G., O. Utermohlen, J. Heukeshoven, F. Lehmann-Grube, and W. Deppert. 1998. Relationship among immunodominance of single $CD8^+$ T cell epitopes, virus load, and kinetics of primary antiviral CTL response. *J. Immunol. 160:2923*.
13. Christinck, E. R., M. A. Luscher, B. H. Barber, and D. B. Williams. 1991. Peptide binding to class I MHC on living cells and quantitation of complexes required for CTL lysis. *Nature 352:67*.
14. Kageyama, S., T. J. Tsomides, Y. Sykulev, and H. N. Eisen. 1995. Variations in the number of peptide-MHC class I complexes required to activate cytotoxic T cell responses. *J. Immunol. 154:567*.
15. Schwarz, K., R. de Giuli, G. Schmidtke, S. Kostka, M. van den Broek, K. Kim, C. M. Crews, R. Kraft, and M. Groettrup. 2000. The selective proteasome inhibitors lactacystin and expoxomicin can be used to either up- or down-regulate antigen presentation at non-toxic doses. *J. Immunol. 164:6147*.
16. Groettrup, M., A. Soza, U. Kuckelkorn, and P. M. Kloetzel. 1996. Peptide antigen production by the proteasome: complexity provides efficiency. *Immunol. Today 17:429*.
17. Voges, D., P. Zwickl, and W. Baumeister. 1999. The 26S proteasome: a molecular machine designed for controlled proteolysis. *Annu. Rev. Biochem. 68:1015*.
18. Gileadi, U., H. T. MoinsTeisserenc, I. Correa, B. L. Booth, P. R. Dunbar, A. K. Sewell, J. Trowsdale, R. E. Phillips, and V. Cerundolo. 1999. Generation of an immunodominant CTL epitope is affected by proteasome subunit composition and stability of the antigenic protein. *J. Immunol. 163:6045*.
19. Schwarz, K., M. van den Broek, S. Kostka, R. Kraft, A. Soza, G. Schmidtke, P. M. Kloetzel, and M. Groettrup. 2000. Overexpression of the proteasome subunits LMP2, LMP7, and MECL-1 but not PA28α/β enhances the presentation of an immunodominant lymphocytic choriomeningitis virus T cell epitope. *J. Immunol. 165:768*.
20. Sijts, A. J. A. M., S. Standera, R. E. M. Toes, T. Ruppert, N. J. C. M. Beekman, P. A. vanVeelen, F. A. Ossendorp, C. J. M. Melief, and P. M. Kloetzel. 2000. MHC class I antigen processing of an adenovirus CTL epitope is linked to the levels of immunoproteasomes in infected cells. *J. Immunol. 164:4500*.
21. Schultz, E. S., J. Chapiro, C. Lurquin, S. Claverol, O. BurletSchiltz, G. Warnier, V. Russo, S. Morel, F. Levy, T. Boon, et al. 2002. The production of a new MAGE-3 peptide presented to cytolytic T lymphocytes by HLA-B40 requires the immunoproteasome. *J. Exp. Med. 195:391*.
22. Morel, S., F. Levy, O. BurletSchiltz, F. Brasseur, M. ProbstKepper, A. L. Peitrequin, B. Monsarrat, R. VanVelthoven, J. C. Cerottini, T. Boon, et al. 2000. Processing of some antigens by the standard proteasome but not by the immunoproteasome results in poor presentation by dendritic cells. *Immunity 12:107*.
23. Van Kaer, L., P. G. Ashton-Rickardt, M. Eichelberger, M. Gaczynska, K. Nagashima, K. L. Rock, A. L. Goldberg, P. C. Doherty, and S. Tonegawa. 1994. Altered peptidase and viral-specific T cell response in LMP 2 mutant mice. *Immunity 1:533*.
24. Fehling, H. J., W. Swat, C. Laplace, R. Kuehn, K. Rajewsky, U. Mueller, and H. von Boehmer. 1994. MHC class I expression in mice lacking proteasome subunit LMP-7. *Science 265:1234*.
25. Chen, W. S., C. C. Norbury, Y. J. Cho, J. W. Yewdell, and J. R. Bennink. 2001. Immunoproteasomes shape immunodominance hierarchies of antiviral $CD8^+$ T cells at the levels of T cell repertoire and presentation of viral antigens. *J. Exp. Med. 193:1319*.
26. Dubiel, W., G. Pratt, K. Ferrell, and M. Rechsteiner. 1992. Purification of an 11S regulator of the multicatalytic proteinase. *J. Biol. Chem. 267:22369*.
27. Chu-Ping, M., C. A. Slaughter, and G. N. DeMartino. 1992. Identification, purification and characterization of a protein activator (PA28) of the 20S proteasome (macropain). *J. Biol. Chem. 267:10515*.
28. Groettrup, M., T. Ruppert, L. Kuehn, M. Seeger, S. Standera, U. Koszinowski, and P. M. Kloetzel. 1995. The interferon-γ-inducible 11S regulator (PA28) and the LMP2/LMP7 subunits govern the peptide production by the 20S proteasome in vitro. *J. Biol. Chem. 270:23808*.
29. Groettrup, M., A. Soza, M. Eggers, L. Kuehn, T. P. Dick, H. Schild, H.-G. Rammensee, U. H. Koszinowski, and P.-M. Kloetzel. 1996. A role for the proteasome regulator PA28α in antigen presentation. *Nature 381:166*.
30. Schwarz, K., M. Eggers, A. Soza, U. H. Koszinowski, P. M. Kloetzel, and M. Groettrup. 2000. The proteasome regulator PA28α/β can enhance antigen presentation without affecting 20S proteasome subunit composition. *Eur. J. Immunol. 30:3672*.
31. Van Hall, T., A. Sijts, M. Camps, R. Offringa, C. Melief, P. M. Kloetzel, and F. Ossendorp. 2000. Differential influence on cytotoxic T lymphocyte epitope presentation by controlled expression of either proteasome immunosubunits or PA28. *J. Exp. Med. 192:483*.
32. Yamano, T., S. Murata, N. Shimbara, N. Tanaka, T. Chiba, K. Tanaka, K. Yui, and H. Udono. 2002. Two distinct pathways mediated by PA28 and hsp90 in major histocompatibility complex class I antigen processing. *J. Exp. Med. 196:185*.
33. Preckel, T., W. Fung-Leung, Z. Cai, A. Vitiello, L. Salter-Cid, O. Winqvist, T. G. Wolfe, M. von Herrath, A. Angulo, P. Ghazal, et al. 1999. Impaired immunoproteasome assembly and immune responses in $PA28^{-/-}$ mice. *Science 286:2162*.
34. Murata, S., H. Udono, N. Tanahashi, N. Hamada, K. Watanabe, K. Adachi, T. Yamano, K. Yui, N. Kobayashi, M. Kasahara, et al. 2001. Immunoproteasome assembly and antigen presentation in mice lacking both PA28α and PA28β. *EMBO J. 20:5898*.
35. Aden, D. P., and B. B. Knowles. 1976. Cell surface antigens coded for by the human chromosome 7. *Immunogenetics 3:209*.
36. Bruns, M., J. Cihak, G. Müller, and F. Lehmann-Grube. 1983. Lymphocytic choriomeningitis virus. VI. Isolation of a glycoprotein mediating neutralization. *Virology 130:247*.
37. Schwarz, K., M. van den Broek, R. de Giuli, W. W. Seelentag, N. Shastri, and M. Groettrup. 2000. The use of LCMV-specific Tcell hybridomas for the quantitative analysis of MHC class I restricted antigen presentation. *J. Immunol. Methods 237:199*.
38. Aebischer, T., S. Oehen, and H. Hengartner. 1990. Preferential usage of Vα4 and Vβ10 T cell receptor genes by lymphocytic choriomeningitis virus glycoprotein-specific H-$2D^b$-restricted cytotoxic T cells. *Eur. J. Immunol. 20:523*.
39. Khan, S., M. van den Broek, K. Schwarz, R. de Giuli, P. A. Diener, and M. Groettrup. 2001. Immunoproteasomes largely replace constitutive proteasomes during an antiviral and antibacterial immune response in the liver. *J. Immunol. 167:6859*.
40. Probst, H. C., K. Tschannen, A. Gallimore, M. Martinic, M. Basler, T. Dumrese, E. Jones, and M. F. van den Broek. 2003. Immunodominance of an antiviral cytotoxic T cell response is shaped by the kinetics of viral protein expression. *J. Immunol. 171:5415*.
41. Macagno, A., M. Gilliet, F. Sallusto, A. Lanzavecchia, F. O. Nestle, and M. Groettrup. 1999. Dendritic cells up-regulate immunoproteasomes and the proteasome regulator PA28 during maturation. *Eur. J. Immunol. 29:4037*.
42. Macagno, A., L. Kuehn, R. de Giuli, and M. Groettrup. 2001. Pronounced up-regulation of the PA28α/β proteasome regulator but little increase in the steady state content of immunoproteasomes during dendritic cell maturation. *Eur. J. Immunol. 31:3271*.
43. Rodriguez, F., S. Harkins, M. K. Slifka, and J. L. Whitton. 2002. Immunodominance in virus-induced $CD8^+$ T-cell responses is dramatically modified by DNA immunization and is regulated by γ interferon. *J. Virol. 76:4251*.
44. Butz, E. A., and M. J. Bevan. 1998. Differential presentation of the same MHC class I epitopes by fibroblasts and dendritic cells. *J. Immunol. 160:2139*.
45. Groettrup, M., S. Standera, R. Stohwasser, and P. M. Kloetzel. 1997. The subunits MECL-1 and LMP2 are mutually required for incorporation into the 20S proteasome. *Proc. Natl. Acad. Sci. USA 94:8970*.
46. Griffin, T. A., D. Nandi, M. Cruz, H. J. Fehling, L. VanKaer, J. J. Monaco, and R. A. Colbert. 1998. Immunoproteasome assembly: cooperative incorporation of interferon γ (IFN-γ)-inducible subunits. *J. Exp. Med. 187:97*.
47. De, M., K. Jayarapu, L. Elenich, J. J. Monaco, R. A. Colbert, and T. A. Griffin. 2003. β2 subunit propeptides influence cooperative proteasome assembly. *J. Biol. Chem. 278:6153*.
48. Wherry, E. J., J. N. Blattman, K. Murali-Krishna, R. van der Most, and R. Ahmed. 2003. Viral persistence alters CD8 T-cell immunodominance and tissue distribution and results in distinct stages of functional impairment. *J. Virol. 77:4911*.
49. Fuller, M. J., and A. J. Zajac. 2003. Ablation of CD8 and CD4 T cell responses by high viral loads. *J. Immunol. 170:477*.

Chapter 5

Immune defects in MECL-1 deficient mice

Michael Basler, Jacqueline Möbius, & Marcus Groettrup

1. Abstract

The proteasome is responsible for the generation of most peptide ligands of MHC class I molecules either in their final form or in the form of N-terminally extended precursors. IFN-γ treatment leads to a replacement of the proteasome's active site subunits δ, MB1, and MC14 by the inducible subunits LMP2, LMP7, and MECL-1. To date, no evidence has been obtained for a role of MECL-1 in antigen presentation, like it has been demonstrated for LMP2 and LMP7. In this study, we investigated the poorly understood exchange of MECL-1 for MC14 with the help of MECL-1 gene targeted mice. Infection of mice with lymphocytic choriomeningitis virus elicited a markedly reduced CTL response to GP276-286/D^b and NP205-212/K^b in MECL-$1^{-/-}$ mice. We demonstrated that the impaired CTL response to GP276-286 was not attributed to a decreased generation of this epitope by antigen presenting cells, leaving open the possibility that the CTL repertoire was altered in MECL-1 deficient mice. Differences in $V_ß10$ usage of LCMV-infected MECL-1 mice support this idea. Taken together, we demonstrated a role of MECL-1 in antigen processing.

2. Introduction

Cytotoxic T lymphocytes (CTL) recognize peptide epitopes presented on MHC class I molecules, which allows CTLs to monitor our body for cells harbouring intracellular pathogens.

The proteasome is the main protease in the cytoplasm and the nucleus which is responsible for the generation of most peptide ligands of MHC class I molecules (Groettrup et al., 1996b) (Voges et al., 1999). The proteolytic core complex of the proteasome system is the 20S proteasome which is constructed like a cylinder of four stacked rings. The outer two rings consist of seven different α-type subunits that bind to regulatory complexes of the 20S core particle, whereas the two inner rings are made up of seven different subunits of the β-type (Groll et al., 1997). Three of the β-subunits designated δ, MB1, and MC14 (Z) bear the active centers of the 20S proteasome. The catalytic activities of the proteasome have been classified with the help of fluorogenic peptides as chymotrypsin-like (cleavage C-terminal of hydrophobic aa), trypsin-like (cleavage C-terminal of basic aa), and caspase-like (also known as peptidyl-glutamyl-peptide hydrolysing (PGPH); cleavage C-terminal of acidic aa)). Upon stimulation of cells with the inflammatory cytokine interferon-γ (IFN-γ), these constitutively expressed subunits are replaced by inducible subunits named LMP2, LMP7, and MECL-1

during the *de novo* assembly of 20S proteasomes. In contrast to LMP2 and LMP7 the MECL-1 subunit is not encoded in the MHC locus and the discovery of this third subunit exchange (MECL-1 for MC14) lagged behind several years (Groettrup et al., 1996a; Hisamatsu et al., 1996; Nandi et al., 1996). Recently, De et al. reported that in ConA blasts derived from MECL-1 deficient mice incorporation of MECL-1 into proteasomes is dependent on LMP2 and to a lesser extent on LMP7, but LMP2 and LMP7 are integrated independently of MECL-1 into proteasomes (De et al., 2003).

Analysis with small fluorogenic substrates showed that the exchange of LMP2 for δ down-regulates the cleavages C-terminal of acidic residues (caspase-like activity) and favours the cleavage C-terminal of hydrophobic residues (chymotrypsin-like activity). Contradicting results have been obtained for the exchange of LMP7 for MB1 and MECL-1 for MC14. Salzmann et al. reported that overexpression of a mutant MECL-1 (T1A) led to a complete loss in trypsin-like activity (Salzmann et al., 1999).

LMP2- and LMP7-deficient mice have been analysed intensively. LMP2 gene targeted mice displayed no change in MHC class I ligand expression, but the numbers of $CD8^+$ was reduced in blood, spleen and thymus. LMP7 deficient mice display reduced MHC class I surface expression (Fehling et al., 1994). Some epitopes are affected by LMP2- and LMP7 gene targeted mice, but the bulk of MHC class I ligands can still be generated in these mice (Van Kaer et al., 1994) (Fehling et al., 1994). Chen et al. examined the effects of immunoproteasomes on the immunodominance hierarchy in the T_{CD8+} response to influenza virus (IV) infection in LMP2-deficient mice (Chen et al., 2001). T_{CD8+} responses to the two most dominant determinants dropped markedly, whereas responses to two subdominant epitopes were enhanced. The altered immunogenicity of some epitopes can be attributed to changes in epitope presentation, whereas the CTL response to one determinant ($NP_{366-374}$) was reduced due to alterations in the T_{CD8+} repertoire (Chen et al., 2001). Also for LMP7 gene targeted mice was reported that they posses an altered T cell repertoire. Vaccination of $LMP7^{-/-}$ mice with cells derived from wildtype mice, but not vice versa, elicited a strong CTL response (Toes et al., 2001). This indicates that the incorporation of immunosubunits influences the repertoire of peptides presented to CTLs and thereby the overall specificity of the CTL response.

In this work, we used the infection with lymphocytic choriomeningitis virus (LCMV) to study the characteristics of antigen processing and presentation in MECL-1 gene targeted mice. The cytotoxic immune response to LCMV is essential for elimination of the virus from infected mice. In C57BL/6 mice, this response is strongly dominated by CTLs specific for the GP-

derived GP33-41D^b, GP34-41K^b, and NP-derived NP396-404D^b and the subdominant epitopes GP276-286/D^b, GP92-101/D^b GP118-125/K^b and NP205-212/K^b (van der Most et al., 1996) (Gallimore et al., 1998) (van der Most et al., 2003).

We found that proteasomes isolated from LCMV infected liver of MECL-1 deficient mice had a slightly impaired incorporation of LMP2, which correlated with an enhanced caspase-like activity. Furthermore naïve MECL-1 gene targeted mice displayed a reduction of CD8$^+$ splenocytes of approximately 20% compared to wild type mice. Analysis of splenocytes derived from LCMV-infected MECL-1$^{-/-}$ mice revealed a markedly reduced CTL-response to GP276 and NP205. The reduction of GP276 was not due to an impaired antigen presentation as assessed by determining the amount of GP276 presented in splenocytes or on macrophages. This result would be consistent with a change of T cell repertoire in MECL-1 deficient mice. Taken together, we demonstrated that MECL-1 is an important component in the MHC-I antigen processing pathway.

4. Results

Mutant mice lack MECL-1

Analysis of genomic DNA of MECL-1$^{-/-}$ and wild type mice by PCR confirmed the gene disruption in MECL-1$^{-/-}$ mice (data not shown). To verify the absence of MECL-1 protein expression in these mice purified spleen proteasomes were separated by two-dimensional gel electrophoresis (2D-PAGE). MECL-1 is constitutively expressed in spleens of C57BL/6 wildtyp mice (Fig. 1A) but completely absent in MECL-1 deficient mice. Western blot analysis of 2D-Gels from LCMV-WE infected liver (Fig. 1B) with a MECL-1 specific antiserum confirmed the lack of MECL-1. Additionally, C57BL/6 western blots revealed several so far uncharacterised isoforms of MECL-1 (Fig. 1B).

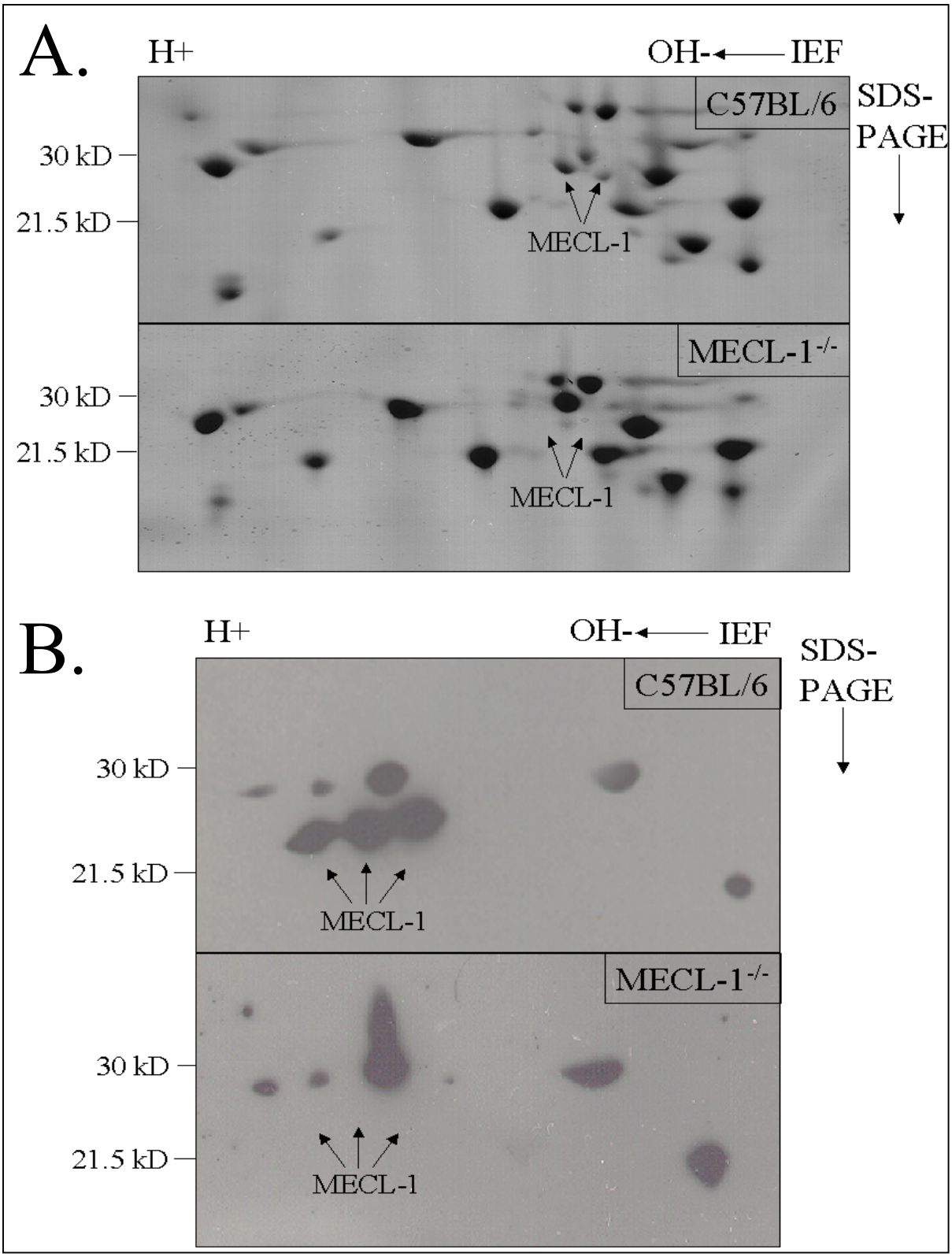

Figure 1: Composition of 20S proteasome subunits from C57BL/6 and MECL-1$^{-/-}$ mice. **A:** IEF/SDS-PAGE analysis of 70µg 20S proteasome purified from the spleen of uninfected C57BL/6 (upper panel) and MECL-1$^{-/-}$ (lower panel) mice. The proteins were visualized by coomassie blue staining. The position of the proteasome subunit MECL-1 is indicated. **B:** IEF/SDS-PAGE of 70µg 20S proteasome purified from the liver of LCMV-WE (d8 post infection with 200pfu) infected C57BL/6 (upper panel) and MECL-1$^{-/-}$ (lower panel) mice were analysed by Western blot with a rabbit polyclonal antibody recognizing MECL-1. Different MECL-1 specific spots are marked.

LMP2 incorporation into immunoproteasomes of LCMV infected livers is reduced in MECL-1 deficient mice

Dependency of MECL-1 incorporation into proteasome on LMP2 and LMP7 has been studied in different systems. It was proposed that efficient LMP2 incorporation is dependent on MECL-1 (Groettrup et al., 1997). De et al. found in ConA blasts of MECL-1 deficient mice that LMP7 as well as LMP2 are inserted independently of MECL-1 into proteasomes (De et al., 2003). To analyse the incorporation of LMP2 and LMP7 in MECL-1 deficient mice, MECL-$1^{-/-}$ and C57BL/6 mice were infected with 200pfu LCMV-WE. 8d later the proteasome composition of infected livers was analysed by 2D-PAGE (Fig. 2). Incorporation of LMP7 into proteasomes was not affected in MECL-$1^{-/-}$ mice compared to wildtype mice. In contrast, LMP2 was slightly but consistently reduced in MECL-deficient mice. It seems that LMP2 incorporation into proteasomes in LCMV infected livers occurs in the absence of MECL-1 but less efficiently.

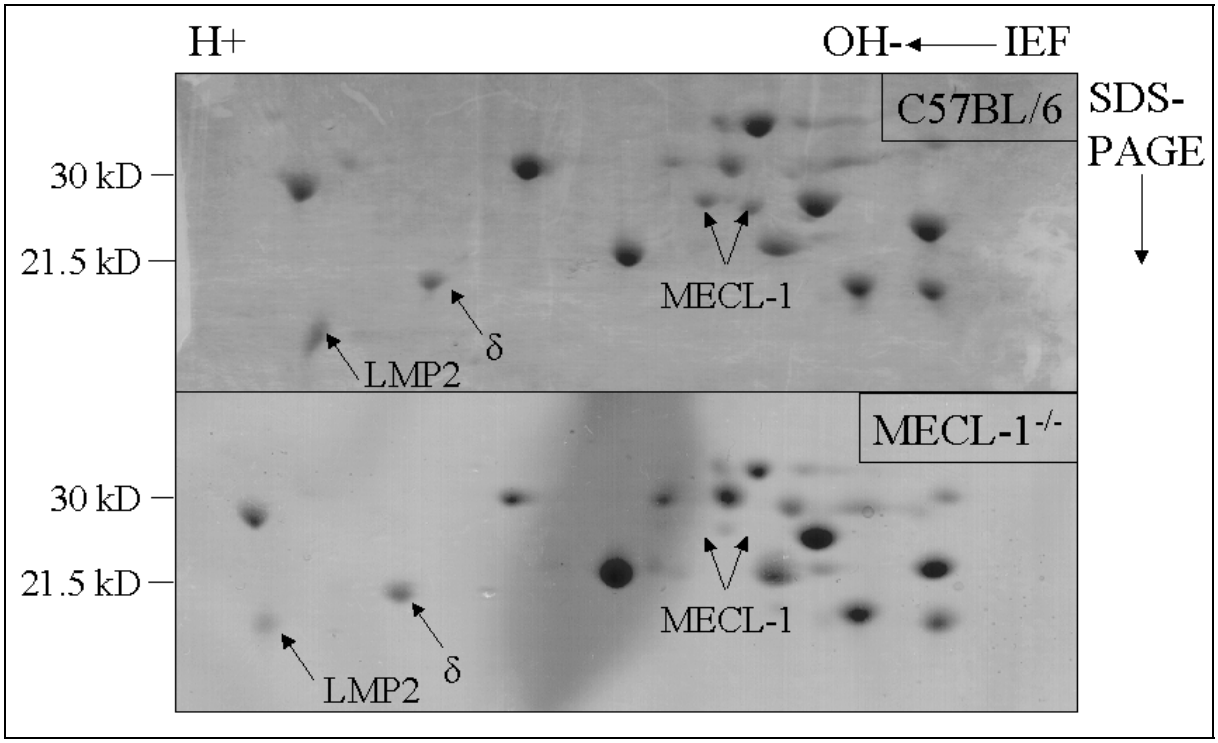

Figure 2: Composition of 20S proteasome subunits from LCMV-WE infected livers of C57BL/6 and MECL-$1^{-/-}$ mice. IEF/SDS-PAGE analysis of 70µg 20S proteasome purified from livers of LCMV-WE infected C57BL/6 (upper panel) and MECL-$1^{-/-}$ (lower panel) mice. The proteins were visualized by coomassie staining. The positions of the proteasome subunits LMP2, δ, and MECL-1 are indicated.

MECL-1 deficient proteasomes have an enhanced caspase-like activity

To investigate the role of MECL-1 in peptide degradation, the peptide hydrolysing activities of purified proteasomes from LCMV infected liver of C57BL/6 and MECL-1$^{-/-}$ were compared with help of fluorogenic peptides. No differences in hydrolysing Bz-VGR-AMC and (Z)-GGL-AMC were observed (Fig. 3). In contrast, Z-LLE-βNA was cleaved more efficiently by MECL-1 deficient proteasomes than by proteasomes from wildtype mice. This is in agreement with an enhanced caspase-like activity in proteasomes of LMP2 deficient mice (Van Kaer et al., 1994), since LMP2 incorporation in MECL-1 deficient mice is slightly reduced (Fig. 2). In contrast to immunoproteasomes carrying an inactive MECL-1 mutation (T1A) (Salzmann et al., 1999), the absence of MECL-1 did not lead to a reduction in trypsin like activity (Fig. 3).

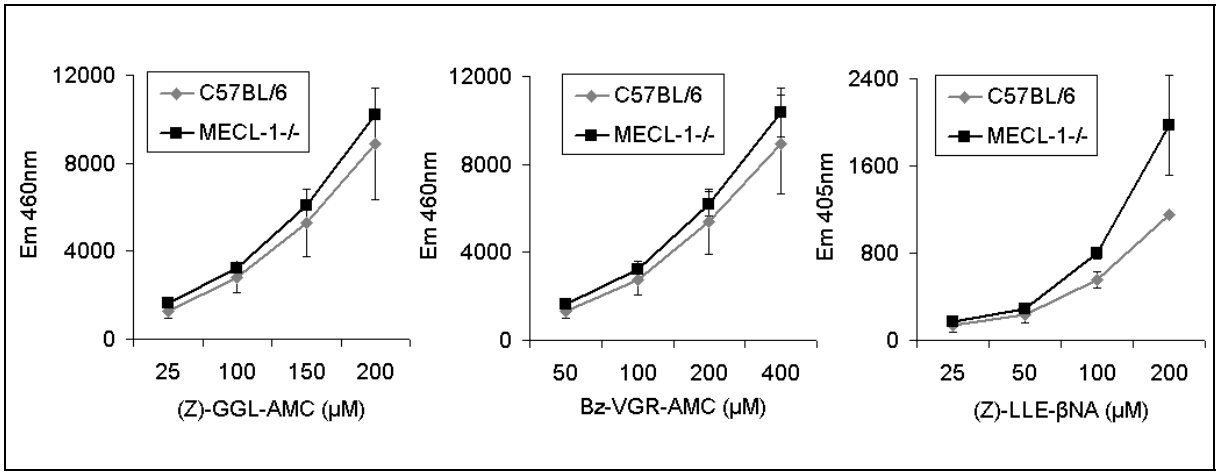

Figure 3: Peptide hydrolyzing activity of 20S proteasomes purified from the livers of LCMV-infected C57BL/6 and MECL-1$^{-/-}$ mice. The purified 20S proteasomes from livers of LCMV-WE-infected C57BL/6 and MECL-1$^{-/-}$ mice (the same preparations as analysed in Fig. 2) were assayed for hydrolysis of the indicated fluorogenic substrates at various concentrations. The activities are calculated from fluorescence of the AMC or ßNA leaving groups after 60 min of incubation. Values represent the mean ± SD of triplicate cultures.

Impaired CTL response against GP276 in LCMV-WE infected MECL-1 deficient mice

LMP2- and LMP7 deficient mice display only marginal immunological defects, which were mostly epitope specific (Van Kaer et al., 1994) (Fehling et al., 1994). To characterize MECL-1 deficient mice in a model system of viral infection, we infected these mice with LCMV-WE and determined virus titers in spleens four days later. No significant differences in virus titers were obtained in control and knock out mice (data not shown). The CTL response in C57BL/6 mice after LCMV-WE infection is directed against two dominant and several subdominant epitopes. In order to compare the anti-LCMV T_{CD8+} response of wildtype and MECL-1

deficient mice, these mice were infected intravenously with LCMV-WE and splenocytes were assayed on d8 after infection for responses to six defined LCMV epitopes by intracellular cytokine staining for interferon-γ (Fig. 4A). CTL responses to the dominant epitopes GP33 and NP396 and the subdominant epitopes GP92 and GP118 were similar whereas responses to GP276 and NP205 (Fig. 4A,B) were reduced.

In order to confirm the observed reduction in the generation of GP276 specific CTLs in MECL-1 deficient mice, we performed double stainings of splenocytes from MECL-$1^{-/-}$ and C57BL/6 control mice for CD8 and for GP276 specific T cell receptor (tetramer staining) on day 8 post infection with LCMV-WE (Fig. 4C). Similar results as shown in Fig. 4A,B were obtained with this assay. To distinguish the contribution of antigen presentation versus T_{CD8+} repertoire formation to the reduced generation of GP276-286-specific CTLs, further experiments were performed.

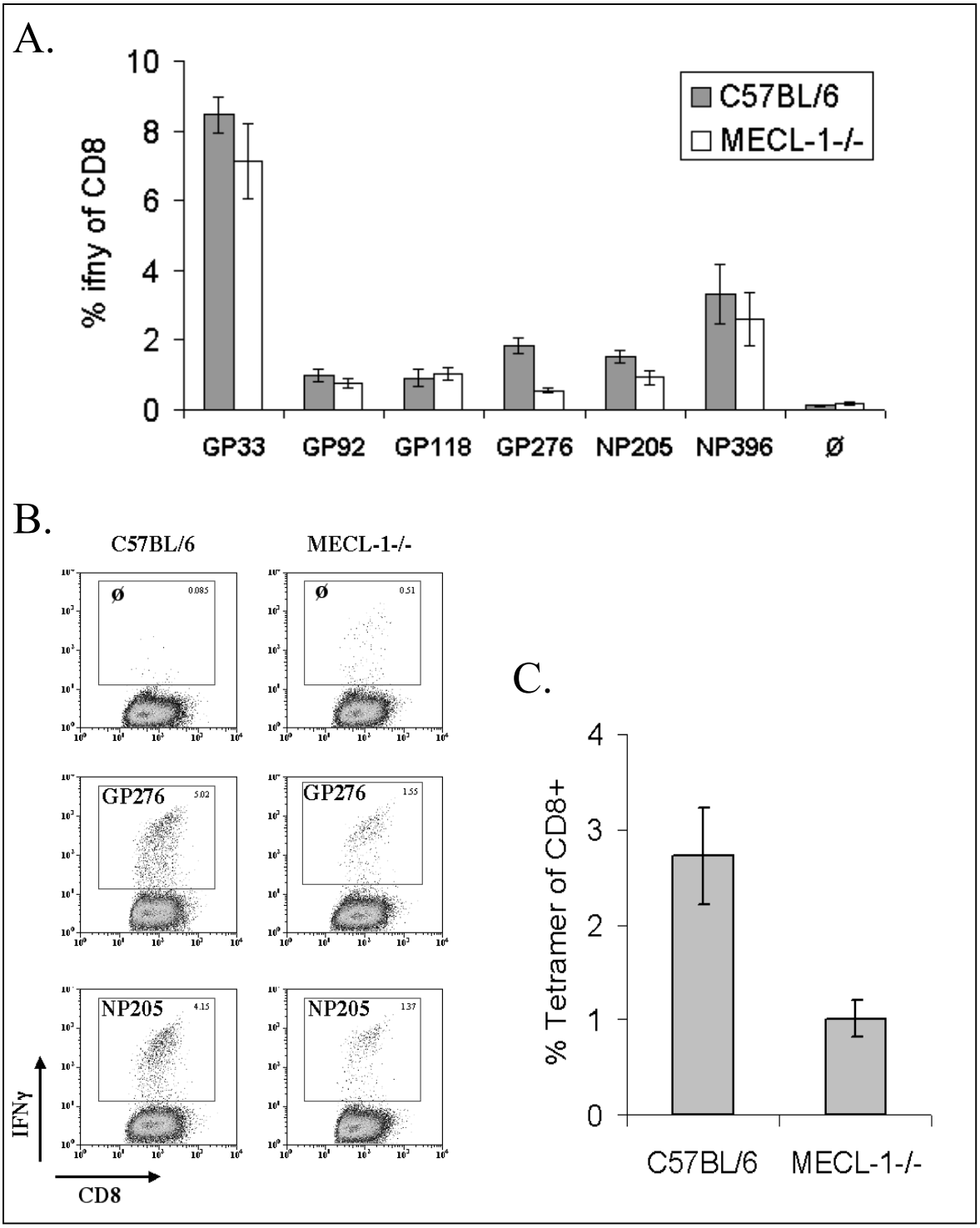

Figure 4: CTL responses in LCMV-WE infected MECL-1$^{-/-}$ and C57BL/6 mice. MECL-1-/- and C57BL/6 mice were infected with 200pfu LCMV-WE i.v.. **A:** Spleen cells were harvested 8d later, stimulated in vitro, and screened for reactivity against the panel of LCMV epitopes listed (x-axis) by flow cytometry for CD8$^+$ T cells expressing intracellular IFN-γ (y-axis). The values represent the mean of three different mice. One representative experiment out of four is shown. **B:** FACS plots of LCMV-infected C57BL/6 (wildtype), and MECL-1$^{-/-}$ mice after 5h *in vitro* stimulation with GP276 or NP205. Ø represents LCMV-infected mice without *in vitro* peptide stimulation. The y-axis shows intracellular IFN-γ produced by CD8-positive (x-axis) splenocytes. **C:** CTL response in LCMV-infected C57BL/6 (wild type), and MECL-1$^{-/-}$ mice was analysed by GP276-specific tetramers. The y-axis shows tetramer positive CTLs. The values represent the mean of three different mice.

No alteration of GP276 presentation in MECL-1 deficient mice

Recently, we have shown that immunoproteasomes lead to a diminished presentation of GP276 (Basler et al., 2004). To investigate the role of antigen presentation in MECL-1 gene targeted mice, thioglycollate-elicited peritoneal macrophages from MECL-1 deficient as well as C57BL/6 control mice were infected *in vitro* for 20 h with LCMV-WE and analysed for GP276 presentation with GP276-specific T cell hybridomas (Fig. 5A). GP276 presentation was not affected in LCMV infected MECL-1 deficient macrophages. In order to determine the amount of antigen presented directly *in vivo*, we intravenously infected MECL-$1^{-/-}$ and control C57BL/6 mice with high dose ($2x10^7$ pfu) or low dose (200 pfu) and analysed the status of GP33 and GP276 presentation in the spleen on day two or four after infection, respectively. Splenocytes from these mice were used as stimulators for IFN-γ production (ICS) by mono-specific CTL-lines specific for GP33 and GP276. To exclude that activated T_{CD8+} in infected spleens falsify the activation status of mono-specific CTLs, a normal intracellular IFN-γ staining (ICS) with infected splenocytes but without mono-specific CTLs was performed. No IFN-γ producing CTLs were detected on d2 and d4 after LCMV-WE infection in spleens (data not shown). As shown in Fig. 5B,C neither GP33 nor GP276 is presented differently in spleens on d2 (high dose) or d4 (low dose) post LCMV-WE infection.

Analysis of peptide fragments from *in vitro* digests of a 25mer (including GP276-286) with purified proteasomes from LCMV infected liver of MECL-$1^{-/-}$ and C57BL/6 control mice by HPLC electron spray ionisation mass spectrometry (HPLC-ESI-MS) did not reveal significant differences between MECL-$1^{-/-}$ and C57BL/6 proteasomal fragmentation (data not shown). Due to fact that the diminished CTL response to GP276 in MECL-1 deficient mice (Fig. 4) is not caused by reduced antigen presentation (Fig. 5B,C) one could assume that the impaired CTL response might be attributed to a defect in the T cell repertoire.

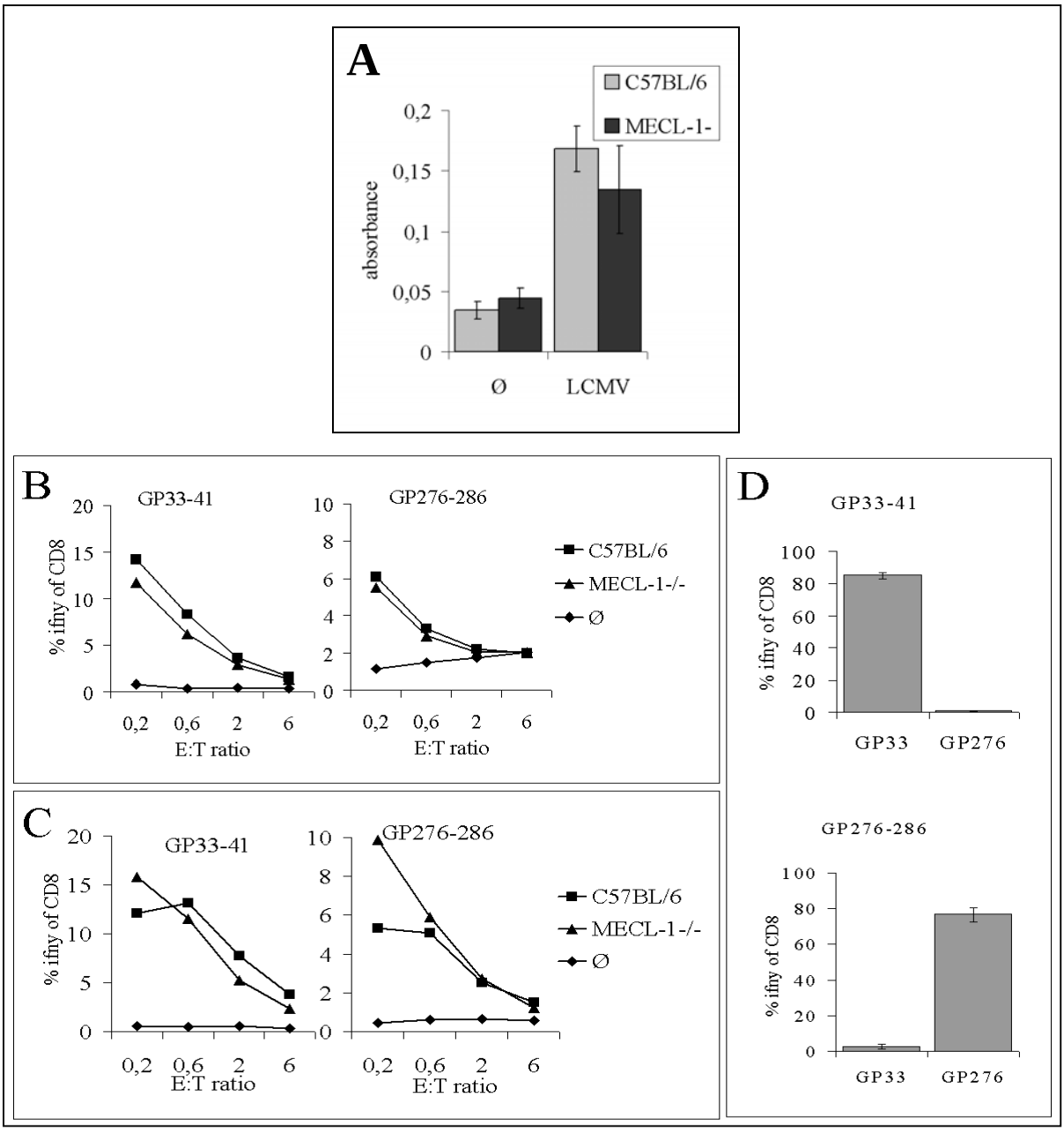

Figure 5: A: Presentation of LCMV-gp276–286 epitopes by LCMV-infected macrophages from C57BL/6, and MECL-1$^{-/-}$ mice. Peritoneal macrophages were infected with LCMV-WE *in vitro* 1 day before addition of T cell hybridomas specific for gp276. Uninfected macrophages are marked with Ø. The y-axis shows absorbance of enzymatically converted chromogen at 570 nm in lacZ assays. The values are the means ± SD of three replicate cultures. The experiment has been repeated twice, giving similar results. **B,** and **C:** LCMV-infected splenocytes derived from C57BL/6 or MECL$^{-/-}$ present the LCMV GP-derived CTL epitopes GP33 and GP276 *ex vivo* similarly. MECL-1$^{-/-}$ and C57BL/6 mice were infected i.v. with 2 x 10^7 pfu (**B.**) or 200 pfu (**C.**) LCMV-WE, their splenocytes were isolated at d2 or d4 post infection, respectively, and were used as APC for GP33–41- or GP276-286 specific CTL-lines. Activation of CTL-lines was analysed by staining for CD8 and intracellular IFN-γ. Shown are the percentages of IFN-γ-positive cells of CD8$^+$ cells as determined by flow cytometry. The percentage of intracellular IFN-γ (y-axis) produced by CTL-lines is plotted versus E:T ratio (effector (CTL-lines) to target (splenocytes)). One experiment out of three is shown. D: Specificity of GP33 and GP76 specific CTL-lines. GP33-specific (upper panel) or GP276-specific (lower panel) CTL-lines were incubated with splenocytes pulsed with GP33 or GP276 (x-axis). Activation of CTL-lines was analysed by staining for CD8 and intracellular IFN-γ (y-axis).

MECL-1 gene targeted mice have reduced numbers of CD8$^+$ T cells

It has been reported that LMP2$^{-/-}$ deficient mice displayed an altered T_{CD8+} response to several influenza epitopes, which was influenced by a modified T cell repertoire in these mice (Chen et al., 2001). To determine whether MECL-1 deficient mice have a defect in numbers of T cells, splenocytes from naïve MECL-1$^{-/-}$ and C57BL/6 control mice were stained for CD8 and analysed by FACS. Cells were gated on lymphocytes and their percentage of CD8$^+$ cells is shown in Fig. 6. MECL-1 gene targeted mice displayed a significant reduction of CD8$^+$ cells of 20%. The number of CD4+ cells was not affected (data not shown). Similar results were reported for LMP2$^{-/-}$ mice (Van Kaer et al., 1994). The reduced numbers of CTLs in MECL-1$^{-/-}$ mice might indicate that these mice have a modified T cell repertoire.

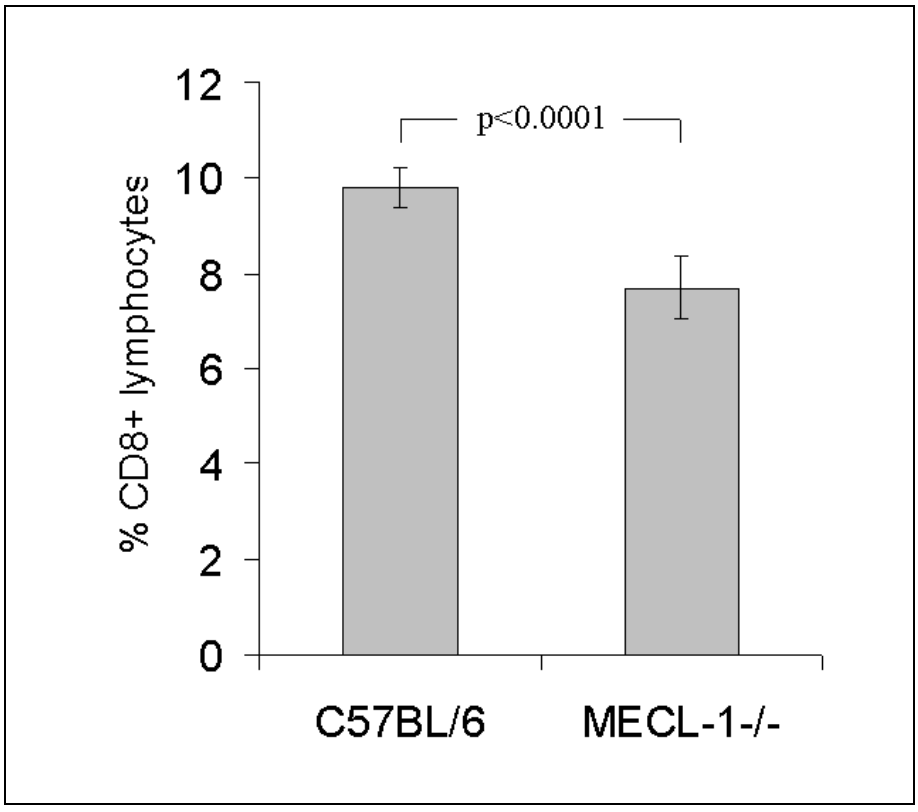

Figure 6: Proportions of splenocytes derived from C57BL/6 or MECL-1$^{-/-}$ mice that are CD8$^+$ determined by flow cytometry. Values are the means ± SD of 8 mice. Values of p were determined by unpaired t test and are considered to be statistically significant when $p < 0.05$.

The generation of V_β10b-specific CTLs is impaired in LCMV-infected MECL-1 deficient mice

In order to investigate whether the impaired generation of GP276 specific CTLs in MECL-1 deficient mice is due to an altered CTL repertoire splenocytes from naïve and LCMV-WE

infected (8d post infection with 200pfu LCMV-WE) C57BL/6, MECL-1$^{-/-}$ mice were stained with $V_ß$ specific antibodies (Fig. 7). It has been reported that T cell lines specific for GP276 were using exclusively the $V_ß10$ variable segment for their T cell receptors (Aebischer et al., 1990). Naïve MECL-1$^{-/-}$ mice showed no difference in $V_ß10$ usage compared to C57BL/6. In contrast, after LCMV infection the extent of CTLs using $V_ß10$ was significantly increased in C57BL/6 mice compared to MECL-1 deficient mice. $V_ß6$ and $V_ß9$ were not affected in naïve and LCMV-infected mice (data not shown).

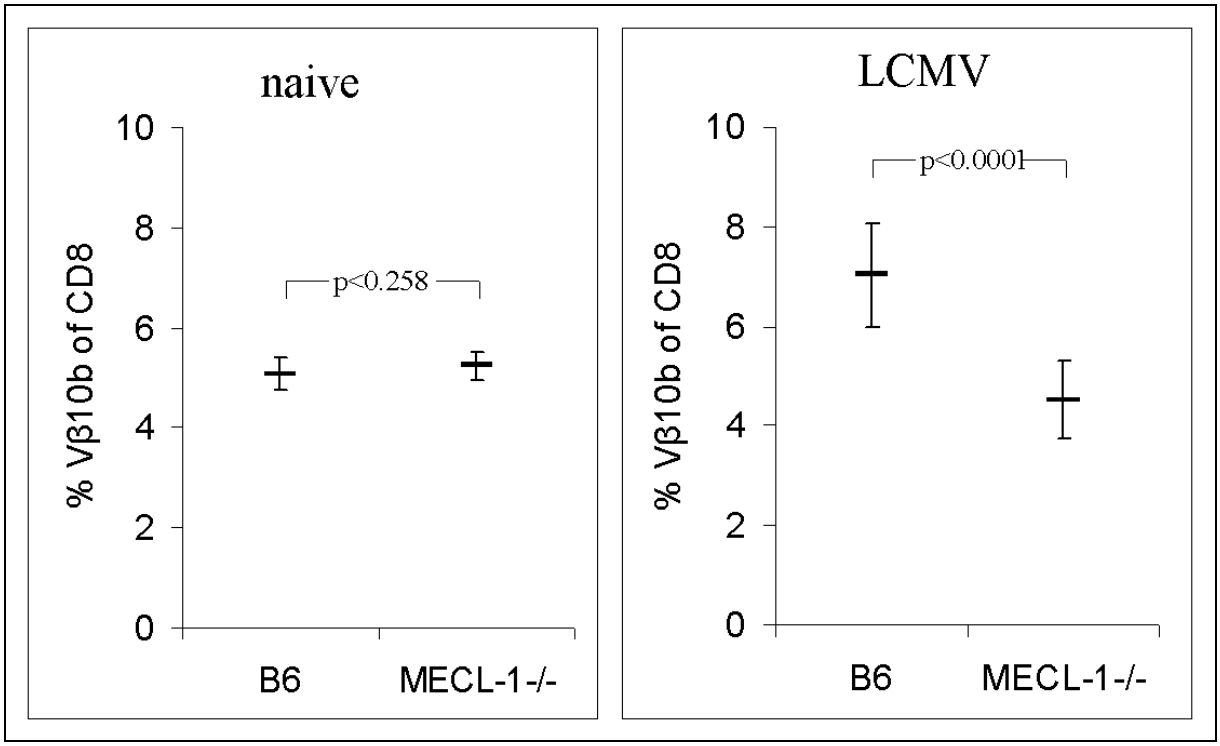

Figure 7: Analysis of Vß10 variable segments of TCRs from C57BL/6, and MECL-1$^{-/-}$ mice. Splenocytes from naive or LCMV-infected (8 days post infection with 200 PFU of LCMV-WE i.v.) mice were stained for CD8 and Vß10b, and analyzed by flow cytometry. Values are the means ± SD of 6 (naive) or 10 (infected) mice. Values of p were determined by unpaired t test and are considered to be statistically significant when $p < 0.05$.

4. Discussion

To date the reason for the expression of the three cytokine-inducible proteasome subunits LMP2, LMP7, and MECL-1 replacing their constitutive counterparts, is still not clear. A minor part of ligands for MHC-I is affected by the immunoproteasome subunits, but the bulk of MHC-I ligands can still be produced in the absence of LMP2 and LMP7 (Arnold et al., 1992; Momburg et al., 1992). The subunit exchange of MECL-1 was discovered several years

after LMP2 and LMP7 (Groettrup et al., 1996a; Hisamatsu et al., 1996; Nandi et al., 1996) and the *in vivo* function of MECL-1 is poorly characterized. In this study, we analysed the immune response to the well-characterized model virus LCMV in MECL-1 gene targeted mice. Proteasomes isolated from LCMV-WE infected liver derived from MECL-1 deficient mice displayed an only slightly reduced incorporation of LMP2 (Fig. 2). Similar results were obtained with LPS blasts from MECL-1 deficient mice showing unchanged LMP2 and LMP7 incorporation in the absence of MECL-1 (De et al., 2003). In contrast, $LMP2^{-/-}$ deficient mice have an impaired MECL-1 incorporation and the absence of LMP7 reduced the level of LMP2 and MECL-1, and resulted in an accumulation of their precursors (De et al., 2003). Therefore defects in MECL-1 deficient mice are exclusively attributed to a loss in MECL-1 and not to other immunosubunits like in $LMP2^{-/-}$ or $LMP7^{-/-}$ mice.

Analysis of proteasomes from LCMV infected liver by western blot revealed three different isoforms of MECL-1 with similar molecular weights but different isoelectric points, suggesting posttranslational modifications as a cause for this polymorphism. Kuckelkorn et al. found that MECL-1 is expressed as different isoforms in liver, thymus, small intestine, and colon but the molecular basis of this polymorphism remained unclear (Kuckelkorn et al., 2002).

Analysis of cleavage specificity of MECL-1 deficient proteasomes isolated from LCMV-WE infected livers with the help of small fluorogenic substrates showed no difference in cleavage after basic aa (trypsin-like activity) (Fig. 3) as it has been reported for proteasomes containing an inactive MECL-1 (T1A) (Salzmann et al., 1999). Probably, the constitutive MC14 subunit can compensate the trypsin-like activity in MECL-1 deficient proteasomes.

Infection of MECL-1 gene targeted mice with LCMV-WE proceeded normally with virus titers on d4 comparable to C57BL/6 wildtype mice (data not shown). Analysis of a panel of LCMV-specific CTL epitopes revealed an impeded CTL-response to GP276 and NP205 (Fig. 4). Recently, we have reported that immunoproteasomes impair presentation of the LCMV glycoprotein derived T cell epitope GP276 (Basler et al., 2004). To investigate whether the reduced CTL response to GP276 in MECL-1 deficient mice is due to a presentation defect, fragmentation of a 25mer containing GP276 by MECL-1 or C57BL/6 immunoproteasomes was analysed by HPLC-ESI-MS (data not shown). No significant difference in fragmentation could be observed between the two types of proteasome. Additionally, neither *in vitro* infected thioglycollate-elicited macrophages derived from $MECL\text{-}1^{-/-}$ nor *ex vivo* analysis of antigen presentation in spleens of $MECL\text{-}1^{-/-}$ revealed reduced GP276 presentation in MECL-1 gene targeted mice (Fig. 5). These findings

suggested that the loss of MECL-1 has an effect on the T_{CD8+} repertoire, like it has been reported for LMP2 gene targeted mice (Chen et al., 2001). The authors showed that the CTL-response to several influenza epitopes was changed in $LMP2^{-/-}$ mice, which was due to both, changes in epitope presentation as well as to differences in the CTL precursor frequency. Graft transplantation and adoptive transfer experiments from wildtype mice to LMP7-deficient mice revealed that the CTL repertoire is altered in $LMP7^{-/-}$ mice, probably due to changes in peptide presentation in the thymus (Toes et al., 2001). As MECL-1, as well as the other immunoproteasome subunits, are expressed in the thymus (Barton et al., 2004; Nil et al., 2004; Stohwasser et al., 1997), one can assume that MECL-1 can shape the T cell repertoire by influencing positive and negative selection. T_{CD8+} cells in splenocytes of naïve MECL-1 deficient mice were reduced about 20% compared to wildtype mice, as it has been reported for $LMP2^{-/-}$ mice (Van Kaer et al., 1994), which might indicate an altered T cell repertoire. Recently, Nil et al. reported that immunoproteasome subunits are expressed in the negative selection mediating thymus-derived dendritic cells, macrophages and medullary thymic epithelial cells (mTEC). In contrast, RT-PCR analysis of cortical epithelial cells (cTEC), which are responsible for positive selection, revealed that immunoproteasome subunits are not present in these cells (Nil et al., 2004). Therefore the defect of MECL-1 deficient mice to respond to GP276 would probably arise from elimination of GP276-specific CTLs by negative selection in the thymus. It has been shown that specific CTLs can recognize different peptides, a phenomenon called molecular mimicry (Kammer et al., 1999). Assuming that GP276 specific CTLs are negatively selected in the thymus, a self-peptide, mimicking GP276, is expressed in the thymus of MECL-1 gene targeted mice, which is absent in wildtype mice.
Taken together, we demonstrated immune defects in MECL-1 deficient mice, indicating that MECL-1 is an important parameter in the design of vaccines against cancers and viruses and to prevent autoimmune diseases.

5. Materials and methods

Mice, viruses, cells, and media

C57BL/6 mice ($H\text{-}2^b$) mice were originally obtained from Charles River, Germany. MECL-1 gene targeted mice (De et al., 2003) were provided by Dr. John Monaco (Cincinnati, USA). All knock out mice were backcrossed onto the C57BL/6 background for at least 10

generations. Mice were kept in a specific pathogen-free facility and used at 6-10 weeks of age.

LCMV-WE was originally obtained from F. Lehmann-Grube (Hamburg, Germany) and propagated on the fibroblast line L929. Mice were infected with 200pfu (low dose) LCMV-WE i.v. and the specific CTL response was analysed at d8 post infection. To determine the amount of antigen presented in spleens derived from C57BL/6 and MECL-$1^{-/-}$, mice were infected with 200pfu (low dose) or $2x10^7$pfu (high dose) LCMV-WE i.v and analysed on d4 or d2, respectively.

DC2.4 (H-2^b) is a mouse dendritic cell line (A kind gift from Dr. K. Rock, University of Massachusetts Medical School). All media were purchased from (Invitrogen-Life Technologies, Karlsruhe, Germany) and contained GlutaMAX, 10% FCS, and 100U/ml penicillin/streptomycin.

Synthetic peptides

The synthetic peptides GP33-41 (KAVYNFATC), GP92-101 (CSANNSHHYI), GP118-125 (ISHNFCNL), GP276-286 (SGVENPGGYCL), NP205-212 (YTVKYPNL) and NP396-404 (FQPQNGQFI) were obtained from Echaz Microcollections (Tubingen, Germany).

Purification of 20S proteasome from mouse organs and fluorogenic assays

The lysis of organ tissues, the purification of 20S proteasomes from liver and spleen, and the quantification of the 20S proteasome from uninfected and LCMV infected (8d post infection with 200pfu LCMV-WE i.v.) C57BL/6, MECL$^{-/-}$ mice were performed as previously described (Groettrup et al., 1995). Purified proteasomes were analysed by two-dimensional gel electrophoresis. Hydrolytic assays for proteasome activity employing fluorogenic assays were performed as detailed previously (Schmidtke et al., 1999).

Two-dimensional gel electrophoresis

IEF/SDS-PAGE and NEPHGE/SDS-PAGE were performed exactly as previously described (Groettrup et al., 1996a).

Western blotting

Proteins from 2-D Gels were blotted onto nitrocellulose (Schleicher & Schuell BioSciences, Dassel, Germany), blocked with PBS/5% (w/v) low fat dry milk/0.2% Tween) for 1h and agitated overnight at 4°C with a rabbit polyclonal antibody recognizing MECL-1 (Groettrup et al., 1997). The blots were washed three times and incubated for 2h with HRP-conjugated goat anti-rabbit antibody (DakoCytomation, Glostrup, Denmark). After extensive washing with PBS/0.2% Tween 20, proteins were visualized on x-ray films by enhanced chemiluminescence.

Flow cytometry

For $V_ß$ staining splenocytes from uninfected or LCMV (8 days post infection with 200pfu LCMV-WE i.v.) infected C57BL/6 and MECL-$1^{-/-}$ mice were treated with 1.66% NH_4Cl (w/v), washed twice, and incubated for 30min with biotin-conjugated anti $V_ß$10b (BD PharMingen) antibodies on ice. Samples were washed twice and incubated for another 30min with streptavidin-conjugated FITC and Cy5-conjugated mouse anti-CD8 (BD PharMingen). After two washes, cells were acquired with the use of a FACScan™ flow cytometer (Becton Dickinson, Mountain View, CA) and analysed with the FLOWJO software (Tree Star, San Carlos, CA). Differences between groups were assessed by unpaired t-test (www.graphpad.com). P values less than 0.05 are considered to be statistically significant.

Intracellular staining for interferon-γ (ICS)

$2x10^6$ splenocytes were incubated in round-bottom 96-well plates with 10^{-7}M of the specific peptide in 100µl IMDM10% + brefeldin A (10µg/ml) for 5h at 37°C. Cells were incubated for 20min at 4°C with Cy5-conjugated mouse anti-CD8 (clone 53-6.7, BD PharMingen). Following fixation with 4% paraformaldehyde at 4°C for 5min, the cells were incubated overnight with fluorescein-conjugated mouse anti-IFN-γ (clone XMG1.2, BD PharMingen) in PBS containing 2% FCS and 0.1% (w/v) saponin (Sigma). Samples were washed twice and acquired with the use of FACScan™ flow cytometer (Becton Dickinson, Mountain View, CA) and analysed by the FlowJo software (Tree Star, San Carlos, CA).

Tetramer staining

Tetrameric complexes containing biotinylated H-2D^b, β_2-microglobulin, GP276-286 peptide, and streptavidin-PE were a kind gift of M. van den Broek. 5x10^5 cells were incubated with 0.5µl tetramer in 50µl FACS buffer (PBS containing 2% FCS, 2mM NaN3, 2mM EDTA) for 10min at 37°C. After adding 1µl of anti-CD8α-Cy5 cells were incubated at 4°C for 30min. Samples were washed three times and acquired with the use of FACScan™ flow cytometer (Becton Dickinson, Mountain View, CA) and analysed by the FlowJo software (Tree Star, San Carlos, CA).

Lac Z assay

For the lacZ assay, LCMVGP276-286/H-2D^b specific T cell hybridomas (Schwarz et al., 2000) were cocultured overnight with 2.5 x 10^4 stimulator cells in 96-well plates. As stimulator cells *in vitro* infected (moi of 1; 24h) thioglycollate-elicited peritoneal macrophages from C57BL/6 and MECL-1$^{-/-}$ mice were used. The lacZ based colour reaction was performed and measured as detailed elsewhere (Schwarz et al., 2000).

Peptide-specific CTL lines

Splenocytes from LCMV-WE memory mice (at least one month post infection with 200 PFU LCMV-WE i.v) were restimulated with irradiated (10000rad) and peptide-loaded (10^{-7} M) (gp33–41 (KAVYNFATC, D^b), or gp276–286 (SGVENPGGYCL, D^b)) DC2.4 in the presence of 40U/ml IL-2. Cultures were restimulated weekly as described above at a ratio of 10:1. An additional density centrifugation step was carried out 1-2 days before using CTLs in *in vitro* antigen presentation experiments. CTLs were used in ICS at an E:T ratio of 0.2 in the first dilution.

6. References

Aebischer, T., Oehen, S. and Hengartner, H. (1990) Preferential usage of Va4 and Vb10 T cell receptor genes by lymphocytic choriomeningitis virus glycoprotein-specific H-2D^b-restricted cytotoxic T cells. *Eur. J. Immunol.*, **20**, 523-531.

Arnold, D., Driscoll, J., Androlewicz, M., Hughes, E., Cresswell, P. and Spies, T. (1992) Proteasome subunits encoded in the MHC are not generally required for the processing of peptides bound by MHC class I molecules. *Nature*, **360**, 171-174.

Barton, L.F., Runnels, H.A., Schell, T.D., Cho, Y.J., Gibbons, R., Tevethia, S.S., Deepe, G.S. and Monaco, J.J. (2004) Immune defects in 28-kDa proteasome activator gamma-deficient mice. *J Immunol*, **172**, 3948-3954.

Basler, M., Youhnovski, N., Van Den Broek, M., Przybylski, M. and Groettrup, M. (2004) Immunoproteasomes down-regulate presentation of a subdominant T cell epitope from lymphocytic choriomeningitis virus. *J Immunol*, **173**, 3925-3934.

Chen, W.S., Norbury, C.C., Cho, Y.J., Yewdell, J.W. and Bennink, J.R. (2001) Immunoproteasomes shape immunodominance hierarchies of antiviral CD8(+) T cells at the levels of T cell repertoire and presentation of viral antigens. *J. Exp. Med.*, **193**, 1319-1326.

De, M., Jayarapu, K., Elenich, L., Monaco, J.J., Colbert, R.A. and Griffin, T.A. (2003) Beta 2 subunit propeptides influence cooperative proteasome assembly. *J Biol Chem*, **278**, 6153-6159.

Fehling, H.J., Swat, W., Laplace, C., Kuehn, R., Rajewsky, K., Mueller, U. and von Boehmer, H. (1994) MHC class I expression in mice lacking proteasome subunit LMP-7. *Science*, **265**, 1234-1237.

Gallimore, A., Dumrese, T., Hengartner, H., Zinkernagel, R.M. and Rammensee, H.-G. (1998) Protective immunity does not correlate with the hierarchy of virus-specific cytotoxic T cell responses to naturally processed peptides. *J. Exp. Med.*, **187**, 1647-1657.

Groettrup, M., Kraft, R., Kostka, S., Standera, S., Stohwasser, R. and Kloetzel, P.-M. (1996a) A third interferon-γ-induced subunit exchange in the 20S proteasome. *Eur. J. Immunol.*, **26**, 863-869.

Groettrup, M., Ruppert, T., Kuehn, L., Seeger, M., Standera, S., Koszinowski, U. and Kloetzel, P.M. (1995) The interferon-γ-inducible 11S regulator (PA28) and the LMP2/LMP7 subunits govern the peptide production by the 20S proteasome in vitro. *J. Biol. Chem.*, **270**, 23808-23815.

Groettrup, M., Soza, A., Kuckelkorn, U. and Kloetzel, P.M. (1996b) Peptide antigen production by the proteasome: complexity provides efficiency. *Immunol. Today*, **17**, 429-435.

Groettrup, M., Standera, S., Stohwasser, R. and Kloetzel, P.M. (1997) The subunits MECL-1 and LMP2 are mutually required for incorporation into the 20S proteasome. *Proc. Natl. Acad. Sci. USA*, **94**, 8970-8975.

Groll, M., Ditzel, L., Löwe, J., Stock, D., Bochtler, M., Bartunik, H.D. and Huber, R. (1997) Structure of 20 S proteasome from yeast at 2.4A resolution. *Nature*, **386**, 463-471.

Hisamatsu, H., Shimbara, N., Saito, Y., Kristensen, P., Hendil, K.B., Fujiwara, T., Takahashi, E.-i., Tanahashi, N., Tamura, T., Ichihara, A. and Tanaka, K. (1996) Newly identified pair of proteasomal subunits regulated reciprocally by interferon γ. *J. Exp. Med.*, **183**, 1-10.

Kammer, A.R., van der Burg, S.H., Grabscheid, B., Hunziker, I.P., Kwappenberg, K.M.C., Reichen, J., Melief, C.J.M. and Cerny, A. (1999) Molecular mimicry of human cytochrome P450 by Hepatitis C virus at the level of cytotoxic T cell recognition. *J. Exp. Med.*, **190**, 169-176.

Kuckelkorn, U., Ruppert, T., Strehl, B., Jungblut, P.R., Zimny-Arndt, U., Lamer, S., Prinz, I., Drung, I., Kloetzel, P.M., Kaufmann, S.H. and Steinhoff, U. (2002) Link between organ-specific antigen processing by 20S proteasomes and CD8(+) T cell-mediated autoimmunity. *J. Exp. Med.*, **195**, 983-990.

Momburg, F., Ortiz-Navarrete, V., Neefjes, J., Goulmy, E., van-de-Wal, Y., Spits, H., Powis, S.J., Butcher, G.W., Howard, J.C., Walden, P. and Haemmerling, G. (1992) Proteasome subunits encoded by the major histocompatibility complex are not essential for antigen presentation. *Nature*, **360**, 174-177.

Nandi, D., Jiang, H. and Monaco, J.J. (1996) Identification of MECL-1 (LMP-10) as the third IFN-γ-inducible proteasome subunit. *J. Immunol.*, **156**, 2361-2364.

Nil, A., Firat, E., Sobek, V., Eichmann, K. and Niedermann, G. (2004) Expression of housekeeping and immunoproteasome subunit genes is differentially regulated in positively and negatively selecting thymic stroma subsets. *Eur J Immunol*, **34**, 2681.

Salzmann, U., Kral, S., Braun, B., Standera, S., Schmidt, M., Kloetzel, P.M. and Sijts, A. (1999) Mutational analysis of subunit i beta 2 (MECL-1) demonstrates conservation of cleavage specificity between yeast and mammalian proteasomes. *FEBS Lett*, **454**, 11-15.

Schmidtke, G., Holzhütter, H., Bogyo, M., Kairies, N., Groll, M., de Giuli, R., Emch, S. and Groettrup, M. (1999) How an inhibitor of the HIV-1 protease modulates proteasome activity. *J. Biol. Chem.*, **274**, 35734-35740.

Schwarz, K., de Giuli, R., Schmidtke, G., Kostka, S., van den Broek, M., Kim, K., Crews, C.M., Kraft, R. and Groettrup, M. (2000) The selective proteasome inhibitors lactacystin and expoxomicin can be used to either up- or downregulate antigen presentation at non-toxic doses. *J. Immunol.*, **164**, 6147-6157.

Stohwasser, R., Standera, S., Peters, I., Kloetzel, P.-M. and Groettrup, M. (1997) Molecular cloning of the mouse proteasome subunits MC14 and MECL-1: reciprocally regulated tissue expression of interferon-γ - modulated proteasome subunits. *Eur. J. Immunol.*, **27**, 1182-1187.

Toes, R.E.M., Nussbaum, A.K., Degermann, S., Schirle, M., Emmerich, N.P.N., Kraft, M., Laplace, C., Zwinderman, A., Dick, T.P., Muller, J., Schonfisch, B., Schmid, C., Fehling, H.J., Stevanovic, S., Rammensee, H.G. and Schild, H. (2001) Discrete cleavage motifs of constitutive and immunoproteasomes revealed by quantitative analysis of cleavage products. *J. Exp. Med.*, **194**, 1-12.

van der Most, R.G., Murali-Krishna, K., Lanier, J.G., Wherry, E.J., Puglielli, M.T., Blattman, J.N., Sette, A. and Ahmed, R. (2003) Changing immunodominance patterns in antiviral CD8 T-cell responses after loss of epitope presentation or chronic antigenic stimulation. *Virology*, **315**, 93-102.

van der Most, R.G., Sette, A., Oseroff, C., Alexander, J., Murali-Krishna, K., Lau, L.L., Southwood, S., Sidney, J., Chestnut, R.W., Matloubian, M. and Ahmed, R. (1996) Analysis of cytotoxic T cell responses to dominant and subdominant epitopes during acute and chronic lymphocytic choriomeningitis virus infection. *J. Immunol.*, **157**, 5543-5554.

Van Kaer, L., Ashton-Rickardt, P.G., Eichelberger, M., Gaczynska, M., Nagashima, K., Rock, K.L., Goldberg, A.L., Doherty, P.C. and Tonegawa, S. (1994) Altered peptidase and viral-specific T cell response in LMP 2 mutant mice. *Immunity*, **1**, 533-541.

Voges, D., Zwickl, P. and Baumeister, W. (1999) The 26S proteasome: A molecular machine designed for controlled proteolysis. *Annu. Rev. Biochem.*, **68**, 1015-1068.

Chapter 6

Immunodominance of an antiviral cytotoxic T cell response is shaped by the kinetics of viral protein expression

Hans Christian Probst, Kathrin Tschannen, Awen Gallimore, Marianne Martinic, Michael Basler, Tilman Dumrese, Emma Jones, and Maries F. van den Broek

Published in Journal of Immunology 2003:171(10):5415-22

The Journal of Immunology

Immunodominance of an Antiviral Cytotoxic T Cell Response Is Shaped by the Kinetics of Viral Protein Expression[1]

Hans Christian Probst,* Kathrin Tschannen,* Awen Gallimore,[2†] Marianne Martinic,* Michael Basler,[‡] Tilman Dumrese,* Emma Jones,[†] and Maries F. van den Broek[3]*

Lymphocytic choriomeningitis virus (LCMV) infection induces a protective CTL response consisting of gp- and nucleoprotein (NP)-specific CTL. We find that a small load of LCMV led to immunodominance of NP-CTL, whereas a large viral load resulted in dominance of gp-CTL. This is the first study describing that immunodominance is not fixed after infection with a given pathogen, but varies with the viral load instead. We assumed higher Ag sensitivity for NP-CTL, which would explain their preferential priming at low viral load, as well as their overstimulation resulting in selective exhaustion at high viral load. The higher Ag sensitivity of NP-CTL was due to faster kinetics of NP-epitope presentation. Thus, we uncover a novel factor that impinges upon immunodominance and is related to the kinetics of virus protein expression. We propose that CTL against early viral proteins swiftly interfere with virus replication, resulting in efficient protection. If these "early" CTL fail in immediate virus control, they are activated in the face of higher viral load compared with "late" CTL and are therefore prone to be exhausted. Thus, the observed absence of early CTL in persistent infections might not be the cause, but rather the consequence of viral persistence. ***The Journal of Immunology,*** **2003, 171: 5415–5422.**

The $CD8^+$ CTL recognize peptides presented by MHC class I molecules on the surface of APC (1). These peptides are predominantly generated from endogenous proteins in a proteasome- and TAP-dependent fashion (2–4). Viral peptides will therefore be presented on infected cells by MHC class I molecules, and as a result, virus-specific CTL are important effectors to control virus replication and spread (5–9).

Infection of C57BL/6 ($H\text{-}2^b$) mice with lymphocytic choriomeningitis virus (LCMV)[5] induces a strong and protective CTL response that is dominated by four epitopes: gp-derived gp33–41/D^b, gp34–41/K^b, and gp276–286/D^b and nucleoprotein (NP)-derived NP396–404/D^b. The response in BALB/c ($H\text{-}2^d$) mice is strongly dominated by NP118–126/L^d, but also responses to gp283–292/K^d are detectable (10–17). After infection with LCMV-Armstrong (Arm), the CTL response in C57BL/6 mice is dominated by NP396-CTL (15, 17), whereas infection of mice with faster replicating strains such as LCMV-WE, LCMV-Docile (Doc), or LCMV-Arm Clone13 or -t1b (18) results in immunodominance of gp33-CTL (10, 18, 19).

Preferential priming of NP396-CTL at low virus load and immunodominance of gp33-CTL at high virus load suggest that NP396-CTL are more sensitive to Ag in some way and selective exhaustion (18, 20, 21) of NP396-CTL may explain their gradual disappearance upon increasing viral load. Several studies described the association between decreased CTL responses and high viral load and disease progression in HIV infection (22–24) or infection with LCMV (20). Exhaustion of specific CTL in persistent infections is facilitated in the absence of $CD4^+$ cells (18, 25–27), but can also happen in the presence of fully functional $CD4^+$ cells (21).

We have performed experiments to delineate the relationship among virus burden, immunodominance, and protection against persistent infection. Other studies have previously identified differences in Ag processing, T cell repertoires, and MHC/peptide/TCR avidities as important factors in controlling immunodominance. It was, however, clear from our early experiments that neither of these factors could account for the shifting pattern of immunodominance observed following infection of mice with viruses of different replicative capacities. In fibroblasts that were infected with LCMV in vitro, the NP was detected substantially before gp by immunoprecipitation (28). In this study, we show that this kinetic difference in protein production has consequences for LCMV-derived Ag processing and presentation: LCMV-infected cells presented NP-derived CTL epitopes 8 h before they presented gp-derived epitopes. NP-CTL indeed seemed to interact with LCMV-infected cells in vivo before gp-CTL, as we show that priming of gp-CTL in vivo was prevented by the presence of NP-CTL, but not vice versa. In addition, we show that selective expansion of NP-CTL at low viral load is a feature intrinsic to LCMV, as it did not occur after infection with recombinant vaccinia virus carrying LCMV CTL epitopes.

We propose that the kinetic difference in Ag presentation explains the preferential priming of NP-CTL at low viral load, their selective exhaustion at high viral load, as well as their relatively high protective capacity in vivo (19). Thus, we discovered a novel factor that impinges on immunodominance and which is related to the kinetics of Ag presentation.

*Institute of Experimental Immunology, University of Zurich, Zurich, Switzerland; [†]Institute of Molecular Medicine, John Radcliffe Hospital, Oxford, United Kingdom; and [‡]Department of Immunology, University of Constance, Constance, Germany.

Received for publication November 12, 2002. Accepted for publication September 3, 2003.

The costs of publication of this article were defrayed in part by the payment of page charges. This article must therefore be hereby marked *advertisement* in accordance with 18 U.S.C. Section 1734 solely to indicate this fact.

[1] This work was supported are supported by the Swiss National Science Foundation (to H.C.P. and M.M.), the Wellcome Trust (to A.G.), and the Cloëtta Foundation and the European Community (QLG1-CT-1999-00202, to M.F.B.)

[2] Current address: Medical Biochemistry, University of Wales College of Medicine, Heath Hospital, Cardiff, CF-14 4XN, U.K..

[3] Address correspondence and reprint requests to Dr. Maries F. van den Broek, Institute of Experimental Immunology, Schmelzbergstrasse 12, CH 8091 Zurich, Switzerland. E-mail address: maries@pathol.unizh.ch

[4] Abbreviations used in this paper: LCMV, lymphocytic choriomeningitis virus; NP, nucleoprotein; Arm, Armstrong; DC, dendritic cell; Doc, Docile; m.o.i., multiplicity of infection; VV, vaccinia virus; ICS, intracellular staining; CTL_p, precursor CTL.

0022-1767/03/$02.00

Materials and Methods

Mice

C57BL/6 (H-2^b) and BALB/c (H-2^d) mice were bred in the Institut für Labortierkunde, University of Zurich (Zurich, Switzerland). 318 TCR-transgenic mice expressing the P14 TCR that is specific for LCMV gp33–41/D^b are on a C57BL/6 background (29). $CB6F_1$ (H-$2^{b\times d}$) were obtained from Charles River Breeding Laboratories (Hannover, Germany). DIETER mice have a pure C57BL/6 background and expression of gp33–41 and NP396–404 as a transgene can be induced in their dendritic cells (DC) (30). All mice were kept under specific pathogen-free conditions and were at least 6 wk old at the beginning of the experiments. Animal experiments were performed in compliance with Swiss national and cantonal laws (Kantonales Veterinäramt Zürich) on animal protection.

Viruses

LCMV-WE was originally obtained from Dr. F. Lehmann-Grube (Heinrich Pette Institute, Hamburg, Germany) (31), LCMV-Arm was obtained from Dr. M. Oldstone (The Scripps Clinic and Research Foundation, La Jolla, CA) (32) and LCMV-Doc was a variant isolated from a LCMV-WE carrier mouse and was obtained from C. Pfau (Department of Biology, Rensselaer Polytechnic Institute, Washington, DC) (33). LCMV was propagated on L929 cells at a low multiplicity of infection (m.o.i.). Vaccinia virus (VV), strain WR, was originally obtained from Dr. B. Moss (National Institutes of Health, Bethesda, MD). rVV carrying one of the two immunodominant CTL epitopes of LCMV in the context of H-2^b were generated by cloning synthetic oligonucleotides encoding for the peptide sequence (5′-CATG-xxx-xxx-xxx-TA-3′ and 5′-CTAGAT-xxx-xxx-xxx-3′, where xxx represents the peptide coding sequence and the underlined sequence the added start codon) into the *Nco*I/*Bgl*II-digested transfer vector pSC11.3OR2 (34). The minigene sequences were: gp33 = AAAGCTGTGTACAATTTCGC CACCTGT (MKAVYNFATC) and NP396 = TTTCAACCACAAAAT GGGCAATTCATA (MFQPQNGQFI). Recombinant viruses were selected using 5-bromo-2′-deoxyuridine and recombinant plaques were identified by β-galactosidase activity as described elsewhere (35). rVV were plaque purified three times on BSC40 cells. As a control, VV expressing the vesicular stomatitis virus gp (VVc) was used. All VV were propagated at a low m.o.i. on BSC40 cells.

Dendritic cells

Bone marrow-derived DC were generated from the femora and tibiae of DIETER mice as previously described (36). Mice were primed by i.v. injection of 5×10^5 DC.

Cell lines

MC57G are methylcholanthrene-induced fibrosarcoma cells of C57BL/6 origin. EL-4 are dimethylbenzanthrene-induced thymoma cells of C57BL/6 origin. P815 are mastocytoma cells from BALB/c origin. BSC40 cells are a subclone of the green African monkey kidney cell line BSC-1. NP118–126/L^d-specific and gp34–41/K^b-specific T cell hybridomas carrying the *lacZ* reporter construct were a kind gift from M. Groettrup (University of Constance, Constance, Germany). The NP118 hybridoma recognizes NP118–126 (RPQASGVYM) plus H-$2L^d$, the gp34 hybridoma gp34–41 (AVYNFATC) plus H-$2K^b$ (37, 38).

Peptide-specific CTL lines

Splenocytes from LCMV-WE memory mice (injected with 100 PFU LCMV-WE at least 2 mo before) were restimulated with irradiated and peptide-loaded (10^{-8} M), thioglycolate-elicited macrophages (1 ml of thioglycolate i.p. at day −3) at a ratio of 20:1 in the presence of 25 U/ml IL-2. Cultures were restimulated every week as described above at a ratio of 5:1. After three rounds of restimulation, CTL were found to be of single specificity. BALB/c memory CTL were restimulated with NP118–126 (RPQASGVYM, L^d) or with gp283–292 (GYCLTKWMIL, K^d) and C57BL/6 memory CTL were restimulated with gp33–41 (KAVYNFATC, D^b), gp276–286 (SGVENPGGYCL, D^b), or with NP396–404 (FQPQNGQFI, D^b).

CTL assays

To measure direct ex vivo LCMV-specific CTL responses, splenocytes were tested for cytolytic activity toward peptide-loaded (10^{-7} M) or unloaded ^{51}Cr-labeled EL-4 or P815 target cells in a 5-h assay. The CTL activity of LCMV-specific memory CTL was measured 5 days after in vitro restimulation of splenocytes with peptide-loaded (10^{-8} M), irradiated, syngeneic thioglycolate macrophages (responder:stimulator = 20:1) in the presence of 25 U/ml IL-2. Standard dilutions of cultures were tested for cytolytic activity on peptide-loaded ^{51}Cr-labeled EL-4 or P815 cells in a 5-h assay.

Staining with tetrameric MHC class I-peptide complexes

Tetrameric complexes containing biotinylated H-$2D^b$ or H-$2L^d$, β_2-microglobulin, the relevant peptide, and extravidin-PE were generated as described previously (39, 40). Approximately 5×10^5 cells were stained with 0.5–1 μg of tetramer in 25 μl of FACS buffer (FB: PBS plus 2% FCS plus 0.01% NaN_3 plus 20 mM EDTA) at 37°C for 10 min. One microliter of anti-CD8α-FITC (clone 53-6.7) was added and staining was continued for 30 min at 4°C. Cells were washed three times, fixed (FACS Lysis Solution; BD Biosciences, Mountain View, CA) and were analyzed by flow cytometry (FACScan; BD Biosciences) using CellQuest software. For tetramer dissociation assays, cells were stained with tetramer as above, anti-CD8α-FITC, anti-CD4-biotin, anti-B220-biotin, and anti-I-A^b-biotin, for 30 min at 4°C, were washed once, were stained with streptavidin-CyChrome for 20 min at 4°C (all BD PharMingen, San Diego, CA), and were washed three times. Cells were suspended in 0.5 ml of FACS buffer containing propidium iodide and 150 μg/ml mouse monoclonal IgG2a anti-D^b (T21–460, obtained from G. Hämmerling, Deutsches Krebsforschungszentrum, Heidelberg, Germany) to prevent rebinding of dissociated tetramer at $t = 0$. Samples were incubated on ice for the indicated times and tetramer staining was analyzed on $CD8^+$, $CD4^-$, $B220^-$, I-A^{b-}, and propidium iodide-ve cells. We measured the rate of decay using flow cytometry and we obtained linear decay plots of the natural logarithm of the normalized fluorescence vs time, indicating that tetramer dissociation was occurring stochastically and that the resulting tetramer staining half-lives should be proportional to the half-lives of the respective TCR-peptide-MHC complexes (41).

Intracellular cytokine staining (ICS) for IFN-γ

One million splenocytes were incubated in 200 μl of IMDM plus 10% FCS and antibiotics for 6 h at 37°C with 10^{-6} M of the specific peptide or with medium alone as a negative control. To enhance intracellular accumulation of IFN-γ, brefeldin A was added at a final concentration of 5 μg/ml for the whole duration of the culture. For staining, cells were put at 4°C, washed with FACS buffer (FB, see above), and stained with anti-CD8β-PE (BD PharMingen) for 30 min at 4°C. Cells were washed twice with FB and fixed with 100 μl of 4% paraformaldehyde in PBS for 5 min at 4°C. Two milliliters of permeabilization buffer (PB: FB plus 0.1% w/v saponin) were added and cells were incubated for 10 min at 4°C. Cells were spun down and stained intracellularly with anti-mouse-IFN-γ-FITC (clone AN18; BD PharMingen) in PB for >60 min at 4°C. After three washes with PB, cells were resuspended in FB and analyzed by flow cytometry as described above.

Kinetics of Ag presentation by LCMV-infected $CB6F_1$ macrophages

Thioglycolate-elicited macrophages were isolated and infected with LCMV-Arm or with LCMV-WE at a m.o.i. of 2 and were further incubated at 37°C for the indicated times. Infected macrophages were harvested ($t = 0$) and brefeldin A was added to a final concentration of 5 μg/ml to freeze cells in their state of Ag presentation. The degree of infection was measured by intracellular staining for LCMV NP using FITC-labeled monoclonal rat-anti-LCMV NP (VL4 (42)), followed by FACS analysis. Macrophages of the same batch were used as targets in a chromium release assay and as stimulators in ICS using peptide-specific CTL lines as effectors/responders. For these experiments, part of the macrophages were labeled with ^{51}Cr (in the presence of brefeldin A) and were incubated with titrated numbers of peptide-specific CTL in a 5-h Cr release assay in the presence of brefeldin A. Another part of the macrophages was used as stimulators of IFN-γ production in a 6-h ICS in the presence of brefeldin A (3×10^5 macrophages plus 3×10^5 tetramer-positive CTL) as described above. In the chromium release assay as well as in ICS, macrophages loaded with titrated amounts of each of the five peptides (10^{-6}–10^{-12} M) were included as a sensitivity control for the individual CTL lines.

Kinetics of Ag presentation by cells from LCMV-infected mice

$CB6F_1$ mice were infected i.v. with 2×10^7 PFU of LCMV-WE. The high inoculum size was chosen to ensure maximal numbers of infected cells in the spleen. At defined time points after infection, spleens were homogenized and used as APCs. Five $\times 10^4$ T cell hybridoma cells were incubated overnight in 96-well round-bottom plates at 37°C with 1.5×10^5 splenocytes from infected $CB6F_1$ mice or with 1.5×10^5 naive $CB6F_1$ splenocytes with titrated amounts of the relevant antigenic peptide in 200 μl of medium containing 5 μg/ml brefeldin A to freeze their condition of Ag

presentation. After incubation, cultures were processed as described previously (43). Briefly, cells were washed with PBS and were subsequently fixed with PBS containing 2% formaldehyde and 0.2% glutaraldehyde for 5 min at 4°C. The plates were washed with PBS and overlaid with 50 μl of staining solution (1 mg/ml 5-bromo-4-chloro-3-indolyl β-D-galactoside, 5 mM potassium ferrocyanide, 5 mM potassium ferricyanide, and 2 mM $MgCl_2$ in PBS). T cell hybridomas that were stimulated through the TCR can be visualized by blue staining, resulting from a *lacZ* reporter gene under control of the IL-2 promoter/enhancer (37). Triplicate cultures were microscopically examined, and the number of blue cells per well was counted after overnight incubation at 37°C.

Measurement of virus titers

LCMV titers were determined in the spleens and livers at indicated time points after infection. To determine LCMV titers, organs were removed, homogenized in MEM/2% FCS, and titrated by 10-fold dilution onto monolayers of MC57G cells in 24-well plates. LCMV was detected after 2 days of incubation at 37°C by an immunofocus assay using an LCMV NP-specific mAb (VL4), as previously described (42). The detection limit of this focus forming assay is 100 PFU/ml.

Results

Immunodominance is influenced by the LCMV inoculum and is not related to T cell intrinsic features such as TCR affinity or the capacity to expand

Since LCMV is a noncytopathic virus that replicates massively in its natural host, the mouse, simple titration of the inoculum does not cover a wide range of viral loads. To circumvent this problem and to be able to analyze immunodominance at gradually increasing viral loads, we took advantage of different viral isolates that are known to have different replication rates, such that LCMV-Arm < LCMV-WE < LCMV-Doc. We infected C57BL/6 mice with titrated (10-fold dilutions) amounts of different LCMV strains and measured virus titers 5 days later in the spleen. We then chose the inoculum size to analyze immunodominance such that we had a graded increase in viral load (see Fig. 1). We infected C57BL/6 mice with 10^2 or 10^6 PFU of LCMV-Arm, with 10^0, 10^2, or 10^6 PFU of LCMV-WE, or with 10^2 of 10^6 PFU of LCMV-Doc. The viral load was measured in spleen at days 6, 8, and 15 (Fig. 1*A*, *upper panels*) and in liver (comparable to spleen, data not shown) and was found to increase in the following order: 10^2 PFU LCMV-Arm $<10^6$ PFU LCMV-Arm $<10^0$ PFU LCMV-WE $<10^2$ PFU LCMV-WE $<10^2$ PFU LCMV-Doc $<10^6$ PFU LCMV-WE $<10^6$ PFU LCMV-Doc. Virus was not detectable anymore at day 50 in any of the mice, except for mice infected with 10^6 PFU LCMV-Doc (50,000 PFU/spleen), which is in accordance with previously published findings (20). Tetramer staining 15 days after infection (Fig. 1*A*, *middle panels*) showed clear immunodominance of NP396-CTL at low viral load, which gradually decreased with increasing viral load. This resulted in immunodominance of gp33-CTL at higher viral loads. Functional analysis of the CTL by ICS ex vivo at day 15 after infection made the observed difference even more clear (Fig. 1*A*, *lower panels*): At low viral load, NP396-CTL were immunodominant, whereas they were functionally undetectable (although physically present to some extent) after infection with 10^6 PFU LCMV-WE. In contrast, the number of gp33-CTL increased at increasing viral load. High-dose (10^6 PFU) LCMV-Doc resulted in such high amounts of rapidly spreading virus that also gp-specific CTL were functionally and physically exhausted (20, 40, 44), ultimately resulting in lifelong virus persistence. The apparent higher sensitivity to exhaustion of NP-CTL might be explained by a lower naive precursor CTL (CTL_p) frequency of NP-CTL compared with gp-CTL; however, this possibility cannot account for the preferential priming of NP-CTL at low virus load. The viral loads after infection with 10^6 PFU LCMV-Arm and 1 PFU LCMV-WE were apparently similar (Fig. 1*A*, *upper panels*); however, the immunodominance profile was found to be different

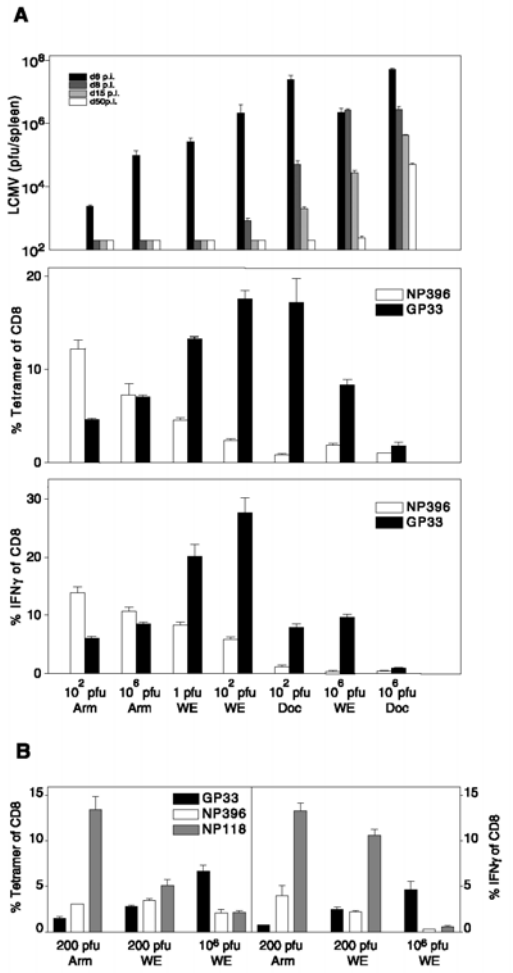

FIGURE 1. NP396-specific CTL are preferentially primed under conditions of low viral load and are gradually exhausted as viral load increases. *A*, C57BL/6 mice were infected with 10^0, 10^2, or 10^6 PFU of LCMV-Arm, LCMV-WE, or LCMV-Doc. *Upper panels,* Viral titers were measured in the spleen at indicated time points after infection. *Middle panels,* The physical presence of gp33- and NP396-CTL in the spleen was measured at day 15 after infection by tetramers. *Lower panels,* The functional presence of gp33- and NP396-CTL in the spleen was measured at day 15 after infection by ICS. The values are the mean of three mice; one representative experiment of four is shown. *B,* $CB6F_1$ mice were infected with 10^2 PFU of LCMV-Arm and 10^2 or 10^6 PFU of LCMV-WE. *Left panel,* The physical presence of gp33-, NP396-, and NP118-CTL in blood was measured at day 29 after infection by tetramers. *Right panel,* The functional presence in the spleen was measured at day 29 after infection by ICS. The values represent the mean of two mice; one experiment of two is shown. ■, gp33; □, NP396; ▨, NP118.

(Fig. 1*A*, *middle* and *lower panels*). This is possibly attributable to the fact that the resolution of the plaque assay is not sufficient to detect small, but probably biologically relevant differences in viral load immediately after infection. Moreover, analysis of the gp- and NP-CTL response after infection of $CB6F_1$ mice with 10^2 PFU LCMV-Arm and 10^2 or 10^6 PFU LCMV-WE demonstrated that the NP396- and the NP118-specific response behaved similarly (i.e., going down upon increasing virus load) and opposite to the gp33-specific response (i.e., increasing upon higher virus load) (Fig. 1*B*). Because the NP118 response is a very strong one, selective exhaustion of NP-CTL at high virus load is unlikely to

result from low CTL_p frequencies. The preferential priming of NP-CTL at low viral load and their exhaustion upon increasing Ag levels suggests that NP-CTL have somehow a higher sensitivity to Ag than gp-CTL. We considered the possibility that CTL bearing TCR with high affinity were preferentially activated at low virus load and were more likely to be overstimulated and exhausted (18, 20) at higher virus load. As a consequence, we had to assume that NP396-CTL generally have a TCR of higher affinity compared with gp33-CTL. The most reliable manner to determine TCR affinities is probably by BiaCore; however, this method cannot be applied on polyclonal T cell populations. Therefore, we used tetramer dissociation on ex vivo-prepared CTL as a measure for the TCR affinities of polyclonal, but mono-specific CTL populations after infection with LCMV (41). We always included 318 TCR-transgenic T cells that are specific for gp33/D^b (29) as a reproducibility control. We found comparable tetramer dissociation kinetics of gp33-CTL and of NP396-CTL after infection with LCMV (Fig. 2, *A* and *B*), suggesting no apparent difference in TCR affinity between the two specificities. In addition, we found no difference in TCR affinities between infection with LCMV-WE and -Arm

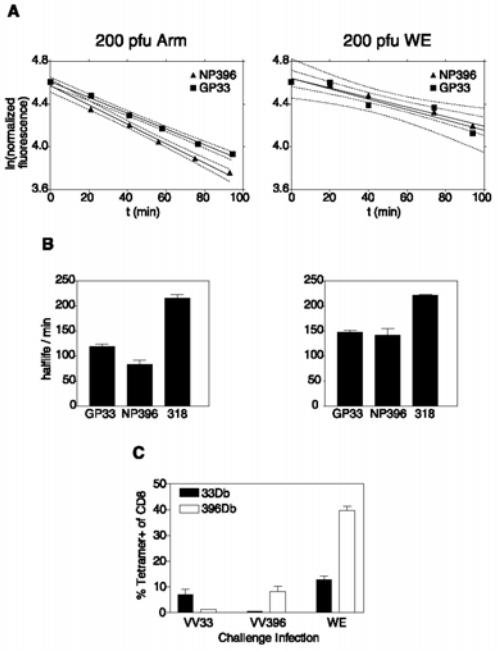

FIGURE 2. gp33- and NP396-specific CTL show similar TCR affinity as measured by tetramer dissociation rates and are not intrinsically different with respect to their ability to expand in vivo. C57BL/6 mice were infected i.v. with 10^2 PFU of LCMV-Arm or -WE, and splenocytes were stained with tetramer as described in *Materials and Methods* 35 days later. Tetramer-stained cells were incubated on ice for the indicated times in the presence of saturating amounts of a monoclonal anti-D^b Ab to prevent rebinding of dissociated tetramer as described elsewhere (41). The dissociation of tetramers was measured by FACS. *A,* Representative decay plots of one LCMV-Arm- and one LCMV-WE-infected mouse. Decay plots show the natural logarithm of the normalized fluorescence vs time. *B,* The mean of calculated half-lives of TCR-peptide-H-2D^b interaction of three individual mice is plotted. *C,* C57BL/6 mice were primed with 5×10^5 syngeneic DIETER DC transgenic for gp33 and NP396 (30) and were challenged 10 days later with 2×10^6 PFU of VV33, 2×10^6 PFU of VV396, or with 10^2 PFU of LCMV-WE. Expansion of gp33- and of NP396-CTL was measured in the blood by tetramers 8 days after challenge. Results represent the mean of two individual mice, and one representative experiment of two is shown.

(Fig. 2, *A* and *B*). Also, by titrating peptides in ICS for IFN-γ or on targets in a CTL assay, we did not find substantial differences between gp33–41 and NP396–404 (data not shown) provided that in these particular experiments we used the optimized D^b binder KAVYNFATM, with an affinity for D^b comparable to NP396–404, instead of the natural peptide KAVYNFATC. In addition, when we used the natural peptide (KAVYNFATC) and corrected for lower affinity to D^b (12), we also did not see differences in peptide titrations. The interaction of the TCR with H-2D^b/gp33–41 is not affected if the naturally occurring cysteine on position 9 is replaced by a methionine (45). Thus, the change of immunodominance after infection with different amounts of virus cannot be explained by differences in TCR affinity of polyclonal NP396- and gp33-CTL populations.

To distinguish between factors intrinsic to the responding CTL populations and LCMV-specific features, we primed mice with 5×10^5 bone marrow-derived DIETER DC transgenic for gp33–41 and NP396–404 (30) and challenged them 10 days later with 2×10^6 PFU rVV expressing gp33–41 or NP396–404 as a minigene (VV33, VV396) or with 100 PFU LCMV-WE. We found that gp33-CTL and NP396-CTL expanded to a similar extent after VV minigene challenge (Fig. 2*C*). In contrast, NP396-CTL expanded considerably stronger than gp33-CTL after LCMV challenge. This indicated that the difference in expansion seen in LCMV-challenged mice is not an intrinsic property of the individual CTL populations but rather depends on LCMV as such.

LCMV-infected macrophages present LCMV NP-derived CTL epitopes with increased kinetics compared with LCMV gp-derived CTL epitopes

Using infected cells in vitro, it has been shown that the LCMV NP is detectable at least 12 h before LCMV gp on the protein level (28). Thus, NP-derived epitopes can be presented before gp-derived epitopes, which may have important consequences for CTL induction: NP-CTL will be primed before gp-CTL and they will thus start controlling the virus before most gp-specific precursors had the chance to interact with their nominal peptide on LCMV-infected cells. Therefore, NP-CTL generally will be primed in the face of higher viral load than gp-CTL and can interfere with priming of gp-CTL at the same time. We investigated the existence of kinetic differences in the onset of presentation between gp-and NP-derived epitopes by infecting thioglycolate-elicited $CB6F_1$ (H-2^{bxd}) macrophages with LCMV-Arm or -WE at a m.o.i. of 2, resulting in infection of 100% of the macrophages as demonstrated by intracellular staining with an mAb against LCMV NP (VL4 (42)). Subsequently, their status of Ag presentation was frozen at different time points after infection by brefeldin A, and these macrophages were used as stimulators for IFN-γ production (ICS) by mono-specific CTL lines specific for three gp-derived (gp33–41/D^b, gp276–286/D^b, gp283–292/K^d) and two NP-derived (NP118–126/L^d, NP396–404/D^b) epitopes. We found that gp-derived epitopes were detectable by CTL after 7–8 h of infection and reached their maximum after 10 h, whereas NP-derived epitopes reached their maximum around 2 h after infection (Fig. 3). This was true for both LCMV-Arm (Fig. 3, *left panels*) and -WE (Fig. 3, *middle panels*), excluding the possibility that differences in immunodominance seen in vivo after infection with LCMV-Arm (NP396 immunodominant) or -WE (gp33 immunodominant) were due to differences in Ag processing or presentation between the two LCMV strains. Because differences in Ag sensitivity between the individual CTL lines would obscure our data, we included $CB6F_1$ macrophages loaded with titrated amounts of peptide in the same experiment to check the Ag sensitivity of CTL lines. Half-maximal stimulation of IFN-γ production required 10^{-10} M gp33,

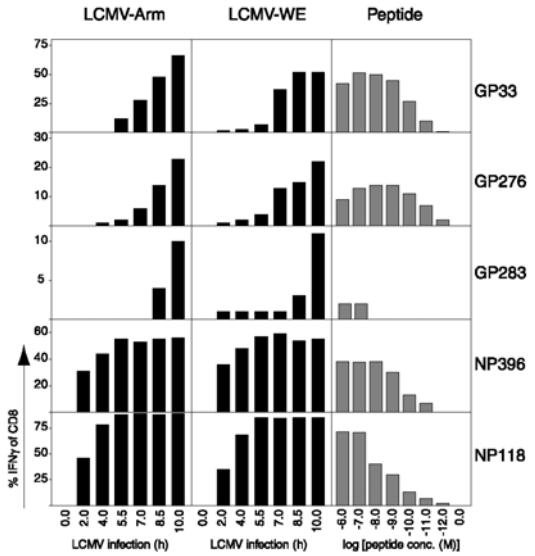

FIGURE 3. NP-derived CTL epitopes are presented to CTL with faster kinetics than gp-derived CTL epitopes. Thioglycolate-elicited $CB6F_1$ macrophages were infected with LCMV-Arm (*left panels*) or LCMV-WE (*middle panels*) with a m.o.i. of 2, and the state of Ag presentation was frozen at indicated time points by addition of brefeldin A (5 μg/ml). Subsequently, these macrophages were used to induce IFN-γ production by five independent, peptide-specific CTL lines as a readout. CTL were incubated with infected macrophages in the presence of brefeldin A for 6 h and were surface stained for CD8β and intracellularly for IFN-γ. *Right panels,* The same CTL lines were incubated as described above with $CB6F_1$ macrophages loaded with titrated amounts of peptide to determine the peptide sensitivity of the individual CTL lines. One representative experiment of four is shown.

10^{-11} M gp276, between 10^{-9} and 10^{-10} M NP396, and 10^{-8}M NP118 (Fig. 3, *right panels*). This indicates that gp-CTL lines were slightly more sensitive to Ag compared with the NP-CTL lines, excluding that faster detection of NP epitopes was due to higher Ag sensitivity of NP-CTL lines. However, the gp283-CTL line appeared relatively Ag insensitive ($>10^{-7}$ M required) and gp283–292 also became detectable extremely late (8.5 h) after infection (Fig. 3). This may be explained by the fact that $CB6F_1$ macrophages express limited numbers of the gp283–292-presenting H-2K^d molecule, whereas substantially higher numbers of H-2D^b and H-2L^d are expressed (data not shown). Using the same macrophages (infected for different times with LCMV-Arm or -WE or loaded with titrated peptide) as targets for peptide-specific CTL lines in a 5-h ^{51}Cr release assay, the above-mentioned kinetic differences were confirmed: NP-CTL lines (data not shown).

LCMV-infected splenocytes ex vivo present LCMV NP-derived CTL epitopes with increased kinetics compared with LCMV gp-derived CTL epitopes

LCMV is known to infect a variety of cells in vivo, such as DC and macrophages (46), and, therefore, in vitro-infected, thioglycolate-elicited macrophages may not represent the physiologically relevant population presenting LCMV-derived epitopes in vivo. To analyze the kinetics of Ag presentation in vivo, we infected $CB6F_1$ mice with 2×10^7 PFU LCMV-WE and used their splenocytes at different time points after infection as APC for NP118–126/L^d- or gp34–41/K^b-specific T cell hybridomas (38, 43). To exclude the possibility that differences in Ag sensitivity between the two hybridomas would influence our result, we included uninfected $CB6F_1$ macrophages with titrated amounts of peptide in the same experiment. For both hybridomas, maximal numbers of blue cells were found at 10^{-7} M peptide or higher and background numbers were found below 10^{-10} M peptide. This shows that the gp34/K^b-specific and the NP11/L^d-specific hybridoma were equally sensitive to Ag.

The kinetics of Ag presentation by in vivo-infected splenocytes were similar to those by in vitro-infected, thioglycolate-elicited macrophages (Fig. 4). gp34-specific T cells were activated by splenocytes that were infected for 12 h or more, and splenocyte infection for 20 h or more induced maximal numbers. In contrast, infection of splenocytes for 4 h or more resulted in the presentation of the NP118 epitope and maximal levels were reached after 12 h. The maximal numbers of activated hybridomas after incubation with infected splenocytes were ~50% of the maximal values observed after incubation with peptide in both cases. This may be explained by the fact that peptides were present throughout the overnight culture, thus avoiding the influence of peptide off-rates as is the case with infected splenocytes in the presence of brefeldin A.

Presentation by in vivo-infected splenocytes displayed a delay of ~2 h for both epitopes (NP and gp derived) compared with the in vitro-infected macrophages (Fig. 3). This may be explained by the lower peptide sensitivity of the hybridomas (~10^{-8} M (64)) compared with the mono-specific CTL lines we used (Fig. 3) or by the fact that it takes LCMV slightly longer to infect cells in vivo than in vitro, where the cells were infected at a high m.o.i. and in very close contact with the virus.

Kinetic differences in the presentation of LCMV-derived CTL epitopes can be visualized in vivo

To show the relevance of faster kinetics of presentation of NP-derived epitopes in vivo, we designed the following experiment:

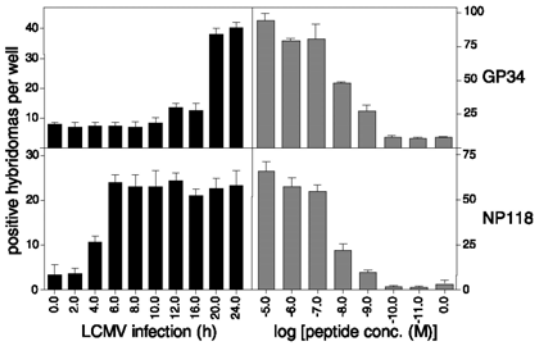

FIGURE 4. LCMV-infected splenocytes ex vivo present LCMV NP-derived CTL epitopes with increased kinetics compared with LCMV gp-derived CTL epitopes. $CB6F_1$ mice were infected i.v. with 2×10^7 PFU of LCMV-WE, their splenocytes were isolated at different time points after infection and were used as APC for NP118–126/L^d- or for gp34–41/K^b-specific T cell hybridomas. Five $\times$ 10^4 T cell hybridomas were incubated overnight at 37°C with 1.5×10^5 LCMV-infected splenocytes (*left panels*) or with 1.5×10^5 uninfected splenocytes in the presence of titrated amounts of peptide (*right panels*). Five micrograms of brefeldin A per milliliter was present throughout the culture period to freeze the status of Ag presentation by the infected splenocytes. After stimulation through the TCR, T cell hybridomas can be visualized by blue staining, resulting from a *lacZ* reporter gene under control of the IL-2 promoter/enhancer (37). Cultures were microscopically examined, and the number of blue cells per well was counted. Values represent the mean ± SD of triplicate cultures. One mouse was used per time point of infection. One representative experiment of two is shown.

We reasoned that "early" memory CTL (e.g., NP-CTL) recognize infected cells and start to eliminate them before "late" CTL (e.g., gp-CTL) had the chance to interact with their Ag, and thus substantially interfere with the priming of the latter. As a consequence, early memory CTL (e.g., NP-CTL) should block priming of late CTL (e.g., gp-CTL) upon infection with LCMV, but not vice versa. Thus, we primed mice with VV33, VV396, or VVc and challenged them 30 days later with 100 PFU LCMV-WE to investigate whether we could prime gp-CTL in the face of a pre-existing NP-CTL memory response and vice versa. It is important to note that priming with VV33 or with VV396 protects mice against subsequent LCMV challenge, resulting in very low (undetectable) LCMV levels (data not shown). We measured the frequency of gp33- and NP396-CTL in the spleen by tetramer staining (Fig. 5) at day 9 after LCMV challenge and confirmed the data by a primary ex vivo CTL assay 9 days after LCMV infection (data not shown).

After VV396 priming, pre-existing memory NP396-CTL were found to expand massively upon LCMV challenge (Fig. 5). gp33-CTL were not primed by LCMV in the presence of memory NP396-CTL (Fig. 5). This can be explained by different kinetics of Ag presentation: NP396-CTL could start to control LCMV-infected cells before gp33-CTL could efficiently interact with them, resulting in inhibition of gp33-CTL priming. In the reverse situation, VV33 priming results in enhanced expansion of gp33-CTL after LCMV challenge compared with VVc priming, thus demonstrating the increased number of gp33-specific precursors due to VV33 priming (Fig. 5). Interestingly, and in contrast with the situation described above, pre-existing memory gp33-CTL did not interfere with the priming of NP396-CTL (cf VVc and VV33 in Fig. 5). This shows that gp33-CTL, even although present as memory cells and at increased CTL_p numbers, could not interfere with the priming of NP396-CTL. Because gp is presented with delayed kinetics compared with NP, gp33-CTL were too late to interfere with NP396-CTL priming. The ex vivo CTL assay performed on day 9 confirmed the tetramer data (data not shown). It is unlikely that differences in priming between VV33 and VV396 are responsible for the observed findings: Priming with VV33 or with VV396 resulted in a specific CTL response of similar size as determined by tetramer analysis (0.8–1.0% of the $CD8^+$ at day 10 after infection) and by limiting dilution analysis (1 in 10^4 splenocytes at day 7 after infection). The frequency of specific memory CTL was comparable for VV33- and VV396-infected mice over at least 5 wk as measured by protection against LCMV challenge (data not shown).

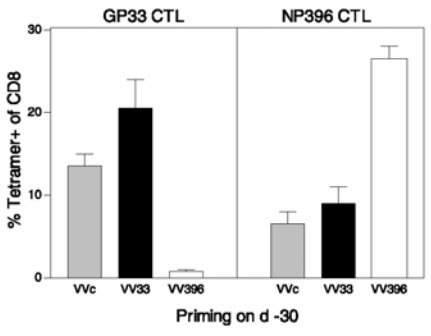

FIGURE 5. NP396-specific memory inhibits priming of gp33-specific cells, but not vice versa. C57BL/6 mice were primed by i.p. injection of 2×10^6 PFU of rVV33, rVV396, or rVVc and challenged 30 days later with 10^2 PFU of LCMV-WE. The expansion of gp33- and NP396-CTL was measured in the blood by tetramer staining after 9 days. Results represent the mean of three individual mice. One representative experiment of three is shown.

Discussion

LCMV infection induces a protective CTL response against both gp- and NP-derived epitopes. We describe here that inocula leading to a relatively low virus load (e.g., LCMV-Arm) resulted in immunodominance of NP-CTL, whereas increasing viral load (e.g., LCMV-WE or -Doc) coincided with decreasing NP-CTL, ultimately resulting in immunodominance of gp-CTL. We explained this finding by a higher sensitivity to Ag of NP-CTL compared with gp-CTL: NP-CTL thus would be preferentially activated by low levels of Ag and (partially) exhausted (18, 20, 44) upon increasing viral load. It has been suggested (46) that different strains of LCMV infect different cells in vivo: this would preclude comparison between strains as we do here. We infected C57BL/6 mice with 10^6 PFU of LCMV-Arm, -WE, or -Doc and stained splenocytes for subset markers and LCMV NP. We found that, independent of the strain used to infect, 5–8% of $CD11c^+$, 0.7–1.5% of $CD11b^+$, and $<0.5\%$ of $CD19^+$ or $TCR\alpha\beta^+$ cells stained positive for LCMV NP. This excludes that changes in immunodominance were due to different tropism of the individual strains. Comparison of the gp33- and the NP396-specific CTL response after infection with 1 or with 100 PFU of LCMV-WE demonstrates that the gp33-specific response increased, whereas the NP396 response decreased with higher viral load (Fig. 1). The data of Ou et al. (44) can be interpreted along the same line: They showed that infection of mice deficient for the IFN-$\alpha\beta$ receptor (A129 mice) with 100 PFU of LCMV-WE or with 10^5 PFU of LCMV-Arm resulted in a substantially higher viral load and in selective exhaustion of NP396-CTL when compared with wild-type control mice. Thus, also without varying the virus strain/dose used for infection, but by choosing the conditions such that the virus replicates to higher titers, NP-CTL were found to gradually disappear. We considered that the higher Ag sensitivity of NP-CTL could be due to 1) higher TCR affinity of NP-CTL, 2) prolonged presentation of NP compared with gp by infected cells (47), or 3) different kinetics of presentation of NP vs gp epitopes (28). We found no difference in TCR affinity as measured by tetramer dissociation (41) between NP396- and gp33-CTL or by peptide titration in CTL assay and in ICS. The finding that in mice persistently infected with LCMV gp expression was not found after day 15, whereas NP could be detected in all mice even after 80 days, has been used to explain the relatively high sensitivity to overstimulation of NP-CTL (18). However, the prolonged presence of a stable protein, like NP, does not mean that CTL epitopes are generated continuously: It has been proposed by Yewdell et al. (48) that the majority of the MHC class I-binding peptides are derived from defective ribosomal products and thus heavily depend on protein neosynthesis. Two studies supported this hypothesis (49, 50), and we showed recently for LCMV NP that no CTL epitopes were generated from this long-lived protein, unless neosynthesis took place (51). Therefore, the relevance of the observation that gp is not as persistent as NP in chronically infected mice to (over)stimulation of NP-CTL is not certain. We cannot formally exclude the possible contribution of cross-priming to the phenomenon we describe here. However, we do not expect cross-priming to be an important pathway for priming a CTL response against a pathogen that very efficiently infects DC.

We analyzed the kinetics of presentation of NP- and of gp-derived epitopes by LCMV-WE- and -Arm-infected macrophages, because we argued that faster presentation of NP-derived epitopes could account for a better protective capacity on a per cell basis

(19), for better priming at limited viral load, and for higher sensitivity to exhaustion at high viral load. We found that, independent of the LCMV strain used, both NP-derived epitopes were sufficiently presented to stimulate CTL as early as 2.5 h after infection, whereas it took at least 8 h before three different gp-derived epitopes were recognized. It is unlikely that different traveling times of particular MHC class I molecules from the endoplasmic reticulum to the cell surface account for the kinetic differences observed here, as H-2D^b is the restricting element of one NP-derived and two gp-derived peptides. To formally exclude the possibility that in vitro-infected, thioglycolate-elicited macrophages differed with respect to Ag presentation from those cells that are naturally infected by LCMV in vivo, we used splenocytes isolated from LCMV-infected mice at different time points after infection as APC to stimulate gp- or NP-specific T cell hybridomas (37, 38, 43). Using this approach, we found similar kinetic differences between the presentation of gp- and NP-derived epitopes. We used above readouts for Ag presentation rather than peptide elution from MHC class I molecules, because the latter method requires a large amount of cells ($>5 \times 10^8$ per time point and virus) that is impossible to obtain from other sources than from cell lines, the latter being probably abnormal in Ag processing or presentation.

As a result of faster kinetics of NP presentation, NP-CTL encounter their nominal peptide on every infected cell before gp-CTL do and will therefore be activated earlier and probably in the face of higher viral loads. The consequences of delayed gp presentation were demonstrated in vivo: pre-existing memory NP-CTL inhibited priming of gp-CTL, whereas pre-existing memory gp-CTL did not interfere with NP-CTL priming. In an attempt to investigate consequences of kinetic differences in epitope presentation for in vivo priming in a direct manner, we analyzed the expansion kinetics of NP- and gp-specific CTL at different early time points after infection. To this end, we performed ICS at 3, 4, 5, 6, 7, 8, and 9 days after infection. We detected LCMV-specific CTL from day 5 onward; however, we did not find substantial differences in expansion kinetics of NP- vs gp-CTL (data not shown). Detection of specific CTL by tetramers was unreliable as long as virus was still present (approximately until day 7), probably due to TCR down-regulation. Kinetic differences of 8 h may not lead to detectable differences in expansion kinetics, because the time required for initial T cell activation and proliferation is much longer than 8 h, thus masking possible initial differences. Moreover, it may well be that possible differences in expansion kinetics could not be detected anymore by day 5 because most of the virus usually is eliminated by then and a substantial part of the NP-CTL may be exhausted before they could expand to numbers that allow detection. No comparative data on naive CTL_p frequencies are currently available. Alternatively, small differences in the frequencies of CTL_p could probably cover up differences in expansion kinetics.

Kinetic differences in epitope presentation may also explain the finding that a NP118-CTL escape mutant of LCMV, that still expressed the gp283 CTL epitope, was controlled slower than the wild-type virus in BALB/c mice, but equally fast in $CB6F_1$ mice (that could use an additional NP-derived epitope, NP396) (13). It was found in the same study that the 118-CTL escape mutant efficiently primed subdominant gp283-CTL in BALB/c mice, but not in $CB6F_1$ mice, whereas LCMV-WE did not prime gp283-CTL in either mouse strain: Absence of an early NP-specific response in BALB/c mice (but not in $CB6F_1$ mice) results in slower virus control and allows the priming of otherwise subdominant and later gp-specific responses. Results obtained by mathematical analysis of the LCMV-specific CTL response in BALB/c mice (52) can also be explained by kinetic differences in epitope generation.

Based on our findings, we propose the general rule that CTL against early epitopes normally clear most of the virus and are at risk to be exhausted if the initial viral load is relatively high. Experiments showing that early NP-CTL are 100 times more effective in protecting mice against LCMV compared with late gp-CTL (Ref. 19 and M. F. van den Broek and H. C. Probst, unpublished data) fit this hypothesis. Data on specific CTL responses in other viral infections than LCMV seem to support the general applicability of our hypothesis. Vaccination of macaques with early simian immunodeficiency virus proteins (Rev, Tat) induced a protective immunity that was substantially more effective than vaccination with late simian immunodeficiency virus proteins (Pol, Gag) (53). Along the same line, longitudinal analysis of the HIV-specific CTL response in individuals with a high HIV load revealed that Rev- and Tat-specific CTL were the first to disappear (54–56). In analogy to what we described here for LCMV infection, namely, evidence for early activation of specific CTL followed by their gradual functional or even physical disappearance after they were unable to eliminate the Ag in due time can be found in a variety of infections, such as HIV (57, 58), hepatitis B (59–61), and hepatitis C (62) and also in tumor-bearing patients (63).

We propose that CTL against early viral proteins swiftly interfere with virus replication, resulting in efficient protection. If these early CTL fail in immediate virus control, they are activated in the face of higher viral load compared with late CTL and are therefore prone to be exhausted.

Thus, the observed absence of CTL in persistent infections might not be the cause, but rather the consequence of viral persistence.

Acknowledgments

We thank Nathalie Oetiker-Jeanguenat and Anita Dürmüller (Institute of Experimental Immunology, Zurich, Switzerland) for help with some experiments, Günter Hämmerling (Deutsches Krebsforschungszentrum, Heidelberg, Germany) for the anti-D^b Ab T21-460, Marcus Groettrup (University of Constance, Constance, Germany) for the LCMV-specific T cell hybridomas, and Vincenzo Cerundolo (Institute of Molecular Medicine, Oxford, U.K.) for the plasmid pSC11.3OR2. We are indebted to Rolf Zinkernagel and Hans Hengartner (Institute of Experimental Immunology) for continued support and helpful discussions. We thank Paul Klenerman (Institute of Molecular Medicine) for reading this manuscript and for helpful suggestions.

References

1. Rammensee, H., K. Falk, and O. Rötschke. 1993. Peptides naturally presented by MHC class I molecules. *Annu. Rev. Immunol. 11:213.*
2. Momburg, F., and G. Hämmerling. 1998. Generation and TAP-mediated transport of peptides for MHC class I molecules. *Adv. Immunol. 68:191.*
3. Townsend, A., J. Bastin, K. Gould, G. Brownlee, M. Andrew, B. Coupar, D. Boyle, S. Chan, and G. Smith. 1988. Defective presentation to class I restricted CTL in vaccinia-infected cells is overcome by enhanced degradation of antigen. *J. Exp. Med. 168:1211.*
4. Groettrup, M., A. Soza, U. Kuckelkorn, and P. Kloetzel. 1996. Peptide antigen production by the proteasome: complexity provides efficiency. *Immunol. Today 17:429.*
5. Zinkernagel, R., and P. Doherty. 1979. MHC-restricted cytotoxic T cells: studies on the biological role of polymorphic major transplantation antigens determining T-cell restriction specificity, function and responsiveness. *Adv. Immunol. 27:52.*
6. Kägi, D., B. Ledermann, K. Bürki, P. Seiler, B. Odermatt, K. Olsen, E. Podack, R. Zinkernagel, and H. Hengartner. 1994. Cytotoxicity mediated by T cells and natural killer cells is greatly impaired in perforin-deficient mice. *Nature 369:31.*
7. Riddell, S., K. Watanabe, J. Goodrich, C. Li, M. Agha, and P. Greenberg. 1992. Restoration of viral immunity in immunodeficient humans by adoptive transfer of T cell clones. *Science 257:238.*
8. Rickinson, A., and B. Moss. 1997. Human CTL responses to Epstein-Barr virus infection. *Annu. Rev. Immunol. 15:405.*
9. Guidotti, L., T. Ishikawa, M. Hobbs, B. Matzke, R. Schreiber, and F. Chisari. 1996. Intracellular inactivation of hepatitis B virus by cytotoxic T lymphocytes. *Immunity 4:25.*
10. Gallimore, A., H. Hengartner, and R. Zinkernagel. 1998. Hierarchies of antigen-specific cytotoxic T cell responses. *Immunol. Rev. 164:29.*

11. Van der Most, R., A. Sette, C. Oseroff, J. Alexander, K. Murali-Krishna, L. Lau, S. Southwood, J. Sidney, R. Chestnut, M. Matloubian, and R. Ahmed. 1996. Analysis of CTL responses to dominant and subdominant epitopes during acute and chronic LCMV infection. *J. Immunol. 157:5543.*
12. Van der Most, R., K. Murali-Krishna, J. Whitton, C. Oseroff, J. Alexander, S. Southwood, J. Sidney, R. Chestnut, A. Sette, and R. Ahmed. 1998. Identification of D^b- and K^b-restricted subdominant CTL responses in LCMV-infected mice. *Virology 240:158.*
13. Weidt, G., O. Utermöhlen, J. Heukeshoven, F. Lehmann-Grube, and W. Deppert. 1998. Relationship among immunodominance of single $CD8^+$ T cell epitopes, viral load, and kinetics of primary antiviral CTL response. *J. Immunol. 160:2923.*
14. Sourdive, D., K. Murali-Krishna, J. Altman, A. Zajac, J. Whitmire, C. Pannetier, P. Kourilsky, B. Evavold, A. Sette, and R. Ahmed. 1998. Conserved T cell receptor repertoire in primary and memory CD8 T cell responses to an acute viral infection. *J. Exp. Med. 188:71.*
15. Murali-Krishna, K., J. Altman, M. Suresh, D. Sourdive, A. Zajac, J. Miller, J. Slansky, and R. Ahmed. 1998. Counting antigen-specific CD8 T cells: a reevaluation of bystander activation during viral infection. *Immunity 8:177.*
16. Butz, E., and M. Bevan. 1998. Massive expansion of antigen-specific $CD8^+$ T cells during acute virus infection. *Immunity 8:167.*
17. Blattman, J., D. Sourdive, K. Murali-Krishna, R. Ahmed, and J. Altman. 2000. Evolution of the T cell repertoire during primary, memory, and recall responses to viral infection. *J. Immunol. 165:6081.*
18. Zajac, A., J. Blattman, K. Murali-Krishna, D. Sourdive, M. Suresh, J. Altman, and R. Ahmed. 1998. Viral immune evasion due to persistence of activated T cells without effector function. *J. Exp. Med. 188:2205.*
19. Gallimore, A., T. Dumrese, H. Hengartner, R. Zinkernagel, and H. Hengartner. 1998. Protective immunity does not correlate with the hierarchy of virus-specific CTL responses to naturally processed peptides. *J. Exp. Med. 187:1647.*
20. Moskophidis, D., F. Lechner, H. Pircher, and R. Zinkernagel. 1993. Virus persistence in acutely infected immunocompetent mice by exhaustion of antiviral cytotoxic effector T cells. *Nature 362:758.*
21. Oxenius, A., R. Zinkernagel, and H. Hengartner. 1998. Comparison of activation versus induction of unresponsiveness of virus-specific CD4 and CD8 T cells upon acute versus persistent virus infection. *Immunity 9:449.*
22. Pantaleo, G., J. Demarest, T. Schacker, M. Vaccarezza, O. Cohen, M. Daucher, C. Graziosi, S. Schnittmann, T. Quinn, and G. Shaw. 1997. The qualitative nature of the primary immune response to HIV infection is a prognosticator of disease progression independent of the initial level of plasma viremia. *Proc. Natl. Acad. Sci. USA 94:254.*
23. Klein, M., C. van Baalen, A. Holwerda, S. kerkhof Garde, R. Bende, I. Keet, J. eeftinck-Schattenkerk, A. Osterhaus, H. Schitemaker, and F. Miedema. 1995. Kinetics of Gag-specific CTL responses during the clinical course of HIV-1 infection: a longitudinal analysis of rapid progressors and long-term asymptomatics. *J. Exp. Med. 181:1365.*
24. Ogg, G., X. Jin, S. Bonhoeffer, P. Dunbar, M. Nowak, S. Monard, J. Segal, Y. Cao, S. Rowland-Jones, and Cerundolo, V. 1998. Quantitation of HIV-1-specific CTL and plasma load of viral RNA. *Science 279:2103.*
25. Battegay, M., D. Moskophidis, A. Rahemtulla, H. Hengartner, T. Mak, and R. Zinkernagel. 1994. Enhanced establishment of a virus carrier state in adult $CD4^+$ T cell-deficient mice. *J. Virol. 68:4700.*
26. Matloubian, M., R. Concepcion, and R. Ahmed. 1994. $CD4^+$ T cells are required to sustain $CD8^+$ CTL responses during chronic viral infection. *J. Virol. 68:8056.*
27. Cardin, R., J. Brooks, S. Sarawar, and P. Doherty. 1996. Progressive loss of $CD8^+$ T cell-mediated control of a gamma-herpesvirus in the absence of $CD4^+$ T cells. *J. Exp. Med. 184:863.*
28. Bruns, M., T. Kratzberg, W. Zeller, and F. Lehmann-Grube. 1990. Mode of replication of lymphocytic choriomeningitis virus in persistently infected cultivated mouse L cells. *Virology 177:615.*
29. Pircher, H., D. Moskophidis, U. Rohrer, K. Bürki, H. Hengartner, and R. Zinkernagel. 1990. Viral escape by selection of CTL-resistant variants in vivo. *Nature 346:629.*
30. Probst, H. C., J. Lagnel, G. Kollias, and M. van den Broek. 2003. Inducible transgenic mice reveal resting dendritic cells as potent inducers of $CD8^+$ T cell tolerance. *Immunity 18:713.*
31. Lehmann-Grube, F. 1971. Lymphocytic choriomeningitis virus. *Virol. Monogr. 10:1.*
32. Buchmeier, M., R. Welsh, F. Dutko, and M. Oldstone. 1980. The virology and immunology of LCMV infection. *Adv. Immunol. 30:275.*
33. Pfau, C., J. Valenti, D. Pevear, and K. Hunt. 1982. Lymphocytic choriomeningitis killer cells are lethal only in weakly disseminated murine infections. *J. Exp. Med. 156:79.*
34. Cerundolo, V., A. Kelly, T. Elliott, J. Trowsdale, and A. Townsend. 1995. Genes encoded in the major histocompatibility complex affecting the generation of peptides for TAP transport. *Eur. J. Immunol. 25:554.*
35. Moss, B., and P. Earl. 1998. Expression of proteins in mammalian cells using vaccinia viral vectors. In *Current Protocols in Molecular Biology.* F. M. Ausubel, R. Brent, R. E. Kingston, D. D. Moore, J. G. Seidman, J. A. Smith, and K. Struhl, eds. Wiley, New York, pp. 16.15.1–16.15.5.
36. Inaba, K., M. Inaba, N. Romani, H. Aya, M. Deguelin, S. Ikehara, S. Muramatsu, and R. Steinman. 1992. Generation of large numbers of dendritic cells from mouse bone marrow cultures supplemented with granulocyte/monocyte-colony stimulating factor. *J. Exp. Med. 176:1693.*
37. Shastri, N., and F. Gonzalez. 1993. Endogenous generation and presentation of the ovalbumin peptide/K^b complex to T cells. *J. Immunol. 150:2724.*
38. Schwarz, K., M. van den Broek, R. de Giuli, W. Seelentag, N. Shastri, and M. Groettrup. 2000. The use of LCMV-specific T-cell hybridomas for the quantitative analysis of MHC class I restricted antigen presentation. *Immunol. Methods 237:199.*
39. Altman, J., P. Moss, P. Goulder, D. Barouch, M. McHeyzer-Williams, J. Bell, A. McMichael, and M. Davis. 1996. Phenotypic analysis of antigen-specific T lymphocytes. *Science 274:94.*
40. Gallimore, A., A. Glithero, A. Godkin, A. Tissot, A. Plückthun, T. Elliott, H. Hengartner, and R. Zinkernagel. 1998. Induction and exhaustion of LCMV-specific T lymphocytes visualised using soluble tetrameric MHC class I-peptide complexes. *J. Exp. Med. 187:1373.*
41. Savage, P., J. Boniface, and M. Davis. 1999. A kinetic basis for T cell receptor repertoire selection during an immune response. *Immunity 10:485.*
42. Battegay, M., S. Cooper, A. Althage, J. Bänzinger, H. Hengartner, and R. Zinkernagel. 1991. Quantification of LCMV with an immunological focus assay in 24 or 96 well plates. *J. Virol. Methods 33:191.*
43. Usherwood, E., T. Hogg, and D. Woodland. 1999. Enumeration of antigen-presenting cells in mice infected with Sendai virus. *J. Immunol. 162:3350.*
44. Ou, R., S. Zhou, L. Huang, L., and D. Moskophidis. 2001. Critical role for α/β and γ interferons in persistence of LCMV by clonal exhaustion of cytotoxic T cells. *J. Virol. 75:8407.*
45. Achour, A., J. Michaelson, R. Harris, J. Odeberg, P. Grufman, J. Sandberg, V. Levitsky, K. Kärre, T. Sandalova, and G. Schneider. 2002. A structural basis for LCMV immune evasion: subversion of H-$2D^b$ and H-$2K^b$ presentation of gp33 revealed by comparative crystal structure analysis. *Immunity 17:757.*
46. Sevilla, N., S. Kunz, A. Holz, H. Lewicki, D. Homann, H. Yamada, K. Campbell, J. de la Torre, and M. Oldstone. 2000. Immunosuppression and resultant viral persistence by specific viral targeting of dendritic cells. *J. Exp. Med. 192:1249.*
47. Oldstone, M., and M. Buchmeier. 1982. Restricted expression of viral glycoprotein in cells of persistently infected mice. *Nature 300:360.*
48. Yewdell, J., L. Anton, and J. Bennink. 1996. Defective ribosomal products (DriPs): a major source of antigenic peptides for MHC class I molecules. *J. Immunol. 157:1823.*
49. Schubert, U., L. Anton, J. Gibbs, C. Norbury, J. Yewdell, and A. Bennink. 2000. Rapid degardation of a large fraction of newly synthesized proteins by proteasomes. *Nature 404:770.*
50. Reits, E., J. Vos, M. Gromme, M., and J. Neefjes. 2000. The major substrates for TAP in vivo are derived from newly synthesized proteins. *Nature 404:774.*
51. Khan, S., R. de Giuli, G. Schmidtke, M. Bruns, M. Buchmeier, M. van den Broek, and M. Groettrup. 2001. Cutting edge: neosynthesis is required for the presentation of a T cell epitope from a long-lived viral protein. *J. Immunol. 167:4801.*
52. De Boer, R. 2001. Recruitment times, proliferation, and apoptosis rates during the $CD8^+$ T cell response to LCMV. *J. Virol. 75:10663.*
53. Geretti, A., and A. Osterhaus. 2001. Virus replication and evolution drive the kinetics and specificity of SIV-specific CTL. *Immunol. Rev. 183:109.*
54. Van Baalen, C., O. Pontesilli, R. Huisman, A. Geretti, M. Klein, F. de Wolf, F. Miedema, R. Gruters, and A. Osterhaus. 1997. Human immunodeficiency virus type 1 Rev and Tat specific CTL frequencies inversely correlate with rapid progression to AIDS. *J. Gen. Virol. 78:1913.*
55. Addo, M., M. Atfeld, E. Rosenberg, R. Elridge, M. Philips, K. Habeeb, A. Khatri, C. Brander, G. Robbins, G. Mazzara, et al. 2001. The HIV-1 regulatory proteins Tat and Rev are frequently targeted by CTL derived from HIV-1-infected individuals. *Proc. Natl. Acad. Sci. USA 98:1781.*
56. Novitsky, V., N. Rybak, M. McLane, P. Gilbert, P. Chingwedere, I. Klein, S. Gaolekwe, S. Chang, T. Peter, I. Thior, et al. 2001. Identification of HIV-1C Gag-, Tat-, Rev-, and Nef-specific Elispot-based CTL responses for AIDS vaccine design. *J. Virol. 75:9210.*
57. Appay, V., R. Dunbar, M. Callan, P. Klenerman, G. Gillespie, L. Papagno, G. Ogg, A. King, F. Lechner, C. Spina, et al. 2000. HIV-specific $CD8^+$ T cells produce antiviral cytokines but are impaired in cytolytic function. *J. Exp. Med. 192:63.*
58. Kostense, S., G. Ogg, E. Manting, G. Gillespie, J. Joling, K. Vandenberghe, E. Veenhof, D. van Baarle, S. Jurriaans, M. Klein, and F. Miedema. 2001. High viral burden in the presence of major HIV-specific $CD8^+$ T cell expansions: evidence for impaired CTL effector function. *Eur. J. Immunol. 31:677.*
59. Lechner, F., N. Gruener, S. Urbani, J. Uggeri, T. Santantonio, A. Kammer, A. Cerny, R. Phillips, C. Ferrari, G. Pape, and P. Klenerman. 2000. $CD8^+$ T lymphocyte responses are induced during acute hepatitis C virus infection but are not sustained. *Eur. J. Immunol. 30:2479.*
60. Lechner, F., D. Wong, P. Dunbar, R. Chapman, R. Chung, P. Dohrenwend, G. Robbins, R. Phillips, P. Klenerman, and B. Walker. 2000. Analysis of successful immune responses in persons infected with hepatitis C virus. *J. Exp. Med. 191:1499.*
61. Sing, K., A. Ladhams, S. Arnold, H. Parmar, X. Chen, J. Cooper, L. Butterworth, K. Stuart, D. D'Arcy, and W. Cooksley. 2001. A longitudinal analysis of CTL precursor frequencies to the hepatitis B virus in chronically infected patients. *J. Viral Hepatitis 8:19.*
62. Erickson, A:, Y. Kimura, S. S. Igarashi, J. Eichelberger, M. Houghton, J. Sidney, D. McKinney, A. Sette, A. Hughes, and C. Walker. 2001. The outcome of hepatitis C virus infection is predicted by escape mutations in epitopes targeted by CTL. *Immunity 15:883.*
63. Lee, P., C. Yee, P. Savage, L. Fong, D. Brockstedt, J. Weber, D. Johnson, S. Swetter, J. Thompson, P. Greenberg, M. Roederer, and M. Davis. 1999. Characterization of circulating T cells specific for tumor-associated antigens in melanoma patients. *Nat. Med. 5:677.*

Chapter 7

A cytomegalovirus inhibitor of gamma interferon signaling controls immunoproteasome induction

Selina Khan, Albert Zimmermann, Michael Basler, Marcus Groettrup, & Hartmut Hengel

Published in Journal of Virology 2004:78(4):1831-42.

JOURNAL OF VIROLOGY, Feb. 2004, p. 1831–1842 Vol. 78, No. 4
0022-538X/04/$08.00+0 DOI: 10.1128/JVI.78.4.1831–1842.2004

A Cytomegalovirus Inhibitor of Gamma Interferon Signaling Controls Immunoproteasome Induction

Selina Khan,[1]† Albert Zimmermann,[2] Michael Basler,[3] Marcus Groettrup,[1,3]* and Hartmut Hengel[2]*

Research Department, Cantonal Hospital St. Gallen, CH-9007 St. Gallen, Switzerland,[1] and Division of Viral Infections, Robert Koch-Institut, Nordufer 20, D-13353 Berlin,[2] and Division of Immunology, Department of Biology, University of Constance, D-78457 Konstanz,[3] Germany

Received 8 July 2003/Accepted 24 October 2003

Both human and mouse cytomegaloviruses (HCMV and MCMV) avoid peptide presentation through the major histocompatibility complex (MHC) class I pathway to CD8$^+$ T cells. Within the MHC class I pathway, the vast majority of antigenic peptides are generated by the proteasome system, a multicatalytic protease complex consisting of constitutive subunits, three of which can be replaced by enzymatically active gamma interferon (IFN-γ)-inducible subunits, i.e., LMP2, LMP7, and MECL1, to form the so-called immunoproteasomes. Here, we show that steady-state levels of immunoproteasomes are readily formed in response to MCMV infection in the liver. In contrast, the incorporation of immunoproteasome subunits was prevented in MCMV-infected, as well as HCMV-infected, fibroblasts in vitro. Likewise, the expression of the IFN-γ-inducible proteasome regulator PA28αβ was also impaired in MCMV-infected cells. Both MCMV and HCMV did not alter the constitutive-subunit composition of proteasomes in infected cells. Quantitative assessment of LMP2, MECL1, and LMP7 transcripts revealed that the inhibition of immunoproteasome formation occurred at a pretranscriptional level. Remarkably, a targeted deletion of the MCMV gene *M27*, encoding an inhibitor of STAT2 that disrupts IFN-γ receptor signaling, largely restored transcription and protein expression of immunoproteasome subunits in infected cells. While CMV block peptide transport and MHC class I assembly by posttranslational strategies, immunoproteasome assembly, and thus the repertoire of proteasomal peptides, is controlled by pretranscriptional mechanisms. We hypothesize that the blockade of immunoproteasome formation has considerable consequences for shaping the CD8$^+$-T-cell repertoire during the effector phase of the immune response.

Human cytomegalovirus (HCMV), a prototype member of the betaherpesvirus subfamily, is an important pathogen and can cause a wide range of disease manifestations. Primary infection in the immunocompetent host is usually asymptomatic, whereas in the immunocompromised host infection or virus reactivation from latency can cause severe and even fatal disease. Mouse cytomegalovirus (MCMV) shows a similar pathobiology and has a collinear genome (47). Studies of humans and of the mouse have revealed that virus-specific CD8$^+$ T lymphocytes represent the dominant effector arm of protective immunity. For immune recognition, the infected cells present virus-derived peptides on their major histocompatibility complex (MHC) class I molecules to CD8$^+$ cytotoxic T lymphocytes. The processing and presentation of viral peptides is therefore the basis for immune recognition of infected cells, and a change in or lack of peptide supply can undermine the efficiency of T-cell recognition and result in immune evasion of the virus. Both HCMV and MCMV avoid peptide presentation by the expression of several viral glycoproteins (gps) controlling distinct checkpoints of the MHC class I presentation pathway. Specifically, the HCMV *US6*-encoded gp shuts off the translocation of peptides across the endoplasmic reticulum membrane by the transporter associated with antigen processing (TAP) (2, 31). MHC class I complex formation and transport to the cell surface is blocked by the HCMV gps US2, US11, and US3. MCMV affects peptide presentation by the gps m152/gp40 (70), m06/gp48 (57), and m04/gp34 (37, 40).

The majority of endogenous proteins are degraded via the ubiquitin-proteasome pathway. In this pathway, the proteolytic core is the 20S proteasome. Although it is freely accessible in the cytoplasm and nucleoplasm, its geometry prevents the uncontrolled access of substrates. The 20S proteasome is shaped like a closed cylinder constituted from four stacked rings. Each of the two outer rings is composed of seven different subunits of the α type, whereas each of the two inner rings is constituted from seven different β-type subunits. Both β-rings contain a copy of the subunits delta (β1), MB1 (β5), and Z (β2), which bear the active centers facing the luminal side of the 20S proteasome. Upon stimulation of cells with gamma interferon (IFN-γ), these three subunits are replaced by the IFN-γ-inducible subunits LMP2, LMP7, and MECL-1, respectively (8, 11, 13, 24), to form so-called immunoproteasomes. These subunit replacements have been shown to alter the different catalytic activities of the proteasome (42) and to promote the production of peptide ligands for MHC class I molecules (12, 63, 69). Overexpression of the immunoproteasome subunits LMP2, LMP7, and MECL1 in cell lines enhanced the presentation of

* Corresponding author. Mailing address for Hartmut Hengel: Division of Viral Infections, Robert Koch-Institut, Nordufer 20, D-13353 Berlin, Germany. Phone: 49 1888 754 2502. Fax: 49 1888 754 2328. E-mail: hengelh@rki.de. Mailing address for Marcus Groettrup: Lehrstuhl für Immunologie, Universität Konstanz, Universitätsstrasse 10, D-78457 Konstanz, Germany. Phone: 49 7531 882130. Fax: 49 7531 883102. E-mail: Marcus.Groettrup@uni-konstanz.de.

† Present address: Department of Immunohematology and Blood Bank, University Hospital, 2300 RC Leiden, The Netherlands.

different viral epitopes, such as the NP118 epitope of the lymphocytic choriomeningitis virus (LCMV) nucleoprotein (62) or an epitope derived from the GagL protein of Moloney murine leukemia virus (68). Further evidence for the significance of the proteasome in antigen processing comes from studies using proteasome inhibitors, which have been found to abolish MHC class I antigen presentation (59). In addition, mice deficient in LMP2 and LMP7 showed some deficiencies in peptide processing and presentation (12, 69).

26S proteasome holoenzymes consist of catalytic 20S proteasomes and one or two copies of the 19S regulatory complex. Moreover, so-called hybrid proteasomes, which consist of 20S proteasomes bound by the 19S regulator (PA700), as well as an 11S regulator (PA28α/β), have been described (28). PA700 and PA28 serve to control the hydrolytic activity of the 20S core particle. PA28αβ consists of two subunits, α and β, which form hexa- or heptameric rings that can bind to one or both sides of the 20S proteasome (18). Both subunits of PA28 are inducible by IFN-γ (1), and PA28 has been shown to play a role in antigen presentation and the generation of peptide ligands for MHC class I molecules (10, 23, 50).

Since the proteasome is the key protease generating peptides for the MHC class I antigen presentation pathway, we analyzed the impact of HCMV and MCMV infection on the proteasome subunit composition. We hypothesized that CMVs may alter the makeup of the proteasome and its regulatory complex, PA28αβ, to affect the cleavage and presentation of antigenic peptides. The formation of immunoproteasomes was dramatically induced during acute MCMV replication in the liver. In clear contrast, MCMV, as well as HCMV, prevented the incorporation of the IFN-γ-inducible proteasome subunits LMP2, MECL1, and LMP7 in infected cells in vitro. Moreover, the expression of the proteasome regulator PA28αβ was also affected by MCMV infection. The blockade of immunoproteasome assembly was due to pretranscriptional inhibition and required the expression of the MCMV gene *M27*, encoding an inhibitor of IFN-γ receptor signaling (A. Zimmermann, M. Trilling, M. Wagner, M. Wilborn, I. Bubic, T. Ziade, S. Jonjic, U. H. Koszinowski, and H. Hengel, submitted for publication). The data identify different cellular compartments and opposing principles of proteasome regulation by CMV infection in infected cells versus neighboring cells in infected tissues. The findings predict differences between the repertoires of viral peptides generated by immunoproteasomes in professional antigen-presenting cells (APC) on one hand and by housekeeping proteasomes in productively infected cells on the other.

MATERIALS AND METHODS

Mice. Female BALB/cJ (*H-2*^{d}) mice were purchased from the University of Konstanz (Konstanz, Germany). The mice were kept in a conventional pathogen-free environment and used at 8 to 9 weeks of age.

Viruses, cells, and infection conditions. The Smith strain of MCMV (ATCC VR-194) and the MCMV mutant ΔM27 (Zimmermann et al., submitted) were propagated in third-passage mouse embryo fibroblasts (MEF) and purified by being pelleted through a sucrose cushion before the virus titers were determined by a standard plaque assay. Tissue cultures were infected with MCMV at a multiplicity of infection of 10 and harvested at the appropriate times postinfection (p.i.). The animals were infected by intraperitoneal injection with 10^6 PFU of MCMV before they were sacrificed on day 6 p.i. and their organs were removed. Stocks of HCMV strain AD 169 were prepared using human MRC5 cells (30). Infectious supernatants were harvested when 100% of the cells showed cytopathic effects. Virus titers were determined by a standard plaque assay. HCMV infection was enhanced by centrifugation at 800 × *g* for 30 min. In all experiments, MRC5 cells were infected with HCMV at a multiplicity of infection of 5 to 10. The cells were processed further as indicated below.

Purification of 26S proteasome from mouse livers. The 26S proteasome was purified from uninfected and MCMV-infected BALB/c mouse livers according to a protocol originally designed for the purification of 26S proteasomes from rabbit muscle, which we adopted for mouse liver tissue (9). The livers were homogenized in TSDG buffer (10 mM Tris–HCl, 1 mM dithiothreitol [DTT], 1 mM NaN_3, 25 mM NaCl, 10 mM $MgCl_2$, 0.1 mM EDTA, 10% glycerol, 2 mM ATP, 50 mM NaF, 0.1 mM Na_8VO_4, pH 7.5) using a Dounce 40-ml glass homogenizer. The homogenate was centrifuged for 20 min at 20,000 × *g*, and the supernatant was filtered through a layer of glass wool; the supernatant was centrifuged once more, this time for 45 min at 100,000 × *g*, and recovered after filtering it over the glass wool. The clarified crude lysate was adsorbed onto the DEAE-TSK 650S resin (Tosoh Biosep, Stuttgart, Germany) that had been equilibrated in TSDG buffer (2 g of liver tissue per g of DEAE matrix) by being tumbled end over end for at least 1 h at 4°C. Subsequently, unbound proteins were removed by washing the DEAE gel with TSDG buffer. The DEAE resin was suspended in 50 ml of TSDG and poured into the column (C10/20; 1 by 15 cm; Pharmacia, Zürich, Switzerland). After the column was packed, 20 ml of TSDG was pumped over the column at 1 ml/min. The column was washed with 20 ml of 75 mM KCl in TSDG, bound proteins were eluted with a linear gradient (190 ml) of 75 to 400 mM KCl in TSDG buffer, and 2-ml fractions were collected. After elution, peptidase activity was measured using the fluorogenic peptide substrate *N*-succinyl-LLVY-7-amido-4-methylcoumarin (Suc-LLVY-MCA) at a final concentration of 200 μM. The fluorogenic-peptide assay was performed exactly as previously described (22). Fractions with peak activity were pooled, and the 26S proteasome sample was concentrated by ultracentrifugation at 100,000 × *g* for 21 h at 4°C. The 26S proteasome precipitated by ultracentrifugation was subjected to Sepharose 6B using a column with the dimensions 1.6 by 98 cm (Pharmacia C16/100; Amersham Bioscience, Zürich, Switzerland) in TSDG buffer, proteins were eluted with a flow rate of 0.4 ml/min, and 2-ml fractions were collected and tested for proteasome activity. The pooled active fractions were then applied to an arginine-Sepharose column (Amersham Bioscience) with the dimensions 1.5 by 6 cm and equilibrated in TSDG, and unbound proteins were washed away with 20 ml of TSDG. The proteins were eluted with a linear gradient (300 ml) from 25 to 400 mM KCl in TSDG buffer at a flow rate of 1 ml/min, and 3-ml fractions were collected. The fractions containing peak activity were pooled and subjected to another ultracentrifugation at 100,000 × *g* for 21 h at 4°C. After the concentration step, the precipitated proteasome was loaded onto glycerol gradients of 20 to 40% glycerol in Kopp buffer (20 mM Tris, 1.2 mM $MgCl_2$, 0.1 mM EDTA, 1 mM DTT, 1 mM NaN_3, pH 7.5) and centrifuged for 20 h at 100,000 × *g*. After the run, 0.5-ml fractions were recovered and peptidase activity was measured. Fractions with peak activity were pooled and processed further for nondenaturing polyacrylamide gel electrophoresis (PAGE) and two-dimensional gel electrophoresis. The purified 26S proteasome was separated by isoelectric focusing (IEF) using the Immobiline DryStrip pH gradient strips from Amersham BioScience, and the second dimension was performed on a vertical 12.5% sodium dodecyl sulfate (SDS) gel. Subsequently, the gels were silver stained. For quantification, the gels were scanned and analyzed using AIDA software (Fuji, Tokyo, Japan).

Nondenaturing PAGE and substrate overlay. Nondenaturing polyacrylamide gels (2.5% [wt/vol] stacking gels and 4% [wt/vol] separating gel) were prepared using Bio-Rad Mini Protean electrophoresis units and gels (10 by 8 cm by 0.75 mm). The gels were run at 10 mA per gel for 2 h at 4°C. Thereafter, the gel was covered with substrate buffer (30 mM Tris, pH 7.5, 10 mM KCl, 1 mM DTT, 5 mM $MgCl_2$, 2 mM ATP, 100 μg of creatine kinase/ml, 100 mM creatine phosphate) containing 200 μM Suc-LLVY-MCA and incubated in a humid chamber for 10 min at 37°C. Activity was then visualized by exposing the gel to UV light (365-nm wavelength). Subsequently, the gels were stained with Coomassie blue.

IFN-γ treatment and metabolic labeling. MEF were stimulated with 100 U of mouse IFN-γ/ml (Alexis Biochemicals, Grünberg, Germany), and MRC5 cells were stimulated with 500 U of human IFN-γ/ml (Alexis Biochemicals) for periods as described in the figure legends. Thereafter, subconfluent monolayers of cells were either harvested for real-time reverse transcription (RT)-PCR and Western blot analysis or cells were labeled with [^{35}S]methionine and [^{35}S]cysteine (1,200 Ci/mmol; Amersham-Pharmacia, Freiburg, Germany) at a concentration of 500 μCi/ml for 6 h in methionine-free medium before overnight chase. After being washed with 2% phosphate-buffered saline (PBS), the cells were lysed in lysis buffer for immunoprecipitation.

Immunoprecipitation and NEPHGE. The labeled cells were lysed in buffer A (25 mM Tris–HCl, pH 7.5, 1 mM DTT, 2 mM ATP, 2 mM $MgCl_2$) containing 0.2 mg of creatine kinase/ml and 40 mM creatine phosphate as an ATP-regenerating

system (28). After sonication, the lysates were clarified by centrifugation and precleared for 60 min using protein G-Sepharose beads. The supernatants were incubated overnight with protein G-Sepharose, precoated with the monoclonal antibody MCP444 (mouse anti-human HN3; generously provided by Klavs Hendil, Copenhagen, Denmark) (29) or a polyclonal anti-proteasome serum generated in rabbits against purified 20S proteasome (61). The beads were washed five times in 1 ml of buffer A and once in 25 mM ammonium acetate, pH 7.5, and the immunoprecipitated proteasome was then separated by nonequilibrium pH gradient electrophoresis (NEPHGE)–SDS-PAGE as described previously (28). The dried gels were exposed to Kodak BioMaxMR films for 7 days. For quantification, the films were scanned and analyzed using AIDA software.

Real-time RT-PCR. Extraction of total RNA from cells and real-time RT-PCR were conducted as described previously (39). The primers used for the LMP2, LMP7, delta, and hypoxanthine phosphoribosyltransferase PCR amplifications were as described previously (39), whereas the primers for PA28α PCR amplification were 5′-AAGAGAAGAAGAAAGGGGACG-3′ and 5′-AGCTTGGT GTGAAGGTTGG-3′, with an annealing temperature of 60°C. The sense and antisense primers used for MECL1 were 5′-CGTCTGCCCTTTACTGC-3′ and 5′-CCACTTCATTCCACCTCC-3′, with an annealing temperature of 60°C. In each run, the mock samples (uninfected and unstimulated cells) were compared to IFN-γ-stimulated and MCMV-infected samples. The value calculated by the quantification analysis was always within the range covered by three concentrations of the mock sample, which was taken as arbitrary units to construct the standard curve for linear regression with r equal to 1.0 and a P value of <0.0001. The amounts of template cDNAs were normalized to those of hypoxanthine phosphoribosyltransferase mRNA. The amplification was checked by melting-curve analysis of the products.

Western blotting. Cells were lysed in buffer B (50 mM Tris, pH 7.5, 5 mM $MgCl_2$, 1 mM EDTA, 0.5% Triton) followed by sonication, and the lysates were clarified by centrifugation. Thereafter, the lysates were boiled for 5 min in Laemmli sample buffer (10 mM Tris, pH 6.8, 10.4 mM SDS, 38 nM bromophenol blue, 2.5% glycerol) and separated by SDS-PAGE. The proteins were blotted onto nitrocellulose (Schleicher & Schüll, Dassel, Germany), which was blocked with PBS–5% (wt/vol) low-fat dry milk–0.1% Tween 20 for 1 h and agitated overnight at 4°C with the appropriate antibodies in PBS–5% low-fat dry milk. Immunoblots were performed with the following antibodies: anti-MCMV pp89 monoclonal antibody Croma 101, anti-β-actin (Sigma, Munich, Germany), anti-proteasome subunit C7 (α1; a kind contribution of Klaus Scherrer, Paris, France), anti-LMP2, anti-LMP7, anti-MECL-1, and anti-PA28α (39). The blots were washed and incubated for 1 h with a horseradish peroxidase-conjugated secondary antibody, goat anti-rabbit immunoglobulin G (Jackson ImmunoResearch, West Grove, Pa.). After extensive washing with PBS–0.1% Tween 20, the proteins were visualized on X-ray films by chemiluminescence. For quantification, the films were scanned and analyzed using AIDA software.

RESULTS

Induction of immunoproteasomes during MCMV infection in vivo. Recently, it was shown that LCMV infection results in a rapid and dramatic induction of immunoproteasome formation in vivo that is mediated by cytokines, particularly IFN-γ (39). In MCMV-infected mice, IFN-γ has been demonstrated to govern the yield of processing, as well as the presentation of the MCMV ie1/pp89-derived, *H-2 L^d*-restricted peptide YPHFMPTNL, in infected organs (15, 32). On the other hand, MCMV has been demonstrated to block IFN-γ-induced antiviral responses (43), the MHC class I presentation function in infected fibroblasts (32), and IFN-γ-induced MHC class II expression in infected macrophages (27). To determine whether immunoproteasomes are formed in MCMV-infected tissues in vivo, BALB/c mice were infected intraperitoneally with 10^6 PFU of MCMV, and 26S proteasomes were purified from the livers (see Materials and Methods) of MCMV-infected and control animals on day 6 p.i. At this point, MCMV replication reaches high titers of ~4 to 5 $\log_{10}$ PFU per g of tissue (67; Zimmermann et al., submitted). The purified 26S proteasomes from uninfected and infected mice were separated on IEF–SDS-PAGE two-dimensional gels before the gels were silver stained (Fig. 1A and B) and quantified using the invariant subunit MN3 (β7) as a standard (Fig. 1C). The assignment of proteasome subunits was performed according to their migratory positions in two-dimensional gels, which were previously identified by protein microsequencing (21). The immunoproteasome subunit LMP2 was markedly upregulated during MCMV infection, while LMP7 was already quite prominent in uninfected mice. However, since both of the corresponding constitutive subunits delta and MB1 disappear from the MCMV-infected liver, a further replacement of MB1 by LMP7 must also have occurred. Changes in the subunit pattern of the 19S regulator or among enzymatically inactive subunits of the 20S proteasome were not observed. To verify that the purified 26S proteasome was indeed intact and enzymatically active, the preparation was subjected to a native acrylamide gel electrophoresis. 26S proteasomes were visualized by overlaying the gel with the fluorogenic peptide substrate Suc-Leu-Leu-Val-Tyr methyl-coumaryl-7-amide (Fig. 1E). Proteolytic activity was found at one distinct band of the 26S proteasome preparation. This band migrated significantly more slowly than the proteolytic activity of a purified 20S proteasome preparation. In summary, this finding indicated that under steady-state conditions, functional immunoproteasomes are readily generated in response to acute MCMV infection in vivo.

HCMV infection prevents the formation of immunoproteasomes. Like MCMV, HCMV was reported to prevent IFN-γ receptor-mediated cellular responses, like an elevation of MHC class II expression, by interfering with JAK/STAT signaling (45, 46). In view of the dramatic upregulation of immunoproteasome formation during MCMV replication in the liver, we wanted to settle the question of whether immunoproteasomes are formed in IFN-γ-exposed infected cells. To study proteasome assembly, human MRC5 fibroblasts were metabolically labeled for 6 h using [^{35}S]methionine and [^{35}S]cysteine before overnight chase. After the lysis of cells, the proteasomes were immunoprecipitated using the monoclonal antibody MCP444, which recognizes the beta subunit HN3 (β7) (29) and does not interfere with the binding of the regulatory complexes to the 20S proteasome. The precipitation of immune complexes was conducted under conditions maintaining the interaction between the 20S proteasome and the PA700 complex (28). The immunoprecipitated 26S proteasome was subsequently separated by NEPHGE and SDS-PAGE (Fig. 2A to D). Quantification of the induction of immunoproteasomes is shown in Fig. 2E. Treatment of MRC5 cells with IFN-γ resulted in the incorporation of the immunoproteasome subunits LMP2 and LMP7 into the proteasome by replacing the subunits delta and MB1 (Fig. 2B), as reported previously with other cell lines (3, 14). Infection of MRC5 cells with HCMV for 72 h did not significantly change the relative amount of incorporated LMP7 in relation to the MB1 subunits compared to uninfected cells (Fig. 2C versus A and E). In contrast, LMP2 expression was decreased three- to fourfold after HCMV infection. Next, we assessed the IFN-γ-induced increase of immunoproteasomes in HCMV-infected MRC5 cells. Remarkably, IFN-γ treatment of HCMV-infected cells did not enhance the levels of incorporated immunoproteasome subunits (Fig. 2D), whereas an almost-complete exchange of LMP7 for MB1 occurred in uninfected MRC5 cells after stimulation with IFN-γ. Again, no changes in the subunit pattern of the 19S regulator or among

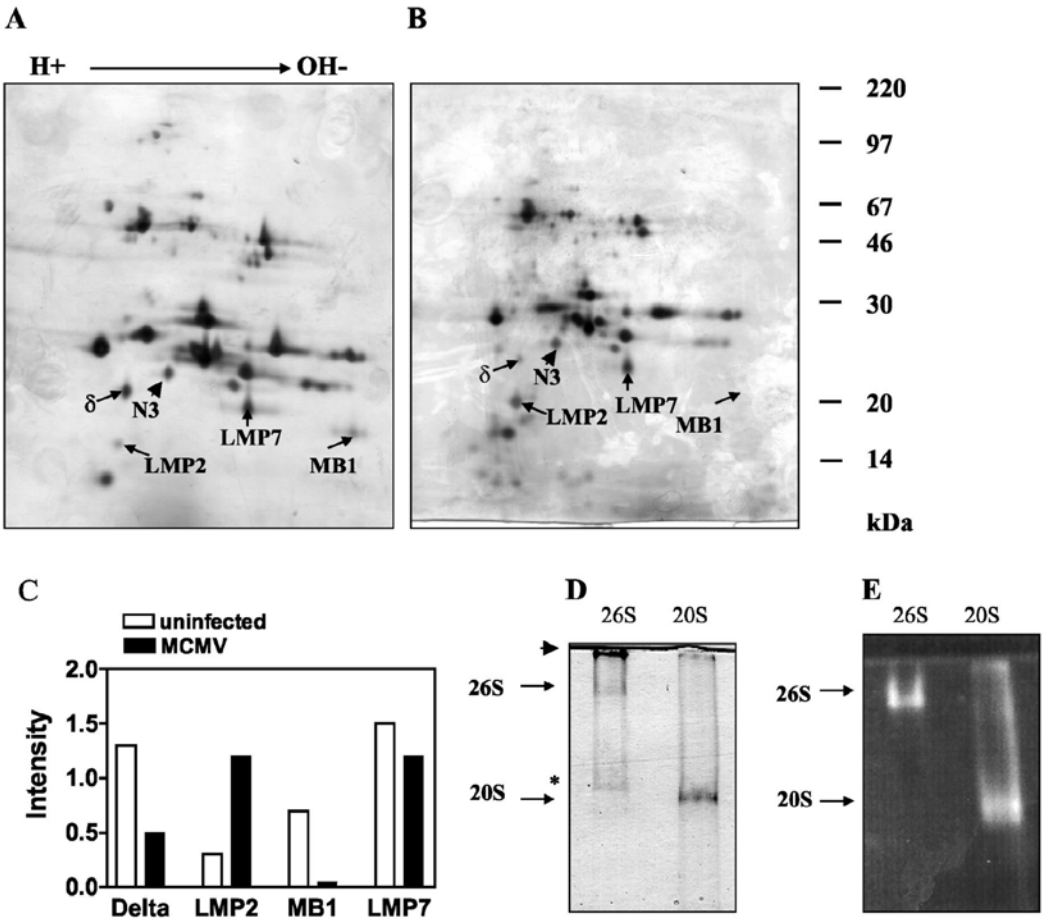

FIG. 1. (A and B) Two-dimensional IEF–SDS-PAGE of 26S proteasome purified from the livers of uninfected and MCMV-infected mice. Purified 26S proteasomes (100 μg) from uninfected (A) or MCMV-infected (B) BALB/c mice were separated by IEF–SDS-PAGE, and the gels were silver stained. The constitutive subunits N3, delta, and MB1 and the immunoproteasome subunits LMP2 and LMP7 are indicated. (C) Densitometric evaluation of the indicated proteasome subunits from the two-dimensional gels shown in panels A and B. The intensity values are standardized on the expression of the constitutive and invariant β-type subunit N3, setting the intensity of N3 to 1. (D and E) Nondenaturing PAGE of the purified 26S proteasome. Purified proteasomes were electrophoresed for 2 h at 10 mA on a 4.5% native polyacrylamide gel, and 30 μg of proteins was loaded in each lane. Lanes: 26S, 26S proteasomes; 20S, purified 20S proteasome. Enzyme activity was localized by a peptide overlay using the fluorogenic peptide Suc-LLVY-MCA (E), and the proteins were subsequently stained with Coomassie blue (D). The arrowhead in panel D indicates the top of the gel, whereas the asterisk indicates a band corresponding to the PA700 complex, as determined by Western blot analysis (data not shown). The gels shown were reproduced three times each.

enzymatically inactive subunits of the 20S proteasome were apparent. In conclusion, the data demonstrated an impaired generation of immunoproteasomes in HCMV-infected cells.

Inhibition of IFN-γ-mediated immunoproteasome induction in MCMV-infected cells. To find out whether the induction of immunoproteasomes in MCMV-infected fibroblasts is blocked, as observed in HCMV infection, we analyzed MEF 30 h p.i. As shown in Fig. 3, MCMV infection led to an inhibition of the IFN-γ-mediated induction and incorporation of LMP2 and LMP7 into proteasomes (compare Fig. 3B with D), while mock-infected MEF exposed to IFN-γ responded with an increase of LMP2- and LMP7-containing proteasomes (compare Fig. 3A with B). A quantification of the expression of the respective subunits revealed that MCMV infection led to a four- to fivefold inhibition of LMP2 and LMP7 induction in IFN-γ-stimulated infected MEF compared to uninfected MEF. The expression of the immunoproteasome subunits in MCMV-infected cells decreased by two- to fourfold compared to uninfected MEF cells. Taken together, the findings indicated that the generation of immunoproteasomes is inhibited to similar degrees in HCMV- and MCMV-infected cells in vitro. This effect could be due to either decreased synthesis of immunoproteasome subunits or inhibition of immunoproteasome subunit incorporation during 20S proteasome assembly.

Changes in steady-state levels of immunoproteasome subunits LMP2, LMP7, MECL-1, and PA28. To test whether MCMV infection decreases the steady-state levels of the immunoproteasome subunits LMP2, LMP7, MECL-1, and PA28,

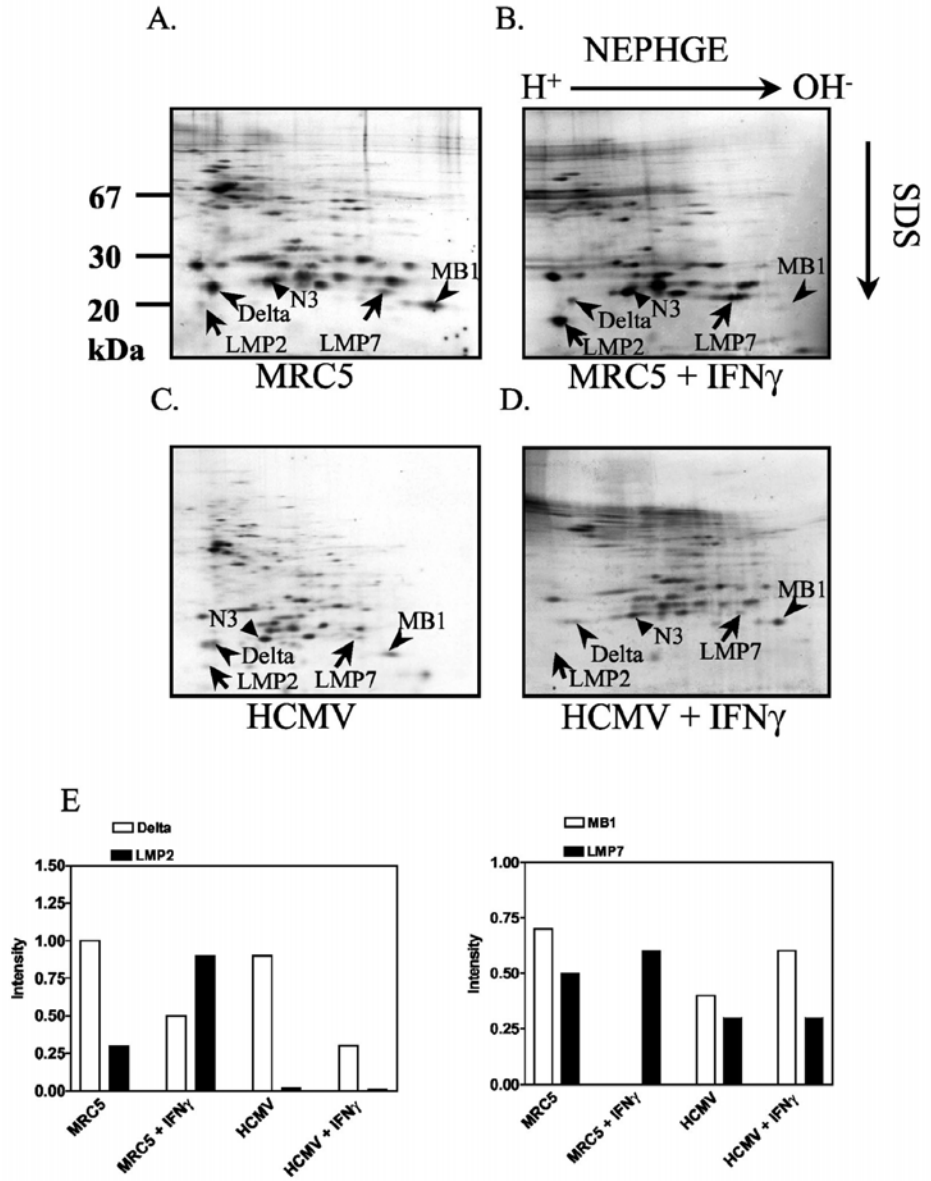

FIG. 2. HCMV infection reduces the IFN-γ-dependent induction of immunoproteasomes. MRC5 cells were left uninfected (A and B) or were infected with the HCMV strain AD169 for 72 h (C and D). IFN-γ (500 U/ml) was added for 24 h after 48 h of infection (D) or for 24 h to uninfected cells (B) prior to pulse-chase labeling and immunoprecipitation of the proteasome. Proteasome subunits were separated by NEPHGE–SDS-PAGE. The invariant β subunit N3 and the IFN-γ-inducible subunits LMP2 and LMP7, as well as their constitutively expressed homologues delta and MB1, are indicated. (E) Quantification of radioactivity in the two-dimensional gels. Intensity values are standardized on the expression of the constitutive and invariant β-type subunit N3. The gels shown are from one experiment out of three.

Western blot analysis was performed. As shown in Fig. 4A, the total proteasome content remained unchanged following MCMV infection, as indicated by the same levels of the constitutive subunit C7 (α1). Upon stimulation of MEF cells with IFN-γ for 24 h, the abundances of the immunoproteasome subunits LMP2, LMP7, and MECL-1 were strongly elevated. MCMV infection alone resulted in a modest but significant induction of these subunits in vitro. Interestingly, MCMV infection inhibited the induction of LMP2, LMP7, and MECL-1 when the cells were infected for 6 h with MCMV before they were treated with IFN-γ for 6, 12, or 24 h. In order to achieve a more quantitative evaluation of steady-state immunoproteasome expression levels, we analyzed titrated amounts of lysates on Western blots probed with C7-, LMP2-, and MECL-1-specific antibodies (Fig. 4B). Quantification by densitometry in the linear range of detection yielded 15- and 57-fold induction

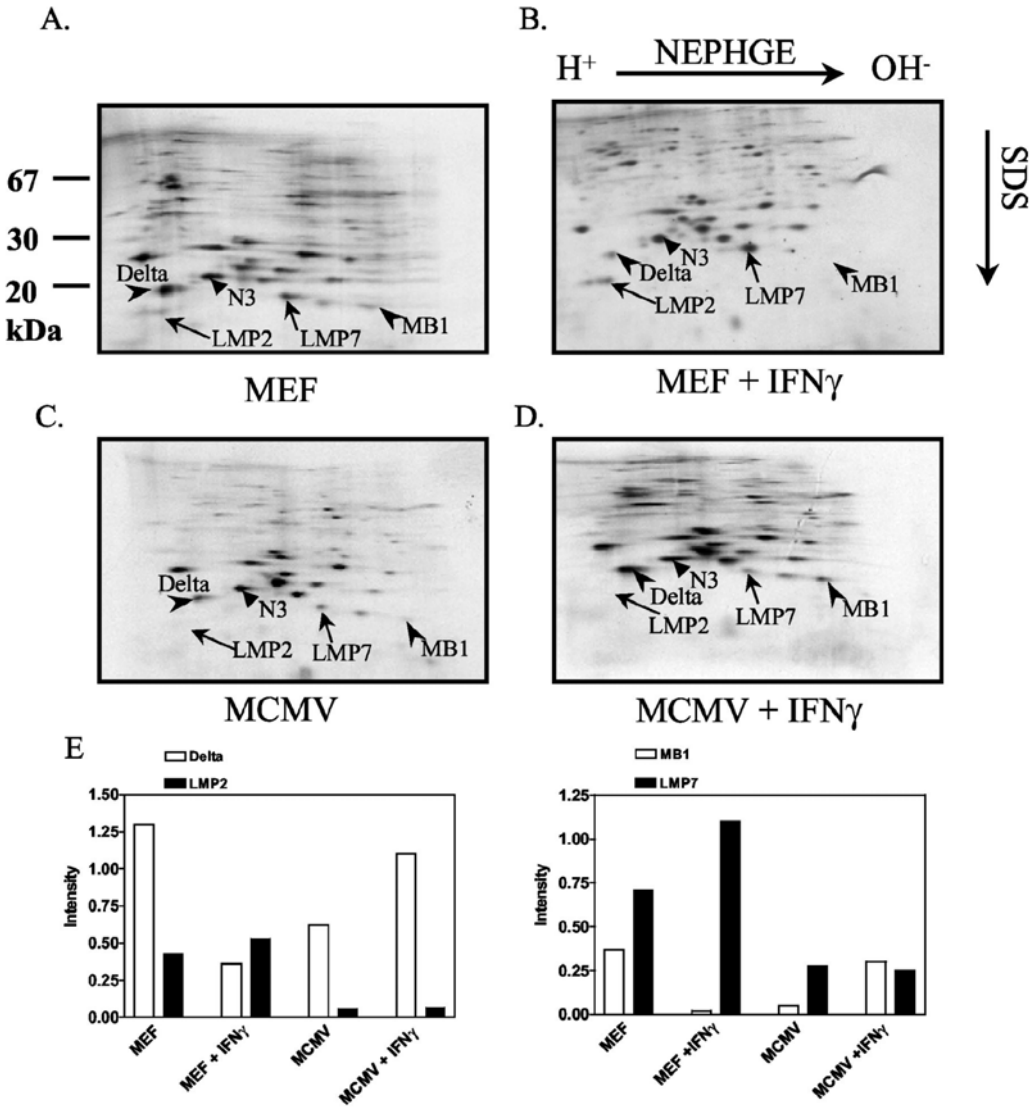

FIG. 3. MCMV suppresses the IFN-γ-dependent induction of the immunoproteasome subunits LMP2 and LMP7. MEF were left uninfected (A and B) or infected with MCMV for 30 h (C and D). After 6 h of infection, 100 U of mouse IFN-γ/ml was added (D), or it was added to uninfected cells (B) prior to pulse-chase labeling. Proteasomes were immunoprecipitated and separated by NEPHGE–SDS-PAGE. The IFN-γ-inducible subunits LMP2 and LMP7 and their constitutively expressed homologues delta and MB1 are indicated, along with the constitutive β-type subunit N3. (E) Quantitative evaluation of the two-dimensional gels, as indicated in the legend to Fig. 2. The gels shown are from one experiment out of three independent experiments.

of LMP2 and MECL-1, respectively, after stimulation with IFN-γ for 24 h, which was inhibited 3- and 1.5-fold, respectively, when the cells were infected with MCMV. The proteasome regulator PA28αβ, which enhances the processing of several viral epitopes (61, 68), was enhanced 27-fold by IFN-γ treatment in uninfected cells and 13-fold in MCMV-infected cells (Fig. 4A). In summary, these findings suggested that MCMV impedes the synthesis, assembly, or stability of immunoproteasome components.

MCMV inhibits gene transcription of immunoproteasomes and the PA28αβ regulator. To determine whether the MCMV-mediated inhibition of the synthesis of immunoproteasome subunits and the PA28α activator occurred at a pretranscriptional or posttranscriptional level, real-time RT-PCR was conducted to assess the mRNA levels of LMP2, MECL1, LMP7, and PA28α gene transcription. The results from one of two independent experiments are listed in Table 1. As expected, incubation of MEF with IFN-γ resulted in up to a 100-fold

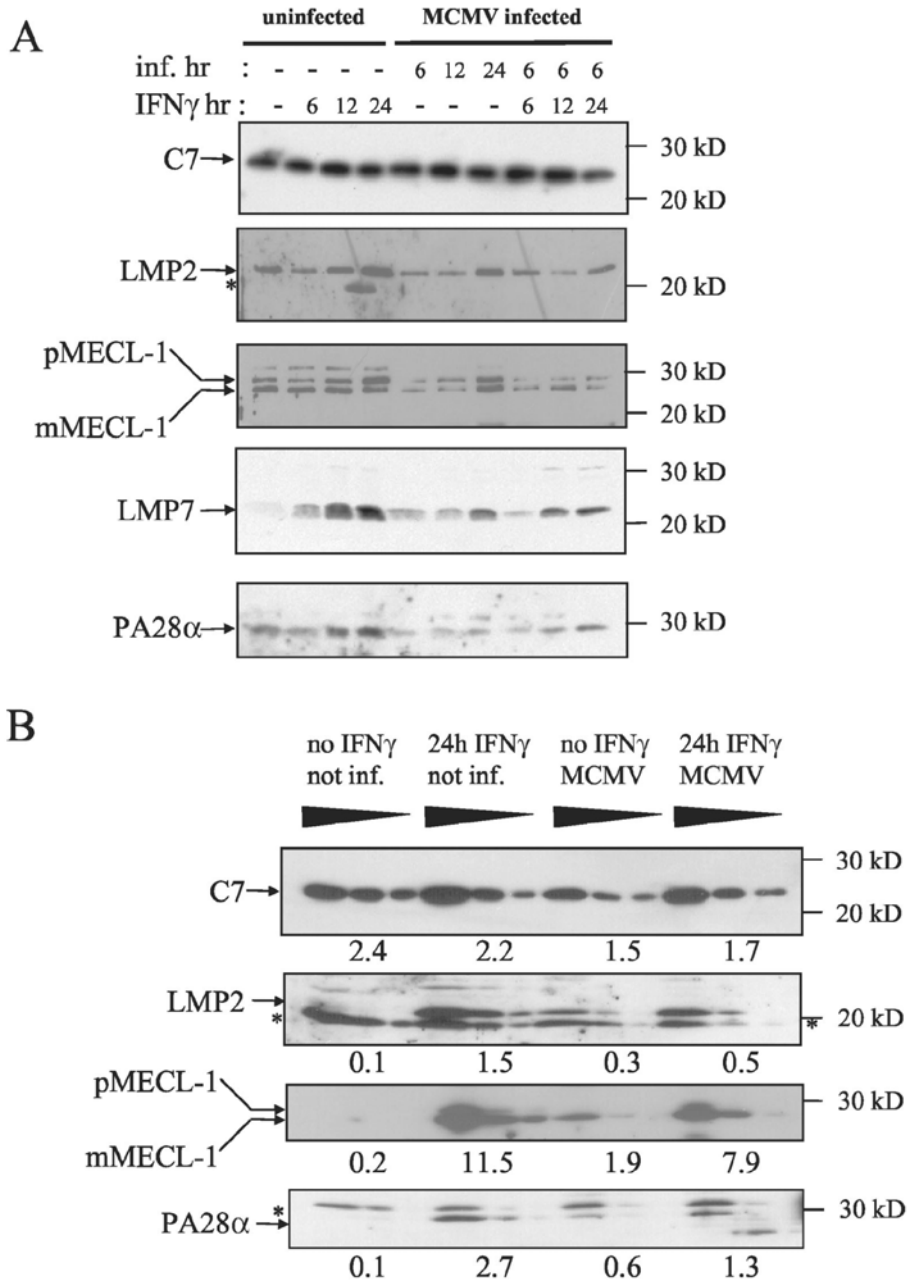

FIG. 4. Steady-state levels of the proteasome subunits LMP2, LMP7, and MECL-1 and the proteasome regulator subunit PA28α. MEF were left uninfected (−) or were infected (inf.) with MCMV for 6, 12, or 24 h as indicated before they were stimulated with 100 U of mouse IFN-γ/ml for 6, 12, or 24 h as shown at the top of each panel. (A) Crude cell lysates were separated by SDS-PAGE and blotted. The Western blots were probed with antibodies specific for the constitutive proteasome subunit C7 (α1); the immunoproteasome subunits LMP2, LMP7, and MECL-1; and the α subunit of the proteasome regulator PA28. For MECL-1 both the precursor (pMECL-1) and the mature subunit (mMECL-1) are visible. The asterisks indicate cross-reactive irrelevant bands. (B) For a semiquantitative assessment of steady-state protein expression, threefold dilutions of lysates were analyzed on Western blots specific for C7, LMP2, MECL-1, and PA28α. IFN-γ treatment was performed for 24 h with or without MCMV infection 6 h before the onset of IFN-γ stimulation. The bands were analyzed by densitometry in the linear range of detection, and the raw density data of volume integration minus background density are indicated below the samples.

increase in the mRNA levels of the immunoproteasome subunits LMP2, LMP7, MECL1, and PA28α. Plateau levels were reached 12 to 24 h after the exposure of cells to IFN-γ for LMP2 and LMP7. MCMV infection alone induced LMP2 and LMP7 transcription ~2- to 4-fold compared to uninfected cells. The mRNA level for the constitutive β subunit delta remained virtually unchanged, indicating that the inhibition of the IFN-γ-inducible expression of immunoproteasome and PA28α genes was not due to a general effect on proteasome gene transcription during MCMV infection. The data demonstrated that IFN-γ induction of immunoproteasome gene transcription is inhibited in MCMV-infected cells.

The MCMV gene *M27* is essential for the full suppression of immunoproteasome subunits. The MCMV early gene *M27* has been shown to downregulate STAT2 and thereby confers resistance in viral replication to IFN-γ in vitro and in vivo (Zimmermann et al., submitted). As a consequence, the replication of a ΔM27 mutant is completely blocked in the presence of IFN-γ. We surmised from this finding that IFN-γ-induced transcription of immunoproteasome genes might be restored in ΔM27-infected cells. When the levels of LMP2 and LMP7 transcripts were quantitated by real-time PCR, a significant induction by IFN-γ was found, which reached a little lower values than in mock-infected IFN-γ-treated MEF (Table 1). Western blot analysis revealed that levels of MECL-1 and LMP7 (Fig. 5) were also significantly higher in ΔM27-infected cells than in wild-type MCMV-infected cells. However, the expression levels in ΔM27-infected cells were not as high as in uninfected controls, leaving open the possibility that other MCMV-encoded genes may contribute to immunoproteasome suppression. In conclusion, the data indicated that MCMV already prevents immunoproteasome formation at the stage of IFN-γ receptor signal transduction.

DISCUSSION

Here, we demonstrate that proteasomes are subject to CMV regulation and identify how CMV infection modulates proteasome subunit composition. In response to acute MCMV infection, mice generate strong induction of immunoproteasomes in the liver, i.e., the constitutive proteolytically active subunits delta, MB1, and Z are rapidly replaced by the IFN-γ-inducible subunits LMP2, LMP7, and MECL-1 within the 20S core proteasome complex. In sharp contrast, the formation of immunoproteasomes in vitro is blocked in MCMV-infected, as well as HCMV-infected, fibroblasts treated with high doses of IFN-γ. Further analysis of the viral blockade of immunoproteasome formation revealed a decrease in protein expression and gene transcription, suggesting that CMV infection results in a state of unresponsiveness to IFN-γ-induced immunoproteasome gene induction. The diminished incorporation of LMP2 and LMP7 into the proteasome after IFN-γ treatment of HCMV-infected cells is in agreement with a recent study by Miller and colleagues reporting that HCMV leads to a transcriptional downregulation of IFN-γ-sensitive genes within the MHC class II locus (including TAP1, TAP2, LMP2, and LMP7 genes) (46). Taking advantage of an MCMV mutant, ΔM27 (Zimmermann et al., submitted), which lacks an inhibitor of STAT2, we identified IFN-γ receptor signaling as a critical step

TABLE 1. Real-time RT-PCR analysis of mRNA in MEF after MCMV infection and/or IFN-γ treatment[a]

Time (h)	Level																							
	LMP2					LMP7					δ					MECL1					PA28α				
	Mock + IFN-γ	MCMV (wt)	MCMV (wt) + IFN-γ	ΔM27	ΔM27 + IFN-γ	Mock + IFN-γ	MCMV (wt)	MCMV (wt) + IFN-γ	ΔM27	ΔM27 + IFN-γ	Mock + IFN-γ	MCMV (wt)	MCMV (wt) + IFN-γ	ΔM27	ΔM27 + IFN-γ	Mock + IFN-γ	MCMV (wt)	MCMV (wt) + IFN-γ	ΔM27	ΔM27 + IFN-γ	Mock + IFN-γ	MCMV (wt)	MCMV (wt) + IFN-γ	ΔM27	ΔM27 + IFN-γ
0	1	1	1	1	1	1	1	1	1	1	1	1	1	ND	ND	1	1	1	ND	ND	1	1	1	ND	ND
6	31	4.2	5	4.5	13.8	14	3.1	5.2	5.3	30	1.6	1.5	1.8	ND	ND	6.9	1.9	1.4	ND	ND	6.3	1.5	2.4	ND	ND
12	126	4.0	21	10.8	94	127	2.5	11	17.9	32	1.5	1.4	1.5	ND	ND	14.2	1.8	4.1	ND	ND	9.2	1.9	3.2	ND	ND
24	90	4.6	2.7	14.8	108	35	2.3	0.8	9.3	51	1.3	1.0	0.8	ND	ND	89	3.2	21	ND	ND	21	4.8	4.8	ND	ND

[a] Indicated as relative levels (LMP2/HPRT, LMP7/HPRT, δ/HPRT, MECL1/HPRT, and PA28α/HPRT). wt, wild type; Mock, mock infected; ND, not done.

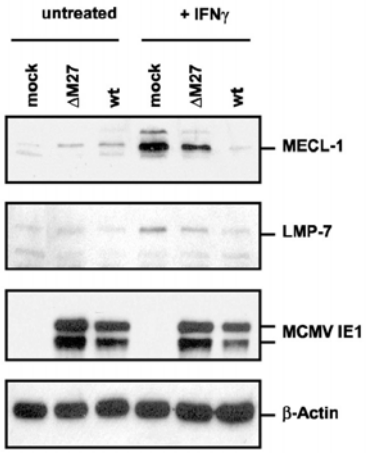

FIG. 5. Steady-state levels of MECL-1 and LMP7 in wild-type (wt) MCMV- and ΔM27-infected MEF. Equivalent amounts of cell lysates of mock- and MCMV-infected MEF, either unstimulated or stimulated with IFN-γ (+ IFN-γ), were separated by SDS-PAGE and blotted. Western blot analysis was performed using antibodies specific for MECL-1, LMP7, MCMV IE1 (pp89 and pp76), and β-actin.

for CMV interference with immunoproteasome gene expression and function.

Immunoproteasome induction in vivo. At first glance, our in vitro and in vivo findings appear paradoxical. The likely explanation of the strong increase in the steady-state levels of immunoproteasomes in response to MCMV infection in the liver is a scenario in which (i) uninfected bystander cells in infected tissue become exposed to inflammatory cytokines, like IFN-γ and tumor necrosis factor alpha, known to induce immunoproteasome synthesis (3, 11, 13) and (ii) immune cells which constitutively express immunoproteasome subunits immigrate in great numbers into sites of virus replication in the liver (48). Hepatic 20S proteasomes have an extraordinarily long half-life of 12 to 15 days, as demonstrated in metabolically labeled rats (66), indicating that the replacement of constitutive proteasomes by immunoproteasomes in MCMV-infected livers occurs surprisingly fast. A strong increase in immunoproteasome formation has also been documented in the livers of mice during viral, bacterial, and fungal infections with LCMV, *Listeria monocytogenes*, and *Histoplasma capsulatum* (6, 39). This effect was markedly reduced in IFN-γ-deficient mice, indicating that this cytokine is indeed a leading factor driving proteasome replacement in vivo (39). On the organ level and under steady-state conditions, the inflammatory increase far surpasses the direct inhibition of immunoproteasome formation in infected cells. The fact that only a small fraction of liver parenchyma is productively infected with MCMV (26, 49) resolves the seeming paradox between the in vitro and in vivo findings.

Prevention of immunoproteasome assembly: restriction of peptide antigen complexity? A pertinent question concerns what consequences the downregulation of immunoproteasomes may have for antigen presentation and clearance of CMV-infected cells. There is ample evidence that immunoproteasomes have altered peptidolytic properties. This is based on the fact that of the 14 different proteasomal subunits, only the three enzymatically active components, i.e., delta, Z, and MB1, have IFN-γ-inducible counterparts. Incorporation of LMP2, MECL1, and LMP7 is carried out interdependently, favoring the assembly of homogeneous immunoproteasomes (19, 25). As a result, two different types of proteasomes are built, those with constitutively expressed catalytic subunits and immunoproteasomes. Proteasomal peptides can be subdivided into three distinct subsets, those exclusively cleaved by constitutive proteasomes, those exclusively generated by immunoproteasomes, and common peptides produced by both proteasome types. Thus, immunoproteasomes generate a distinct and different repertoire of MHC class I ligands in inflamed tissues than in uninflamed tissues, which express very low levels of LMP2, LMP7, and MECL-1 (64). The immunoproteasome-dependent change in epitope production may serve to focus the specificity of the $CD8^+$-T-cell response but also to avoid autoimmune assaults, since different peptides are processed from normal tissues and from sites of inflammation (20).

Given the fact that proteasome assembly is regulated by opposing principles in CMV-infected cells on the one hand and professional APC on the other, direct consequences for the processing of viral epitopes and the specificity of responding antiviral $CD8^+$ T cells are likely. During the initial priming phase of the immune response $CD8^+$ T cells are activated by dendritic cells (DC) constitutively expressing immunoproteasomes (44). Irrespective of whether the DC is cross-presenting CMV peptides from exogenous antigens (5, 65) or processing peptides from proteins synthesized within the cell, a repertoire of viral peptides divergent from that in CMV-infected cells lacking immunoproteasomes should be expected. The deviation in epitope production during the priming versus the effector phase of the immune response should lead to a reduction in the overall antigenicity of CMV. The CMV inhibition of immunoproteasome formation restricts the diversity of epitopes presented in productively infected nonhematopoietic stromal and parenchymal tissue. Additionally, in these cell types, the MHC class I function is most efficiently downregulated by a multitude of CMV inhibitors (7). Taking these data together, it is tempting to speculate that CMV misleads the $CD8^+$-T-cell response when primed by peptides derived from infected or cross-presenting professional APC that are not generated by CMV-infected nonhematopoietic cells lacking immunoproteasomes.

Potential implications of the specificity of the antiviral $CD8^+$-cytotoxic-T-lymphocyte response. The mechanism of immune deviation may contribute to the relatively low number of MHC class I-restricted immunodominant CMV epitopes compared with the very large MCMV and HCMV proteome encompassing ~200 antigenic proteins (for a review, see references 51 and 52). In this context, it is worth mentioning that the $CD8^+$-T-effector–memory cell population in latently MCMV-infected mice is surprisingly focused on very few peptides in both the *H-2*^{d} (34, 36) and the *H-2*^{b} haplotypes (17). In relation to humans, the expansion of a similar $CD8^+$-effector–memory population has been demonstrated which is characterized by relatively few peptides (16, 38). Interestingly, the MCMV- and HCMV-specific T-cell populations remain small in CD62L and may therefore effectively patrol and protect nonlymphoid tissue (4, 35).

Moreover, one should predict that naturally processed CMV peptides exhibiting a privileged immunogenicity and able to induce dominant and protective $CD8^+$-T-cell reponses in vivo belong to a set of shared epitopes which is generated by both housekeeping proteasomes and immunoproteasomes. Although there are so far few experimental data on the proteasome-dependent processing of CMV peptides, this assumption holds true for the *H-2L*^{d}-restricted immunodominant MCMV pp89-derived epitope YPHFMPTNL (35, 53–55). In previous studies, this epitope was found to be efficiently processed by both types of 20S proteasomes from a precursor peptide in vitro (8, 22), as well as naturally processed in vivo in IFN-γ-treated and untreated fibroblasts and in bone marrow-derived hematopoietic cells and parenchymal cells in mice, respectively (32, 33). The degradation studies of a 25-mer peptide derived from the MCMV IE-pp89 protein using purified proteasomes and PA28αβ showed that, compared to the 20S proteasome alone, an enhancement in the generation of the 11-mer precursor peptide DMYPHFMPTNL occurred when PA28αβ was present (10). This 11-mer precursor was recently demonstrated to be efficiently transported into the endoplasmic reticulum by TAPs for final processing of its N-terminal end (41). Neither overexpression of LMP2 and LMP7 in *ie1*/pp89-transfected fibroblasts nor treatment with IFN-γ affected pp89 antigen presentation (23). Based on these data, we make the tacit assumption that these features also apply to other immunodominant CMV epitopes and that the processing of such peptides remains efficient in the absence of LMP2, LMP7, and MECL-1. Furthermore, we conjecture that T-cell epitopes of HCMV and MCMV which rely on immunoproteasomes will not significantly contribute to the cellular immune response against these viruses. This would be a potential mechanism of CMV immune escape which is also applicable to the oncogenic adenovirus strain 12, which shuts off the expression of immunoproteasomes on a transcriptional level (60).

The MCMV mutant ΔM27 is not able to counteract IFN-γ-mediated gene expression and inhibition of viral replication due to downregulation of STAT2 (Zimmermann et al., submitted). This let us conclude that the viral interference with IFN-γ signaling is responsible for the prevention of immunopreatosome expression. This mutant, which still expresses the whole "machinery" of MHC class I inhibitors, is dramatically attenuated in vivo (Zimmermann et al., submitted). It is conceivable that the IFN-γ-induced expression of cellular immune response genes, including immunoproteasome components, is responsible for the attenuated phenotype by increasing antigenicity to $CD8^+$ T cells. The analysis of the $CD8^+$-T-cell response induced by this mutant could allow us to test the hypothesis that inhibition of immunoproteasome gene expression shapes the protective T-cell response and the accumulation of memory T cells. A better understanding of the biochemical basis of the processing of protective epitopes with privileged immunogenicity and salient antigenicity will promote the design of CMV vaccines and the selection of optimal peptides used to expand $CD8^+$ T cells in vitro for adoptive immunotherapy against CMV disease (56, 58).

ACKNOWLEDGMENTS

We are grateful to Katja Wichmann and Rita de Giuli for expert technical assistance. We warmly acknowledge the technical help and advice of Lother Kuehn for the purification of 26S proteasomes. We thank Klavs Hendil for providing the antibody MCP444, Klaus Scherrer for the C7 antibody, and Stipan Jonjic for pp89 monoclonal antibody Croma 101.

This study was supported by the Deutsche Forschungsgemeinschaft through SFB 421 project A8 and EU QLRT-2001-01112 and by grant 31-52284 from the Swiss National Science Foundation.

REFERENCES

1. **Ahn, J. Y., N. Tanahashi, K. Akiyama, H. Hisamatsu, C. Noda, K. Tanaka, C. H. Chung, N. Shibmara, P. J. Willy, J. D. Mott, et al.** 1995. Primary structures of two homologous subunits of PA28, a gamma-interferon-inducible protein activator of the 20S proteasome. FEBS Lett. **366**:37–42.
2. **Ahn, K., A. Gruhler, B. Galocha, T. R. Jones, E. J. Wiertz, H. L. Ploegh, P. A. Peterson, Y. Yang, and K. Fruh.** 1997. The ER-luminal domain of the HCMV glycoprotein US6 inhibits peptide translocation by TAP. Immunity **6:**613–621.
3. **Aki, M., N. Shimbara, M. Takashina, K. Akiyama, S. Kagawa, T. Tamura, N. Tanahashi, T. Yoshimura, K. Tanaka, and A. Ichihara.** 1994. Interferon-gamma induces different subunit organizations and functional diversity of proteasomes. J. Biochem. (Tokyo) **115:**257–269.
4. **Appay, V., P. R. Dunbar, M. Callan, P. Klenerman, G. M. Gillespie, L. Papagno, G. S. Ogg, A. King, F. Lechner, C. A. Spina, S. Little, D. V. Havlir, D. D. Richman, N. Gruener, G. Pape, A. Waters, P. Easterbrook, M. Salio, V. Cerundolo, A. J. McMichael, and S. L. Rowland-Jones.** 2002. Memory CD8+ T cells vary in differentiation phenotype in different persistent virus infections. Nat. Med. **8:**379–385.
5. **Arrode, G., C. Boccaccio, J. Lule, S. Allart, N. Moinard, J. P. Abastado, A. Alam, and C. Davrinche.** 2000. Incoming human cytomegalovirus pp65 (UL83) contained in apoptotic infected fibroblasts is cross-presented to $CD8^+$ T cells by dendritic cells. J. Virol. **74:**10018–10024.
6. **Barton, L. F., M. Cruz, R. Rangwala, G. S. Deepe, Jr., and J. J. Monaco.** 2002. Regulation of immunoproteasome subunit expression in vivo following pathogenic fungal infection. J. Immunol. **169:**3046–3052.
7. **Benz, C., U. Reusch, W. Muranyi, W. Brune, R. Atalay, and H. Hengel.** 2001. Efficient downregulation of major histocompatibility complex class I molecules in human epithelial cells infected with cytomegalovirus. J. Gen. Virol. **82:**2061–2070.
8. **Boes, B., H. Hengel, T. Ruppert, G. Multhaup, U. H. Koszinowski, and P. M. Kloetzel.** 1994. Interferon gamma stimulation modulates the proteolytic activity and cleavage site preference of 20S mouse proteasomes. J. Exp. Med. **179:**901–909.
9. **Dahlmann, B., L. Kuehn, and H. Reinauer.** 1995. Studies on the activation by ATP of the 26 S proteasome complex from rat skeletal muscle. Biochem. J. **309:**195–202.
10. **Dick, T. P., T. Ruppert, M. Groettrup, P. M. Kloetzel, L. Kuehn, U. H. Koszinowski, S. Stevanovic, H. Schild, and H. G. Rammensee.** 1996. Coordinated dual cleavages induced by the proteasome regulator PA28 lead to dominant MHC ligands. Cell **86:**253–262.
11. **Driscoll, J., M. G. Brown, D. Finley, and J. J. Monaco.** 1993. MHC-linked LMP gene products specifically alter peptidase activities of the proteasome. Nature **365:**262–264.
12. **Fehling, H. J., W. Swat, C. Laplace, R. Kuhn, K. Rajewsky, U. Muller, and H. von Boehmer.** 1994. MHC class I expression in mice lacking the proteasome subunit LMP-7. Science **265:**1234–1237.
13. **Gaczynska, M., K. L. Rock, and A. L. Goldberg.** 1993. Gamma-interferon and expression of MHC genes regulate peptide hydrolysis by proteasomes. Nature **365:**264–267.
14. **Gaczynska, M., K. L. Rock, T. Spies, and A. L. Goldberg.** 1994. Peptidase activities of proteasomes are differentially regulated by the major histocompatibility complex-encoded genes for LMP2 and LMP7. Proc. Natl. Acad. Sci. USA **91:**9213–9217.
15. **Geginat, G., T. Ruppert, H. Hengel, R. Holtappels, and U. H. Koszinowski.** 1997. IFN-gamma is a prerequisite for optimal antigen processing of viral peptides in vivo. J. Immunol. **158:**3303–3310.
16. **Gillespie, G. M., M. R. Wills, V. Appay, C. O'Callaghan, M. Murphy, N. Smith, P. Sissons, S. Rowland-Jones, J. I. Bell, and P. A. Moss.** 2000. Functional heterogeneity and high frequencies of cytomegalovirus-specific $CD8^+$ T lymphocytes in healthy seropositive donors. J. Virol. **74:**8140–8150.
17. **Gold, M. C., M. W. Munks, M. Wagner, U. H. Koszinowski, A. B. Hill, and S. P. Fling.** 2002. The murine cytomegalovirus immunomodulatory gene m152 prevents recognition of infected cells by M45-specific CTL but does not alter the immunodominance of the M45-specific CD8 T cell response in vivo. J. Immunol. **169:**359–365.
18. **Gray, C. W., C. A. Slaughter, and G. N. DeMartino.** 1994. PA28 activator protein forms regulatory caps on proteasome stacked rings. J. Mol. Biol. **236:**7–15.
19. **Griffin, T. A., D. Nandi, M. Cruz, H. J. Fehling, L. V. Kaer, J. J. Monaco, and R. A. Colbert.** 1998. Immunoproteasome assembly: cooperative incorporation of interferon gamma (IFN-γ)-inducible subunits. J. Exp. Med. **187:**97–104.

20. **Groettrup, M., S. Khan, K. Schwarz, and G. Schmidtke.** 2001. Interferon-gamma inducible exchanges of 20S proteasome active site subunits: why? Biochimie **83:**367–372.
21. **Groettrup, M., R. Kraft, S. Kostka, S. Standera, R. Stohwasser, and P. M. Kloetzel.** 1996. A third interferon-gamma-induced subunit exchange in the 20S proteasome. Eur. J. Immunol. **26:**863–869.
22. **Groettrup, M., T. Ruppert, L. Kuehn, M. Seeger, S. Standera, U. Koszinowski, and P. M. Kloetzel.** 1995. The interferon-gamma-inducible 11 S regulator (PA28) and the LMP2/LMP7 subunits govern the peptide production by the 20 S proteasome in vitro. J. Biol. Chem. **270:**23808–23815.
23. **Groettrup, M., A. Soza, M. Eggers, L. Kuehn, T. P. Dick, H. Schild, H. G. Rammensee, U. H. Koszinowski, and P. M. Kloetzel.** 1996. A role for the proteasome regulator PA28α in antigen presentation. Nature **381:**166–168.
24. **Groettrup, M., A. Soza, U. Kuckelkorn, and P. M. Kloetzel.** 1996. Peptide antigen production by the proteasome: complexity provides efficiency. Immunol. Today **17:**429–435.
25. **Groettrup, M., S. Standera, R. Stohwasser, and P. M. Kloetzel.** 1997. The subunits MECL-1 and LMP2 are mutually required for incorporation into the 20S proteasome. Proc. Natl. Acad. Sci. USA **94:**8970–8975.
26. **Grzimek, N. K., J. Podlech, H. P. Steffens, R. Holtappels, S. Schmalz, and M. J. Reddehase.** 1999. In vivo replication of recombinant murine cytomegalovirus driven by the paralogous major immediate-early promoter-enhancer of human cytomegalovirus. J. Virol. **73:**5043–5055.
27. **Heise, M. T., M. Connick, and H. W. T. Virgin.** 1998. Murine cytomegalovirus inhibits interferon gamma-induced antigen presentation to CD4 T cells by macrophages via regulation of expression of major histocompatibility complex class II-associated genes. J. Exp. Med. **187:**1037–1046.
28. **Hendil, K. B., S. Khan, and K. Tanaka.** 1998. Simultaneous binding of PA28 and PA700 activators to 20 S proteasomes. Biochem. J. **332:**749–754.
29. **Hendil, K. B., P. Kristensen, and W. Uerkvitz.** 1995. Human proteasomes analysed with monoclonal antibodies. Biochem. J. **305:**245–252.
30. **Hengel, H., C. Esslinger, J. Pool, E. Goulmy, and U. H. Koszinowski.** 1995. Cytokines restore MHC class I complex formation and control antigen presentation in human cytomegalovirus-infected cells. J. Gen. Virol. **76:**2987–2997.
31. **Hengel, H., J. O. Koopmann, T. Flohr, W. Muranyi, E. Goulmy, G. J. Hammerling, U. H. Koszinowski, and F. Momburg.** 1997. A viral ER-resident glycoprotein inactivates the MHC-encoded peptide transporter. Immunity **6:**623–632.
32. **Hengel, H., P. Lucin, S. Jonjic, T. Ruppert, and U. H. Koszinowski.** 1994. Restoration of cytomegalovirus antigen presentation by gamma interferon combats viral escape. J. Virol. **68:**289–297.
33. **Hengel, H., U. Reusch, G. Geginat, R. Holtappels, T. Ruppert, E. Hellebrand, and U. H. Koszinowski.** 2000. Macrophages escape inhibition of major histocompatibility complex class I-dependent antigen presentation by cytomegalovirus. J. Virol. **74:**7861–7868.
34. **Holtappels, R., N. K. Grzimek, C. O. Simon, D. Thomas, D. Dreis, and M. J. Reddehase.** 2002. Processing and presentation of murine cytomegalovirus pORFm164-derived peptide in fibroblasts in the face of all viral immunosubversive early gene functions. J. Virol. **76:**6044–6053.
35. **Holtappels, R., M. F. Pahl-Seibert, D. Thomas, and M. J. Reddehase.** 2000. Enrichment of immediate-early 1 (m123/pp89) peptide-specific CD8 T cells in a pulmonary CD62L(lo) memory-effector cell pool during latent murine cytomegalovirus infection of the lungs. J. Virol. **74:**11495–11503.
36. **Karrer, U., S. Sierro, M. Wagner, A. Oxenius, H. Hengel, U. H. Koszinowski, R. E. Phillips, and P. Klenerman.** 2003. Memory inflation: continuous accumulation of antiviral CD8+ T cells over time. J. Immunol. **170:**2022–2029.
37. **Kavanagh, D. G., M. C. Gold, M. Wagner, U. H. Koszinowski, and A. B. Hill.** 2001. The multiple immune-evasion genes of murine cytomegalovirus are not redundant: m4 and m152 inhibit antigen presentation in a complementary and cooperative fashion. J. Exp. Med. **194:**967–978.
38. **Khan, N., M. Cobbold, R. Keenan, and P. A. Moss.** 2002. Comparative analysis of CD8+ T cell responses against human cytomegalovirus proteins pp65 and immediate early 1 shows similarities in precursor frequency, oligoclonality, and phenotype. J. Infect. Dis. **185:**1025–1034.
39. **Khan, S., M. van den Broek, K. Schwarz, R. de Giuli, P. A. Diener, and M. Groettrup.** 2001. Immunoproteasomes largely replace constitutive proteasomes during an antiviral and antibacterial immune response in the liver. J. Immunol. **167:**6859–6868.
40. **Kleijnen, M. F., J. B. Huppa, P. Lucin, S. Mukherjee, H. Farrell, A. E. Campbell, U. H. Koszinowski, A. B. Hill, and H. L. Ploegh.** 1997. A mouse cytomegalovirus glycoprotein, gp34, forms a complex with folded class I MHC molecules in the ER which is not retained but is transported to the cell surface. EMBO J. **16:**685–694.
41. **Knuehl, C., P. Spee, T. Ruppert, U. Kuckelkorn, P. Henklein, J. Neefjes, and P. M. Kloetzel.** 2001. The murine cytomegalovirus pp89 immunodominant H-2Ld epitope is generated and translocated into the endoplasmic reticulum as an 11-mer precursor peptide. J. Immunol. **167:**1515–1521.
42. **Kuckelkorn, U., S. Frentzel, R. Kraft, S. Kostka, M. Groettrup, and P. M. Kloetzel.** 1995. Incorporation of major histocompatibility complex-encoded subunits LMP2 and LMP7 changes the quality of the 20S proteasome polypeptide processing products independent of interferon-gamma. Eur. J. Immunol. **25:**2605–2611.
43. **Lucin, P., S. Jonjic, M. Messerle, B. Polic, H. Hengel, and U. H. Koszinowski.** 1994. Late phase inhibition of murine cytomegalovirus replication by synergistic action of interferon-gamma and tumour necrosis factor. J. Gen. Virol. **75:**101–110.
44. **Macagno, A., M. Gilliet, F. Sallusto, A. Lanzavecchia, F. O. Nestle, and M. Groettrup.** 1999. Dendritic cells up-regulate immunoproteasomes and the proteasome regulator PA28 during maturation. Eur. J. Immunol. **29:**4037–4042.
45. **Miller, D. M., B. M. Rahill, J. M. Boss, M. D. Lairmore, J. E. Durbin, J. W. Waldman, and D. D. Sedmak.** 1998. Human cytomegalovirus inhibits major histocompatibility complex class II expression by disruption of the Jak/Stat pathway. J. Exp. Med. **187:**675–683.
46. **Miller, D. M., Y. Zhang, B. M. Rahill, K. Kazor, S. Rofagha, J. J. Eckel, and D. D. Sedmak.** 2000. Human cytomegalovirus blocks interferon-gamma stimulated up-regulation of major histocompatibility complex class I expression and the class I antigen processing machinery. Transplantation **69:**687–690.
47. **Mocarski, E. S., and C. T. Courcelle.** 2001. Cytomegaloviruses and their replication, p. 2629–2673. *In* D. M. Knipe and P. M. Howley (ed.), Fields virology, 4th ed. Lippincott, Williams and Wilkins, Philadelphia, Pa.
48. **Olver, S. D., P. Price, and G. R. Shellam.** 1994. Cytomegalovirus hepatitis: characterization of the inflammatory infiltrate in resistant and susceptible mice. Clin. Exp. Immunol. **98:**375–381.
49. **Podlech, J., R. Holtappels, N. Wirtz, H. P. Steffens, and M. J. Reddehase.** 1998. Reconstitution of CD8 T cells is essential for the prevention of multiple-organ cytomegalovirus histopathology after bone marrow transplantation. J. Gen. Virol. **79:**2099–2104.
50. **Preckel, T., W. P. Fung-Leung, Z. Cai, A. Vitiello, L. Salter-Cid, O. Winqvist, T. G. Wolfe, M. Von Herrath, A. Angulo, P. Ghazal, J. D. Lee, A. M. Fourie, Y. Wu, J. Pang, K. Ngo, P. A. Peterson, K. Fruh, and Y. Yang.** 1999. Impaired immunoproteasome assembly and immune responses in PA28$^{-/-}$ mice. Science **286:**2162–2165.
51. **Reddehase, M. J.** 2002. Antigens and immunoevasins: opponents in cytomegalovirus immune surveillance. Nat. Rev. Immunol. **2:**831–844.
52. **Reddehase, M. J.** 2000. The immunogenicity of human and murine cytomegaloviruses. Curr. Opin. Immunol. **12:**390–396.
53. **Reddehase, M. J., and U. H. Koszinowski.** 1984. Significance of herpesvirus immediate early gene expression in cellular immunity to cytomegalovirus infection. Nature **312:**369–371.
54. **Reddehase, M. J., W. Mutter, K. Munch, H. J. Buhring, and U. H. Koszinowski.** 1987. CD8-positive T lymphocytes specific for murine cytomegalovirus immediate-early antigens mediate protective immunity. J. Virol. **61:**3102–3108.
55. **Reddehase, M. J., J. B. Rothbard, and U. H. Koszinowski.** 1989. A pentapeptide as minimal antigenic determinant for MHC class I-restricted T lymphocytes. Nature **337:**651–653.
56. **Reddehase, M. J., F. Weiland, K. Munch, S. Jonjic, A. Luske, and U. H. Koszinowski.** 1985. Interstitial murine cytomegalovirus pneumonia after irradiation: characterization of cells that limit viral replication during established infection of the lungs. J. Virol. **55:**264–273.
57. **Reusch, U., W. Muranyi, P. Lucin, H. G. Burgert, H. Hengel, and U. H. Koszinowski.** 1999. A cytomegalovirus glycoprotein re-routes MHC class I complexes to lysosomes for degradation. EMBO J. **18:**1081–1091.
58. **Riddell, S. R., K. S. Watanabe, J. M. Goodrich, C. R. Li, M. E. Agha, and P. D. Greenberg.** 1992. Restoration of viral immunity in immunodeficient humans by the adoptive transfer of T cell clones. Science **257:**238–241.
59. **Rock, K. L., C. Gramm, L. Rothstein, K. Clark, R. Stein, L. Dick, D. Hwang, and A. L. Goldberg.** 1994. Inhibitors of the proteasome block the degradation of most cell proteins and the generation of peptides presented on MHC class I molecules. Cell **78:**761–771.
60. **Rotem-Yehudar, R., M. Groettrup, A. Soza, P. M. Kloetzel, and R. Ehrlich.** 1996. LMP-associated proteolytic activities and TAP-dependent peptide transport for class 1 MHC molecules are suppressed in cell lines transformed by the highly oncogenic adenovirus 12. J. Exp. Med. **183:**499–514.
61. **Schwarz, K., M. Eggers, A. Soza, U. H. Koszinowski, P. M. Kloetzel, and M. Groettrup.** 2000. The proteasome regulator PA28α/β can enhance antigen presentation without affecting 20S proteasome subunit composition. Eur. J. Immunol. **30:**3672–3679.
62. **Schwarz, K., M. van Den Broek, S. Kostka, R. Kraft, A. Soza, G. Schmidtke, P. M. Kloetzel, and M. Groettrup.** 2000. Overexpression of the proteasome subunits LMP2, LMP7, and MECL-1, but not PA28 alpha/beta, enhances the presentation of an immunodominant lymphocytic choriomeningitis virus T cell epitope. J. Immunol. **165:**768–778.
63. **Sibille, C., K. G. Gould, K. Willard-Gallo, S. Thomson, A. J. Rivett, S. Powis, G. W. Butcher, and P. De Baetselier.** 1995. LMP2+ proteasomes are required for the presentation of specific antigens to cytotoxic T lymphocytes. Curr. Biol. **5:**923–930.
64. **Stohwasser, R., S. Standera, I. Peters, P. M. Kloetzel, and M. Groettrup.** 1997. Molecular cloning of the mouse proteasome subunits MC14 and MECL-1: reciprocally regulated tissue expression of interferon-gamma-modulated proteasome subunits. Eur. J. Immunol. **27:**1182–1187.
65. **Tabi, Z., M. Moutaftsi, and L. K. Borysiewicz.** 2001. Human cytomegalovirus

pp65- and immediate early 1 antigen-specific HLA class I-restricted cytotoxic T cell responses induced by cross-presentation of viral antigens. J. Immunol. **166:**5695–5703.

66. **Tanaka, K., and A. Ichihara.** 1989. Half-life of proteasomes (multiprotease complexes) in rat liver. Biochem. Biophys. Res. Commun. **159:**1309–1315.
67. **Trgovcich, J., D. Stimac, B. Polic, A. Krmpotic, E. Pernjak-Pugel, J. Tomac, M. Hasan, B. Wraber, and S. Jonjic.** 2000. Immune responses and cytokine induction in the development of severe hepatitis during acute infections with murine cytomegalovirus. Arch. Virol. **145:**2601–2618.
68. **van Hall, T., A. Sijts, M. Camps, R. Offringa, C. Melief, P. M. Kloetzel, and F. Ossendorp.** 2000. Differential influence on cytotoxic T lymphocyte epitope presentation by controlled expression of either proteasome immunosubunits or PA28. J. Exp. Med. **192:**483–494.
69. **Van Kaer, L., P. G. Ashton-Rickardt, M. Eichelberger, M. Gaczynska, K. Nagashima, K. L. Rock, A. L. Goldberg, P. C. Doherty, and S. Tonegawa.** 1994. Altered peptidase and viral-specific T cell response in LMP2 mutant mice. Immunity **1:**533–541.
70. **Ziegler, H., R. Thale, P. Lucin, W. Muranyi, T. Flohr, H. Hengel, H. Farrell, W. Rawlinson, and U. H. Koszinowski.** 1997. A mouse cytomegalovirus glycoprotein retains MHC class I complexes in the ERGIC/cis-Golgi compartments. Immunity **6:**57–66.

Chapter 8

Long-lived signal peptide of lymphocytic choriomeningitis virus glycoprotein pGP-C

Marc Froeschke, Michael Basler, Marcus Groettrup, & Bernhard Dobberstein

Published in Journal of Biological Chemistry 2003:278(43):41914-20.

THE JOURNAL OF BIOLOGICAL CHEMISTRY
Vol. 278, No. 43, Issue of October 24, pp. 41914–41920, 2003
Printed in U.S.A.

Long-lived Signal Peptide of Lymphocytic Choriomeningitis Virus Glycoprotein pGP-C*[S]

Received for publication, March 6, 2003, and in revised form, July 15, 2003
Published, JBC Papers in Press, August 12, 2003, DOI 10.1074/jbc.M302343200

Marc Froeschke‡, Michael Basler§, Marcus Groettrup§, and Bernhard Dobberstein‡¶

From the ‡Zentrum für Molekulare Biologie der Universität Heidelberg, Im Neuenheimer Feld 282, D-69120 Heidelberg and the §University of Constance, Department of Immunology, Universitätsstrasse 10, D-78457 Konstanz, Germany

Signal peptides (SPs) direct nascent secretory and membrane proteins to the membrane of the endoplasmic reticulum. They are usually cleaved from the nascent polypeptide by signal peptidase and then further proteolytically processed. The SP of the pre-glycoprotein (pGP-C) of the lymphocytic choriomeningitis virus $SP^{GP\text{-}C}$ (signal peptide of pGP-C) shows different properties: 1) The $SP^{GP\text{-}C}$ is unusually long (58 amino acid residues) and contains two hydrophobic segments interrupted by a lysine residue. 2) The $SP^{GP\text{-}C}$ is cleaved only from a subset of pGP-C proteins. A substantial portion of pGP-C accumulates that still contains the $SP^{GP\text{-}C}$. 3) The cleaved $SP^{GP\text{-}C}$ is rather long-lived ($t_{1/2}$ of more than 6 h). 4) The cleaved $SP^{GP\text{-}C}$ resides in the membrane and is resistant to digestion with proteinase K even in the presence of detergents, suggesting a very compact structure. 5) $SP^{GP\text{-}C}$ accumulates in virus particles. These unusual features of the cleaved $SP^{GP\text{-}C}$ suggest that $SP^{GP\text{-}C}$ not only targets the nascent pGP-C to the endoplasmic reticulum membrane but also has additional functions in lymphocytic choriomeningitis virus life cycle.

Most secretory and membrane proteins are synthesized as preproteins with an N-terminal signal peptide (SP)[1] (1, 2). Signal peptides are usually 15–25 amino acid residues in length and are typically comprised of three distinct regions: a central hydrophobic core of 7–10 residues (h-region), a polar N-terminal region that can be very variable in length and is usually positively charged, and a C-terminal region that contains the cleavage site for the signal peptidase (3). In eukaryotes, SPs target nascent secretory and membrane proteins to the endoplasmic reticulum (ER) and mediate insertion of the nascent polypeptides into the translocon (4). Membrane insertion is thought to occur in a loop-like fashion such that the N terminus of the SP is exposed on the cytoplasmic side of the membrane. Signal peptidase then cleaves the SP on the lumenal side of the membrane (5, 6). Cleavage usually occurs cotranslationally; however in some cases, SP cleavage is delayed or does not occur at all. Delayed cleavage is observed for the US11 SP (7) and the SP of the human immunodeficiency virus-1 (HIV-1) glycoprotein 160 (gp160) (8). The SP of the human cytomegalovirus (HCMV) US2 gene product is not even cleaved at all (9). Mutational analyses of several preproteins revealed that the efficiency and fidelity of SP cleavage can be influenced by mutations within the signal sequence itself but also by mutations in the mature protein (10–12).

After cleavage from the preprotein, SPs are thought to be either directly degraded or processed by signal peptide peptidase (SPP) into distinct fragments that are released from the membrane (13, 14). SPP has recently been shown to be a presenilin-type intramembrane-cleaving protease (15). Several determinants for processing by SPP have been identified: the SP has to be cleaved from the preprotein and the hydrophobic core region has to contain helix-breaking residues. Moreover, as yet ill-defined features of the SP flanking regions can affect SP processing (16).

SP fragments resulting from processing by SPP can be functionally active. In the case of the hormone preprolactin and the human immunodeficiency virus-1 (HIV-1) gp160, the N-terminal portion of the respective SP is released into the cytosol and binds to calmodulin in a Ca^{2+}-dependent manner (17). This implies that these SP-derived fragments may influence signal transduction pathways in the cell (17).

SPs can also play a role in immunorecognition. SPs of the polymorphic major histocompatibility complex (MHC) class I molecules contain a highly conserved sequence that is capable of binding to nonpolymorphic MHC class I molecules (HLA-E in human) (18). The peptide-HLA-E complex interacts at the cell surface with an inhibitory receptor on natural killer cells and thereby monitors the level of MHC class I molecule expression (19). Presentation of the SP-derived epitope is dependent on the transporter associated with antigen processing that transports peptides generated by the proteasome into the ER lumen (20).

The glycoproteins (GP-1 and GP-2) of the lymphocytic choriomeningitis virus (LCMV) are synthesized as a type I precursor glycoprotein C (pGP-C) that is processed during intracellular transport into GP-1 and GP-2 (21). The predicted SP of LCMV pGP-C ($SP^{GP\text{-}C}$) is rather unusual: it is longer than average SPs, comprising 58 amino acid residues, and has two hydrophobic regions separated by a lysine residue. An epitope derived from the core region, amino acid residues 33–41/43 of the $SP^{GP\text{-}C}$ (gp33), is presented by MHC class I molecules to cyto-

* This work was funded by the Deutsche Forschungsgemeinschaft Grant SFB 352/B1 (to B. D.) and Grant 31-52284 from the Swiss National Science foundation (to M. G.). The costs of publication of this article were defrayed in part by the payment of page charges. This article must therefore be hereby marked "*advertisement*" in accordance with 18 U.S.C. Section 1734 solely to indicate this fact.

[S] The on-line version of this article (available at http://www.jbc.org) contains supplementary figures 1S–3S showing Western blot analysis of supernatant and pellet fractions after cell fractionation, Western blot analysis of L929 cells and purified virus particles, and sequence alignment of the predicted signal sequences of some arenavirus glycoproteins.

¶ To whom correspondence should be addressed: Tel.: 49-6221-546825; Fax: 49-6221-545892; E-mail: dobberstein@zmbh.uni-heidelberg.de.

[1] The abbreviations used are: SP, signal peptide; SPP, signal peptide peptidase; pGP-C, pre-glycoprotein C; pGP-C-HA, C-terminal HA-tagged pGP-C; $pGP\text{-}C_{142}$, truncated (amino acid residues 1–142) pGP-C; $SP^{GP\text{-}C}$, signal peptide of pGP-C; ER, endoplasmic reticulum; HA, hemagglutinin; HCMV, human cytomegalovirus; LCMV (WE), lymphocytic choriomeningitis virus strain WE; gp, glycoprotein; HIV, human immunodeficiency virus; HIV-1 gp160, glycoprotein 160 of HIV-1; PNGase F, protein *N*-glycanase F; MHC, major histocompatibility complex; Tricine, *N*-[2-hydroxy-1,1-bis(hydroxymethyl)ethyl]glycine.

toxic T lymphocytes (21–24). Presentation requires a functional transporter associated with antigen processing (25) and proteasome activity (26). We have investigated the cleavage and fate of the SP^{GP-C} in transfected and LCMV-infected cells.

EXPERIMENTAL PROCEDURES

Plasmids—The expression plasmid pSV51l/pGP-C was derived from the widely used original cDNA of LCMV (WE) S RNA (27) and the pSV51l expression vector (28). A DNA fragment including the entire coding region for LCMV (WE) pGP-C (GenBank™ accession number M22138: base pairs 17–1,579) was cloned into pSV51l using an additionally introduced *Bam*HI site (pSV51l/pGP-C).

A DNA fragment encoding pGP-C-HA was generated by polymerase chain reaction using the forward primer 5′-GGA TCT CTA GAG TCG ACC CC-3′ and the backward primer 5′-CTG GAT CCT CAA GCG TAA TCT GGA ACA TCG TAT GGG TAG CGT CTT TTC CAG ATA G-3′. The PCR product was inserted into the *Bam*HI site of pSV51l (pSV51l/pGP-C-HA).

Cells and Virus—HeLa and L929 cells were obtained from American Type Culture Collection (Manassas, VA). MC57 cells have been described previously (29). HeLa, MC57, and L929 cells were grown under recommended conditions. The LCMV (WE) strain was originally obtained from F. Lehmann-Grube (30).

Peptides and Antibodies—Synthetic peptides deduced from the SP^{GP-C} and including amino acid residues 7–18 (MFEALPHIIDEV, SP7), 30–41 (TSIKAVYNFATC, SP30), and 48–57 (SFLFLAGRSC, SP48) were coupled to keyhole limpet hemocyanin and injected into rabbits to raise anti-SP7, -SP30, and -SP48 antibodies. Antisera were immunopurified. KL25 is a mouse monoclonal antibody reactive with the LCMV glycoprotein GP-1 (31).

Transfection, Infection, and LCMV Particle Preparation—Expression vectors were transfected into HeLa cells by the calcium phosphate precipitation method for 20–24 h (32). The cells were grown for an additional 48 h. MC57 cells were infected for 24 h with LCMV (WE) (multiplicity of infection, 0.05). LCMV particles were prepared as described (33) without using a continuous sucrose gradient.

Metabolic Labeling and Immunoprecipitation—After transfection, about 1×10^6 cells were starved in Met/Cys-free Dulbecco's modified Eagle's medium plus 10% fetal calf serum for 150 min at 37 °C and labeled with 0.15 mCi/ml [^{35}S]Met/Cys for 30 min. Labeling medium was removed, and cells were washed with phosphate-buffered saline and either directly analyzed or chased in complete Dulbecco's modified Eagle's medium for the indicated time periods.

Cells were harvested and lysed for 15 min on ice in 100 mM NaCl, 20 mM HEPES/KOH (pH 7.3), 5 mM $MgCl_2$, 1% (w/v) Triton X-100, 100 μg/ml phenylmethylsulfonyl fluoride, 10 μg/ml aprotinin, 10 μg/ml leupeptin, and 10 μg/ml pepstatin. Equal aliquots were used for immunoprecipitation (34).

After infection 2×10^6 confluent cells were starved in Met/Cys-free RPMI 1640 plus 10% dialyzed fetal calf serum for 45 min at 37 °C and labeled with 0.1 mCi/ml [^{35}S]Met/Cys for 60 min. Labeling medium was removed, and cells were washed with phosphate-buffered saline and chased in complete medium for the indicated time periods. Cells were harvested and lysed for 45 min on ice in 150 mM NaCl, 50 mM Tris-HCl (pH 8.0), 1 mM EDTA, 0.85 mM phenylmethylsulfonyl fluoride, 10 μM leupeptin, 2.8 μM pepstatin, 0.75 μM aprotinin, and 2% (v/v) Nonidet P-40. Equal aliquots were used for immunoprecipitation. The beads were boiled in the appropriate sample buffer (35, 36), and proteins were then analyzed by SDS-PAGE followed by phosphorimaging using a BAS 1500 (Fuji, Tokyo, Japan). Protein amounts have been quantified using MacBas2.0 program.

Cell Fractionation and Treatments of Isolated Membranes—Transfected HeLa cells were harvested, resuspended in 20 volumes of hypotonic buffer (5 mM HEPES/KOH (pH 7.4), 0.5 mM $MgCl_2$, 10 μg/ml aprotinin, 10 μg/ml leupeptin, and 10 μg/ml pepstatin), incubated on ice for 10 min, and broken up by using a Dounce homogenizer. The homogenate was adjusted to 0.25 M sucrose and centrifuged at 4 °C, 13,800 × *g* for 5 min. The supernatant was loaded on a high salt sucrose cushion (500 mM sucrose, 500 mM KOAc, 50 mM HEPES/KOH (pH 7.6), 2 mM MgOAc, 1 mM dithiothreitol, and 10 mg/ml phenylmethylsulfonyl fluoride) and centrifuged at 4 °C, 100,000 × *g* for 30 min. The resulting pellet (membranes) was resuspended in hypotonic buffer, adjusted to 100 mM NaCl and 0.25 M sucrose, and aliquots were treated on ice with different combinations of 0.5 mg/ml proteinase K, 0.5 mg/ml trypsin, 1% (w/v) Triton X-100, or increasing concentrations of SDS (0.2, 0.5, and 1.0%) as indicated in the legend for Fig. 4.

For carbonate extraction, one aliquot of membranes was treated with 1/10 volume of 1 M Na_2CO_3 (pH 11) for 15 min on ice and loaded on a sucrose cushion (250 mM sucrose, 100 mM Na_2CO_3, pH 11). After centrifugation (4 °C, 130,000 × *g*, 10 min), the supernatant was taken off, and the pellet was resuspended in hypotonic buffer adjusted to 100 mM NaCl and 0.25 M sucrose.

PNGase F Treatment of Immunoprecipitated Proteins—Immunoprecipitated proteins bound to resin were incubated with 100 units of PNGase F (New England Biolabs, Schwalbach, Germany) in a final volume of 30 μl as specified by the supplier and incubated for 12 h at 37 °C.

Western Blot Analysis—Proteins of total cell lysates, fractions of membranes, cytosol, or LCMV particles were separated by SDS-PAGE, transferred to nitrocellulose, and identified using anti-SP7, anti-Sec61β, or anti-α-tubulin antibodies by standard Western blot analysis technique (32).

RESULTS

Characterization of Antibodies Directed against the pGP-C Signal Peptide (SP^{GP-C})—To characterize the SP of the LCMV glycoprotein pGP-C (SP^{GP-C}) (Fig. 1*A*), antibodies against three different segments of the SP^{GP-C} were raised in rabbits. The peptides used for immunization comprised amino acid residues 7–18 (SP7), 30–41 (SP30), and 48–57 (SP48) (Fig. 1*B*). Antibodies were affinity-purified and used to immunoprecipitate a fragment of pGP-C, comprising amino acid residues 1–142 ($pGP\text{-}C_{142}$) (Fig. 1*A*), which was synthesized *in vitro*. An aliquot of the translation reaction (Fig. 1*C*, *lane 1*) and the immunoprecipitates (*lanes 2–13*) were separated by SDS-PAGE, and $pGP\text{-}C_{142}$ was visualized by phosphorimaging. Only the anti-SP7 antibody was able to immunoprecipitate $pGP\text{-}C_{142}$ (Fig. 1*C*, *lane 2*). The specificity of the reaction was demonstrated by the addition of the SP7 or an unrelated (control) peptide. No immunoprecipitation is seen when the specific peptide SP7 is included in the reaction (*lane 3*), whereas a control peptide had no effect (*lane 4*). The preimmune serum did not immunoprecipitate $pGP\text{-}C_{142}$ (*lane 5*). Antibodies raised against the other two SP peptides, SP30 and SP48, did not immunoprecipitate $pGP\text{-}C_{142}$ (*lanes 6–13*). Anti-SP7 antibody was used for the further studies.

Identification of (p)GP-C-HA and SP Cleavage from pGP-C—SPs are usually cleaved very rapidly after their membrane insertion from the nascent or just completed secretory or membrane protein. To follow cleavage of the SP^{GP-C} from pGP-C, we initially used a cell-free system in which $pGP\text{-}C_{142}$ was synthesized in the presence of rough microsomal membranes (13). Cleavage of the SP^{GP-C} from $pGP\text{-}C_{142}$ was very inefficient as compared with SP cleavage from the secretory protein preprolactin (data not shown). We therefore reasoned that SP^{GP-C} cleavage from pGP-C might be inherently inefficient. To test this hypothesis, we transfected HeLa cells with a plasmid expressing HA epitope-tagged LCMV pGP-C (pGP-C-HA) (Fig. 1*A*). Cells were labeled with [^{35}S]Met/Cys for 30 min. The extract was treated with PNGase F to remove *N*-linked carbohydrates from pGP-C-HA and thereby obtain a more distinct banding pattern. Unglycosylated (p)GP-C-HA ((p)GP-C-HA*) was immunoprecipitated with anti-HA or anti-SP7 antibodies (Fig. 2*A*). Both antibodies immunoprecipitated a major band of about 55 kDa, the expected molecular mass of unglycosylated (p)GP-C-HA, (p)GP-C-HA* (*lanes 3* and *4*). In the anti-HA immunoprecipitates, we cannot detect a smaller form representing mature GP-C-HA*, suggesting either that pGP-C-HA* and GP-C-HA* are not resolved by the gel system used or that GP-C-HA* is degraded. In addition, the anti-SP7 antibody immunoprecipitates a peptide of about 6 kDa. The 6-kDa peptide comigrates with *in vitro* synthesized SP^{GP-C} comprising the N-terminal 58 amino acid residues of pGP-C (SP58) (Fig. 2*B*, *lane 2*). This suggests that the complete SP^{GP-C} accumulates.

To investigate whether the SP^{GP-C} is stable enough to be detected under steady state conditions, we used Western blot-

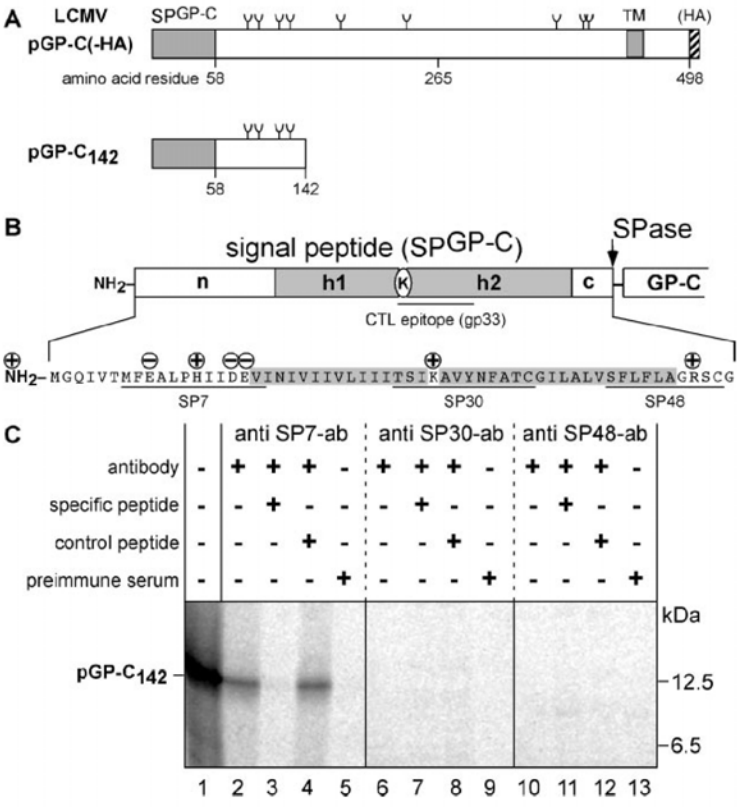

FIG. 1. *A*, outline of LCMV pGP-C tagged at its C terminus with a HA tag (pGP-C-HA). The signal peptide (SP^{GP-C}), the transmembrane region (*TM*), and the HA tag (HA) are indicated. The *forked symbols* indicate potential sites for *N*-glycosylation. $pGP\text{-}C_{142}$ is a fragment of pGP-C synthesized in an *in vitro* system from a truncated pGP-C mRNA. *B*, outline of SP^{GP-C}. The N-terminal (*n*), hydrophobic (h1, h2), the C-terminal (*c*) regions, and the site for signal peptidase (*SPase*) cleavage are indicated. The position of the lysine residue between the h1 and h2 region (*K*) and positively (+) and negatively (−) charged amino acid residues in the SP^{GP-C} are indicated. The immunodominant epitope of cytotoxic T lymphocytes (CTL), gp33 and peptide sequences (SP7, SP30, and SP48) that were used to raise antibodies are *underlined*. *C*, characterization of anti-SP7, -SP30, and -SP48 antibodies by immunoprecipitation of *in vitro* synthesized $pGP\text{-}C_{142}$. Proteins were separated on a 15% SDS gel and $pGP\text{-}C_{142}$ visualized by phosphorimaging. The respective specific peptides or unrelated peptides were added as indicated.

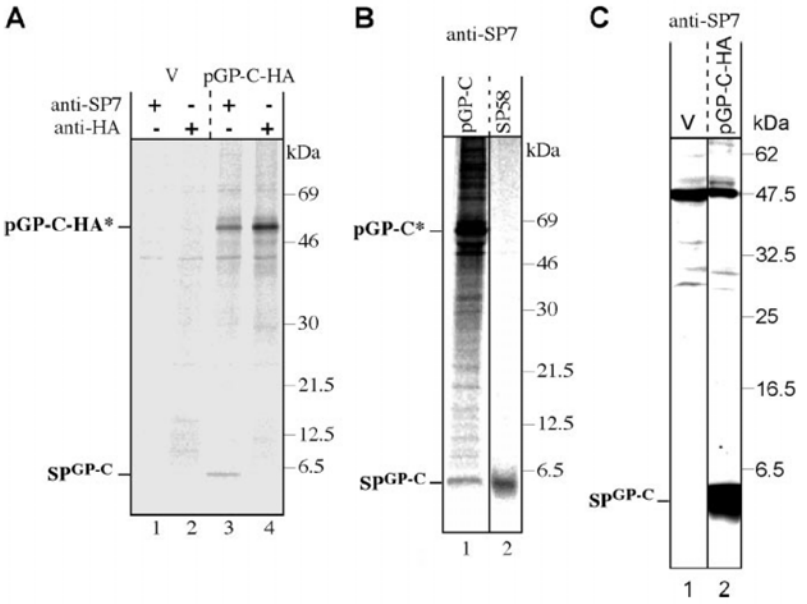

FIG. 2. **Identification of pGP-C(-HA) and SP^{GP-C} in transfected HeLa cells.** In *A*, HeLa cells were transfected with plasmid pSV51l (*V*) or pSV51l/pGP-C-HA and labeled for 30 min. with [^{35}S]Met/Cys. Antigens were immunoprecipitated with anti-SP7 or anti-HA antibodies and PNGase F-treated. Proteins were separated by SDS-PAGE, and unglycosylated pGP-C-HA* and SP^{GP-C} were visualized by phosphorimaging. *B*, size estimation of SP^{GP-C}. Transfected cells expressing SP^{GP-C} were analyzed as in *A* (*lane 1*). To obtain a molecular size standard of the SP^{GP-C}, we translated a truncated mRNA coding for the N-terminal 58 amino acids of pGP-C (SP58) (*lane 2*). SP^{GP-C} and *in vitro* synthesized SP58 comigrate (*cf. lanes 1* and *2*). *C*, identification of SP^{GP-C} by Western blotting. Transfected cells expressing pGP-C-HA as described in *A* were prepared for Western blotting using a Tricine type gel and probed with anti-SP7 antibody. SP^{GP-C} is seen in cells expressing pGP-C-HA (*lane 2*) but not in cells transfected with control vector (*V*) (*lane 1*).

ting. A cell extract from transfected HeLa cells was separated on an SDS-PAGE Tricine gel that separates peptides with high resolution, and a Western blot was probed with the anti-SP7 antibody. As can be seen in Fig. 2*C*, the SP^{GP-C} can be detected in cells expressing pGP-C-HA (*lane 2*) but not in cells transfected with the empty vector (*lane 1*).

Stability of the Cleaved SP^{GP-C}—To follow cleavage of the SP^{GP-C} from pGP-C-HA, we pulse-labeled transfected HeLa cells for 30 min and chased them with medium containing unlabelled amino acids for 3 and 6 h (Fig. 3*A*). Aliquots of the samples were treated with PNGase F as indicated in the figure. The anti-SP7 antibody was used to immunoprecipitate pGP-C-HA and the cleaved SP^{GP-C}. SP7 or control peptides were added to the samples as indicated. After the labeling and PNGase F treatment, the 55-kDa pGP-C-HA* and a prominent small peptide are immunoprecipitated with the anti-SP7 antibody (Fig. 3*A*, *lane 4*). Both, the 55-kDa protein and the 6-kDa peptide (SP^{GP-C}) are no longer immunoprecipitated when the SP7 peptide is included in the immunoprecipitation (*lanes 7* and *8*). During the 3- and 6-h chase period, the amount of the

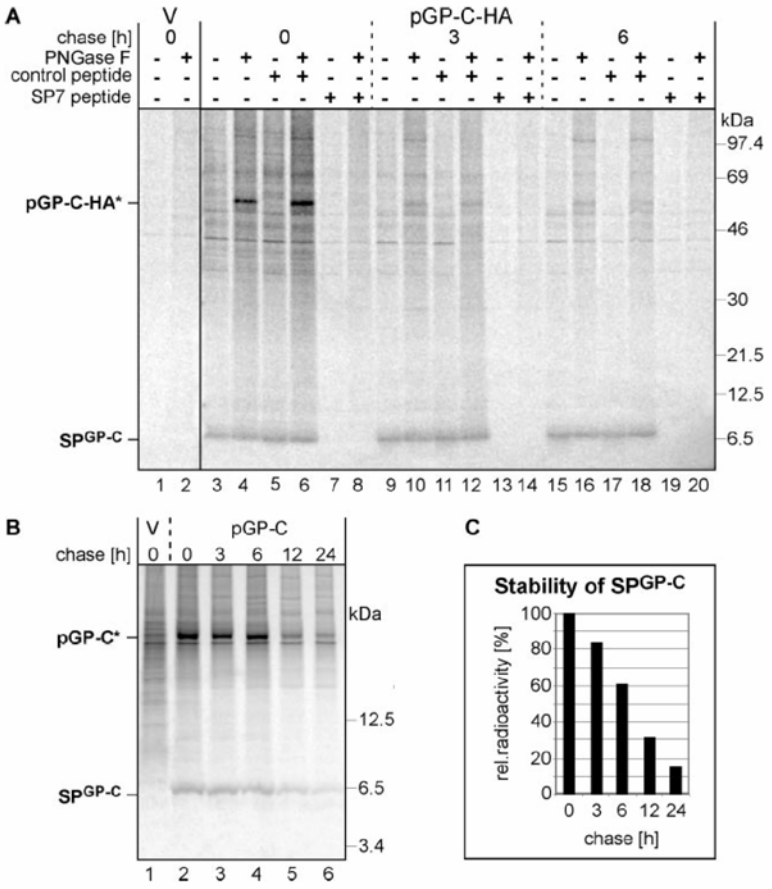

FIG. 3. **Pulse-chase analysis of pGP-C-HA.** In *A*, transfected HeLa cells expressing pGP-C-HA were labeled for 30 min and chased for the times indicated. Solubilized proteins were immunoprecipitated with anti-SP7 antibody and aliquots of these proteins were treated with PNGase F and further analyzed as described in the legend for Fig. 2. The positions of unglycosylated pGP-C-HA* and SP^{GP-C} are shown. *V*, pSV51l. *B*, transfected HeLa cells expressing pGP-C were labeled and immunoprecipitated as described under *A* but chased for 3, 6, 12, and 24 h. Unglycosylated pGP-C* and SP^{GP-C} are indicated. *C*, quantification of the amount of SP^{GP-C} as shown under *B*.

55-kDa protein is substantially reduced, whereas the amount of SP^{GP-C} is not markedly altered (*lanes 4*, *10*, and *16*).

To expand the chase times and see whether the HA tag affects the stability of pGP-C or the SP^{GP-C}, we expressed pGP-C as described above but used chase times of 3, 6, 12, and 24 h. To rule out the possibility that SP^{GP-C} migrates at the gel front, we again used the SDS-PAGE Tricine gel system that separates peptides with high resolution. SP^{GP-C} immunoprecipitated by the anti-SP7 antibody is still detectable after 24 h of chase labeling (Fig. 3*B*). From a quantification of the amount of SP^{GP-C} detectable at the chase times, we calculated a half-life of more than 6 h for SP^{GP-C} (Fig. 3*C*).

Membrane Association and Protease Sensitivity of SP^{GP-C}—To investigate the membrane association of SP^{GP-C}, we pulse-labeled transfected cells and prepared a cytoplasmic and membrane fraction by centrifugation of a cell homogenate. As markers for cytosol and ER membranes, antibodies against α-tubulin and Sec61β were used, respectively (see supplementary data, Fig. 1*S*). SP^{GP-C} was exclusively found in the membrane fraction (Fig. 4, *cf. lanes 2* and *3*). Carbonate (pH 11) extraction was also not able to remove SP^{GP-C} from the membrane fraction (*cf. lanes 10* and *11*). To test whether the SP^{GP-C} was accessible on the cytoplasmic side of the membrane, proteinase K was added to the membrane and cytoplasmic fractions. Neither proteinase K (*lanes 4* and *5*) nor trypsin (data not shown) were able to cleave the SP^{GP-C}. To see whether the resistance against protease digestion was due to the membrane barrier or is an intrinsic property of the SP^{GP-C}, we solubilized the membranes with either the nondenaturing detergent Triton X-100 or increasing concentrations (0.2, 0.5, and 1.0%) of SDS (30 min on ice). Although pGP-C-HA was digested under these conditions, SP^{GP-C} was not (*lanes 6–9*).

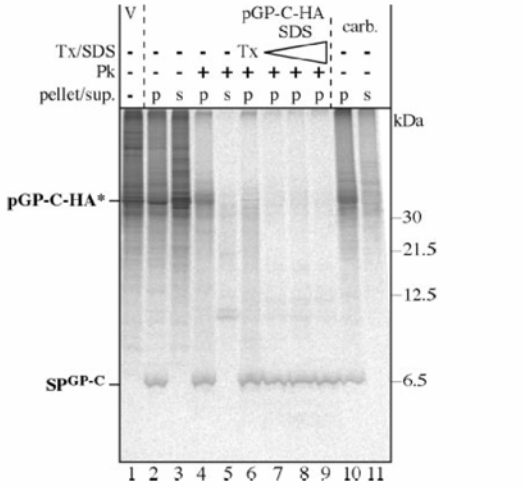

FIG. 4. **Membrane association of SP^{GP-C}.** Transfected pulse-labeled HeLa cells were fractionated into supernatants (*s*) and pellets (*p*) by centrifugation (*lanes 2* and *3*). Aliquots were treated with proteinase K (*Pk*), Triton X-100 (*Tx*), or 0.2, 0.5, or 1% SDS on ice as indicated. Antigens from each fraction were immunoprecipitated with the anti-SP7 antibody. An aliquot of the pellet fraction was extracted with carbonate (pH 11) and separated into supernatant and pellet by centrifugation as indicated (*lanes 10* and *11*). pGP-C-HA* and the SP^{GP-C} are indicated.

SP^{GP-C} after Infection with LCMV—To investigate the cleavage and fate of SP^{GP-C} during viral biogenesis and maturation,

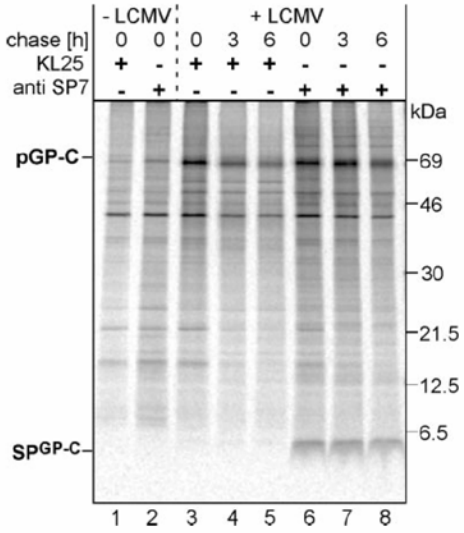

FIG. 5. **Pulse-chase labeling of LCMV-infected cells.** LCMV-infected and -uninfected cells were [^{35}S]Met/Cys-labeled and chased for 3 and 6 h. Antigens were immunoprecipitated with the KL25 antibody recognizing an epitope in the GP-1 protein or with the anti-SP7 antibody and separated on a Laemmli gel. The positions of pGP-C and SP^{GP-C} are indicated.

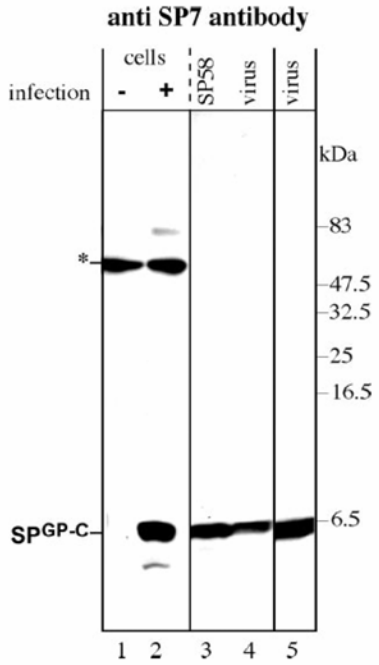

FIG. 6. **Identification of SP^{GP-C} in LCMV particles by Western blot analysis.** Proteins from LCMV-uninfected and -infected cells (*lanes 1* and *2*) and purified virus particles (*lanes 4* and *5*) were separated by SDS-PAGE and probed by Western blotting with anti-SP7 antibody. The position of the SP^{GP-C} is indicated. *, a cellular protein cross-reacting with the anti-SP7 antibody. An *in vitro* synthesized peptide (SP58) comprising amino acid residues 1–58 of SP^{GP-C} is used as a size marker (*lane 3*). In *lane 5*, a longer exposure of *lane 4* is shown.

we infected MC57 mouse fibroblasts with LCMV. 24 h after infection, cells were labeled with [^{35}S]Met/Cys for 60 min and chased for 3 or 6 h with medium containing nonlabeled amino acids. An antibody recognizing an epitope in the mature GP-1 protein (KL25) and the anti-SP7 antibody were used in immunoprecipitations. As compared with the noninfected cells (Fig. 5, *lanes 1* and *2*), an intensively labeled protein of about 70 kDa was immunoprecipitated with the KL25 antibody as well as the anti-SP7 antibody (*lanes 3–8*). The amount of this protein was reduced at the 3 and 6 h chase times. The size of this protein (70 kDa) and the fact that the protein is immunoprecipitated by KL25 as well as the SP7 antibody suggests that it is mainly pGP-C. Cleaved SP^{GP-C} is clearly detectable in anti-SP7 immunoprecipitates even after 6 h of chase (*lanes 6–8*). Thus the high stability of the SP^{GP-C} is not restricted to transfected cells but is also a property of the SP^{GP-C} during virus infection.

To see whether the cleaved SP^{GP-C} also accumulates in the virus, we purified LCMV particles from culture supernatants of acute infected L929 cells and identified the SP^{GP-C} by using the anti-SP7 antibody and Western blot analysis. As can be seen in Fig. 6, the SP^{GP-C} is detected in the infected cells (*lane 2*) as well as in the purified LCMV particles (*lanes 4* and *5*). The SP^{GP-C} comigrates with *in vitro* synthesized SP^{GP-C} (SP58), indicating that the entire SP accumulates (*cf. lanes 3* and *4*). The purity of the virus particle preparation is indicated by the absence of the cellular 50-kDa protein cross-reacting with the anti-SP7 antibody (*cf.* Fig. 6, *lanes 1* and *2* with *lane 5*). Furthermore, a marker protein for the ER, Sec61β, could not be detected in the LCMV particle preparation (see supplementary data, Fig. 2*S*). In infected cells, the anti-SP7 antibody recognized a peptide smaller than SP^{GP-C} by about 1–2 kDa. This peptide might represent an SPP processing product of the SP^{GP-C} (15).

DISCUSSION

Signal peptides are usually cleaved from their preprotein shortly after membrane insertion and are then rapidly proteolytically processed and/or degraded (3, 6). The SP of LCMV pGP-C is different with respect to cleavage from the preprotein and its processing and degradation (for a schematic representation, see Fig. 7). The SP^{GP-C} is not cleaved from all glycoprotein molecules, and pGP-C accumulates for several hours in transfected and infected cells. More unexpected is that the cleaved SP^{GP-C} is unusually stable, having a half-life of more than 6 h, and accumulates in LCMV particles.

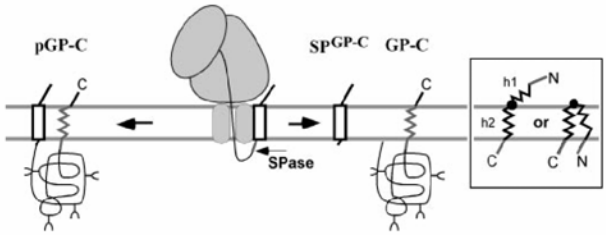

FIG. 7. **Proposed model for signal peptide cleavage from pGP-C.** During membrane insertion, the SP of pGP-C is only cleaved from a subset of synthesized molecules. SP^{GP-C} has a half-life of more than 6 h. It may span the membrane twice as it harbors two hydrophobic regions, h1 and h2 (*boxed inset*), and has a compact structure that is resistant to mild proteolysis even in the presence of detergents. *SPase*, signal peptidase.

SP^{GP-C} Cleavage from pGP-C—We raised an antibody (anti-SP7) that specifically recognizes the signal peptide of LCMV pGP-C. Specificity was demonstrated by using competing and control peptides in immunoprecipitations. In transfected and LCMV-infected cells, pGP-C and the cleaved signal peptide SP^{GP-C} could be detected and found to be rather long-lived. We were unable to resolve or detect mature GP-C. This may be due to the gel system used or may indicate degradation of GP-C. The recombinant LCMV (WE) pGP-C we used in this study is derived from persistent infected cells. During progression from acute to persistent infection, pGP-C accumulates 12 point mu-

tations (between amino acids 94 and 457), which are exclusively found in the mature part of the glycoprotein but not in its signal peptide (amino acids 1–58). One (L110P) of these point mutations prevents processing into GP-1 and GP-2 (37). However, accumulation of pGP-C and $SP^{GP\text{-}C}$ is also seen in acute infected cells and therefore reflects an intrinsic property of pGP-C and is not due to the mutations accumulating in GP-C in persistent infected cells.

Inefficient SP cleavage has also been found for some other viral membrane proteins. A fraction of newly synthesized HCMV US11 molecules retains the SP after the US11 has been completed (7). Delayed cleavage is caused by amino acid residues in the N-terminal part of the US11 SP. A second region that affects the rate and extent of SP cleavage is the transmembrane region of US11 (7). A precursor form of the HIV-1 gp160 has also been found to accumulate. In this case, the SP cleavage has been shown to be a prerequisite for intracellular transport of gp160. The SP of pre-gp160 interferes with gp160 folding and surface expression (8, 38). Whether similar functions can be assigned to the $SP^{GP\text{-}C}$ awaits further experimentation.

$SP^{GP\text{-}C}$ Accumulation in Infected Cells and in LCMV Particles—In contrast to other SPs, the cleaved $SP^{GP\text{-}C}$ is not rapidly processed and degraded. It accumulates in transfected cells expressing pGP-C as well as in LCMV-infected cells producing virus particles. Stability is thus not dependent on other factors encoded by the viral genome. The basis for the high stability of the $SP^{GP\text{-}C}$ probably lies in the structural features of $SP^{GP\text{-}C}$. Although an average signal peptide comprises about 20 amino acid residues, the $SP^{GP\text{-}C}$ extends over 58 amino acid residues and is characterized by two hydrophobic regions separated by a lysine residue (Fig. 1*B*). The N-terminal h1 region includes 15 uncharged amino acid residues, of which 11 are hydrophobic. The h2 region contains 20 uncharged amino acid residues. Membrane insertion of signal peptides of a secretory or type I membrane protein is thought to occur in a loop-like fashion such that the N terminus is exposed on the cytoplasmic side, and the cleavage site for signal peptidase is exposed on the lumenal side (Fig. 7). Given that the two hydrophobic regions of $SP^{GP\text{-}C}$ are both of sufficient length and hydrophobicity to span the membrane, it is well conceivable that $SP^{GP\text{-}C}$ spans the membrane twice. We have demonstrated using carbonate extraction that all $SP^{GP\text{-}C}$ peptides are integrated in the membrane. As cleavage sites of signal peptidase are usually in proximity to the hydrophobic segment of a signal peptide, we consider it very likely that the h2 region spans the membrane during membrane insertion such that signal peptidase has access to the cleavage site on the lumenal side of the ER. The h1 region is also of sufficient hydrophobicity to span the membrane. If this is true, the N terminus would have to translocate across the membrane, and the h1 and h2 regions would span the membrane in antiparallel configuration (Fig. 7). Several observations argue for such a configuration: 1) Protease added to membrane vesicles does not cleave the $SP^{GP\text{-}C}$. If only the h2 region would span the membrane, the more than 30 amino acid residues of the N terminus would be exposed on the cytoplasmic side accessible to the added protease. 2) The $SP^{GP\text{-}C}$ is very resistant to proteolysis even in the presence of detergents, suggesting a compact structure as formed in the suggested antiparallel configuration of the two h regions. 3) The N-terminal hydrophilic region contains an excess of acidic amino acid residues over basic ones. A statistical analysis has revealed that clusters of positively charged amino acid residues are mostly found on the cytoplasmic side of membrane-spanning proteins (39). As judged by this criterion, the slightly negatively charged N-terminal region of the $SP^{GP\text{-}C}$ would be compatible with translocation across the ER membrane.

An unusually long and stable SP has also been found for the foamy virus envelope glycoprotein (Env) (40). The foamy virus SP^{Env} is 148 amino acid residues in length and contains a single hydrophobic region located between residues 70 and 90. This SP becomes glycosylated and is found in virus particles. What structural features of this SP prevent proteolytic processing and rapid degradation is not yet known.

Possible Implications of $SP^{GP\text{-}C}$ Cleavage and Stability—What relevance could the accumulation of pGP-C and the rather stable $SP^{GP\text{-}C}$ have for the LCMV life cycle? pGP-C might represent a biosynthetic intermediate that could be converted posttranslationally to transport competent GP-C by cleavage of the SP. Alternatively, pGP-C might be a substrate for the ER-associated degradation system. Clearly, further work is required to distinguish between these two or other possibilities.

LCMV is the prototype of the arenaviridae. Glycoproteins of other arenaviridae are synthesized with SPs of similar length. In addition, these SPs show sequence similarity and also contain two hydrophobic segments separated by one or two positively charged amino acid residues (see supplementary data, Fig. 3*S*). Cleavage of Lassa virus signal peptide was recently shown to be necessary for GP-C processing into GP-1 and GP-2 and maturation in the secretory pathway (41).

The unusual stability and accumulation of $SP^{GP\text{-}C}$ strongly argues for functions besides targeting to the ER membrane. An attractive hypothesis would be that $SP^{GP\text{-}C}$ plays a role for virus assembly or formation and stabilization of the virus particle itself. Our finding that $SP^{GP\text{-}C}$ is present in purified virus particles in substantial amounts supports such a notion.

A striking biosynthetic and structural similarity can be found between the $SP^{GP\text{-}C}$ and the 6K peptide of Semliki Forest virus and Sindbis virus (42). The 6K peptides of these viruses are synthesized as part of a polyprotein between the two glycoproteins P62 and E1 and are excised by two proteases to give the final 6K products. The 6K peptides comprise 55–58 amino acid residues and have an acidic, hydrophilic N-terminal region and two hydrophobic segments interrupted by 1 or 2 basic amino acid residues. 6K, like $SP^{GP\text{-}C}$, is thought to be cleaved at its C-terminal side by signal peptidase (42). It is known that Semliki Forest virus 6K is required for efficient virus budding and is found in the virus in submolar amounts (43–47).

A function in virus budding and integration into virus particles has also been shown for the SP of foamy virus Env protein (40). However, this SP does not share many structural similarities with the $SP^{GP\text{-}C}$.

The signal peptide of pGP-C contains the immunodominant MHC class I restricted T cell epitope (gp33) comprising amino acid residues 33–41/43 (23, 24). A quite obvious consequence of $SP^{GP\text{-}C}$ stability is that the T cell epitope will not directly be released, and thus the T cell response will be delayed. Generation of the $SP^{GP\text{-}C}$-derived T cell epitope requires a functional proteasome, suggesting that the $SP^{GP\text{-}C}$ is eventually released from the membrane into the cytosol, where it becomes proteolytically processed (26). Whether processing of cleaved $SP^{GP\text{-}C}$ is relevant for generating the gp33 T cell epitope is unclear. Alternatively, mistargeted pGP-C accumulating during biosynthesis in the cytosol may be degraded by the proteasome and generate the gp33 T cell epitope.

Work described here strongly suggests that the SP of pGP-C is more than a targeting device to the ER. It may function at further stages of the LCMV life cycle.

Acknowledgments—We thank Rita de Giuli for excellent technical assistance and Michael Buchmeier, Bruno Martoglio, and Martin Pool

for advice. We thank Rolf M. Zinkernagel for bringing to our attention the signal peptide of LCMV and Joachim Hombach for providing the cDNA of the LCMV S RNA.

REFERENCES

1. Blobel, G. (1980) *Proc. Natl. Acad. Sci. U. S. A.* **77,** 1496–1500
2. von Heijne, G. (1990) *J. Membrane Biol.* **115,** 195–201
3. von Heijne, G. (1985) *J. Mol. Biol.* **184,** 99–105
4. Walter, P., and Johnson, A. E. (1994) *Annu. Rev. Cell Biol.* **10,** 87–119
5. Blobel, G., and Dobberstein, B. (1975) *J. Cell Biol.* **67,** 835–851
6. Martoglio, B., and Dobberstein, B. (1998) *Trends Cell Biol.* **8,** 410–415
7. Rehm, A., Stern, P., Ploegh, H. L., and Tortorella, D. (2001) *EMBO J.* **20,** 1573–1582
8. Li, Y., Bergeron, J. J., Luo, L., Ou, W. J., Thomas, D. Y., and Kang, C. Y. (1996) *Proc. Natl. Acad. Sci. U. S. A.* **93,** 9606–9611
9. Gewurz, B. E., Ploegh, H. L., and Tortorella, D. (2002) *J. Biol. Chem.* **277,** 11306–11313
10. Russel, M., and Model, P. (1981) *Proc. Natl. Acad. Sci. U. S. A.* **78,** 1717–1721
11. von Heijne, G. (1983) *Eur. J. Biochem.* **133,** 17–21
12. Andrews, D. W., Perara, E., Lesser, C., and Lingappa, V. R. (1988) *J. Biol. Chem.* **263,** 15791–15798
13. Lyko, F., Martoglio, B., Jungnickel, B., Rapoport, T. A., and Dobberstein, B. (1995) *J. Biol. Chem.* **270,** 19873–19878
14. Klappa, P., Dierks, T., and Zimmermann, R. (1996) *Eur. J. Biochem.* **239,** 509–518
15. Weihofen, A., Binns, K., Lemberg, M. K., Ashman, K., and Martoglio, B. (2002) *Science* **296,** 2215–2218
16. Lemberg, M. K., and Martoglio, B. (2002) *Mol. Cell.* **10,** 735–744
17. Martoglio, B., Graf, R., and Dobberstein, B. (1997) *EMBO J.* **16,** 6636–6645
18. Braud, V., Jones, E. Y., and McMichael, A. (1997) *Eur. J. Immunol.* **27,** 1164–1169
19. Braud, V. M., Allan, D. S., O'Callaghan, C. A., Soderstrom, K., D'Andrea, A., Ogg, G. S., Lazetic, S., Young, N. T., Bell, J. I., Phillips, J. H., Lanier, L. L., and McMichael, A. J. (1998) *Nature* **391,** 795–799
20. Bai, A., and Forman, J. (1997) *J. Immunol.* **159,** 2139–2146
21. Burns, J. W., and Buchmeier, M. J. (1993) in *The Arenaviridae* (Salvato, M. S., ed), pp. 17–35, Plenum Press, New York
22. Klavinskis, L. S., Whitton, J. L., Joly, E., and Oldstone, M. B. (1990) *Virology* **178,** 393–400
23. Buchmeier, M. J., and Zinkernagel, R. M. (1992) *Science* **257,** 1142
24. Hudrisier, D., Oldstone, M. B., and Gairin, J. E. (1997) *Virology* **234,** 62–73
25. Hombach, J., Pircher, H., Tonegawa, S., and Zinkernagel, R. M. (1995) *J. Exp. Med.* **182,** 1615–1619
26. Gallimore, A., Schwarz, K., van den Broek, M., Hengartner, H., and Groettrup, M. (1998) *Mol. Immunol.* **35,** 581–591
27. Romanowski, V., Matsuura, Y., and Bishop, D. H. (1985) *Virus Res.* **3,** 101–114
28. Huylebroeck, D., Maertens, G., Verhoeyen, M., Lopez, C., Raeymakers, A., Jou, W. M., and Fiers, W. (1988) *Gene (Amst.)* **66,** 163–181
29. Aden, D. P., and Knowles, B. B. (1976) *Immunogenetics* **3,** 209
30. Lehmann-Grube, F. (1971) *Virol. Monogr.* **10,** 1
31. Bruns, M., Cihak, J., Muller, G., and Lehmann-Grube, F. (1983) *Virology* **130,** 247–251
32. Maniatis, T., Fritsch, E. F., and Sambrook, J. (1982) *Molecular cloning: A Laboratory Manual*, Cold Spring Harbor Laboratory, Cold Spring Harbor, NY
33. Buchmeier, M. J., Elder, J. H., and Oldstone, M. B. (1978) *Virology* **89,** 133–145
34. Lipp, J., and Dobberstein, B. (1986) *Cell* **46,** 1103–1112
35. Laemmli, U. K. (1970) *Nature* **227,** 680–685
36. Schägger, H., and von Jagow, G. (1987) *Anal. Biochem.* **166,** 368–379
37. Beyer, W. R., Miletic, H., Ostertag, W., and von Laer, D. (2001) *J. Virol.* **75,** 1061–1064
38. Li, Y., Luo, L., Thomas, D. Y., and Kang, C. Y. (2000) *Virology* **272,** 417–428
39. Hartmann, E., Rapoport, T. A., and Lodish, H. F. (1989) *Proc. Natl. Acad. Sci. U. S. A.* **86,** 5786–5790
40. Lindemann, D., Pietschmann, T., Picard-Maureau, M., Berg, A., Heinkelein, M., Thurow, J., Knaus, P., Zentgraf, H., and Rethwilm, A. (2001) *J. Virol.* **75,** 5762–5771
41. Eichler, R., Lenz, O., Strecker, T., and Garten, W. (2003) *FEBS Lett.* **538,** 203–206
42. Garoff, H., Kondor-Koch, C., and Riedel, H. (1982) *Curr. Top. Microbiol. Immunol.* **99,** 1–50
43. Gaedigk-Nitschko, K., Ding, M. X., Levy, M. A., and Schlesinger, M. J. (1990) *Virology* **175,** 282–291
44. Liljestrom, P., Lusa, S., Huylebroeck, D., and Garoff, H. (1991) *J. Virol.* **65,** 4107–4113
45. Lusa, S., Garoff, H., and Liljestrom, P. (1991) *Virology* **185,** 843–846
46. Loewy, A., Smyth, J., von Bonsdorff, C. H., Liljestrom, P., and Schlesinger, M. J. (1995) *J. Virol.* **69,** 469–475
47. Yao, J. S., Strauss, E. G., and Strauss, J. H. (1996) *J. Virol.* **70,** 7910–7920

Chapter 9

Discussion

The adaptive immune system has evolved in higher vertebrates to defend them efficiently against infections and perhaps also against cancers. The class I pathway allows the immunosurveillance of proteins, which are synthesized within virtually all types of cells. Proteasomes are highly abundant in eukaryotic cells and play a major role in antigen processing. The aim of this study was to analyse different parameters in the MHC-I antigen processing pathway, focused on the role of the three proteasome inducible immune subunits LMP2, LMP7, and MECL-1.

Chapter 2 describes the role of ubiquitylation in antigen processing. To date, it is not known whether ubiquitin is required for antigen processing and when addressing this question with a temperature sensitive E1 cell line in the past contradictory results were obtained (Cox et al., 1995; Michalek et al., 1996). In this thesis, ubiquitin and dominant negative mutant forms of ubiquitin were expressed in a tetracycline inducible manner to investigate whether ubiquitin is required for the presentation of ligands for MHC-I. No change in total ubiquitylation and MHC-I surface expression was observed after induction of ubiquitin or its mutant forms. Since the induced ubiquitin can not outcompete endogenous ubiquitin no conclusion can be drawn whether ubiquitin is required for antigen processing, but at least, ubiquitin is not limiting (if required at all). An alternative approach to address the role of ubiquitylation in antigen processing could be the elimination of the E1 enzyme by inducible small interference RNA (siRNA). The shut-off of the ubiquitin-activating enzyme E1 would prevent ubiquitylation of all proteins and thereby ubiquitylation in antigen processing could be investigated.

In chapter 3 the role of Hsp90 in the processing of LCMV derived epitopes was investigated. Treatment of LCMV infected cells with geldanamycin, an inhibitor of Hsp90, led to a dose dependent reduction in presentation of the LCMV-derived epitope NP118, but other LCMV-derived epitopes were not affected. Different experiments to assign the role of Hsp90 in processing of NP118 failed. The dependency of NP118 on Hsp90 seems to be cell and virus specific.

The main part of this thesis, Chapter 4 and 5, describes the role of LMP2, LMP7 and MECL-1 in the processing of LCMV-derived epitopes. Chapter 4 analyses the proteasomal processing of GP276-286, a subdominant epitope in LCMV-WE infected C57BL/6 mice. It is shown that the treatment of cells with IFN-γ enhanced the presentation of GP33–41, whereas presentation of the GP276–286 epitope from the same glycoprotein was markedly reduced. Different read-out systems proved that GP276-286 is made more efficiently by constitutive proteasomes compared to immunoproteasomes. Overexpression of the active site subunits of

immunoproteasomes LMP2, LMP7, and MECL-1 as well as overexpression of LMP2 alone suppressed the presentation of the GP276–286 epitope. Infection of thioglycollate-elicited peritoneal macrophages derived from LMP2- and LMP7-deficient mice with LCMV-WE, as well as infection of these mice with a recombinant vaccinia virus expressing the LCMV glycoprotein showed an enhanced generation of GP276–286 epitope. *In vitro* digests demonstrated that fragmentation by immunoproteasomes, but not constitutive proteasomes, led to a preferential destruction of the GP276 epitope. In the past, the phenomenon of immunodominance has been investigated intensively in the LCMV system, but the reasons for the subdominance of GP276 remained unclear (Aebischer et al., 1990; Gallimore et al., 1998a; Gallimore et al., 1998b; van der Most et al., 2003; van der Most et al., 1998). We show that LMP2 and LMP7 can at least in part contribute to the subdominance of GP276 and immunosubunits can shape the epitope hierarchy of CTL responses *in vivo*. Another factor that determines immunodominance is the kinetic of viral protein expression (chapter 6). It is reported that a small load of LCMV led to immunodominance of NP-CTL, whereas a large viral load resulted in dominance of GP-CTL. Immunodominance is an extremely complex phenomenon due to contribution of many different factors (discussed in chapter 1). Analysis of single components leads to general knowledge that is important to develop vaccines that induce effective and protective CTL responses to different pathogens or cancers resistant to humoral immunity.

The proteasomal active site subunit exchange of MECL-1 for MC14 was discovered relatively late compared to LMP2 and LMP7 and little is known about this exchange in respect to antigen processing for MHC-I (Groettrup et al., 1996; Hisamatsu et al., 1996; Nandi et al., 1996). In this thesis, the contribution of MECL-1 in antigen processing was analyzed with the help of MECL-1 gene targeted mice (chapter 5). Infection of these mice with LCMV-WE elicited a strong CTL response to a panel of different peptides. The intensity of the CTL response to two different epitopes, NP205 and GP276, was markedly reduced. The impaired CTL response to GP276 in MECL-$1^{-/-}$ mice could not be assigned to a defect in the presentation of this epitope. Analysis of $V\beta_{10b}$, the preferred Vß-chain in the TCR of GP276-specific CTLs (Aebischer et al., 1990), in naïve and LCMV infected MECL-1 gene targeted mice revealed that they are present in MECL-$1^{-/-}$ mice but they do not proliferate after LCMV infection. Staining of CD8 in splenocytes showed that MECL-1 deficient mice have a 20% reduction of CD8 positive cells compared to wildtype mice. Similar results were reported for LMP2- and PA28γ-gene targeted mice. Chen et al. reported an altered hierarchy in LMP$2^{-/-}$ mice after infection with influenza virus, which was due to both, changes in peptide

presentation and an altered T_{CD8+} repertoire in these mice (Chen et al., 2001). Since the reduced CTL response to GP276 in MECL-1 deficient mice is not due to an impaired presentation of this epitope it is very likely that the changed CTL response is due to an altered CTL repertoire. Data concerning $v\beta_{10b}$-usage of GP276specific CTLs in MECL-1-deficient mice support this idea. Adoptive transfer experiments of naïve T cells (CD90.2) into CD90.1 mice following an infection with LCMV-WE should confirm an altered CTL repertoire of MECL-1 deficient mice. As MECL-1 is constitutively expressed in cells responsible for negative selection in the thymus (Nil et al., 2004) one can assume that MECL-1 gene targeted mice have an altered CTL-repertoire. Probably a self-peptide expressed in the thymus of MECL-1 deficient mice causes the elimination of GP276-specific CTLs. Taken together, in chapter 5 it is demonstrated that MECL-1 is an important component of the MHC-I antigen processing pathway.

Both human and mouse cytomegaloviruses (HCMV and MCMV) avoid peptide presentation by several viral glycoproteins controlling different checkpoints of the MHC-I presentation pathway (Basta and Bennink, 2003). The incorporation of immunoproteasome subunits was prevented in MCMV infected, as well as HCMV-infected, fibroblasts *in vitro* (chapter 7). Quantitative assessment of LMP2, MECL-1, and LMP7 transcripts revealed that the inhibition of immunoproteasome formation occurred at a pretranscriptional level. Remarkably, a targeted deletion of the MCMV gene *M27*, encoding an inhibitor of STAT2 that disrupts IFN-γ receptor signaling, largely restored transcription and protein expression of immunoproteasome subunits in infected cells. The fact that viruses have acquired molecules to suppress immunoproteasome formation during evolution highlights the importance of immunoproteasomes for processing of ligands for MHC-I molecules. Moreover, analysis of viral evasion proteins is pivotal in understanding virus host interactions and developing vaccines to modulate immune responses.

The glycoproteins (GP-1 and GP-2) of the lymphocytic choriomeningitis virus (LCMV) are synthesized as a type I precursor glycoprotein C (pGP-C) that is processed during intracellular transport into GP-1 and GP-2. The predicted signal peptide (SP) of LCMV pGP-C (SPGP-C) is unusually long (58aa) compared to the average length of signal peptides. In chapter 8 we have investigated the cleavage and fate of the SPGP-C in transfected and LCMV-infected cells. We found that cleaved SPGP-C is rather long-lived and accumulates in virus particles. These unusual features of the cleaved SPGP-C suggest that SPGP-C not only targets the nascent pGP-C to the endoplasmic reticulum membrane but that it has additional so far unknown functions in lymphocytic choriomeningitis virus life cycle. A consequence of

SPGP-C stability is that the T cell epitope GP33 will not directly be released, and thus the T cell response will be delayed. As we have seen in chapter 6, the time point when a certain protein is synthesized during viral replication, is an important parameter in determining epitope hierarchy. Generation of the SPGP-C-derived T cell epitope GP33 requires a functional proteasome, suggesting that the SPGP-C is eventually released from the membrane into the cytosol, where it becomes proteolytically processed. Whether processing of cleaved SPGP-C is relevant for generating the GP33 T cell epitope is unclear.

During this thesis we also found that immunoproteasomes can affect some epitopes, but others are not affected. Why did nature make such a tremendous effort to replace the proteasomes active site subunits by the three IFN-γ inducible subunits LMP2, LMP7 and MECL-1? At present no simple answer can be given and several arguments indicate that immunoproteasomes are not absolutely required: (1) The bulk of MHC-I ligands can still be generated in cell lines and mice deficient for LMP2 or LMP7 (Arnold et al., 1992) (Momburg et al., 1992). (2) No severe phenotypes have been detected in LMP2, LMP7, and MECL-1 deficient mice (Fehling et al., 1994; Van Kaer et al., 1994). (3) These mice are not handicapped in clearance of several pathogens compared to wildtype mice (Basler et al., 2004; Chen et al., 2001; Fehling et al., 1994; Van Kaer et al., 1994). (4) Chickens do not have immunosubunits (Kaufman et al., 1999). The fact that no severe phenotype has been found in these mice does not exclude an important function of immunoproteasomes. Immunoproteasome are may be not absolutely required for a single individual, but for a whole population of a species they might be pivotal in surviving during evolution.

In the past, different functions have been assigned to the immunosubunits (discussed in chapter1). (1) The LMP subunits may have a docking function to physically link proteasomes to TAP. (2) The ‘optimal loading‘ argument is implying that the subunit exchanges produce a better-suited set of peptides for loading and stabilizing MHC-I molecules. (3) Another concept is that of ‘optimal diversity‘, which suggests, that a broader set of peptides is produced. (4) The change in epitope production may contribute to avoid autoimmune assaults if different peptide epitopes are processed from endogenous housekeeping genes in uninflamed sites as opposed to sites of viral infection.

Didn’t we investigate the right parameters in the past? Are the immunosubunits relevant for another pathway than that for the obvious MHC-I? What makes other organism containing immunoproteasomes different from chickens? May be immunoproteasomes are important in the cleavage of only very rare and so far unidentified proteins and thereby regulating cell

functions. Further analysis of LMP2, LMP7, and MECL-1 deficient mice in autoimmune or cancer models could reveal a special function of these subunits in these diseases. It is also possible that the gene disruption of only one subunit has only a minor effect, may be due to compensation of the loss by the other subunits, whereas generation of LMP2, LMP7 and MECL-1 triple gene deficient mice or even mice with gene disruption of all the inducible proteasome components, including regulators, could have a more drastic effect.

Due to the fact that nature developed the inducible energy requiring immunoproteasome system during evolution and the fact that viruses developed molecules to suppress immunoproteasome formation (chapter 7) one can conclude that these subunits have important so far not identified or not well characterized functions.

Chapter 10

References

Achour, A., Michaelsson, J., Harris, R.A., Odeberg, J., Grufman, P., Sandberg, J.K., Levitsky, V., Karre, K., Sandalova, T. and Schneider, G. (2002) A structural basis for LCMV immune evasion: subversion of H-2D(b) and H-2K(b) presentation of gp33 revealed by comparative crystal structure.Analyses. *Immunity*, **17**, 757-768.

Addo, M.M., Altfeld, M., Rosenberg, E.S., Eldridge, R.L., Philips, M.N., Habeeb, K., Khatri, A., Brander, C., Robbins, G.K., Mazzara, G.P., Goulder, P.J. and Walker, B.D. (2001) The HIV-1 regulatory proteins Tat and Rev are frequently targeted by cytotoxic T lymphocytes derived from HIV-1-infected individuals. *Proc Natl Acad Sci U S A*, **98**, 1781-1786.

Aden, D.P. and Knowles, B.B. (1976) Cell surface antigens coded for by the human chromosome 7. *Immunogenetics*, **3**, 209-221.

Aebischer, T., Oehen, S. and Hengartner, H. (1990) Preferential usage of Va4 and Vb10 T cell receptor genes by lymphocytic choriomeningitis virus glycoprotein-specific H-2D^{b}-restricted cytotoxic T cells. *Eur. J. Immunol.*, **20**, 523-531.

Ahn, J.Y., Tanahashi, N., Akiyama, K.-y., Hisamatsu, H., Noda, C., Tanaka, K., Chung, C.H., Shibmara, N., Willy, P.J., Mott, J.D., Slaughter, C.A. and DeMartino, G. (1995) Primary structures of two homologous subunits of PA28, a γ-interferon-inducible protein activator of the 20S proteasome. *FEBS Lett.*, **366**, 37-42.

Ahn, K., Erlander, M., Leturcq, D., Peterson, P.A., Früh, K. and Yang, Y. (1996) In Vivo characterization of the proteasome regulator PA28. *J. Biol. Chem.*, **271**, 18237-18242.

Ahn, K., Gruhler, A., Galocha, B., Jones, T.R., Wiertz, E.J.H.J., Ploegh, H.L., Peterson, P.A., Yang, Y. and Früh, K. (1997) The ER-luminal domain of the HCMV glycoprotein US6 inhibits peptide translocation by TAP. *Immunity*, **6**, 613-621.

Aki, M., Shimbara, N., Takashina, M., Akiyama, K., Kagawa, S., Tamura, T., Tanahashi, N., Yoshimura, T., Tanaka, K. and Ichihara, A. (1994) Interferon-γ induces different subunit organizations and functional diversity of proteasomes. *J. Biochem.*, **115**, 257-269.

Altman, J.D., Moss, P.A.H., Goulder, P.J.R., Barouch, D.H., McHeyzer-Williams, M.G., Bell, J.I., McMichael, A.J. and Davis, M.M. (1996) Phenotypic analysis of antigen-specific T lymphocytes. *Science*, **274**, 94-96.

Andrews, D.W., Perara, E., Lesser, C. and Lingappa, V.R. (1988) Sequences beyond the cleavage site influence signal peptide function. *J Biol Chem*, **263**, 15791-15798.

Appay, V., Dunbar, P.R., Callan, M., Klenerman, P., Gillespie, G.M., Papagno, L., Ogg, G.S., King, A., Lechner, F., Spina, C.A., Little, S., Havlir, D.V., Richman, D.D., Gruener, N., Pape, G., Waters, A., Easterbrook, P., Salio, M., Cerundolo, V., McMichael, A.J. and Rowland-Jones, S.L. (2002) Memory CD8+ T cells vary in differentiation phenotype in different persistent virus infections. *Nat Med*, **8**, 379-385.

Appay, V., Nixon, D.F., Donahoe, S.M., Gillespie, G.M., Dong, T., King, A., Ogg, G.S., Spiegel, H.M., Conlon, C., Spina, C.A., Havlir, D.V., Richman, D.D., Waters, A., Easterbrook, P., McMichael, A.J. and Rowland-Jones, S.L. (2000) HIV-specific CD8(+) T cells produce antiviral cytokines but are impaired in cytolytic function. *J Exp Med*, **192**, 63-75.

Argon, Y. and Simen, B.B. (1999) GRP94, an ER chaperone with protein and peptide binding properties. *Semin Cell Dev Biol*, **10**, 495-505.

Arnold, D., Driscoll, J., Androlewicz, M., Hughes, E., Cresswell, P. and Spies, T. (1992) Proteasome subunits encoded in the MHC are not generally required for the processing of peptides bound by MHC class I molecules. *Nature*, **360**, 171-174.

Arrode, G., Boccaccio, C., Lule, J., Allart, S., Moinard, N., Abastado, J.P., Alam, A. and Davrinche, C. (2000) Incoming human cytomegalovirus pp65 (UL83) contained in apoptotic infected fibroblasts is cross-presented to CD8(+) T cells by dendritic cells. *J Virol*, **74**, 10018-10024.

Bai, A. and Forman, J. (1997) The effect of the proteasome inhibitor lactacystin on the presentation of transporters associated with antigen processing (TAP)-dependent and TAP-independent peptide epitopes by class I molecules. *J. Immunol.*, **159**, 2139-2146.

Barton, L.F., Cruz, M., Rangwala, R., Deepe, G.S. and Monaco, J.J. (2002) Regulation of immunoproteasome subunit expression in vivo following pathogenic fungal infection. *J Immunol*, **169**, 3046-3052.

Barton, L.F., Runnels, H.A., Schell, T.D., Cho, Y.J., Gibbons, R., Tevethia, S.S., Deepe, G.S. and Monaco, J.J. (2004) Immune defects in 28-kDa proteasome activator gamma-deficient mice. *J Immunol*, **172**, 3948-3954.

Basler, M., Youhnovski, N., Van Den Broek, M., Przybylski, M. and Groettrup, M. (2004) Immunoproteasomes down-regulate presentation of a subdominant T cell epitope from lymphocytic choriomeningitis virus. *J Immunol*, **173**, 3925-3934.

Basta, S. and Bennink, J.R. (2003) A survival game of hide and seek: Cytomegaloviruses and MHC class I antigen presentation pathways. *Viral Immunol*, **16**, 231-242.

Basu, S., Binder, R.J., Ramalingam, T. and Srivastava, P.K. (2001) CD91 is a common receptor for heat shock proteins gp96, hsp90, hsp70, and calreticulin. *Immunity*, **14**, 303-313.

Battegay, M., Cooper, S., Althage, A., Banziger, J., Hengartner, H. and Zinkernagel, R.M. (1991) Quantification of lymphocytic choriomeningitis virus with an immunological focus assay in 24- or 96-well plates. *J. Virol. Methods*, **33**, 191-198.

Battegay, M., Moskophidis, D., Rahemtulla, A., Hengartner, H., Mak, T.W. and Zinkernagel, R.M. (1994) Enhanced establishment of a virus carrier state in adult CD4+ T-cell-deficient mice. *J Virol*, **68**, 4700-4704.

Beninga, J., Rock, K.L. and Goldberg, A.L. (1998) Interferon-gamma can stimulate post-proteasomal trimming of the N terminus of an antigenic peptide by inducing leucine aminopeptidase. *J Biol Chem*, **273**, 18734-18742.

Benz, C., Reusch, U., Muranyi, W., Brune, W., Atalay, R. and Hengel, H. (2001) Efficient downregulation of major histocompatibility complex class I molecules in human epithelial cells infected with cytomegalovirus. *J Gen Virol*, **82**, 2061-2070.

Berwin, B., Hart, J.P., Rice, S., Gass, C., Pizzo, S.V., Post, S.R. and Nicchitta, C.V. (2003) Scavenger receptor-A mediates gp96/GRP94 and calreticulin internalization by antigen-presenting cells. *Embo J*, **22**, 6127-6136.

Bevan, M.J. and Fink, P.J. (1978) The influence of thymus H-2 antigens on the specificity of maturing killer and helper cells. *Immunol Rev*, **42**, 3-19.

Beyer, W.R., Miletic, H., Ostertag, W. and von Laer, D. (2001) Recombinant expression of lymphocytic choriomeningitis virus strain WE glycoproteins: a single amino acid makes the difference. *J Virol*, **75**, 1061-1064.

Beyer, W.R., Popplau, D., Garten, W., von Laer, D. and Lenz, O. (2003) Endoproteolytic processing of the lymphocytic choriomeningitis virus glycoprotein by the subtilase SKI-1/S1P. *J Virol*, **77**, 2866-2872.

Binder, R.J., Han, D.K. and Srivastava, P.K. (2000) CD91: a receptor for heat shock protein gp96. *Nature Immunol.*, **1**, 151-155.

Blattman, J.N., Sourdive, D.J., Murali-Krishna, K., Ahmed, R. and Altman, J.D. (2000) Evolution of the T cell repertoire during primary, memory, and recall responses to viral infection. *J Immunol*, **165**, 6081-6090.

Blobel, G. (1980) Intracellular protein topogenesis. *Proc Natl Acad Sci U S A*, **77**, 1496-1500.

Blobel, G. and Dobberstein, B. (1975) Transfer of proteins across membranes. I. Presence of proteolytically processed and unprocessed nascent immunoglobulin light chains on membrane-bound ribosomes of murine myeloma. *J Cell Biol*, **67**, 835-851.

Boes, B., Hengel, H., Ruppert, T., Multhaup, G., Koszinowski, U.H. and Kloetzel, P.M. (1994) Interferon γ stimulation modulates the proteolytic activity and cleavage site preference of 20S mouse proteasomes. *J. Exp. Med.*, **179**, 901-909.

Braud, V., Jones, E.Y. and McMichael, A. (1997) The human major histocompatibility complex class Ib molecule HLA-E binds signal sequence-derived peptides with primary anchor residues at positions 2 and 9. *Eur. J. Immunol.*, **27**, 1164-1169.

Braud, V.M., Allan, D.S., O'Callaghan, C.A., Soderstrom, K., D'Andrea, A., Ogg, G.S., Lazetic, S., Young, N.T., Bell, J.I., Phillips, J.H., Lanier, L.L. and McMichael, A.J. (1998) HLA-E binds to natural killer cell receptors CD94/NKG2A, B and C. *Nature*, **391**, 795-799.

Braun, B.C., Glickman, M., Kraft, R., Dahlmann, B., Kloetzel, P.M., Finley, D. and Schmidt, M. (1999) The base of the proteasome regulatory particle exhibits chaperone- like activity. *Nat Cell Biol*, **1**, 221-226.

Bruns, M., Cihak, J., Müller, G. and Lehmann-Grube, F. (1983) Lymphocytic choriomeningitis virus. VI. Isolation of a glycoprotein mediating neutralization. *Virology*, **130**, 247-251.

Bruns, M., Kratzberg, T., Zeller, W. and Lehmann-Grube, F. (1990) Mode of replication of lymphocytic choriomeningitis virus in persistently infected cultivated mouse L cells. *Virology*, **177**, 615-624.

Buchmeier, M.J., Elder, J.H. and Oldstone, M.B.A. (1978) Protein structure of lymphocytic choriomeningitis virus: identification of the virus structural and cell associated polypeptides. *Virology*, **89**, 133-145.

Buchmeier, M.J. and Oldstone, M.B.A. (1979) Protein structure of lymphocytic choriomeningitis virus: evidence for a cell-associated precursor of the virion glycopeptides. *Virology*, **99**, 111-120.

Buchmeier, M.J., Welsh, R.M., Dutko, F.J. and Oldstone, M.B.A. (1980) The virology and immunobiology of lymphocytic choriomeningitis virus infection. *Adv. Immunol.*, **30**, 275-331.

Buchmeier, M.J. and Zinkernagel, R.M. (1992) Immunodominant T cell epitope from signal sequence. *Science*, **257**, 1142.

Buchner, J. (1999) Hsp90 & Co. - a holding for folding. *Trends Biochem Sci*, **24**, 136-141.

Bukowski, J.F., Biron, C.A. and Welsh, R.M. (1983) Elevated natural killer cell-mediated cytotoxicity, plasma interferon, and tumor cell rejection in mice persistently infected with lymphocytic choriomeningitis virus. *J Immunol*, **131**, 991-996.

Burns, J.W. and Buchmeier, M.J. (1993) Glycoproteins of the arenaviruses. In Salvato, M.S. (ed.), *The Arenaviridae*. Plenum Press, New York, pp. 17-35.

Butz, E.A. and Bevan, M.J. (1998a) Differential presentation of the same MHC class I epitopes by fibroblasts and dendritic cells. *J. Immunol.*, **160**, 2139-2144.

Butz, E.A. and Bevan, M.J. (1998b) Massive expansion of antigen-specific CD8+ T cells during an acute virus infection. *Immunity*, **8**, 167-175.

Campbell, J.J., Bowman, E.P., Murphy, K., Youngman, K.R., Siani, M.A., Thompson, D.A., Wu, L., Zlotnik, A. and Butcher, E.C. (1998) 6-C-kine (SLC), a lymphocyte adhesion-triggering chemokine expressed by high endothelium, is an agonist for the MIP-3beta receptor CCR7. *J Cell Biol*, **141**, 1053-1059.

Cao, W., Henry, M.D., Borrow, P., Yamada, H., Elder, J.H., Ravkov, E.V., Nichol, S.T., Compans, R.W., Campbell, K.P. and Oldstone, M.B.A. (1998) Identification of a-Dystroglycan as a receptor for lymphocytic choriomeningitis virus and lassa fever virus. *Science*, **282**, 2079-2081.

Cardin, R.D., Brooks, J.W., Sarawar, S.R. and Doherty, P.C. (1996) Progressive loss of CD8+ T cell-mediated control of a gamma-herpesvirus in the absence of CD4+ T cells. *J Exp Med*, **184**, 863-871.

Cascio, P., Call, M., Petre, B.M., Walz, T. and Goldberg, A.L. (2002) Properties of the hybrid form of the 26S proteasome containing both 19S and PA28 complexes. *Embo J*, **21**, 2636-2645.

Cascio, P., Hilton, C., Kisselev, A.F., Rock, K.L. and Goldberg, A.L. (2001) 26S proteasomes and immunoproteasomes produce mainly N-extended versions of an antigenic peptide. *Embo J*, **20**, 2357-2366.

Cerundolo, V., Kelly, A., Elliot, T., Trowsdale, J. and Townsend, A. (1995) Genes encoded in the major histocompatibility complex affecting the generation of peptides for TAP transport. *Eur. J. Immunol.*, **25**, 554-562.

Chen, W., Anton, L.C., Bennink, J.R. and Yewdell, J.W. (2000) Dissecting the multifactorial causes of immunodominance in class I-restricted T cell responses to viruses. *Immunity*, **12**, 83-93.

Chen, W., Syldath, U., Bellmann, K., Burkart, V. and Kolb, H. (1999) Human 60-kDa heat-shock protein: a danger signal to the innate immune system. *J Immunol*, **162**, 3212-3219.

Chen, W.S., Norbury, C.C., Cho, Y.J., Yewdell, J.W. and Bennink, J.R. (2001) Immunoproteasomes shape immunodominance hierarchies of antiviral CD8(+) T cells at the levels of T cell repertoire and presentation of viral antigens. *J. Exp. Med.*, **193**, 1319-1326.

Christinck, E.R., Luscher, M.A., Barber, B.H. and Williams, D.B. (1991) Peptide binding to class I MHC on living cells and quantitation of complexes required for CTL lysis. *Nature*, **352**, 67-70.

Chu-Ping, M., Slaughter, C.A. and DeMartino, G.N. (1992) Identification, purification and characterization of a protein activator (PA28) of the 20S Proteasome (Macropain). *J. Biol. Chem.*, **267**, 10515-10523.

Connell, P., Ballinger, C.A., Jiang, J., Wu, Y., Thompson, L.J., Hohfeld, J. and Patterson, C. (2001) The co-chaperone CHIP regulates protein triage decisions mediated by heat-shock proteins. *Nat Cell Biol*, **3**, 93-96.

Cox, J.H., Galardy, P., Bennink, J.R. and Yewdell, J.W. (1995) Presentation of endogenous and exogenous antigens is not affected by inactivation of E1 ubiquitin-activating enzyme in temperature-sensitive cell lines. *J. Immunol.*, **154**, 511-519.

Craiu, A., Akoplan, T., Goldberg, A. and Rock, K.L. (1997) Two distinct proteolytic processes in the generation of a major histocompatibility complex class I-presented peptide. *Proc. Natl. Acad. Sci. USA*, **94**, 10850-10855.

Cyr, D.M., Hohfeld, J. and Patterson, C. (2002) Protein quality control: U-box-containing E3 ubiquitin ligases join the fold. *Trends Biochem Sci*, **27**, 368-375.

Dahlmann, B., Kuehn, L. and Reinauer, H. (1995) Studies on the activation by ATP of the 26 S proteasome complex from rat skeletal muscle. *Biochem J*, **309 (Pt 1)**, 195-202.

Davis, M.M. and Bjorkman, P.J. (1988) T-cell antigen receptor genes and T-cell recognition. *Nature*, **334**, 395-402.

De Boer, R.J., Oprea, M., Antia, R., Murali-Krishna, K., Ahmed, R. and Perelson, A.S. (2001) Recruitment times, proliferation, and apoptosis rates during the CD8(+) T-cell response to lymphocytic choriomeningitis virus. *J Virol*, **75**, 10663-10669.

De, M., Jayarapu, K., Elenich, L., Monaco, J.J., Colbert, R.A. and Griffin, T.A. (2003) Beta 2 subunit propeptides influence cooperative proteasome assembly. *J Biol Chem*, **278**, 6153-6159.

Deng, Y., Yewdell, J.W., Eisenlohr, L.C. and Bennink, J.R. (1997) MHC affinity, peptide liberation, T cell repertoire, and immunodominance all contribute to the paucity of MHC class I-restricted peptides recognized by antiviral CTL. *J Immunol*, **158**, 1507-1515.

Deveraux, Q., Ustrell, V., Pickart, C. and Rechsteiner, M. (1994) A 26S protease subunit that binds ubiquitin conjugates. *J. Biol. Chem.*, **269**, 7059-7061.

Dick, T.P., Bangia, N., Peaper, D.R. and Cresswell, P. (2002) Disulfide bond isomerization and the assembly of MHC class I-Peptide complexes. *Immunity*, **16**, 87-98.

Dick, T.P., Ruppert, T., Groettrup, M., Kloetzel, P.M., Kuehn, L., Koszinowski, U.H., Stevanovic´, S., Schild, H. and Rammensee, H.-G. (1996) Coordinated dual cleavages by the proteasome regulator PA28 lead to dominant MHC ligands. *Cell*, **86**, 253-262.

Driscoll, J., Brown, M.G., Finley, D. and Monaco, J.J. (1993) MHC-linked LMP gene products specifically alter peptidase activities of the proteasome. *Nature*, **365**, 262-264.

Dubiel, W., Pratt, G., Ferrell, K. and Rechsteiner, M. (1992) Purification of an 11S regulator of the multicatalytic proteinase. *J. Biol. Chem.*, **267**, 22369-22377.

Eggers, M., Boes-Fabian, B., Ruppert, T., Kloetzel, P.-M. and Koszinowski, U.H. (1995) The cleavage preference of the proteasome governs the yield of antigenic peptides. *J. Exp. Med.*, **182**, 1865-1870.

Eichler, R., Lenz, O., Strecker, T. and Garten, W. (2003) Signal peptide of Lassa virus glycoprotein GP-C exhibits an unusual length. *FEBS Lett*, **538**, 203-206.

Eleuteri, A.M., Kohanski, R.A., Cardozo, C. and Orlowski, M. (1997) Bovine spleen multicatalytic proteinase complex (proteasome) - Replacement of X, Y, and Z subunits by LMP7, LMP2, and MECL1 and changes in properties and specificity. *J. Biol. Chem.*, **272**, 11824-11831.

Erickson, A.L., Kimura, Y., Igarashi, S., Eichelberger, J., Houghton, M., Sidney, J., McKinney, D., Sette, A., Hughes, A.L. and Walker, C.M. (2001) The outcome of hepatitis C virus infection is predicted by escape mutations in epitopes targeted by cytotoxic T lymphocytes. *Immunity*, **15**, 883-895.

Fehling, H.J., Swat, W., Laplace, C., Kuehn, R., Rajewsky, K., Mueller, U. and von Boehmer, H. (1994) MHC class I expression in mice lacking proteasome subunit LMP-7. *Science*, **265**, 1234-1237.

Felts, S.J., Owen, B.A., Nguyen, P., Trepel, J., Donner, D.B. and Toft, D.O. (2000) The hsp90-related protein TRAP1 is a mitochondrial protein with distinct functional properties. *J Biol Chem*, **275**, 3305-3312.

Finley, D., Bartel, B. and Varshavsky, A. (1989) The tails of ubiquitin precursors are ribosomal proteins whose fusion to ubiquitin facilitates ribosome biogenesis. *Nature*, **338**, 394-401.

Finley, D. and Chau, V. (1991) Ubiquitination. *Annu Rev Cell Biol*, **7**, 25-69.

Finley, D., Sadis, S., Monia, B.P., Boucher, P., Ecker, D.J., Crooke, S.T. and Chau, V. (1994) Inhibition of proteolysis and cell cycle progression in a multiubiquitination-deficient yeast mutant. *Mol. Cell. Biol.*, **14**, 5501-5509.

Forster, R., Schubel, A., Breitfeld, D., Kremmer, E., Renner-Muller, I., Wolf, E. and Lipp, M. (1999) CCR7 coordinates the primary immune response by establishing functional microenvironments in secondary lymphoid organs. *Cell*, **99**, 23-33.

Fowlkes, B.J. and Schweighoffer, E. (1995) Positive selection of T cells. *Curr Opin Immunol*, **7**, 188-195.

Froeschke, M., Basler, M., Groettrup, M. and Dobberstein, B. (2003) Long-lived signal peptide of lymphocytic choriomeningitis virus glycoprotein pGP-C. *J. Biol. Chem.*, **278**, 41914-41920.

Fujiwara, T., Oda, K., Yokota, S., Takatsuki, A. and Ikehara, Y. (1988) Brefeldin A causes disassembly of the Golgi complex and accumulation of secretory proteins in the endoplasmic reticulum. *J Biol Chem*, **263**, 18545-18552.

Fuller, M.J. and Zajac, A.J. (2003) Ablation of CD8 and CD4 T cell responses by high viral loads. *J Immunol*, **170**, 477-486.

Gaczynska, M., Rock, K.L. and Goldberg, A.L. (1993) Gamma-interferon and expression of MHC genes regulate peptide hydrolysis by proteasomes. *Nature*, **365**, 264-267.

Gaczynska, M., Rock, K.L., Spies, T. and Goldberg, A.L. (1994) Peptidase activities of proteasomes are differentially regulated by the major histocompatibility complex-encoded genes for LMP 2 and LMP 7. *Proc. Natl. Acad. Sci. USA*, **91**, 9213-9217.

Gaedigk-Nitschko, K., Ding, M.X., Levy, M.A. and Schlesinger, M.J. (1990) Site-directed mutations in the Sindbis virus 6K protein reveal sites for fatty acylation and the underacylated protein affects virus release and virion structure. *Virology*, **175**, 282-291.

Gallimore, A., Dumrese, T., Hengartner, H., Zinkernagel, R.M. and Rammensee, H.-G. (1998a) Protective immunity does not correlate with the hierarchy of virus-specific cytotoxic T cell responses to naturally processed peptides. *J. Exp. Med.*, **187**, 1647-1657.

Gallimore, A., Glithero, A., Godkin, A., Tissot, A., Althage, A., Plückthun, A., Elliott, T., Hengartner, H. and Zinkernagel, R. (1998b) Induction and exhaustion of lymphocytic choriomeningitis virus- specific cytotoxic T lymphocytes visuoaized using soluble tetrameric MHC class I peptide complexes. *in the press.*

Gallimore, A., Hengartner, H. and Zinkernagel, R. (1998c) Hierarchies of antigen-specific cytotoxic T-cell responses. *Immunol Rev*, **164**, 29-36.

Gallimore, A., Hombach, J., Dumrese, T., Rammensee, H.G., Zinkernagel, R.M. and Hengartner, H. (1998d) A protective cytotoxic T cell response to a subdominant epitope is influenced by the stability of the MHC class I/peptide complex and the overall spectrum of viral peptides generated within infected cells. *Eur. J. Immunol.*, **28**, 3301-3311.

Gallimore, A., Schwarz, K., van den Broek, M., Hengartner, H. and Groettrup, M. (1998e) The proteasome inhibitor lactacystin prevents the generation of an endoplasmic reticulum leader - derived T cell epitope. *Mol. Immunol.*, **35**, 581-591.

Garbi, N., Tan, P., Diehl, A.D., Chambers, B.J., Ljunggren, H.G., Momburg, F. and Hämmerling, G.J. (2000) Impaired immune responses and altered peptide repertoire in tapasin- deficient mice. *Nat Immunol*, **1**, 234-238.

Garcia, K.C., Degano, M., Stanfield, R.L., Brunmark, A., Jackson, M.R., Peterson, P.A., Teyton, L. and Wilson, I.A. (1996) An alphabeta T cell receptor structure at 2.5 A and its orientation in the TCR-MHC complex. *Science*, **274**, 209-219.

Garoff, H., Kondor-Koch, C. and Riedel, H. (1982) Structure and assembly of alphaviruses. *Curr Top Microbiol Immunol*, **99**, 1-50.

Geginat, G., Ruppert, T., Hengel, H., Holtappels, R. and Koszinowski, U.H. (1997) IFN-gamma is a prerequisite for optimal antigen processing of viral peptides in vivo. *J Immunol*, **158**, 3303-3310.

Geier, E., Pfeifer, G., Wilm, M., LucchiariHartz, M., Baumeister, W., Eichmann, K. and Niedermann, G. (1999) A giant protease with potential to substitute for some functions of the proteasome. *Science*, **283**, 978-981.

Geretti, A.M. and Osterhaus, A.D. (2001) Virus replication and evolution drive the kinetics and specificity of SIV-specific cytotoxic T lymphocytes. *Immunol Rev*, **183**, 109-114.

Gewurz, B.E., Ploegh, H.L. and Tortorella, D. (2002) US2, a human cytomegalovirus-encoded type I membrane protein, contains a non-cleavable amino-terminal signal peptide. *J Biol Chem*, **277**, 11306-11313.

Gileadi, U., MoinsTeisserenc, H.T., Correa, I., Booth, B.L., Dunbar, P.R., Sewell, A.K., Trowsdale, J., Phillips, R.E. and Cerundolo, V. (1999) Generation of an immunodominant CTL epitope is affected by proteasome subunit composition and stability of the antigenic protein. *J. Immunol.*, **163**, 6045-6052.

Gillespie, G.M., Wills, M.R., Appay, V., O'Callaghan, C., Murphy, M., Smith, N., Sissons, P., Rowland-Jones, S., Bell, J.I. and Moss, P.A. (2000) Functional heterogeneity and high frequencies of cytomegalovirus-specific CD8(+) T lymphocytes in healthy seropositive donors. *J Virol*, **74**, 8140-8150.

Glickman, M.H., Rubin, D.M., Coux, O., Wefes, I., Pfeifer, G., Cjeka, Z., Baumeister, W., Fried, V.A. and Finley, D. (1998) A subcomplex of the proteasome regulatory particle required for ubiquitin-conjugate degradation and related to the COP9-signalosome and eIF3. *Cell*, **94**, 615-623.

Glickman, M.H., Rubin, D.M., Fu, H., Larsen, C.N., Coux, O., Wefes, I., Pfeifer, G., Cjeka, Z., Vierstra, R., Baumeister, W., Fried, V. and Finley, D. (1999) Functional analysis of the proteasome regulatory particle. *Mol Biol Rep*, **26**, 21-28.

Gold, M.C., Munks, M.W., Wagner, M., Koszinowski, U.H., Hill, A.B. and Fling, S.P. (2002) The murine cytomegalovirus immunomodulatory gene m152 prevents recognition of infected cells by M45-specific CTL but does not alter the immunodominance of the M45-specific CD8 T cell response in vivo. *J Immunol*, **169**, 359-365.

Gossen, M. and Bujard, H. (1992) Tight control of gene expression in mammalian cells by tetracyclin-response promotors. *Proc. Natl. Acad. Sci. USA*, **89**, 5547-5551.

Gray, C.W., Slaughter, C.A. and DeMartino, G.N. (1994) PA28 activator protein forms regulatory caps on proteasome stacked rings. *J. Mol. Biol.*, **236**, 7-15.

Griffin, T.A., Nandi, D., Cruz, M., Fehling, H.J., VanKaer, L., Monaco, J.J. and Colbert, R.A. (1998) Immunoproteasome assembly: Cooperative incorporation of interferon gamma (IFN-gamma)-inducible subunits. *J. Exp. Med.*, **187**, 97-104.

Griffin, T.A., Slack, J.P., McCluskey, T.S., Monaco, J.J. and Colbert, R.A. (2000) Identification of proteassemblin, a mammalian homologue of the yeast protein UMP1p that is required for normal proteasome assembly. *Mol. Cell Biol. Commun.*, **3**, 212-217.

Groettrup, M., Khan, S., Schwarz, K. and Schmidtke, G. (2001) Interferon-γ inducible exchanges of 20S proteasome active site subunits: Why? *Biochimie*, **83**, 367-372.

Groettrup, M., Kraft, R., Kostka, S., Standera, S., Stohwasser, R. and Kloetzel, P.-M. (1996a) A third interferon-γ-induced subunit exchange in the 20S proteasome. *Eur. J. Immunol.*, **26**, 863-869.

Groettrup, M., Ruppert, T., Kuehn, L., Seeger, M., Standera, S., Koszinowski, U. and Kloetzel, P.M. (1995) The interferon-γ-inducible 11S regulator (PA28) and the LMP2/LMP7 subunits govern the peptide production by the 20S proteasome in vitro. *J. Biol. Chem.*, **270**, 23808-23815.

Groettrup, M., Soza, A., Eggers, M., Kuehn, L., Dick, T.P., Schild, H., Rammensee, H.-G., Koszinowski, U.H. and Kloetzel, P.-M. (1996b) A role for the proteasome regulator PA28α in antigen presentation. *Nature*, **381**, 166-168.

Groettrup, M., Soza, A., Kuckelkorn, U. and Kloetzel, P.M. (1996c) Peptide antigen production by the proteasome: complexity provides efficiency. *Immunol. Today*, **17**, 429-435.

Groettrup, M., Standera, S., Stohwasser, R. and Kloetzel, P.M. (1997) The subunits MECL-1 and LMP2 are mutually required for incorporation into the 20S proteasome. *Proc. Natl. Acad. Sci. USA*, **94**, 8970-8975.

Groll, M., Ditzel, L., Löwe, J., Stock, D., Bochtler, M., Bartunik, H.D. and Huber, R. (1997) Structure of 20 S proteasome from yeast at 2.4A resolution. *Nature*, **386**, 463-471.

Grzimek, N.K., Podlech, J., Steffens, H.P., Holtappels, R., Schmalz, S. and Reddehase, M.J. (1999) In vivo replication of recombinant murine cytomegalovirus driven by the paralogous major immediate-early promoter-enhancer of human cytomegalovirus. *J Virol*, **73**, 5043-5055.

Guidotti, L.G., Ishikawa, T., Hobbs, M.V., Matzke, B., Schreiber, R. and Chisari, F.V. (1996) Intracellular inactivation of the hepatitis B virus by cytotoxic T lymphocytes. *Immunity*, **4**, 25-36.

Hahn, Y.S., Braciale, V.L. and Braciale, T.J. (1991) Presentation of viral antigen to class I major histocompatibility complex-restricted cytotoxic T lymphocyte. Recognition of an immunodominant influenza hemagglutinin site by cytotoxic T lymphocyte is independent of the position of the site in the hemagglutinin translation product. *J. Exp. Med.*, **174**, 733-736.

Harding, C.V., France, J., Song, R., Farah, J.M., Chatterjee, S., Iqbal, M. and Siman, R. (1995) Novel Dipeptide aldehydes are proteasome inhibitors and block the MHC-I antigen-processing pathway. *J. Immunol.*, **155**, 1767-1775.

Hartmann, E., Rapoport, T.A. and Lodish, H.F. (1989) Predicting the orientation of eukaryotic membrane-spanning proteins. *Proc Natl Acad Sci U S A*, **86**, 5786-5790.

Heise, M.T., Connick, M. and Virgin, H.W. (1998) Murine cytomegalovirus inhibits interferon gamma-induced antigen presentation to CD4 T cells by macrophages via regulation of expression of major histocompatibility complex class II associated genes. *J Exp Med*, **187**, 1037-1046.

Hendil, K.B., Khan, S. and Tanaka, K. (1998) Simultaneous binding of PA28 and PA700 activators to 20 S proteasomes. *Biochem. J.*, **332**, 749-754.

Hendil, K.B., Kristensen, P. and Uerkvitz, W. (1995) Human proteasomes analysed with monoclonal antibodies. *Biochem. J.*, **305**, 245-252.

Hengartner, H., Odermatt, B., Schneider, R., Schreyer, M., Walle, G., MacDonald, H.R. and Zinkernagel, R.M. (1988) Deletion of self-reactive T cells before entry into the thymus medulla. *Nature*, **336**, 388-390.

Hengel, H., Esslinger, C., Pool, J., Goulmy, E. and Koszinowski, U.H. (1995) Cytokines restore MHC class I complex formation and control antigen presentation in human cytomegalovirus-infected cells. *J Gen Virol*, **76 (Pt 12)**, 2987-2997.

Hengel, H., Koopmann, J.O., Flohr, T., Muranyi, W., Goulmy, E., Hammerling, G.J., Koszinowski, U.H. and Momburg, F. (1997) A viral ER-resident glycoprotein inactivates the MHC-encoded peptide transporter. *Immunity*, **6**, 623-632.

Hengel, H., Lucin, P., Jonjic, S., Ruppert, T. and Koszinowski, U.H. (1994) Restoration of cytomegalovirus antigen presentation by gamma interferon combats viral escape. *J. Virol.*, **68**, 289-297.

Hengel, H., Reusch, U., Geginat, G., Holtappels, R., Ruppert, T., Hellebrand, E. and Koszinowski, U.H. (2000) Macrophages escape inhibition of major histocompatibility complex class I-dependent antigen presentation by cytomegalovirus. *J. Virol.*, **74**, 7861-7868.

Hershko, A. and Ciechanover, A. (1998) The ubiquitin system. *Annu. Rev. Biochem.*, **67**, 425-479.

Hershko, A., Ciechanover, A. and Varshavsky, A. (2000) The ubiquitin system. *Nature Med.*, **6**, 1073-1081.

Hisamatsu, H., Shimbara, N., Saito, Y., Kristensen, P., Hendil, K.B., Fujiwara, T., Takahashi, E.-i., Tanahashi, N., Tamura, T., Ichihara, A. and Tanaka, K. (1996) Newly identified pair of proteasomal subunits regulated reciprocally by interferon γ. *J. Exp. Med.*, **183**, 1-10.

Hodgins, R.R.W., Ellison, K.S. and Ellison, M.J. (1992) Expression of a ubiquitin derivate that conjugates to protein irreversible produces phenotypes consistent with a ubiquitin deficiency. *J. Biol. Chem.*, **267**, 8807-8812.

Hohfeld, J., Cyr, D.M. and Patterson, C. (2001) From the cradle to the grave: molecular chaperones that may choose between folding and degradation. *Embo Rep*, **2**, 885-890.

Holtappels, R., Grzimek, N.K., Simon, C.O., Thomas, D., Dreis, D. and Reddehase, M.J. (2002) Processing and presentation of murine cytomegalovirus pORFm164-derived peptide in fibroblasts in the face of all viral immunosubversive early gene functions. *J Virol*, **76**, 6044-6053.

Holtappels, R., Pahl-Seibert, M.F., Thomas, D. and Reddehase, M.J. (2000) Enrichment of immediate-early 1 (m123/pp89) peptide-specific CD8 T cells in a pulmonary CD62L(lo) memory-effector cell pool during latent murine cytomegalovirus infection of the lungs. *J Virol*, **74**, 11495-11503.

Hombach, J., Pircher, H., Tonegawa, S. and Zinkernagel, R.M. (1995) Strictly transporter of antigen presentation (TAP)-dependent presentation of an immunodominant cytotoxic T lymphocyte epitope in the signal sequence of a virus protein. *J. Exp. Med.*, **182**, 1615-1619.

Honore, B., Leffers, H., Madsen, P. and Celis, J.E. (1993) Interferon-γ up-regulates a unique set of proteins in human keratinocytes. Molecular cloning and expression of the cDNA encoding the RGD-sequence-containing protein IGUP I-5111. *Eur. J. Biochem.*, **218**, 421-430.

Hudrisier, D., Oldstone, M.B.A. and Gairin, J.E. (1997) The signal sequence of lymphocytic choriomeningitis virus contains an immunodominant cytotoxic T cell epitope that is restricted by both H-2D^b and H-2K^b molecules. *Virology*, **234**, 62-73.

Hunt, D.F., Henderson, R.A., Shabanowitz, J., Sakaguchi, K., Michel, H., Sevilir, N., Cox, A.L., Appella, E. and Engelhard, V.H. (1992) Characterization of peptides bound to the class I MHC molecule HLA-A2.1 by mass spectrometry. *Science*, **255**, 1261-1263.

Huylebroeck, D., Maertens, G., Verhoeyen, M., Lopez, C., Raeymakers, A., Jou, W.M. and Fiers, W. (1988) High-level transient expression of influenza virus proteins from a series of SV40 late and early replacement vectors. *Gene*, **66**, 163-181.

Inaba, K., Inaba, M., Romani, N., Aya, H., Deguchi, M., Ikehara, S., Muramatsu, S. and Steinman, R.M. (1992) Generation of large numbers of dendritic cells from mouse bone marrow cultures supplemented with granulocyte/macrophage colony-stimulating factor. *J. Exp. Med.*, **176**, 1693-1702.

Ishii, T., Udono, H., Yamano, T., Ohta, H., Uenaka, A., Ono, T., Hizuta, A., Tanaka, N., Srivastava, P.K. and Nakayama, E. (1999) Isolation of MHC class I-restricted tumor antigen peptide and its precursors associated with heat shock proteins hsp70, hsp90, and gp96. *J Immunol*, **162**, 1303-1309.

Jiang, H. and Monaco, J.J. (1997) Sequence and expression of mouse proteasome activator PA28 and the related autoantigen Ki. *Immunogenetics*, **46**, 93-98.

Kageyama, S., Tsomides, T.J., Sykulev, Y. and Eisen, H.N. (1995) Variations in the number of peptide-MHC class I complexes required to activate cytotoxic T cell responses. *J Immunol*, **154**, 567-576.

Kägi, D., Ledermann, B., Burki, K., Seiler, P., Odermatt, B., Olsen, K.J., Podack, E.R., Zinkernagel, R.M. and Hengartner, H. (1994) Cytotoxicity mediated by T cells and natural killer cells is greatly impaired in perforin-deficient mice. *Nature*, **369**, 31-37.

Kammer, A.R., van der Burg, S.H., Grabscheid, B., Hunziker, I.P., Kwappenberg, K.M.C., Reichen, J., Melief, C.J.M. and Cerny, A. (1999) Molecular mimicry of human cytochrome P450 by Hepatitis C virus at the level of cytotoxic T cell recognition. *J. Exp. Med.*, **190**, 169-176.

Karrer, U., Sierro, S., Wagner, M., Oxenius, A., Hengel, H., Koszinowski, U.H., Phillips, R.E. and Klenerman, P. (2003) Memory inflation: continuous accumulation of antiviral CD8+ T cells over time. *J Immunol*, **170**, 2022-2029.

Kaufman, J., Milne, S., Göbel, T.W.F., Walker, B.A., Jacob, J.P., Auffray, C., Zoorob, R. and Beck, S. (1999) The chicken B locus is a minimal essential major histocompatibility complex. *Nature*, **401**, 923-925.

Kavanagh, D.G., Gold, M.C., Wagner, M., Koszinowski, U.H. and Hill, A.B. (2001) The multiple immune-evasion genes of murine cytomegalovirus are not redundant: m4 and m152 inhibit antigen presentation in a complementary and cooperative fashion. *J Exp Med*, **194**, 967-977.

Khan, M.T., Wang, K., Auland, M.E., Kable, E.P.W. and Roufogalis, B.D. (1994) Membrane-bound high molecular mass proteinases from human erythrocytes. *Biochim. Biophys. Acta*, **1209**, 215-221.

Khan, N., Cobbold, M., Keenan, R. and Moss, P.A. (2002) Comparative analysis of CD8+ T cell responses against human cytomegalovirus proteins pp65 and immediate early 1 shows similarities in precursor frequency, oligoclonality, and phenotype. *J Infect Dis*, **185**, 1025-1034.

Khan, S., de Giuli, R., Schmidtke, G., Bruns, M., Buchmeier, M., van den Broek, M. and Groettrup, M. (2001a) Cutting Edge: Neosynthesis is required for the presentation of a T cell epitope from a long lived viral protein. *J. Immunol.*, **167**, 4801-4804.

Khan, S., van den Broek, M., Schwarz, K., de Giuli, R., Diener, P.A. and Groettrup, M. (2001b) Immunoproteasomes largely replace constitutive proteasomes during an antiviral and antibacterial immune response in the liver. *J. Immunol.*, **167**, 6859-6868.

Khan, S., Zimmermann, A., Basler, M., Groettrup, M. and Hengel, H. (2004) A cytomegalovirus inhibitor of gamma interferon signaling controls immunoproteasome induction. *J Virol*, **78**, 1831-1842.

Kisselev, A.F., Akopian, T.N. and Goldberg, A.L. (1998) Range of sizes of peptide products generated during degradation of different proteins by archaeal proteasomes. *J. Biol. Chem.*, **273**, 1982-1989.

Kisselev, A.F., Akopian, T.N., Woo, K.M. and Goldberg, A.L. (1999) The sizes of peptides generated from protein by mammalian 26 and 20 S proteasomes - Implications for understanding the degradative mechanism and antigen presentation. *J. Biol. Chem.*, **274**, 3363-3371.

Klappa, P., Dierks, T. and Zimmermann, R. (1996) Cyclosporin A inhibits the degradation of signal sequences after processing of presecretory proteins by signal peptidase. *Eur J Biochem*, **239**, 509-518.

Klavinskis, L.S., Lindsay-Whitton, J., Joly, E. and Oldstone, M.B.A. (1990) Vaccination and protection from a lethal infection: identification, incorporation, and use of a cytotoxic T lymphocyte glycoprotein epitope. *Virology*, **178**, 393-400.

Kleijnen, M.F., Huppa, J.B., Lucin, P., Mukherjee, S., Farrell, H., Campbell, A.E., Ulrich H, K. and Hill, A.B. (1997) A mouse cytomegalovirus glcoprotein, gp 34, forms a complex with folded class I MHC molecules in the ER which is not retained but is transported to the cell surface. *EMBO Journal*, **16 No. 4**, 685-694.

Klein, M.R., van Baalen, C.A., Holwerda, A.M., Kerkhof Garde, S.R., Bende, R.J., Keet, I.P., Eeftinck-Schattenkerk, J.K., Osterhaus, A.D., Schuitemaker, H. and Miedema, F. (1995) Kinetics of Gag-specific cytotoxic T lymphocyte responses during the clinical course of HIV-1 infection: a longitudinal analysis of rapid progressors and long-term asymptomatics. *J Exp Med*, **181**, 1365-1372.

Knowlton, J.R., Johnston, S.C., Whitby, F.G., Realini, C., Zhang, Z.G., Rechsteiner, M. and Hill, C.P. (1997) Structure of the proteasome activator REG alpha (PA28 alpha). *Nature*, **390**, 639-643.

Knuehl, C., Spee, P., Ruppert, T., Kuckelkorn, U., Henklein, P., Neefjes, J. and Kloetzel, P.M. (2001) The murine cytomegalovirus pp89 immunodominant H-2L(D) epitope is generated and translocated into the endoplasmic reticulum as an 11- mer precursor peptide. *J Immunol*, **167**, 1515-1521.

Kohler, A., Bajorek, M., Groll, M., Moroder, L., Rubin, D.M., Huber, R., Glickman, M.H. and Finley, D. (2001a) The substrate translocation channel of the proteasome. *Biochimie*, **83**, 325-332.

Kohler, A., Cascio, P., Leggett, D.S., Woo, K.M., Goldberg, A.L. and Finley, D. (2001b) The axial channel of the proteasome core particle is gated by the Rpt2 ATPase and controls both substrate entry and product release. *Mol Cell*, **7**, 1143-1152.

Kostense, S., Ogg, G.S., Manting, E.H., Gillespie, G., Joling, J., Vandenberghe, K., Veenhof, E.Z., van Baarle, D., Jurriaans, S., Klein, M.R. and Miedema, F. (2001) High viral burden in the presence of major HIV-specific CD8(+) T cell expansions: evidence for impaired CTL effector function. *Eur J Immunol*, **31**, 677-686.

Kuckelkorn, U., Frentzel, S., Kraft, R., Kostka, S., Groettrup, M. and Kloetzel, P.-M. (1995) Incorporation of major histocompatibility complex - encoded subunits LMP2 and LMP7 changes the quality of the 20S proteasome polypeptide processing products independent of interferon-γ. *Eur. J. Immunol.*, **25**, 2605-2611.

Kuckelkorn, U., Ruppert, T., Strehl, B., Jungblut, P.R., Zimny-Arndt, U., Lamer, S., Prinz, I., Drung, I., Kloetzel, P.M., Kaufmann, S.H. and Steinhoff, U. (2002) Link between organ-specific antigen processing by 20S proteasomes and CD8(+) T cell-mediated autoimmunity. *J. Exp. Med.*, **195**, 983-990.

Kuehn, L. and Dahlmann, B. (1996) Reconstitution of proteasome activator PA 28 from isolated subunits: optimal activity is associated with an α,β- heteromultimer. *FEBS Letters*, **394**, 183-186.

Kunisawa, J. and Shastri, N. (2003) The group II chaperonin TRiC protects proteolytic intermediates from degradation in the MHC class I antigen processing pathway. *Mol Cell*, **12**, 565-576.

Laemmli, U.K. (1970) Cleavage of structural proteins during the assembly of the head of bacteriophage T4. *Nature*, **227**, 680-685.

Lam, Y.A., Lawson, T.G., Velayutham, M., Zweier, J.L. and Pickart, C.M. (2002) A proteasomal ATPase subunit recognizes the polyubiquitin degradation signal. *Nature*, **416**, 763-767.

Lanzavecchia, A., Iezzi, G. and Viola, A. (1999) From TCR engagement to T cell activation: a kinetic view of T cell behaviour. *Cell*, **96**, 1-4.

Lechner, F., Gruener, N.H., Urbani, S., Uggeri, J., Santantonio, T., Kammer, A.R., Cerny, A., Phillips, R., Ferrari, C., Pape, G.R. and Klenerman, P. (2000a) CD8+ T lymphocyte responses are induced during acute hepatitis C virus infection but are not sustained. *Eur J Immunol*, **30**, 2479-2487.

Lechner, F., Wong, D.K.H., Dunbar, P.R., Chapman, R., Chung, R.T., Dohrenwend, P., Robbins, G., Phillips, R., Klenerman, P. and Walker, B.D. (2000b) Analysis of successful immune responses in persons infected with hepatitis C virus. *J Exp Med*, **191**, 1499-1512.

Lee, P.P., Yee, C., Savage, P.A., Fong, L., Brockstedt, D., Weber, J.S., Johnson, D., Swetter, S., Thompson, J., Greenberg, P.D., Roederer, M. and Davis, M.M. (1999) Characterization of circulating T cells specific for tumor-associated antigens in melanoma patients. *Nat Med*, **5**, 677-685.

Lehmann-Grube, F. (1971) Lymphocytic choriomeningitis virus. *Virol. Monogr.*, **10**, 1-173.

Leist, T.P., Cobbold, S.P., Waldmann, H., Aguet, M. and Zinkernagel, R.M. (1987) Functional analysis of T lymphocyte subsets in antiviral host defense. *J. Immunol.*, **138**, 2278-2281.

Lemberg, M.K. and Martoglio, B. (2002) Requirements for signal peptide peptidase-catalyzed intramembrane proteolysis. *Mol Cell*, **10**, 735-744.

Li, J., Gao, X.L., Ortega, J.Q., Nazif, T., Joss, L., Bogyo, M., Steven, A.C. and Rechsteiner, M. (2001) Lysine 188 substitutions convert the pattern of proteasome activation by REG gamma to that of REGs alpha and beta. *Embo J.*, **20**, 3359-3369.

Li, Y., Bergeron, J.J., Luo, L., Ou, W.J., Thomas, D.Y. and Kang, C.Y. (1996) Effects of inefficient cleavage of the signal sequence of HIV-1 gp 120 on its association with calnexin, folding, and intracellular transport. *Proc Natl Acad Sci U S A*, **93**, 9606-9611.

Li, Y., Luo, L., Thomas, D.Y. and Kang, C.Y. (2000) The HIV-1 Env protein signal sequence retards its cleavage and down-regulates the glycoprotein folding. *Virology*, **272**, 417-428.

Liljestrom, P., Lusa, S., Huylebroeck, D. and Garoff, H. (1991) In vitro mutagenesis of a full-length cDNA clone of Semliki Forest virus: the small 6,000-molecular-weight membrane protein modulates virus release. *J Virol*, **65**, 4107-4113.

Lindemann, D., Pietschmann, T., Picard-Maureau, M., Berg, A., Heinkelein, M., Thurow, J., Knaus, P., Zentgraf, H. and Rethwilm, A. (2001) A particle-associated glycoprotein signal peptide essential for virus maturation and infectivity. *J Virol*, **75**, 5762-5771.

Lipp, J. and Dobberstein, B. (1986) The membrane-spanning segment of invariant chain (I gamma) contains a potentially cleavable signal sequence. *Cell*, **46**, 1103-1112.

Loewy, A., Smyth, J., von Bonsdorff, C.H., Liljestrom, P. and Schlesinger, M.J. (1995) The 6-kilodalton membrane protein of Semliki Forest virus is involved in the budding process. *J Virol*, **69**, 469-475.

Lord, J.M., Davey, J., Frigerio, L. and Roberts, L.M. (2000) Endoplasmic reticulum-associated protein degradation. *Semin Cell Dev Biol*, **11**, 159-164.

Lucin, P., Jonjic, S., Messerle, M., Polic, B., Hengel, H. and Koszinowski, U.H. (1994) Late phase inhibition of murine cytomegalovirus replication by synergistic action of interferon-gamma and tumour necrosis factor. *J Gen Virol*, **75 (Pt 1)**, 101-110.

Luders, J., Demand, J. and Hohfeld, J. (2000) The ubiquitin-related BAG-1 provides a link between the molecular chaperones Hsc70/Hsp70 and the proteasome. *J. Biol. Chem.*, **275**, 4613-4617.

Lusa, S., Garoff, H. and Liljestrom, P. (1991) Fate of the 6K membrane protein of Semliki Forest virus during virus assembly. *Virology*, **185**, 843-846.

Lyko, F., Martoglio, B., Jungnickel, B., Rapoport, T.A. and Dobberstein, B. (1995) Signal sequence processing in rough microsomes. *J. Biol. Chem.*, **270**, 19873-19878.

Ma, C., Slaughter, C. and DeMartino, G. (1992) Identification, purification, and characterization of a protein activator (PA28) of the 20 S proteasome (macropain). *J. Biol. Chem.*, **267**, 10515 - 10523.

Ma, C.P., Willy, P.J., Slaughter, C.A. and DeMartino, G.N. (1993) PA28, an activator of the 20 S proteasome, is inactivated by proteolytic modification at its carboxyl terminus. *J Biol Chem*, **268**, 22514-22519.

Macagno, A., Gilliet, M., Sallusto, F., Lanzavecchia, A., Nestle, F.O. and Groettrup, M. (1999) Dendritic cells upregulate immunoproteasomes and the proteasome regulator PA28 during maturation. *Eur. J. Immunol.*, **29**, 4037-4042.

Macagno, A., Kuehn, L., de Giuli, R. and Groettrup, M. (2001) Pronounced upregulation of the PA28α/β proteasome regulator but little increase in the steady state content of immunoproteasomes during dendritic cell maturation. *Eur. J. Immunol.*, **31**, 3271-3280.

Martoglio, B. and Dobberstein, B. (1998) Signal sequences: more than just greasy peptides. *Tr Cell Biol*, **8**, 410-415.

Martoglio, B., Graf, R. and Dobberstein, B. (1997) Signal peptide fragments of preprolactin and HIV-1 p-gp160 interact with calmodulin. *EMBO J.*, **16**, 6636-6645.

Matloubian, M., Concepcion, R.J. and Ahmed, R. (1994) CD4+ T cells are required to sustain CD8+ cytotoxic T-cell responses during chronic viral infection. *J Virol*, **68**, 8056-8063.

McClellan, A.J. and Frydman, J. (2001) Molecular chaperones and the art of recognizing a lost cause. *Nat Cell Biol*, **3**, E51-53.

McCusker, D., Wilson, M. and Trowsdale, J. (1999) Organization of the genes encoding the human proteasome activators PA28 alpha and beta. *Immunogenetics*, **49**, 438-445.

McCutchen-Maloney, S.L., Matsuda, K., Shimbara, N., Binns, D.D., Tanaka, K., Slaughter, C.A. and DeMartino, G.N. (2000) cDNA cloning, expression, and functional characterization of PI31, a proline-rich inhibitor of the proteasome. *J. Biol. Chem.*, **275**, 18557-18565.

Meacham, G.C., Patterson, C., Zhang, W., Younger, J.M. and Cyr, D.M. (2001) The Hsc70 co-chaperone CHIP targets immature CFTR for proteasomal degradation. *Nat Cell Biol*, **3**, 100-105.

Meyer, B.J., de la Torre, J.C. and Southern, P.J. (2002) Arenaviruses: genomic RNAs, transcription, and replication. *Curr Top Microbiol Immunol*, **262**, 139-157.

Michalek, M.T., Grant, E.P., Gramm, C., Goldberg, A.L. and Rock, K.L. (1993) A role for the ubiquitin-dependent proteolytic pathway in MHC class I-restricted antigen presentation. *Nature*, **363**, 552-554.

Michalek, M.T., Grant, E.P. and Rock, K.L. (1996) Chemical denaturation and modification of ovalbumin alters its dependence on ubiquitin conjugation for class I antigen presentation. *J. Immunol.*, **157**, 617-624.

Millar, D.G., Garza, K.M., Odermatt, B., Elford, A.R., Ono, N., Li, Z. and Ohashi, P.S. (2003) Hsp70 promotes antigen-presenting cell function and converts T-cell tolerance to autoimmunity in vivo. *Nat Med*, **9**, 1469-1476.

Miller, D.M., Rahill, B.M., Boss, J.M., Lairmore, M.D., Durbin, J.E., Waldman, J.W. and Sedmak, D.D. (1998) Human cytomegalovirus inhibits major histocompatibility complex class II expression by disruption of the Jak/Stat pathway. *J Exp Med*, **187**, 675-683.

Miller, D.M., Zhang, Y., Rahill, B.M., Kazor, K., Rofagha, S., Eckel, J.J. and Sedmak, D.D. (2000) Human cytomegalovirus blocks interferon-gamma stimulated up-regulation of major histocompatibility complex class I expression and the class I antigen processing machinery. *Transplantation*, **69**, 687-690.

Mo, X.Y., Cascio, P., Lemerise, K., Goldberg, A.L. and Rock, K. (1999) Distinct proteolytic processes generate the C and N termini of MHC class I-binding peptides. *J Immunol*, **163**, 5851-5859.

Momburg, F. and Hammerling, G.J. (1998) Generation and TAP-mediated transport of peptides for major histocompatibility complex class I molecules. *Adv Immunol*, **68**, 191-256.

Momburg, F., Ortiz-Navarrete, V., Neefjes, J., Goulmy, E., van-de-Wal, Y., Spits, H., Powis, S.J., Butcher, G.W., Howard, J.C., Walden, P. and Haemmerling, G. (1992) Proteasome subunits encoded by the major histocompatibility complex are not essential for antigen presentation. *Nature*, **360**, 174-177.

Morel, S., Levy, F., BurletSchiltz, O., Brasseur, F., ProbstKepper, M., Peitrequin, A.L., Monsarrat, B., VanVelthoven, R., Cerottini, J.C., Boon, T., Gairin, J.E. and Van den Eynde, B.J. (2000) Processing of some antigens by the standard proteasome but not by the immunoproteasome results in poor presentation by dendritic cells. *Immunity*, **12**, 107-117.

Moskophidis, D., Lechner, F., Pircher, H. and Zinkernagel, R.M. (1993) Virus persistence in acutely infected immunocompetent mice by exhaustion of antiviral cytotoxic effector

T cells [published erratum appears in Nature 1993 Jul 15;364(6434):262] [see comments]. *Nature*, **362**, 758-761.

Murali-Krishna, K., Altman, J.D., Suresh, M., Sourdive, D.J., Zajac, A.J., Miller, J.D., Slansky, J. and Ahmed, R. (1998) Counting antigen-specific CD8 T cells: a reevaluation of bystander activation during viral infection. *Immunity*, **8**, 177-187.

Murata, S., Kawahara, H., Tohma, S., Yamamoto, K., Kasahara, M., Nabeshima, Y., Tanaka, K. and Chiba, T. (1999) Growth retardation in mice lacking the proteasome activator PA28 gamma. *J. Biol. Chem.*, **274**, 38211-38215.

Murata, S., Udono, H., Tanahashi, N., Hamada, N., Watanabe, K., Adachi, K., Yamano, T., Yui, K., Kobayashi, N., Kasahara, M., Tanaka, K. and Chiba, T. (2001) Immunoproteasome assembly and antigen presentation in mice lacking both PA28 alpha and PA28 beta. *Embo J*, **20**, 5898-5907.

Nandi, D., Jiang, H. and Monaco, J.J. (1996) Identification of MECL-1 (LMP-10) as the third IFN-γ-inducible proteasome subunit. *J. Immunol.*, **156**, 2361-2364.

Nandi, D., Woodward, E., Ginsburg, D.B. and Monaco, J.J. (1997) Intermediates in the formation of mouse 20S proteasomes: Implications for the assembly of precursor beta subunits. *EMBO J.*, **16**, 5363-5375.

Neefjes, J.J., Momburg, F. and Haemmerling, G.J. (1993) Selective and ATP-dependent translocation of peptides by the MHC-encoded transporter. *Science*, **261**, 769-771.

Nemoto, T., Ohara-Nemoto, Y., Ota, M., Takagi, T. and Yokoyama, K. (1995) Mechanism of dimer formation of the 90-kDa heat-shock protein. *Eur J Biochem*, **233**, 1-8.

Niedermann, G., Butz, S., Ihlenfeldt, H.G., Grimm, R., Lucchiari, M., Hoschützky, H., Jung, G., Maier, B. and Eichmann, K. (1995) Contribution of proteasome-mediated proteolysis to the hierarchy of epitopes presented by major histocompatibility complex class I molecules. *Immunity*, **2**, 289-299.

Niedermann, G., Grimm, R., Geier, E., Maurer, M., Realini, C., Gartmann, C., Soll, J., Omura, S., Rechsteiner, M.C., Baumeister, W. and Eichmann, K. (1997) Potential immunocompetence of proteolytic fragments produced by proteasomes before evolution of the vertebrate immune system. *J. Exp. Med.*, **186**, 209-220.

Nikaido, T., Shimada, K., Shibata, M., Hata, M., Sakamoto, M., Y.Takasaki, Sato, C., Takahashi, T. and Nishida, Y. (1990) Cloning and nucleotide sequence of cDNA for Ki antigen, a highly conserved nuclear protein detected with sera from patients with systemic lupus erythematosus. *Clin. Exp. Immunol.*, **79**, 209-214.

Nil, A., Firat, E., Sobek, V., Eichmann, K. and Niedermann, G. (2004) Expression of housekeeping and immunoproteasome subunit genes is differentially regulated in positively and negatively selecting thymic stroma subsets. *Eur J Immunol*, **34**, 2681.

Novitsky, V., Rybak, N., McLane, M.F., Gilbert, P., Chigwedere, P., Klein, I., Gaolekwe, S., Chang, S.Y., Peter, T., Thior, I., Ndung'u, T., Vannberg, F., Foley, B.T., Marlink, R., Lee, T.H. and Essex, M. (2001) Identification of human immunodeficiency virus type 1 subtype C Gag-, Tat-, Rev-, and Nef-specific elispot-based cytotoxic T-lymphocyte responses for AIDS vaccine design. *J Virol*, **75**, 9210-9228.

Ogg, G.S., Xia, J., Bonhoeffer, S., Dunbar, P.R., Nowak, M.A., Monard, S., Segal, J.P., Cao, Y., Rowland-Jones, S.L., Cerundolo, V., Hurley, A., Markowitz, M., Ho, D.D., Nixon, D.F. and McMichael, A.J. (1998) Quantitation of HIV-1-specific cytotoxic T lymphocytes and plasma load of viral RNA. *Science*, **279**, 2103-2106.

Oldstone, M.B. and Buchmeier, M.J. (1982) Restricted expression of viral glycoprotein in cells of persistently infected mice. *Nature*, **300**, 360-362.

Olver, S.D., Price, P. and Shellam, G.R. (1994) Cytomegalovirus hepatitis: characterization of the inflammatory infiltrate in resistant and susceptible mice. *Clin Exp Immunol*, **98**, 375-381.

Ortmann, B., Copeman, J., Lehner, P.J., Sadasivan, B., Herberg, J.A., Grandea, A.G., Riddell, S.R., Tampe, R., Spies, T., Trowsdale, J. and Cresswell, P. (1997) A critical role for tapasin in the assembly and function of multimeric MHC class I-TAP complexes. *Science*, **277**, 1306-1309.

Ou, R., Zhou, S.H., Huang, L. and Moskophidis, D. (2001) Critical role for alpha/beta and gamma interferons in persistence of lymphocytic choriomeningitis virus by clonal exhaustion of cytotoxic T cells. *J Virol*, **75**, 8407-8423.

Oxenius, A., Zinkernagel, R.M. and Hengartner, H. (1998) Comparison of activation versus induction of unresponsiveness of virus-specific CD4+ and CD8+ T cells upon acute versus persistent viral infection. *Immunity*, **9**, 449-457.

Ozkaynak, E., Finley, D. and Varshavsky, A. (1984) The yeast ubiquitin gene: head-to-tail repeats encoding a polyubiquitin precursor protein. *Nature*, **312**, 663-666.

Palmer, A., Rivett, A.J., Thomson, S., Hendil, K.B., Butchers, G.W., Fuertes, G. and Knecht, E. (1996) Subpopulations of proteasomes in rat liver nuclei, microsomes and cytosol. *Biochem. J.*, **316**, 401-407.

Pantaleo, G., Demarest, J.F., Schacker, T., Vaccarezza, M., Cohen, O.J., Daucher, M., Graziosi, C., Schnittman, S.S., Quinn, T.C., Shaw, G.M., Perrin, L., Tambussi, G., Lazzarin, A., Sekaly, R.P., Soudeyns, H., Corey, L. and Fauci, A.S. (1997) The qualitative nature of the primary immune response to HIV infection is a prognosticator of disease progression independent of the initial level of plasma viremia. *Proc Natl Acad Sci U S A*, **94**, 254-258.

Pfau, C.J., Valenti, J.K., Pevear, D.C. and Hunt, K.D. (1982) Lymphocytic choriomeningitis virus killer T cells are lethal only in weakly disseminated murine infections. *J Exp Med*, **156**, 79-89.

Picard, D., Khursheed, B., Garabedian, M.J., Fortin, M.G., Lindquist, S. and Yamamoto, K.R. (1990) Reduced levels of hsp90 compromise steroid receptor action in vivo. *Nature*, **348**, 166-168.

Pickart, C.M. and Rose, I.A. (1985) Ubiquitin carboxyl-terminal hydrolase acts on ubiquitin carboxyl-terminal amides. *J Biol Chem*, **260**, 7903-7910.

Pircher, H., Moskophidis, D., Rohrer, U., Burki, K., Hengartner, H. and Zinkernagel, R.M. (1990) Viral escape by selection of cytotoxic T cell-resistant virus variants in vivo. *Nature*, **346**, 629-633.

Planz, O., Ehl, S., Furrer, E., Horvath, E., Bründler, M.-A., Hengartner, H. and Zinkernagel, R.M. (1997) A critical role for neutralizing-antibody-producing B cells, CD4+ T cells and interferons in persisitent and acute infections of mice with lymphocytic choriomeningitis virus: implications for adoptive immunotherapy of virus carriers. *Proc. Natl. Acad. Sci. USA*, **94**, 6874-6879.

Podlech, J., Holtappels, R., Wirtz, N., Steffens, H.P. and Reddehase, M.J. (1998) Reconstitution of CD8 T cells is essential for the prevention of multiple-organ cytomegalovirus histopathology after bone marrow transplantation. *J Gen Virol*, **79 (Pt 9)**, 2099-2104.

Preckel, T., Fung-Leung, W., Cai, Z., Vitiello, A., Salter-Cid, L., Winqvist, O., Wolfe, T.G., von Herrath, M., Angulo, A., Ghazal, P., Lee, J., Fourie, A.M., Wu, Y., Pang, J., Ngo, K., Peterson, P.A., Früh, K. and Yang, Y. (1999) Impaired immunoproteasome assembly and immune responses in PA28$^{-/-}$ mice. *Science*, **286**, 2162-2165.

Princiotta, M.F., Finzi, D., Qian, S.B., Gibbs, J., Schuchmann, S., Buttgereit, F., Bennink, J.R. and Yewdell, J.W. (2003) Quantitating protein synthesis, degradation, and endogenous antigen processing. *Immunity*, **18**, 343-354.

Probst, H.C., Dumrese, T. and van den Broek, M.F. (2002) Cutting edge: competition for APC by CTLs of different specificities is not functionally important during induction of antiviral responses. *J Immunol*, **168**, 5387-5391.

Probst, H.C., Lagnel, J., Kollias, G. and van den Broek, M. (2003a) Inducible transgenic mice reveal resting dendritic cells as potent inducers of CD8+ T cell tolerance. *Immunity*, **18**, 713-720.

Probst, H.C., Tschannen, K., Gallimore, A., Martinic, M., Basler, M., Dumrese, T., Jones, E. and van den Broek, M.F. (2003b) Immunodominance of an antiviral cytotoxic T cell response is shaped by the kinetics of viral protein expression. *J Immunol*, **171**, 5415-5422.

Raasi, S., Schmidtke, G. and Groettrup, M. (2001) The ubiquitin-like protein FAT10 forms covalent conjugates and induces apoptosis. *J. Biol. Chem.*, **276**, 35334-35343.

Rahemtulla, A., Fung-Leung, W.P., Schilham, M.W., Kundig, T.M., Sambhara, S.R., Narendran, A., Arabian, A., Wakeham, A., Paige, C.J., Zinkernagel, R.M. and et al. (1991) Normal development and function of CD8+ cells but markedly decreased helper cell activity in mice lacking CD4. *Nature*, **353**, 180-184.

Rammensee, H.G., Bachmann, J., Emmerich, N.P.N., Bachor, O.A. and Stevanovic, S. (1999) SYFPEITHI: database for MHC ligands and peptide motifs. *Immunogenetics*, **50**, 213-219.

Rammensee, H.G., Falk, K. and Rötzschke, O. (1993) Peptides naturally presented by MHC class I molecules. *Annu. Rev. Immunol.*, **11**, 213-244.

Realini, C., Jensen, C.C., Zhang, Z.G., Johnston, S.C., Knowlton, J.R., Hill, C.P. and Rechsteiner, M. (1997) Characterization of recombinant REG alpha, REG beta, and REG gamma proteasome activators. *J. Biol. Chem.*, **272**, 25483-25492.

Reddehase, M.J. (2000) The immunogenicity of human and murine cytomegaloviruses. *Curr Opin Immunol*, **12**, 390-396.

Reddehase, M.J. (2002) Antigens and immunoevasins: Opponents in cytomegalovirus immune surveillance. *Nat Rev Immunol*, **2**, 831-844.

Reddehase, M.J. and Koszinowski, U.H. (1984) Significance of herpesvirus immediate early gene expression in cellular immunity to cytomegalovirus infection. *Nature*, **312**, 369-371.

Reddehase, M.J., Mutter, W., Munch, K., Buhring, H.J. and Koszinowski, U.H. (1987) CD8-positive T lymphocytes specific for murine cytomegalovirus immediate-early antigens mediate protective immunity. *J Virol*, **61**, 3102-3108.

Reddehase, M.J., Rothbard, J.B. and Koszinowski, U. (1989) A pentapeptide as minimal antigenic determinant for MHC class I-restricted T lymphocytes. *Nature*, **337**, 651-653.

Reddehase, M.J., Weiland, F., Munch, K., Jonjic, S., Luske, A. and Koszinowski, U.H. (1985) Interstitial murine cytomegalovirus pneumonia after irradiation: characterization of cells that limit viral replication during established infection of the lungs. *J Virol*, **55**, 264-273.

Rehm, A., Stern, P., Ploegh, H.L. and Tortorella, D. (2001) Signal peptide cleavage of a type I membrane protein, HCMV US11, is dependent on its membrane anchor. *Embo J*, **20**, 1573-1582.

Reits, E., Griekspoor, A., Neijssen, J., Groothuis, T., Jalink, K., vanVeelen, P., Janssen, H., Calafat, J., Drijfhout, J.W. and Neefjes, J. (2003) Peptide diffusion, protection, and degradation in nuclear and cytoplasmic compartments before antigen presentation by MHC class I. *Immunity*, **18**, 97-108.

Reits, E., Neijssen, J., Herberts, C., Benckhuijsen, W., Janssen, L., Drijfhout, J.W. and Neefjes, J. (2004) A major role for TPPII in trimming proteasomal degradation products for MHC class I antigen presentation. *Immunity*, **20**, 495-506.

Reits, E.A.J., Benham, A.M., Plougastel, B., Neefjes, J. and Trowsdale, J. (1997) Dynamics of proteasome distribution in living cells. *EMBO J.*, **16**, 6087-6094.

Reits, E.A.J., Vos, J.C., Gromme, M. and Neefjes, J. (2000) The major substrates for TAP in vivo are derived from newly synthesized proteins. *Nature*, **404**, 774-778.

Reusch, U., Muranyi, W., Lucin, P., Burgert, H.G., Hengel, H. and Koszinowski, U.H. (1999) A cytomegalovirus glycoprotein re-routes MHC class I complexes to lysosomes for degradation. *Embo J*, **18**, 1081-1091.

Rickinson, A.B. and Moss, D.J. (1997) Human cytotoxic T lymphocyte responses to Epstein-Barr virus infection. *Annu Rev Immunol*, **15**, 405-431.

Riddell, S.R., Watanabe, K.S., Goodrich, J.M., Li, C.R., Agha, M.E. and Greenberg, P.D. (1992) Restoration of viral immunity in immunodeficient humans by the adoptive transfer ofT cell clones. *Science*, **257**, 238-241.

Rivett, A.J., Palmer, A. and Knecht, E. (1992) Electron microscopic localization of the multicatalytic proteinase complex in rat liver and in cultured cells. *J. Histochem. Cytochem.*, **40**, 1165-1172.

Riviere, Y., Ahmed, R., Southern, P.J., Buchmeier, M.J., Dutko, F.J. and Oldstone, M.B.A. (1985) The S RNA segment of lymphocytic choriomeningitis virus codes for the nucleoprotein and glycoproteins 1 and 2. *J Virol.*, **53**, 966-968.

Rock, K.L. and Goldberg, A.L. (1999) Degradation of cell proteins and the generation of MHC class I- presented peptides. *Annu. Rev. Immunol.*, **17**, 739-779.

Rock, K.L., Gramm, C., Rothstein, L., Clark, K., Stein, R., Dick, L., Hwang, D. and Goldberg, A.L. (1994) Inhibitors of the proteasome block the degradation of most cell proteins and the generation of peptides presented on MHC class I molecules. *Cell*, **78**, 761-771.

Rodriguez, F., Harkins, S., Slifka, M.K. and Whitton, J.L. (2002) Immunodominance in virus-induced CD8(+) T-cell responses is dramatically modified by DNA immunization and is regulated by gamma interferon. *J Virol*, **76**, 4251-4259.

Rodriguez, F., Zhang, J. and Whitton, J.L. (1997) DNA immunization: Ubiquitination of a viral protein enhances cytotoxic T-lymphocyte induction and antiviral protection but abrogates antibody induction. *J. Virol.*, **71**, 8497-8503.

Romanowski, V., Matsuura, Y. and Bishop, D.H. (1985) Complete sequence of the S RNA of lymphocytic choriomeningitis virus (WE strain) compared to that of Pichinde arenavirus. *Virus Res*, **3**, 101-114.

Romisch, K. (1999) Surfing the Sec61 channel: bidirectional protein translocation across the ER membrane. *J Cell Sci*, **112**, 4185-4191.

Rotem-Yehudar, R., Groettrup, M., Soza, A., Kloetzel, P.M. and Ehrlich, R. (1996) LMP-associated proteolytic activities and TAP-dependent transport for class I MHC molecules are suppressed in cell lines transformed by the highly oncogenic adenovirus 12. *J. Exp. Med.*, **183**, 499-514.

Russel, M. and Model, P. (1981) A mutation downstream from the signal peptidase cleavage site affects cleavage but not membrane insertion of phage coat protein. *Proc Natl Acad Sci U S A*, **78**, 1717-1721.

Sallusto, F., Lenig, D., Förster, R., Lipp, M. and Lanzavecchia, A. (1999) Two subsets of memory T lymphocytes with distinct homing potentials and effector functions. *Nature*, **401**, 708-712.

Salvato, M.S. and Shimomaye, E.M. (1989) The completed sequence of lymphocytic choriomeningitis virus reveals a unique RNA structure and a gene for a zinc finger protein. *Virology*, **173**, 1-10.

Salzmann, U., Kral, S., Braun, B., Standera, S., Schmidt, M., Kloetzel, P.M. and Sijts, A. (1999) Mutational analysis of subunit i beta 2 (MECL-1) demonstrates conservation of cleavage specificity between yeast and mammalian proteasomes. *FEBS Lett*, **454**, 11-15.

Saric, T., Beninga, J., Graef, C.I., Akopian, T.N., Rock, K.L. and Goldberg, A.L. (2001) Major histocompatibility complex class I-presented antigenic peptides are degraded in cytosolic extracts primarily by thimet oligopeptidase. *J Biol Chem*, **276**, 36474-36481.

Saric, T., Chang, S.C., Hattori, A., York, I.A., Markant, S., Rock, K.L., Tsujimoto, M. and Goldberg, A.L. (2002) An IFN-gamma-induced aminopeptidase in the ER, ERAP1, trims precursors to MHC class I-presented peptides. *Nat Immunol*, **3**, 1169-1176.

Savage, P.A., Boniface, J.J. and Davis, M.M. (1999) A kinetic basis for T cell receptor repertoire selection during an immune response. *Immunity*, **10**, 485-492.

Schaegger, H. and Jagow, G.V. (1987) Tricine-Sodium Dodecyl Sulfate-Polyacrylamide gel electrophoresis for separation of proteins in the range from 1 to 100 kD. *Anal. Biochem.*, **166**, 368-379.

Schlesinger, D.H., Goldstein, G. and Niall, H.D. (1975) The complete amino acid sequence of ubiquitin, an adenylate cyclase stimulating polypeptide probably universal in living cells. *Biochemistry*, **14**, 2214-2218.

Schmidtke, G., Holzhütter, H., Bogyo, M., Kairies, N., Groll, M., de Giuli, R., Emch, S. and Groettrup, M. (1999) How an inhibitor of the HIV-1 protease modulates proteasome activity. *J. Biol. Chem.*, **274**, 35734-35740.

Schmidtke, G., Schmidt, M. and Kloetzel, P.M. (1997) Maturation of mammalian 20S proteasome: purification and characterization of 13S and 16S proteasome precursor complexes. *J. Mol. Biol.*, **268**, 103-112.

Schnaider, T., Somogyi, J., Csermely, P. and Szamel, M. (1998) The Hsp90-specific inhibitor, geldanamycin, blocks CD28-mediated activation of human T lymphocytes. *Life Sci*, **63**, 949-954.

Schubert, U., Anton, L.C., Gibbs, J., Norbury, C.C., Yewdell, J.W. and Bennink, J.R. (2000) Rapid degradation of a large fraction of newly synthesized proteins by proteasomes. *Nature*, **404**, 770-774.

Schultz, E.S., Chapiro, J., Lurquin, C., Claverol, S., BurletSchiltz, O., Warnier, G., Russo, V., Morel, S., Levy, F., Boon, T., VandenEynde, B.J. and vanderBruggen, P. (2002) The production of a new MAGE-3 peptide presented to cytolytic T lymphocytes by HLA-B40 requires the immunoproteasome. *J. Exp. Med.*, **195**, 391-399.

Schwab, S.R., Li, K.C., Kang, C. and Shastri, N. (2003) Constitutive display of cryptic translation products by MHC class I molecules. *Science*, **301**, 1367-1371.

Schwarz, K., de Giuli, R., Schmidtke, G., Kostka, S., van den Broek, M., Kim, K., Crews, C.M., Kraft, R. and Groettrup, M. (2000a) The selective proteasome inhibitors lactacystin and expoxomicin can be used to either up- or downregulate antigen presentation at non-toxic doses. *J. Immunol.*, **164**, 6147-6157.

Schwarz, K., Eggers, M., Soza, A., Koszinowski, U.H., Kloetzel, P.M. and Groettrup, M. (2000b) The proteasome regulator PA28α/β can enhance antigen presentation without affecting 20S proteasome subunit composition. *Eur. J. Immunol.*, **30**, 3672-3679.

Schwarz, K., van den Broek, M., de Giuli, R., Seelentag, W.W., Shastri, N. and Groettrup, M. (2000c) The use of LCMV-specific Tcell hybridomas for the quantitative analysis of MHC class I restricted antigen presentation. *J. Immunol. Meth.*, **237**, 199-202.

Schwarz, K., van den Broek, M., Kostka, S., Kraft, R., Soza, A., Schmidtke, G., Kloetzel, P.M. and Groettrup, M. (2000d) Overexpression of the proteasome subunits LMP2, LMP7, and MECL-1 but not PA28α/β enhances the presentation of an immunodominant lymphocytic choriomeningitis virus T cell epitope. *J. Immunol.*, **165**, 768-778.

Seifert, U., Maranon, C., Shmueli, A., Desoutter, J.F., Wesoloski, L., Janek, K., Henklein, P., Diescher, S., Andrieu, M., delaSalle, H., Weinschenk, T., Schild, H., Laderach, D., Galy, A., Haas, G., Kloetzel, P.M., Reiss, Y. and Hosmalin, A. (2003) An essential

role for tripeptidyl peptidase in the generation of an MHC class I epitope. *Nat Immunol*, **4**, 375-379.

Serwold, T., Gonzalez, F., Kim, J., Jacob, R. and Shastri, N. (2002) ERAAP customizes peptides for MHC class I molecules in the endoplasmic reticulum. *Nature*, **419**, 480-483.

Serwold, T. and Shastri, N. (1999) Specific proteolytic cleavages limit the diversity of the pool of peptides available to MHC class I molecules in living cells. *J Immunol*, **162**, 4712-4719.

Sevilla, N., Kunz, S., Holz, A., Lewicki, H., Homann, D., Yamada, H., Campbell, K.P., Torre, J.C.d.l. and Oldstone, M.B.A. (2000) Immunosuppression and resultant viral persistence by specific viral targeting of dendritic cells. *J. Exp. Med.*, **192**, 1249-1260.

Shastri, N. and Gonzalez, F. (1993) Endogenous generation and presentation of the ovalbumin peptide/K^b complex to T cells. *J. Immunol.*, **150**, 2724-2736.

Shockett, P., Difilippantonio, M., Hellman, N. and Schatz, D.G. (1995) A modified tetracycline-regulated system provides autoregulatory, inducible gene expression in cultured cells and transgenic mice. *Proc. Natl. Acad. Sci. USA*, **92**, 6522-6526.

Sibille, C., Gould, K.G., Willard-Gallo, K., Thomson, S., Rivett, A.J., Powis, S., Butcher, G.W. and De Baetselier, P. (1995) $LMP2^+$ proteasomes are required for the presentation of specific antigens to cytotoxic T lymphocytes. *Curr. Biol.*, **5**, 923-930.

Sijts, A.J.A.M., Ruppert, T., Rehermann, B., Schmidt, M., Koszinowski, U. and Kloetzel, P.M. (2000a) Efficient generation of a hepatitis B virus cytotoxic T lymphocyte epitope requires the structural features of immunoproteasomes. *J. Exp. Med.*, **191**, 503-513.

Sijts, A.J.A.M., Standera, S., Toes, R.E.M., Ruppert, T., Beekman, N.J.C.M., vanVeelen, P.A., Ossendorp, F.A., Melief, C.J.M. and Kloetzel, P.M. (2000b) MHC class I antigen processing of an Adenovirus CTL epitope is linked to the levels of immunoproteasomes in infected cells. *J. Immunol.*, **164**, 4500-4506.

Sing, G.K., Ladhams, A., Arnold, S., Parmar, H., Chen, X., Cooper, J., Butterworth, L., Stuart, K., D'Arcy, D. and Cooksley, W.G. (2001) A longitudinal analysis of cytotoxic T lymphocyte precursor frequencies to the hepatitis B virus in chronically infected patients. *J Viral Hepat*, **8**, 19-29.

Slifka, M.K., Blattman, J.N., Sourdive, D.J., Liu, F., Huffman, D.L., Wolfe, T., Hughes, A., Oldstone, M.B., Ahmed, R. and Von Herrath, M.G. (2003) Preferential escape of subdominant CD8+ T cells during negative selection results in an altered antiviral T cell hierarchy. *J Immunol*, **170**, 1231-1239.

Song, X., Mott, J.D., Kampen, J.v., Pramanik, B., Tanaka, K., Slaughter, C.A. and DeMartino, G.N. (1996) A model for the quarternary structure of the proteasome activator PA 28. *J. Biol. Chem.*, **271**, 26410-26417.

Sourdive, D.J., Murali-Krishna, K., Altman, J.D., Zajac, A.J., Whitmire, J.K., Pannetier, C., Kourilsky, P., Evavold, B., Sette, A. and Ahmed, R. (1998) Conserved T cell receptor repertoire in primary and memory CD8 T cell responses to an acute viral infection. *J Exp Med*, **188**, 71-82.

Srivastava, P.K. and Das, M.R. (1984) The serologically unique cell surface antigen of Zajdela ascitic hepatoma is also its tumor-associated transplantation antigen. *Int J Cancer*, **33**, 417-422.

Stebbins, C.E., Russo, A.A., Schneider, C., Rosen, N., Hartl, F.U. and Pavletich, N.P. (1997) Crystal structure of an Hsp90-geldanamycin complex: targeting of a protein chaperone by an antitumor agent. *Cell*, **89**, 239-250.

Stepanova, L., Leng, X., Parker, S.B. and Harper, J.W. (1996) Mammalian p50Cdc37 is a protein kinase-targeting subunit of Hsp90 that binds and stabilizes Cdk4. *Genes Dev*, **10**, 1491-1502.

Stohwasser, R., Kuckelkorn, U., Kraft, R., Kostka, S. and Kloetzel, P.M. (1996) 20S proteasome from LMP7 knock out mice reveals altered proteolytic activities and cleavage site preferences. *FEBS Lett.*, **383**, 109-113.

Stohwasser, R., Standera, S., Peters, I., Kloetzel, P.-M. and Groettrup, M. (1997) Molecular cloning of the mouse proteasome subunits MC14 and MECL-1: reciprocally regulated tissue expression of interferon-γ - modulated proteasome subunits. *Eur. J. Immunol.*, **27**, 1182-1187.

Stoltze, L., Schirle, M., Schwarz, G., Schroter, C., Thompson, M.W., Hersh, L.B., Kalbacher, H., Stevanovic, S., Rammensee, H.G. and Schild, H. (2000) Two new proteases in the MHC class I processing pathway. *Nat. Immunol.*, **1**, 413-418.

Swain, S.L. (1983) T cell subsets and the recognition of MHC class. *Immunol Rev*, **74**, 129-142.

Tabi, Z., Moutaftsi, M. and Borysiewicz, L.K. (2001) Human cytomegalovirus pp65- and immediate early 1 antigen-specific HLA class I-restricted cytotoxic T cell responses induced by cross-presentation of viral antigens. *J Immunol*, **166**, 5695-5703.

Tamura, Y., Peng, P., Liu, K., Daou, M. and Srivastave, P.K. (1997) Immunotherapy of tumors with autologous tumor-derived heat shock protein preparations. *Science*, **278**, 117-120.

Tanaka, K. and Ichihara, A. (1989) Half-life of proteasomes (multiprotease complexes) in rat liver. *Biochem. Biophys. Res. Commun.*, **159**, 1309-1315.

Tanioka, T., Hattori, A., Masuda, S., Nomura, Y., Nakayama, H., Mizutani, S. and Tsujimoto, M. (2003) Human leukocyte-derived arginine aminopeptidase. The third member of the oxytocinase subfamily of aminopeptidases. *J Biol Chem*, **278**, 32275-32283.

Tiwari, S. and Weissman, A.M. (2001) Endoplasmic reticulum (ER)-associated degradation of T cell receptor subunits - Involvement of ER-associated ubiquitin-conjugating enzymes (E2s). *J Biol Chem*, **276**, 16193-16200.

Toes, R.E.M., Nussbaum, A.K., Degermann, S., Schirle, M., Emmerich, N.P.N., Kraft, M., Laplace, C., Zwinderman, A., Dick, T.P., Muller, J., Schonfisch, B., Schmid, C., Fehling, H.J., Stevanovic, S., Rammensee, H.G. and Schild, H. (2001) Discrete cleavage motifs of constitutive and immunoproteasomes revealed by quantitative analysis of cleavage products. *J. Exp. Med.*, **194**, 1-12.

Townsend, A., Bastin, J., Gould, K., Brownlee, G., Andrew, M., Coupar, B., Boyle, D., Chan, S. and Smith, G. (1988) Defective presentation to class I-restricted cytotoxic T lymphocytes in vaccinia-infected cells is overcome by enhanced degradation of antigen. *J. Exp. Med.*, **168**, 1211-1224.

Townsend, A.R.M., Gotch, F.M. and Davey, J. (1985) Cytotoxic T cells recognize fragments of the influenza nucleoprotein. *Cell*, **42**, 457-467.

Trgovcich, J., Stimac, D., Polic, B., Krmpotic, A., Pernjak-Pugel, E., Tomac, J., Hasan, M., Wraber, B. and Jonjic, S. (2000) Immune responses and cytokine induction in the development of severe hepatitis during acute infections with murine cytomegalovirus. *Arch Virol*, **145**, 2601-2618.

Tsirigotis, M., Zhang, M., Chiu, R.K., Wouters, B.G. and Gray, D.A. (2001) Sensitivity of mammalian cells expressing mutant ubiquitin to protein- damaging agents. *J Biol Chem*, **276**, 46073-46078.

Tsubuki, S., Kawasaki, H., Saito, Y., Miyashita, N., Inomata, M. and Kawashima, S. (1993) Purification and characterization of a Z-Leu-Leu-Leu-MCA degrading protease expected to regulate neurite formation: a novel catalytic activity in proteasome. *Biochem. Biophys. Res. Comm.*, **196**, 1195-1201.

Udono, H. and Srivastava, P.K. (1993) Heat shock protein 70-associated peptides elicit specific cancer immunity. *J. Exp. Med.*, **178**, 1391-1396.

Usherwood, E.J., Hogg, T.L. and Woodland, D.L. (1999) Enumeration of antigen-presenting cells in mice infected with Sendai virus. *J Immunol*, **162**, 3350-3355.

Ustrell, V., Hoffman, L., Pratt, G. and Rechsteiner, M. (2002) PA200, a nuclear proteasome activator involved in DNA repair. *Embo J*, **21**, 3516-3525.

Ustrell, V., Realini, C. and Rechsteiner, M. (1995) Human lymphoblast and erythrocyte multicatalytic proteases: differential peptidase activities and responses to the 11S regulator. *FEBS Lett.*, **376**, 155-158.

van Baalen, C.A., Pontesilli, O., Huisman, R.C., Geretti, A.M., Klein, M.R., de Wolf, F., Miedema, F., Gruters, R.A. and Osterhaus, A.D. (1997) Human immunodeficiency virus type 1 Rev- and Tat-specific cytotoxic T lymphocyte frequencies inversely correlate with rapid progression to AIDS. *J Gen Virol*, **78 (Pt 8)**, 1913-1918.

van der Most, R.G., Murali-Krishna, K., Lanier, J.G., Wherry, E.J., Puglielli, M.T., Blattman, J.N., Sette, A. and Ahmed, R. (2003) Changing immunodominance patterns in antiviral CD8 T-cell responses after loss of epitope presentation or chronic antigenic stimulation. *Virology*, **315**, 93-102.

van der Most, R.G., MuraliKrishna, K., Whitton, J.L., Oseroff, C., Alexander, J., Southwood, S., Sidney, J., Chesnut, R.W., Sette, A. and Ahmed, R. (1998) Identification of D-b- and K-b-restricted subdominant cytotoxic T- cell responses in lymphocytic choriomeningitis virus-infected mice. *Virology*, **240**, 158-167.

van der Most, R.G., Sette, A., Oseroff, C., Alexander, J., Murali-Krishna, K., Lau, L.L., Southwood, S., Sidney, J., Chestnut, R.W., Matloubian, M. and Ahmed, R. (1996) Analysis of cytotoxic T cell responses to dominant and subdominant epitopes during acute and chronic lymphocytic choriomeningitis virus infection. *J. Immunol.*, **157**, 5543-5554.

van Endert, P.M., Saveanu, L., Hewitt, E.W. and Lehner, P. (2002) Powering the peptide pump: TAP crosstalk with energetic nucleotides. *Trends Biochem Sci*, **27**, 454-461.

van Hall, T., Sijts, A., Camps, M., Offringa, R., Melief, C., Kloetzel, P.M. and Ossendorp, F. (2000) Differential influence on cytotoxic T lymphocyte epitope presentation by controlled expression of either proteasome immunosubunits or PA28. *J. Exp. Med.*, **192**, 483-494.

Van Kaer, L., Ashton-Rickardt, P.G., Eichelberger, M., Gaczynska, M., Nagashima, K., Rock, K.L., Goldberg, A.L., Doherty, P.C. and Tonegawa, S. (1994) Altered peptidase and viral-specific T cell response in LMP 2 mutant mice. *Immunity*, **1**, 533-541.

Vigneron, N., Stroobant, V., Chapiro, J., Ooms, A., Degiovanni, G., Morel, S., vanderBruggen, P., Boon, T. and VandenEynde, B.J. (2004) An antigenic peptide produced by peptide splicing in the proteasome. *Science*, **304**, 587-590.

Voges, D., Zwickl, P. and Baumeister, W. (1999) The 26S proteasome: A molecular machine designed for controlled proteolysis. *Annu. Rev. Biochem.*, **68**, 1015-1068.

von Heijne, G. (1983) Patterns of amino acids near signal-sequence cleavage sites. *Eur J Biochem*, **133**, 17-21.

von Heijne, G. (1985) Signal sequences. The limits of variation. *J Mol Biol*, **184**, 99-105.

Wagner, B.J. and Margolis, J.W. (1995) Age-dependent association of isolated bovine lens multicatalytic proteinase complex(proteasome) with heat-shock protein 90, an endogenous inhibitor. *Archives of Biochemistry and Biophysics*, **323 No.2**, 455-462.

Walter, P. and Johnson, A.E. (1994) Signal sequence recognition and protein targeting to the endoplasmic reticulum membrane. *Annu Rev Cell Biol*, **10**, 87-119.

Weidt, G., Utermohlen, O., Heukeshoven, J., Lehmann-Grube, F. and Deppert, W. (1998) Relationship among immunodominance of single CD8+ T cell epitopes, virus load, and kinetics of primary antiviral CTL response. *J Immunol*, **160**, 2923-2931.

Weihofen, A., Binns, K., Lemberg, M.K., Ashman, K. and Martoglio, B. (2002) Identification of signal peptide peptidase, a presenilin-type aspartic protease. *Science*, **296**, 2215-2218.

Weissman, A.M. (2001) Themes and variations on ubiquitylation. *Nature Rev.*, **2**, 169-178.

Welsh, R.M. and Kiessling, R.W. (1980) Natural killer cell response to lymphocytic choriomeningitis virus in beige mice. *Scand. J. Immunol.*, **11**, 363-367.

Wherry, E.J., Blattman, J.N., Murali-Krishna, K., van der Most, R. and Ahmed, R. (2003) Viral persistence alters CD8 T-cell immunodominance and tissue distribution and results in distinct stages of functional impairment. *J. Virol.*, **77**, 4911-4927.

Whitby, F.G., Masters, E.I., Kramer, L., Knowlton, J.R., Yao, Y., Wang, C.C. and Hill, C.P. (2000) Structural basis for the activation of 20S proteasomes by 11S regulators. *Nature*, **408**, 115-120.

Whitesell, L., Mimnaugh, E.G., De Costa, B., Myers, C.E. and Neckers, L.M. (1994) Inhibition of heat shock protein HSP90-pp60v-src heteroprotein complex formation by benzoquinone ansamycins: essential role for stress proteins in oncogenic transformation. *Proc Natl Acad Sci U S A*, **91**, 8324-8328.

Wickner, S., Maurizi, M.R. and Gottesman, S. (1999) Posttranslational quality control: folding, refolding, and degrading proteins. *Science*, **286**, 1888-1893.

Wojcik, C., Tanaka, K., Paweletz, N., Naab, U. and Wilk, S. (1998) Proteasome activator (PA28) subunits, alpha, beta and gamma (Ki antigen) in NT2 neuronal precursor cells and HeLa S3 cells. *Eur. J. Cell Biol.*, **77**, 151-160.

Xu, Y. and Lindquist, S. (1993) Heat-shock protein hsp90 governs the activity of pp60v-src kinase. *Proc Natl Acad Sci U S A*, **90**, 7074-7078.

Yamano, T., Murata, S., Shimbara, N., Tanaka, N., Chiba, T., Tanaka, K., Yui, K. and Udono, H. (2002) Two distinct pathways mediated by PA28 and hsp90 in major histocompatibility complex class I antigen processing. *J Exp Med*, **196**, 185-196.

Yanagi, Y., Yoshikai, Y., Leggett, K., Clark, S.P., Aleksander, I. and Mak, T.W. (1984) A human T cell-specific cDNA clone encodes a protein having extensive homology to immunoglobulin chains. *Nature*, **308**, 145-149.

Yang, Y., Waters, J.B., Frueh, K. and Peterson, P.A. (1992) Proteasomes are regulated by interferon γ: implications for antigen processing. *Proc. Natl. Acad. Sci. USA*, **89**, 4928-4932.

Yao, J.S., Strauss, E.G. and Strauss, J.H. (1996) Interactions between PE2, E1, and 6K required for assembly of alphaviruses studied with chimeric viruses. *J Virol*, **70**, 7910-7920.

Yewdell, J.T. and Bennink, J.R. (1999) Immunodominance in major histocompatibility complex class I- restricted T lymphocyte responses. *Annu. Rev. Immunol.*, **17**, 51-88.

Yewdell, J.W., Anton, L.C. and Bennink, J.R. (1996) Defective ribosomal products (DRiPs) A Major source of antigenic peptides for MHC Class I molecules. *J. Immunol.*, **157**, 1823-1826.

York, I.A., Chang, S.C., Saric, T., Keys, J.A., Favreau, J.M., Goldberg, A.L. and Rock, K.L. (2002) The ER aminopeptidase ERAP1 enhances or limits antigen presentation by trimming epitopes to 8-9 residues. *Nat. Immunol.*, **3**, 1177-1184.

York, I.A., Goldberg, A.L., Mo, X.Y. and Rock, K.L. (1999) Proteolysis and class I major histocompatibility complex antigen presentation. *Immunol Rev*, **172**, 49-66.

York, I.A., Mo, A.X.Y., Lemerise, K., Zeng, W.Y., Shen, Y.L., Abraham, C.R., Saric, T., Goldberg, A.L. and Rock, K.L. (2003) The cytosolic endopeptidase, thimet oligopeptidase, destroys antigenic peptides and limits the extent of MHC class I antigen presentation. *Immunity*, **18**, 429-440.

Young, J.C., Moarefi, I. and Hartl, F.U. (2001) Hsp90: a specialized but essential protein-folding tool. *J Cell Biol*, **154**, 267-273.

Zaiss, D.M., Standera, S., Kloetzel, P.M. and Sijts, A.J. (2002) PI31 is a modulator of proteasome formation and antigen processing. *Proc. Natl.Acad. Sci. U S A*, **99**, 14344-14349.

Zaiss, D.M.W., Standera, S., Holzhütter, H., Kloetzel, P.M. and Sijts, A.J.A.M. (1999) The proteasome inhibitor PI31 competes with PA28 for binding to 20S proteasomes. *FEBS Lett.*, **457**, 333-338.

Zajac, A.J., Blattman, J.N., Murali-Krishna, K., Sourdive, D.J., Suresh, M., Altman, J.D. and Ahmed, R. (1998) Viral immune evasion due to persistence of activated T cells without effector function. *J Exp Med*, **188**, 2205-2213.

Ziegler, H., Thäle, R., Lucin, P., Muranyi, W., Flohr, T., Hengel, H., Farrell, H., Rawlinson, W. and Koszinowski, U.H. (1997) A mouse cytomegalovirus glycoprotein retains MHC class I complexes in the ERGIC/cis - Golgi compartments. *Immunity*, **6**, 57-66.

Zinkernagel, R., Haenseler, E., Leist, T., Cerny, A., Hengartner, H. and Althage, A. (1986) T cell-mediated hepatitis in mice infected with lymphocytic choriomeningitis virus. *J. Exp. Med.*, **164**, 1075-1091.

Zinkernagel, R.M., Callahan, G.N., Klein, J. and Dennert, G. (1978) Cytotoxic T cells learn specificity for self H-2 during differentiation in the thymus. *Nature*, **271**, 251-253.

Zinkernagel, R.M. and Doherty, P. (1974) Restriction of in vitro T-cell mediated cytotoxicity in lymphocytic choriomeningitis within a syngeneic or semi allogeneic system. *Nature*, **248**, 701-702.

Zinkernagel, R.M. and Doherty, P.C. (1979) MHC-restricted cytotoxic T cells: studies on the biological role of polymorphic major transplantation antigens determining T-cell restriction-specificirty, function, and responsiveness. *Adv. Immunol.*, **27**, 51-177.

Chapter 11

Appendix

1. Record of achievement / Eigenabgrenzung

Chapter 2, 3, 4, and 5: Results described in these chapters were exclusively performed by myself or under my direct supervision.

Chapter 6: I characterized and subcloned T cell hybridomas used in Figure 4.

Chapter 7: I performed western blots shown in Fig. 4 and 5 and did the animal work for Fig.1.

Chapter 8: I contributed to Figure 4 and 5 in this chapter by providing the LCMV infected cells used in Figure 4 and performing the LCMV particle preparation for Figure 5.

2. List of publications

Froeschke, M., **Basler, M.**, Groettrup, M. and Dobberstein, B. (2003) Long-lived signal peptide of lymphocytic choriomeningitis virus glycoprotein pGP-C. *J. Biol. Chem.*, **278**, 41914-41920.

Probst, H.C., Tschannen, K., Gallimore, A., Martinic, M., **Basler, M.**, Dumrese, T., Jones, E. and van den Broek, M.F. (2003) Immunodominance of an antiviral cytotoxic T cell response is shaped by the kinetics of viral protein expression. *J Immunol*, **171**, 5415-5422.

Khan, S., Zimmermann, A., **Basler, M.**, Groettrup, M. and Hengel, H. (2004) A cytomegalovirus inhibitor of gamma interferon signaling controls immunoproteasome induction. *J Virol*, **78**, 1831-1842.

Basler, M., Youhnovski, N., Van Den Broek, M., Przybylski, M. and Groettrup, M. (2004) Immunoproteasomes down-regulate presentation of a subdominant T cell epitope from lymphocytic choriomeningitis virus. *J Immunol*, **173**, 3925-3934.

Basta, S., Stoessel, R., **Basler, M.**, Van Den Broek, M., and Groettrup, M. Cross-Presentation Of the DRiP Substrate LCMV-NP Does Not Require De Novo Synthesis and Is Enhanced via Heat Shock Proteins in A Peptide-Independent Manner. Submitted.

Basler, M., Moebius, J., and Groettrup, M. Immune defects in MECL-1 deficient mice. In preparation.

3. Acknowledgments

The work presented in this thesis was carried out between June 2001 and October 2004 at the Kantonsspital in St. Gallen and at the Chair of Immunology at the University of Konstanz under the supervision of Prof. Dr. Marcus Groettrup.

I'm grateful to several people:

Prof. Dr. Marcus Groettrup for giving me the opportunity to perform my PHD in his group. I'm grateful for his interest in my work, his big support and his motivation (especially when experiments didn't go so well).

Prof. Dr. M. Scheffner and Prof. Dr. H. Schild for accepting to be the 'referent' and the 'co-examinator'.

The 'old' PHD students Carolina and Mark-Steffen for having a good time and interesting discussions.

Sam Basta for sharing his knowledge about viral immunology and for a funny time.

The 'Legler group' members (Daniel, Tina, Carolina, and Petra) for accepting me working next to them and for having a good time in the lab.

Gunter Schmidtke and Daniel Legler for fruitful discussions and support.

Ulrike Beck for her helpfulness and her permanent 'drive' to solve problems.

Jacqueline Möbius for her help during her diploma thesis.

The diploma students (Jacqueline, Petra K., Elvira, Ricarda, Petra B., Regina, and Anja) for increasing the temper in our lab and for several cakes and breakfasts.

All the other members of the lab (Eva, Birte, Elisabeth, Nela, Gerardo, and Brigitte) for their helpfulness.

The members of the TFA, especially Andrea.

All the people at the KSSG (Rita, Elke, Selina, Annalisa, and Ying) for their support at the beginning of my PHD.

Maries van den Broek for quickly answering several questions by e-mail and for sharing reagents.

My family and my wife's family for supporting me.

All my friends and the people I forgot to mention.

And the greatest thank to my wife Iris!